



Elastic matching for classification and modelisation of incomplete time series

Thi-Thu-Hong Phan

► To cite this version:

Thi-Thu-Hong Phan. Elastic matching for classification and modelisation of incomplete time series. Signal and Image processing. Université du Littoral Côte d'Opale, 2018. English. NNT : 2018DUNK0483 . tel-02001195

HAL Id: tel-02001195

<https://theses.hal.science/tel-02001195>

Submitted on 31 Jan 2019

HAL is a multi-disciplinary open access archive for the deposit and dissemination of scientific research documents, whether they are published or not. The documents may come from teaching and research institutions in France or abroad, or from public or private research centers.

L'archive ouverte pluridisciplinaire **HAL**, est destinée au dépôt et à la diffusion de documents scientifiques de niveau recherche, publiés ou non, émanant des établissements d'enseignement et de recherche français ou étrangers, des laboratoires publics ou privés.

Numéro d'ordre:
École doctorale SPI - Université Lille Nord-De-France

THESIS

Submitted for the degree of
Doctor of Philosophy (PhD) in Signal Processing
Docteur de l'Université Littoral Côte d'Opale
Discipline: Traitement du signal
Thi-Thu-Hong PHAN
Calais, October 2018

Elastic matching for classification and modélisation of incomplete time series

sous la direction de / Thesis supervisors:

André BIGAND	Maître de Conférences - HDR
Émilie POISSON CAILLAULT	Maître de Conférences

JURY - Thesis committee:

Plamen ANGELOV	Professeur, Lancaster University	Rapporteur / Referee
Christian VIARD GAUDIN	Professeur, Université de Nantes	Rapporteur / Referee
Sylvie Le HÉGARAT-MASCLE	Professeur, Université Paris Sud	Présidente / President
Alain LEFEBVRE	Chercheur expert HDR	Invité / Invited member
	Dir. IFREMER LER Boulogne-sur-mer	

Laboratoire d'Informatique, Signal et Image de la Côte d'Opale – EA 4491
50 rue Ferdinand Buisson – B.P. 719, 62228 Calais Cedex, France

Contents

Notations and Abbreviations	iii
Introduction	5
1 Preliminaries	11
1.1 Time series	12
1.2 Missing data mechanisms	12
1.3 Time series characterization	15
1.3.1 Composition of time series	15
1.3.2 Auto-correlation function (ACF)	16
1.3.3 Correlation	18
1.3.4 Cross-correlation (recurrent data for univariate time series)	18
1.4 Experiments protocol	19
1.4.1 Experimental process for the imputation task	20
1.4.2 Measurements for evaluating imputation methods	20
1.5 Chapter conclusion	24
2 DTW-based imputation approach for univariate time series	25
2.1 Introduction	26
2.2 Literature review of Dynamic Time Warping	28
2.2.1 Classical DTW algorithm	28
2.2.2 DDTW - Derivative Dynamic Time Warping	32
2.2.3 AFBTW - Adaptive Feature Based Dynamic Time Warping	33
2.2.4 Dissimilarity-based elastic matching	34
2.2.5 Dynamic Time Warping-D algorithm (DTW-D)	35
2.2.6 Illustration	35

2.3	Dynamic Time Warping-based imputation for univariate time series	41
2.3.1	The proposed method - DTWBI	41
2.3.2	Validation procedure	44
2.3.3	Results and discussion	47
2.3.4	Conclusion	57
2.4	Comparison of various DTW versions for completing missing values in uni- variate time series	58
2.4.1	Introduction	58
2.4.2	Imputation based on DTW metrics	59
2.4.3	Data presentation	59
2.4.4	Results and discussion	60
2.4.5	Conclusion	64
2.5	Chapter conclusion	66
3	Imputation approaches for uncorrelated multivariate time series	69
3.1	Introduction	69
3.2	Dynamic Time Warping-based uncorrelated multivariate time series imputation	73
3.2.1	DTWUMI - Proposed approach	73
3.2.2	Validation procedure	75
3.2.3	Results and discussion	79
3.2.4	Conclusion	84
3.3	Proposed method based on an hybrid similarity measure	85
3.3.1	Methods based on fuzzy similarity measure	85
3.3.2	FSMUMI-Proposed approach	87
3.3.3	Validation procedure	93
3.3.4	Results and discussion	96
3.3.5	Conclusion	107
3.4	Chapter conclusion	107
4	Applications: Toward classification and forecasting	111
4.1	Classification of phytoplankton species	112
4.1.1	Introduction	112
4.1.2	Feature-extraction algorithm	115
4.1.3	Methodology	116
4.1.4	Experiment and discussion	121
4.1.5	Conclusion	125

4.2	Event detection in a multidimensional time series	125
4.2.1	Data presentation	126
4.2.2	Preprocessing data	129
4.2.3	Event detection	132
4.2.4	Conclusion	134
4.3	Comparative Study on Univariate Forecasting Methods for Meteorological Time Series	136
4.3.1	Introduction	136
4.3.2	Time series forecasting methods	138
4.3.3	Experiment protocol	140
4.3.4	Results and discussion	141
4.3.5	Conclusion	145
4.4	Chapter conclusion	146
	Conclusions and future work	149
	Appendices	155
	A List of publications and valuations related to the thesis	157
	B Illustration of different DTW versions matching	161
	C List of fuzzy rules	165
	D Dynamic Time Warping-based imputation for univariate time series data	169
	Bibliography	179
	List of Tables	197
	List of Figures	199
	Abstract	203

Acknowledgment

Firstly, I would like to take this opportunity to express my deepest appreciation and thank to my supervisors Professor André BIGAND, Associate Professor Emilie POISSON CAILAUT for your support and guidance; you have been tremendous mentors for me. Your meticulous comments were of enormous assistance to me, and without your guidance and persistent help this thesis would not have been possible.

I would like to express my special gratitude to Prof. Plamen ANGELOV and Prof. Christian VIARD GAUDIN for their time and hard work to review my thesis, and for giving me valuable remarks to improve it. I would also like to convey special thanks to Prof. Sylvie Le HÉGARAT-MASCLE and Dr. Alain LEFEBVRE for examining my dissertation.

I am grateful to Wagner Anne, Sandrine Target for their patience and advice to help me improve the quality of my writing. I am also indebted to the members of the IFREMER institute (France), Nguyen Duy Binh (VNUA-Vietnam) for the databases and SCoSI/ULCO (CALCULCO computing platform) for experiments.

Next, I would like to thank the Vietnam International Education Development, Campus France and LISIC laboratory - University of Littoral for funding this thesis. Without their financial support this project could not have happened.

I also would like to acknowledge my colleagues at the Computer Science Department of Vietnam National University of Agriculture for their moral support throughout the whole PhD. I am grateful to Pham Quang Dung and Farouk Yahaya for kindly volunteering to proofread chapters.

I also would like to thank all my lab colleagues at LISIC and friends for their interaction and friendly support during these years. I am greatly indebted to LE Hoang Raymond, Danielle Proust who have constantly motivated me throughout this work. There are so many people I am thankful for, and while I cannot thank each one individually, I am blessed to have had so much support along the way.

Most importantly, I am incredibly grateful to my husband for his love, patience and encouragement during these challenging academic years. I am thankful for my children who always brighten my days and keep life in perspective. I convey special thanks to my parent, my brothers, and sisters. Their love, support and belief were what sustained me thus far.

Notations and Abbreviations

Notations

t	Position of the first missing value of a gap
T	Size of a gap
M	Number of columns/ Number of variables
N	Number of instants
x	Univariate time series
X	Multivariate time series
Q	Query
R	Reference
Qs	The most similar window
Qa	Query after the gap
Qb	Query before the gap
Qas	The most similar window after the gap
Qbs	The most similar window before the gap

Abbreviations

AFBDTW	Adapted Feature Based Dynamic Time Warping
ANN	Artificial Neural Networks
ARIMA	Autoregressive Integrated Moving Average
BSTS	Bayesian Structural Time Series
DDTW	Derivative Dynamic Time Warping
DT	Decision Tree
DTW	Dynamic Time Warping
DTWBI	Dynamic Time Warping-based Imputation
DTWUMI	Dynamic Time Warping-based Uncorrelated Multivariate Imputation
ED	Euclidean Distance
ES	Exponential Smoothing
FB	Fractional Bias

FcM	Fuzzy c-Mean
FCM	Flow CytoMetry
FFNN	Feed-Forward Neural Network
FSD	Fraction of Standard Derivation
FSMUMI	Fuzzy Similarity Measure-based Uncorrelated Multivariate Imputation
FLO	Orange Fluorescence
FLR	Red Fluorescence
FLY	Yellow Fluorescence
FWS	Forward Scatter
k -NN	k -Nearest Neighbors
LDA	Linear Discriminant Analysis
LMCF	Last Mean Carried Forward
LOCF	Last Observation Carried Forward
LR	Linear Regression
MAR	Missing At Random
MCAR	Missing Completely At Random
MNAR	Missing Not At Random
MI	Multiple imputation
MICE	Multiple Imputation by Chained Equations
ML	Maximum Likelihood
MLP	Multi-Layer Perceptron
NA	Not Available
NB	Naive Bayes
NMAE	Normalized Mean Absolute Error
PCA	Principal Component Analysis
RBF	Radial Basis Function
RF	Random Forest
RRF	Regularized Random Forest
GRRF	Guided Regularized Random Forest
GRF	Guided Random Forest
RMSE	Root Mean Standard Error
SARIMA	Seasonal-ARIMA
SD	Standard Deviation
SE	Standard Error
SES	Single Exponential Smoothing
Snaive	Seasonal naive
SVM	Support Vector Machine
SWS	Sideward Scatter

Introduction

Context of the subject

Huge time series can now be considered thanks to the availability of effective low-cost sensors, and the wide deployment of remote sensing systems. But collected data are commonly incomplete for various reasons such as sensor errors, transmission problems, incorrect measurements, bad weather conditions (outdoor sensors) for manual maintenance, etc. Missing data are a major drawback which particularly affects marine samples [1, 2]. An example of recent data is a characterization of seawater collected by the MAREL Carnot station. This station is a marine water monitoring platform in the eastern English Channel located in Boulogne-sur-Mer, France ([3]). Its objective is to find out how the bloom of algae (phytoplankton) disrupted the coastal ecosystem of the eastern Channel. The aforementioned data contain 19 large time series sampled every 20 minutes including fluorescence, turbidity, oxygen saturation, . . . , and measured by sensors. The analysis of this dataset with extraordinary size and shape allows us to reveal events such as algal blooms and to understand phytoplankton processes in detail. But the data include a vast number of missing values viz., 62.2% for phosphate, 59.9% for nitrate, 27.22% for pH, 12.32% for fluorescence and so on.

Most of proposed models for time series analysis suffer from one major drawback, which is their inability to process incomplete datasets, despite their powerful techniques. They usually require complete data, ie. without missing values (MV). Missing data produce a loss of information and can generate inaccurate data interpretation. So how can missing values be dealt with? Ignoring or deleting is a simple way to solve this drawback (also known as complete case analysis). However, this solution has to pay a high price because of losing valuable information, especially when dealing with a small dataset. This is prominent in time series data where the considered values depend on the previous ones. Furthermore, an analysis based on the systematic differences between observed and unobserved data leads to biased and unreliable results [4]. Thus, the filling procedure is a mandatory and precursory pre-processing step before performing other steps such as modeling/classification, etc. The imputation technique is a conventional method to handle the MV problem [5]. In addition, it is necessary to select or propose imputation methods that suit to the type of data and that are consistent with the missing

values mechanism.

For low frequency systems with a monthly sampling or small missing sequence, they can be easily filled in and they do not affect the global results. In this case, a linear or polynomial regression (of order 2) can use to complete missing values. But problems arise when completing missing values of high frequency systems with quick dynamics change such as MAREL Carnot data and purpose [6]. Moreover, the lack of data is not randomly distributed and the size of consecutive missing values (called a gap) is large. The analysis of such data can result in biased interpretations. For example, pH signal contains the largest gap of 234 days, and in this case, we cannot detect phytoplankton bloom (this can only occur in a duration of one day to one month). Thus, imputation techniques such as moving average or regression methods are not effective. Completion becomes more complex when adding variability (and noise) due to the high frequency system.

In other words, for time series data, present values and past ones are often related. Thus, it is important to consider the whole history (i.e. dynamics) of each signal to complete each gap. To deal with the problem of missing values, a natural solution is to look for the same behavior or shape within time series which amounts to retrieving similar values in the series before or after the missing values. Then missing data are completed with the sequence of following/previous similar values.

Approaches and methodology

Dynamic Time Warping (DTW, also called elastic matching) [7] is an effective and well-known method for measuring similarity between two linear/nonlinear time series. The success of DTW in data mining [8], information retrieval and pattern recognition [9, 10, 11] leads us to study its ability to complete missing values in our context of detection and modelization of event states from time series data. This method calculates a geometric distance between two curves to assess their similarity. The method accepts temporal and local expansions. The algorithm consists in mapping pairs of points that minimizes the Euclidean distance between them, so an overall similarity cost is defined as a sum of intensity distance between all paired points.

The elastic matching is widely used in speech or handwriting recognition. Sakoe and Chiba [7] proposed this method to calculate the elastic distance in recognizing spoken words (a word can be pronounced with different sound and length variation). For handwriting recognition, Rath and Manmatha [12] used images of words in their experience and showed that the elastic pairing was an effective method to take into account a spatial variability of the word. DTW matching cost was also used for data classification [13]. Petitjean et al. [14] proposed the DBA (DTW Barycenter Averaging) approach to compute an average of a set of sequences under DTW. Then, DBA was particularly used instead of the Euclidean distance in the K-means algorithm to successfully cluster satellite image time series.

Another class of approaches to handle missing data problem is the fuzzy set theory. This theory makes it possible to deal with imprecise and uncertain circumstances [15]. Imprecision is classically due to sensors. Hence, time series can be considered as fuzzy as pointed out by Chen *et al.* [16]. Unfortunately, time series are also saddled by problems of incompleteness (missing data) and randomness (noise). This inclines us to focus on fuzzy similarity measures by proposing a more generic uncertainty model. Our study follows the success of existing techniques of weighting similarity measures and fuzzy-based similarity measure. Indeed, these methods tend to produce accurate predictions. Some notable areas where weighted similarity measures are employed are numerous as retrieval systems [15], recommendation systems [17], and collaborative filtering [18, 19]. While fuzzy-based similarity measure has also been successfully used in [20, 15, 17].

The robustness of these approaches has opened a new scope by weighting similarity measures based on fuzzy logic to solve the incompleteness problem in time series data. A classical approach to build a new fuzzy-weighted similarity measure is to use a rule-based technique. This technique has been widely implemented in different applications like online learning [21], time series prediction [22], knowledge extraction from data streams [23], equilibrium problem in economics [24] or in [15], and so on. These potentials lead us to deploy a rule-based technique to build a fuzzy-weighted similarity measure which is applied to complete large missing values in uncorrelated multivariate time series.

Contributions of the PhD thesis

The thesis focuses on the investigation and the development of algorithms to complete missing values in time series. Two types of data are studied to propose imputation methods including univariate and uncorrelated multivariate time series. The contributions of the study are stated as follows:

- The first contribution is the proposition of new features allowing better describe global shape and dynamics of a signal (named, shape-feature extraction algorithm). This algorithm is then used to extract features of phytoplankton signals in order to identify phytoplankton species.
- Our second contribution is to propose an effective method, namely DTWBI (DTW Based Imputation), to complete successive missing data in mono-dimensional time series. This method is based on the combination of the proposed shape-feature extraction and Dynamic Time Warping approaches. The performance of the algorithm is compared with published methods on various real and synthetic databases. We then propose a framework to compare the performance of different DTW variants for the univariate imputation task in marine context.
- The third contribution is an extension of DTWBI to fill large missing data in low/un-correlated multivariate time series, called DTWUMI (DTW based Uncorrelated Mul-

tivariate Imputation). This approach is also based on the elastic matching and shape-feature extraction algorithms. A comparison between DTWUMI approach and state-of-the-art algorithms is implemented to assess the performance of the proposed algorithm on different real and simulated databases.

- The fourth contribution focuses on developing a novel approach for filling successive missing values in low/un-correlated multivariate time series with a high level of uncertainty management, namely FSMUMI (Fuzzy Similarity Measure based Uncorrelated Multivariate Imputation). In this way, we propose to use a novel fuzzy weighted similarity measure based on fuzzy grades of basic similarity measures and fuzzy rules. To evaluate the ability of the proposed approach, we compare it with other published methods on various large time series.
- The final contributions are concrete applications of the DTWBI method i) to complete the MAREL Carnot database and then perform a detection and characterization of usual/rare events in these time series and ii) to forecast univariate meteorological time series collected in Vietnam.

Outline of the PhD thesis

The manuscript is divided into three parts: an introductory part presenting general notions and mechanisms related to missing data, the experiment protocol and indicators to evaluate imputation methods (Chapter 1), a main part covering the completion of the missing data in mono-dimensional and multidimensional time series (Chapters 2 and 3), then an application part dedicated to classify phytoplankton species, detect rare/extreme events in a real dataset and forecast univariate meteorological time series (Chapter 4).

Chapter 1 first introduces the definition of univariate/multivariate time series. It then presents the mechanism of missing data described by Little and Rubin ([25]) and our concepts about categorization of missing values. The characterization of univariate time series is also discussed. Finally, the design of the experiments is mentioned including the experimental protocol for the imputation task and criteria using to evaluate completion algorithms.

Chapter 2 is devoted to the first main contribution of this thesis. It provides the basic foundation of Dynamic Time Warping approach and how the DTW works. A review of different versions of DTW is also presented. A new imputation approach (DTWBI) for univariate time series is proposed. This approach is based on the combination of the shape-feature extraction and Dynamic Time Warping methods. Another contribution of this chapter is the proposition of a framework for filling missing values in univariate time series. Thus a comparison of different versions of DTW is performed for the imputation task. The goal is to identify the most suitable methods for the imputation of marine univariate time series ensuring that results are reliable and high quality.

Chapter 3 highlights the second main contribution of this study. We propose two novel methods to estimate missing data for low/un-correlated multivariate time series. In these two approaches, we take advantage of the property of low/un-correlated multivariate data but we exploit this feature in two different aspects. In the first approach, we apply the major principle of DTW method and shape-feature extraction algorithm to complete large missing values. In the second approach, we impute large gaps in low/un-correlated multivariate data with a high level of uncertainty. In this way, we build a new hybrid similarity measure based on fuzzy grades of basic similarity measures and on fuzzy logic rules. Experimental results of the two proposed approaches are compared with results obtained from the state-of-the-art methods.

Chapter 4 corresponds to applications of the shape-feature extraction algorithm and DTWBI approach via three specific developments:

- The first application focuses on the classification of phytoplankton species. Accordingly, we propose the shape-feature extraction algorithm to extract features of phytoplankton signals obtained from flow cytometry (FCM). We then compare the performance of various classifiers on the proposed type of features and two other types of features to find the most convenient features type for the classification of phytoplankton.
- The second part of this chapter is devoted to high frequency MAREL Carnot data. The objective is to complete missing values of this dataset and then carry out a detection of rare/extreme events using multi-level spectral clustering approach.
- The third part is dedicated to compare univariate forecasting methods for meteorological time series. Inspired from the imputation process, we apply DTWBI to forecast univariate time series and perform a comparison of different univariate forecasting algorithms.

Finally, we conclude this PhD thesis with a highlight of our contributions and discuss possibilities for further research that could be investigated.

This thesis is a part of CPER MARCO project (marco.univ-littoral.fr) and is made in collaboration with IFREMER LER-BL (<https://www.ifremer.fr/manchemerdunord/Environnement/LER-Boulogne-sur-Mer>), LOG UMR CNRS (<http://log.cnrs.fr>) and VNUA (<http://www.vnua.edu.vn/>).

Chapter 1

Preliminaries

Contents

1.1	Time series	12
1.2	Missing data mechanisms	12
1.3	Time series characterization	15
1.3.1	Composition of time series	15
1.3.2	Auto-correlation function (ACF)	16
1.3.3	Correlation	18
1.3.4	Cross-correlation (recurrent data for univariate time series)	18
1.4	Experiments protocol	19
1.4.1	Experimental process for the imputation task	20
1.4.2	Measurements for evaluating imputation methods	20
1.5	Chapter conclusion	24

This chapter introduces some background concepts related to time series and also investigates the design of experiments. Section 1.1 discusses what are time series. Missing data definition and missing data mechanisms are then provided in Section 1.2. Section 1.3 mentions the characterization of univariate time series. Finally, Section 1.4 presents the experiments protocol for the imputation task (this technique is applied to mono-dimensional and multidimensional imputation methods) including experimental process and performance measurements of imputation algorithms.

1.1 Time series

A time series is a collection of observations (a sequence of data points), typically consisting of successive measurements made over a time interval.

Lots of useful information can be obtained from collected time series. They are very common in statistics, signal processing, pattern recognition, econometrics, mathematical finance, weather forecasting, intelligent transport and trajectory forecasting, earthquake prediction, control engineering, astronomy, communications engineering, and largely in any domain of applied science and engineering which involves temporal measurements.

Usually, we can distinguish univariate from multivariate time series. We use capital letters to denote multi-variables, and lowercase letters to denote univariate.

Univariate time series refers to data from one variable recorded sequentially in uniform intervals, for example, hourly energy consumption, daily temperature in a city. $x = \{x_t | t = 1, 2, \dots, N\}$ denotes a univariate time series of N successive observations indexed in time.

Multivariate time series is used when a group of time series variables are involved and their interactions may be considered. A multivariate time series is represented as a matrix $X_{N \times M}$ with M collected signals of *length* N . $x(t, i)$ denotes the value of the i -th signal at time t . $x_t = \{x(t, i), i = 1, \dots, M\}$ is the vector at the t -th observation of all variables.

1.2 Missing data mechanisms

Missing data, or missing values infer the existence of observations whose values are either not collected or lost after registering or corresponding to wrong values (out of the sensor range) in the database. In the literature, missing data mechanisms can be divided into three categories. Each category is based on one possible cause: "Missing data are completely random" (Missing Completely At Random, MCAR, in the literature), "Missing data are random" (Missing At Random, MAR) and "Missing data are not random" (Missing Not At Random, MNAR) ([25]). A detailed discussion is presented as follows:

- Missing Completely At Random, MCAR

Missing data are considered as MCAR when the missingness of data is unrelated to any value (the values of missing variable itself or the values of any other variable). This means these missing data points make a random subset of the data and are completely unsystematic. For example, when a person refuses to disclose his income, this does not

affect his actual income nor the income of his family. Similarly, ignoring MCAR missing values does not make the data analysis biased but will increase the standard error of the sample estimates due to the reduced sample size [26].

- Missing At Random, MAR

Missing data are MAR, that means probability of missing values depends only on the observed data, but not the missing data. In the other hand, the missing values of a variable depend on available values of itself and other variables. This makes it possible to estimate missing data based on other variables. For instance, evaluating students participating in a subject includes two exams: midterm exam and final one. In order to take the final exam students must pass the midterm exam. Assuming that a student fail the midterm exam and he/she drops out of the course. Thus, the missing final exam for this student is MAR.

- Missing Not At Random, MNAR

Missing data are MNAR if the propensity of missing values depends on other missing values. Thus with this type of missing data, we cannot estimate incomplete data from existing variables. To extend the previous example, when a student may pass the midterm exam but he/she may be absent at for the final exam.

It is important to understand causes that produce missing data in order to develop an adaptable imputation task. This can in-turn aid in the selection or proposition of an appropriate imputation algorithm ([27]). But in practice, understanding the causes remains a challenging task when missing data cannot be known at all, or when these data have a complex distribution ([28]).

We note that these missing mechanisms are just assumptions about reasons for the lack of data in the context of analysis. Thus from a hypothetical standpoint, they cannot be verified (except for the MCAR hypothesis) and there are no characteristics of the data itself. Similarly, assigning sub-sequences of missing values to "a category can be blurry" ([27]). Commonly, most current research works focus on the three types of missing data previously defined to find out corresponding imputation methods. But Molenberghs et al. advised that it would always be better to check the robustness of the analytical results to different assumptions with sensitivity analysis ([29], Part V). For these reasons, in this study, we consider missing data as 2 types: isolated missing values and gap - missing consecutive values. Let consider some terminologies and a real marine dataset to illustrate the problem.

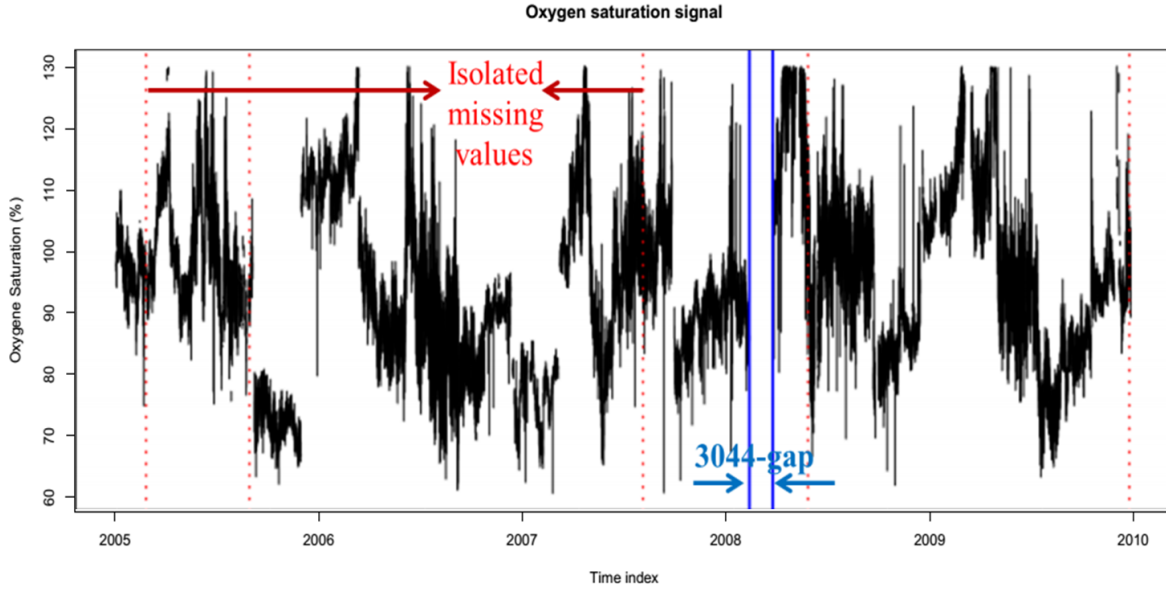


Figure 1.1: Illustration of isolated and T-gap missing values

- Isolated missing value

Given an univariate time series $x = \{x_t | t = 1, 2, \dots, N\}$ with N observations. A single hole at time t is an isolated missing value when observations at time $t - 1$ and $t + 1$ are available. We note $x_t = NA$ (NA stands for Not Available).

- T-gap missing values

A hole of size T , also called gap, is an interval $[t : t + T - 1]$ of consecutive missing values and is denoted $x[t : t + T - 1] = NA$. We define a large gap when T is larger than the known-process change, so it depends on each application.

To clarify these definitions, let us consider the MAREL Carnot dataset ([30]). These data contain single and large holes. For example, oxygen saturation series has 131,472 observations but only 81.9% are available. This series comprises 4,004 isolated missing values and many consecutive missing data. The size of these gaps is highly variable from one hour to few months, the largest gap of this signal is composed of 3,044 missing points corresponding to 42 days. According to Dickley scheme [6] on phytoplankton dynamics, we can only evaluate algae blooms when missing data range from 1 week to 2 weeks. For larger gaps, we cannot detect the phytoplankton boom dynamics or composition.

1.3 Time series characterization

Filling gaps in time series requires firstly to characterize the data. This step is essential, whatever the basis of data, in order to extract useful information from the dataset and makes the dataset easily exploitable. It is particularly interesting to carry out an exploratory of data analysis to choose or propose suitable imputation algorithms.

1.3.1 Composition of time series

Time series analysis means splitting the data into smaller periods in order to easily analyze. The four specific components of time series (including trend, seasonal, cyclical and random change) are presented as follows:

1. *Trend component*: That is the change of variable(s) in terms of monitoring for a long time (denoted m_t). If a trend exists within the time series data (i.e. on the average data), the measurements tend to increase (or decrease) over time. It can be represented by a straight line or a smooth curve of low order (by a graph).
2. *Seasonal component*: This component takes into account intra-interval fluctuations. It means there is a regular and repeated pattern of peaks and valleys within the time series related to a calendar period such as seasons, quarters, months, weekdays, and so on.
3. *Cyclical component*: It is time that a pattern will repeat in the cycle for years. This component represents cyclical change (denoted s_t). In order to evaluate this component, it is necessary to observe values of time series every year.

The difference between this component and the seasonal one is that its cycle lasts more than 1 year.

4. *Random change component*: This component considers random fluctuations around the trend; this could affect the cyclical and seasonal variations of the observed sequence, but it cannot be predicted by previous data in the past of time series. This component (denoted e_t) is not cyclical.

The decomposition of a time series can be carried out according to two models:

The additive model used is:

$$x_t = m_t + s_t + e_t \quad (1.1)$$

The multiplicative model used is:

$$x_t = m_t * s_t * e_t \quad (1.2)$$

Note that the logarithmic transformation of a multiplicative model makes an additive one:

$$\log(m_t * s_t * e_t) = \log(m_t) + \log(s_t) + \log(e_t) \quad (1.3)$$

There are different techniques to decompose time series into components. “Decompose a time series into seasonal, trend and irregular components using moving averages” (R-starts package, [31]) is the most common technique. The function `1.1` determines the trend component using a moving average, and removes it from the time series. Then, the seasonal figure is computed by averaging, for each time unit, over all periods. The seasonal figure is then centered. Finally, the error component is determined by removing trend and seasonal figure (recycled as needed) from the original time series. In this study, we use this technique to analyze all time series data.

Example: Chlorophyll-*a* (Chla) in $\mu\text{g/L}$ - weekly Chlorophyll-*a* time series was measured by Ifremer IGA-Gravelines monitoring [32] from 01/1/1989 to 24/12/2014.

Trend and seasonal analysis are provided in figure 1.2. This figure shows that Chla series has no linear trend and an annual cycle.

1.3.2 Auto-correlation function (ACF)

Besides these four components, when analyzing time series data, we also consider the autocorrelation factor (ACF). This coefficient measures linear dependence between pairs of observations $y(t)$ and $y(t+h)$, $h = 1, 2, \dots$ (h is lagged values, autocorrelation values range from -1 to +1). ACF provides an additional important indication of the properties of time series (i.e. how past and future data points are related). Therefore, it can be used to identify the possible structure of time series data, and to create reliable forecasts and imputations ([27]). High auto-correlation values mean that the future is strongly correlated to the past.

The calculation of the autocorrelation provides an important indication of the properties of a time series such as the determination of frequencies and amplitudes. It is thus possible to find the main periods of a signal from a correlogram. Indeed, when the correlation coefficient tends to 1, we can say that the offset τ corresponds to a period. This coefficient $\rho(\tau)$ is defined via

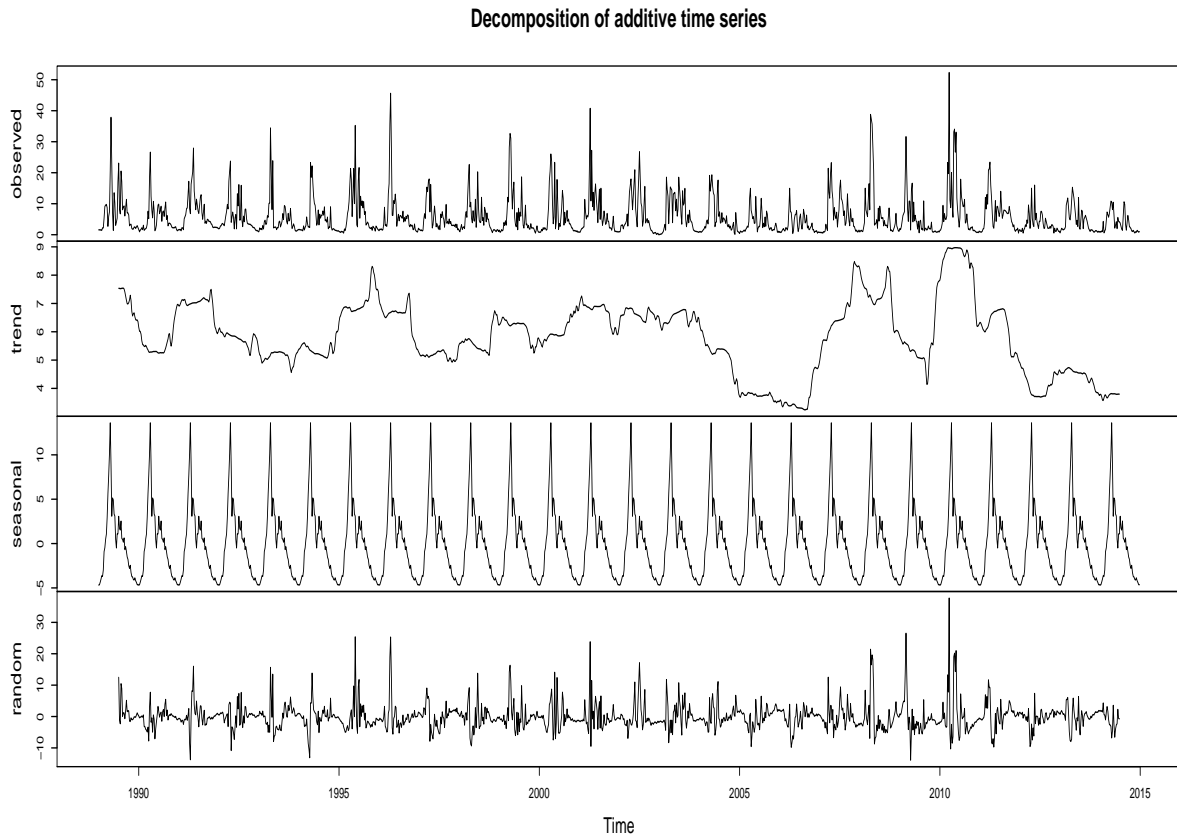


Figure 1.2: Decomposition of weekly data (average) of *Chla* from the Ifremer IGA-Gravelines monitoring station over the period 1989 to 2014 using R-starts package.

the ratio of the functions of the coefficient of auto-covariance $\gamma(\tau)$ [33] as follows:

$$\rho(\tau) = \frac{\gamma(\tau)}{\gamma(0)} \quad (1.4)$$

It should be noted that when the signal is stationary, having a constant variance, the auto-correlation coefficient becomes eq. :

$$\rho(\tau) = \frac{\gamma(\tau)}{\sigma^2} \quad (1.5)$$

When $\rho = -1$ indicates a perfect negative linear relationship, $\rho = 0$ represents no linear relationship, and $\rho = 1$ indicates a perfect positive linear relationship.

Fig. 1.3 shows the auto-correlation of Chlorophyll-*a* series. Values between the blue striped lines of auto-correlation are not statistically significant. Looking at the fig. 1.3, we find that repeating patterns of positive and negative auto-correlations, typical for seasonality: a shift of 52 instants for a correlation coefficient 0.47. This time offset represents 52 weeks (1 year). We

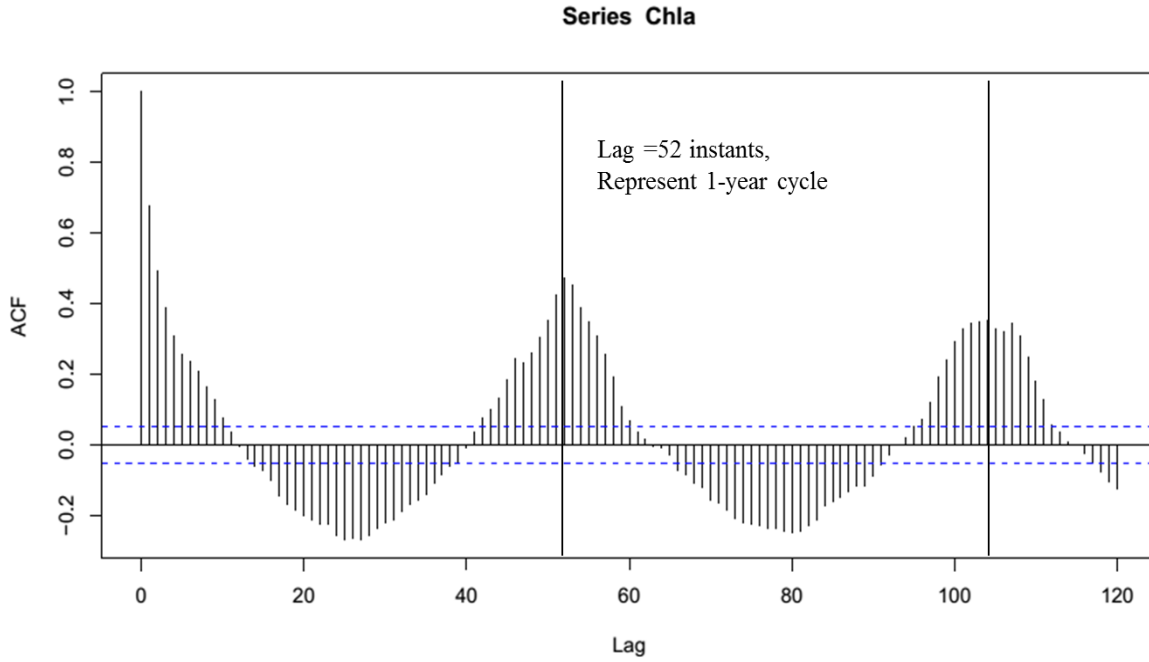


Figure 1.3: ACF of Chla time series

can conclude that the Chlorophyll-*a* signal has a characteristic of 1-year cycle.

1.3.3 Correlation

Correlation (correlation between variables) is a measure of the statistical relationship between two variables. This coefficient can give a suggestion on what convenient methods can be used for the imputation task. This means a dataset presents high correlation between pairs of variables, it might be suitable to use models that exploit information between variables. Here the Pearson product-moment correlation coefficient has been used as a measure. It is calculated by dividing the covariance of two variables by the product of their standard deviation as function 1.11.

1.3.4 Cross-correlation (recurrent data for univariate time series)

Cross correlation (also called lagged correlation) is a common phenomenon of many natural physical systems. It indicates the relationship between two time series: one series may be shifted in time relative to the other one (related to past lags of the other one). This coefficient is particularly important to evaluate the causal relationship between two signals in time, as a function of number of offset observations. We consider N pairs of observations on two time

series x_t and y_t , with h is the lag. Following Chatfield [33], the cross-covariance function is computed as:

$$c_{xy}(h) = \frac{1}{N} \sum_{t=1}^{N-h} (x_t - \bar{x})(y_{t+h} - \bar{y}), h = 0, 1, \dots, N-1 \quad (1.6)$$

or

$$c_{xy}(h) = \frac{1}{N} \sum_{t=1-h}^N (x_t - \bar{x})(y_{t+h} - \bar{y}), h = -1, -2, \dots, -(N-1) \quad (1.7)$$

where \bar{x} and \bar{y} are the means of x_t and y_t respectively.

This cross correlation measure can be calculated by obtaining the covariance between two time series, and normalizing it with respect to the standard deviations of both time series.

$$r_{xy}(h) = \frac{c_{xy}(h)}{\sqrt{c_{xx}(0)c_{yy}(0)}} \quad (1.8)$$

with c_{xx} and c_{yy} are the variances of x_t and y_t .

Two terms of “lead” and “lag” relationships are used to refer to the cross-correlation function as described by equations 1.6 or 1.7. The equation 1.6 means that x_t is shifted h samples back in time relative to y_t . In this case x_t is said to “lead” y_t or y_t is said to “lag” x_t . The equation 1.7 displays the reverse situation.

1.4 Experiments protocol

This part is designed to validate our proposed approaches and to compare with published methods for the imputation task. In this study, we deal with large missing values in two type of data: the first type is univariate time series, while the second one is uncorrelated multivariate time series. In experiments of univariate data, six imputation methods are considered viz., na.interp, na.locf, na.approx, na.aggregate, na.spline and DTWBI. Concerning experiments of multivariate data, we investigate 8 methods including FSMUMI, Amelia, FcM, MI, MICE, missForest, na.approx and DTWUMI. We compare these methods in terms of their efficiency performance, that means the comparison of quantitative and visualization performance. In the following sections, we present the design of the experimental process and the criteria for evaluating methods.

1.4.1 Experimental process for the imputation task

This section introduces detailed descriptions for conducting experiments. The experiments are carried out in order to compare the performance of our proposals with different imputation methods for handling missing values. Indeed, evaluating the ability of imputation methods cannot be done because the actual values are lacking. So we must produce artificial missing data on complete time series to assess the performance of imputation approaches. In this study, T-gap missing type is considered to perform the experiments. Depending on each application, we create simulated gaps with different rates ranging from 1%, 2%, 3%, 4%, 5%, 7.5% and 10% of the complete signal.

Therefore, we use a technique comprising three steps to evaluate the results as follows:

- *The 1st step:* Create artificial missing data by deleting data values from full time series.
- *The 2nd step:* Apply the imputation algorithms previously mentioned to complete missing data. The result of this step thus is time series containing imputed values.
- *The 3rd step:* Assess the performance of proposed methods and compare with published algorithms. In this step, we evaluate the performance of each imputation method by comparing the imputed values with the true values (the original full time series). We use different performance indicators as defined in next section.

1.4.2 Measurements for evaluating imputation methods

In this study, the completion data and observed data are compared to assess the performance of imputation methods. To do this, seven performance indicators are introduced including Similarity (Sim), Normalized Mean Absolute Error (NMAE), Root Mean Squared Error (RMSE), coefficient of determination (R^2), FB (Fractional Bias), FSD (Fraction of Standard Deviation) and FA2. Depending on each application that we use some of these indices. The indicators are computed as follows:

1. Similarity: defines the similar percentage between the imputed values (y) and the respective true values (x). It is calculated by:

$$Sim(y, x) = \frac{1}{T} \sum_{i=1}^T \frac{1}{1 + \frac{|y_i - x_i|}{\max(x) - \min(x)}} \quad (1.9)$$

Where T is the number of missing values. A higher similarity (similarity value $\in [0, 1]$) highlights a better ability method for the task of completing missing values. If signal is a constant ($x = \text{constant}$), we set $\max(x) - \min(x) = 1$.

2. NMAE: The Normalized Mean Absolute Error between the imputed values y and the respective true values time series x is computed as:

$$NMAE(y, x) = \frac{1}{T} \sum_{i=1}^T \frac{|y_i - x_i|}{V_{max} - V_{min}} \quad (1.10)$$

Where V_{max} , V_{min} are the maximum and the minimum values of input time series (time series has missing data) by ignoring the missing values. The NMAE value lies in the range of 0 to ∞ . In case of constant signal, we set $V_{max} - V_{min} = 1$.

A lower NMAE value means better performance method for the imputation task.

3. R^2 score: is calculated as the square of Pearson's coefficient (with p-value) y and x . The coefficient is a measure of the strength of the linear relationship between two variables. In the imputation context, this coefficient measures the degree of association between the imputed values y and the corresponding actual values (x). The R^2 parameter ranges between 0 and 1. Hence, a value closer to 1 indicates a strong predictive ability (imputation values are very close to true values). The correlation coefficient is computed as follows [34]:

$$R = \frac{\sum_{i=1}^T (x_i - \bar{x})(y_i - \bar{y})}{\sqrt{\sum_{i=1}^T (x_i - \bar{x})^2} \sqrt{\sum_{i=1}^T (y_i - \bar{y})^2}} \quad (1.11)$$

4. RMSE: The Root Mean Square Error is a frequently used measure to evaluate the quality of a model (an estimator or a predictor). RMSE is defined as the average squared difference between the imputed values y and the respective true values x . Formally, it is computed as:

$$RMSE(y, x) = \sqrt{\frac{1}{T} \sum_{i=1}^T (y_i - x_i)^2} \quad (1.12)$$

This indicator is very useful for measuring overall precision or accuracy. The range of RMSE lies between 0 to ∞ . A RMSE of zero illustrates that a perfect imputation model but in reality, it cannot be achieved. In general, the most effective method would have the lowest RMSE.

5. FSD (Fraction of Standard Deviation) of y and x is defined as follows:

$$FSD(y, x) = 2 * \frac{|SD(y) - SD(x)|}{SD(y) + SD(x)} \quad (1.13)$$

This fraction indicates whether a method is acceptable or not (here SD stands for Standard Deviation). For the imputation task, if FSD is closer to 0, the imputation values are closer to the real values.

6. FB - Fractional Bias between the imputed values y and the respective true values time series x is defined by eq. 1.14. This parameter determines whether the imputation values are overestimated or underestimated relatively to those observed. A model is considered as perfect when its FB tends to zero, and as acceptable when $-0.3 \leq FB \leq 0.3$

$$FB(y, x) = 2 * \frac{mean(y) - mean(x)}{mean(y) + mean(x)} \quad (1.14)$$

7. FA2: represents the fraction of data points that satisfied smoothing amplitude cover. It is calculated as:

$$FA2(y, x) = \frac{length(0.5 \leq \frac{y}{x} \leq 2)}{length(x)} \quad (1.15)$$

A model is considered perfect when FA2 is equal to 1.

Illustration

We illustrate the computation of these indicators by giving an example. Six different signals are created (including: Query, Reference, Reference2, Reference3, Reference4 and Reference5 (see figure 1.4)) in the following way:

The Query is composed of three periods with three different sine waves.

The Reference is generated from the Query by changing its phase.

Three signals Reference2, Reference3 and Reference4 are just three constant lines.

The final series, Reference5, is yielded by adding small noise to the Query. The noise is generated from a uniform distribution of the same size of the query between 0 and 0.1.

Table 1.1 shows the values of previous criteria between the Query and various references. Zero value means that the two signals are similar.

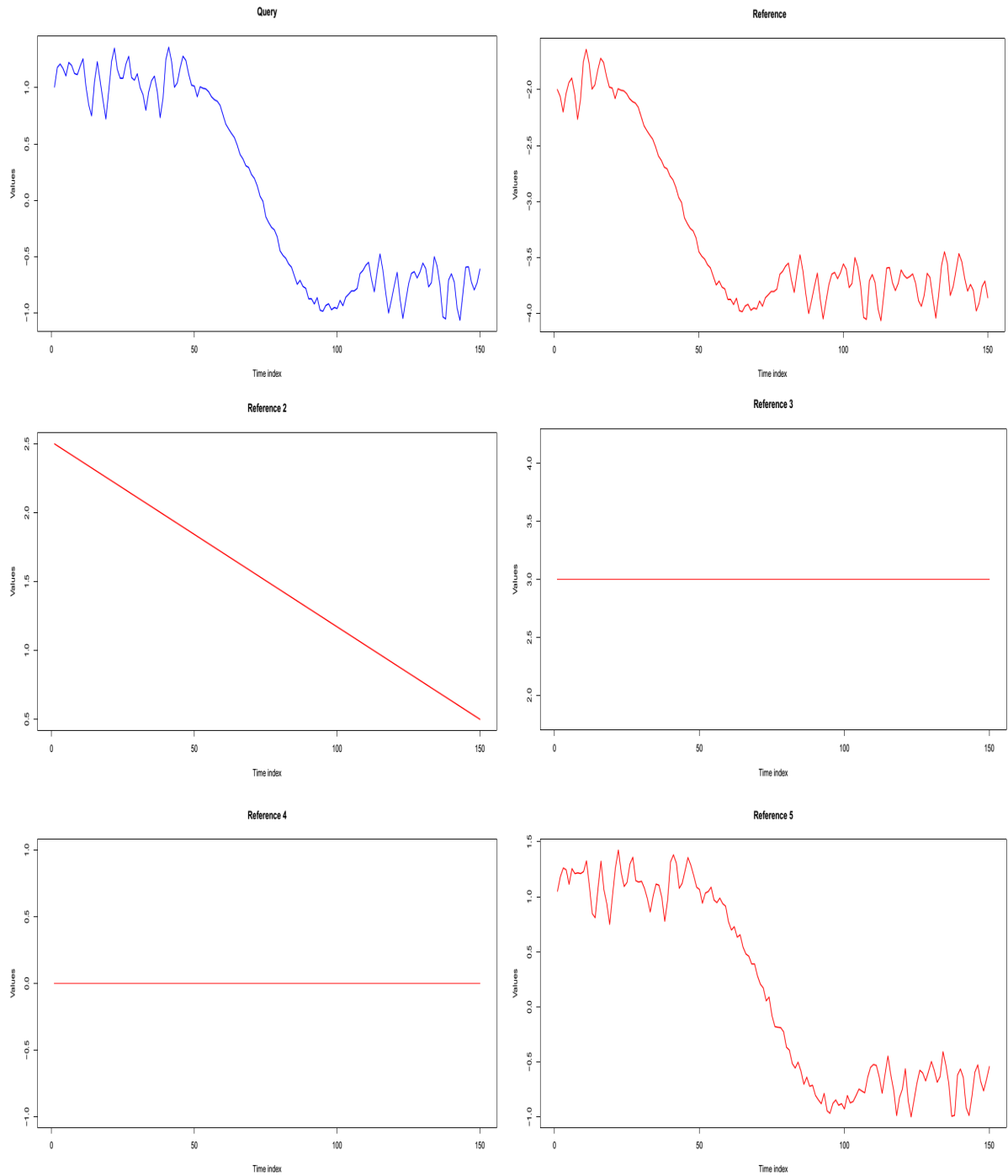


Figure 1.4: Simulated signals

From the results of this table, we obviously find that the Query and Reference5 are very similar. The difference between these two series is "the small noise". Therefore, the similarity, R^2 , FA2 measures are very close to 1. Other indicators viz., RMSE, NMAE, FSD are very small, approaching 0.

In contrast to this case, when we look at results of the first pair (Query and Reference): the lowest similarity, R^2 , FA2, and the highest RMSE, NMAE and FB. This means that the Query and Reference are different.

Values of R^2 for the 3th and 4th cases (Query- Reference3 and Query-Reference4) are NA because the values of SD(Reference3) and SD(Reference4) equal 0.

These indicators are divided into two groups: Group 1 which includes Similarity, R^2 , RMSE, and NMAE, is used to evaluate the accuracy of imputation methods. The remaining indices are used to assess the shape of imputation values generated by imputing methods.

From the above results we can find that these are very useful indicators to evaluate imputation algorithms.

Table 1.1: Values of different indicators between the Query and various references

		1-Sim	$1 - R^2$	RMSE	NMAE	FSD	FB	1-FA2
Query	Reference	0.577	0.466	3.42	1.39	0.16	2.11	1
Query	Reference2	0.36	0.185	1.47	0.58	0.39	1.78	0.78
Query	Reference3	0.533	NA	3.04	1.2	2	1.89	1
Query	Reference4	0.247	NA	0.87	0.34	2	-2	1
Query	Reference5	0.021	0.001	0.06	0.02	0	0.46	0.01

1.5 Chapter conclusion

In this chapter, we first introduce notions of univariate and multivariate time series. Then missing data concept is presented and missing data mechanisms are discussed. The next part of this chapter, we inform the characterization of time series including the decomposition of time series data (trend, seasonality,...), the auto-correlation, the correlation and the recurrent data. Finally, the experiments protocol is mentioned to the validation and evaluation of imputation methods comprising experimental process and performance measurements.

DTW-based imputation approach for univariate time series

Contents

2.1	Introduction	26
2.2	Literature review of Dynamic Time Warping	28
2.2.1	Classical DTW algorithm	28
2.2.2	DDTW - Derivative Dynamic Time Warping	32
2.2.3	AFBTW - Adaptive Feature Based Dynamic Time Warping	33
2.2.4	Dissimilarity-based elastic matching	34
2.2.5	Dynamic Time Warping-D algorithm (DTW-D)	35
2.2.6	Illustration	35
2.3	Dynamic Time Warping-based imputation for univariate time series	41
2.3.1	The proposed method - DTWBI	41
2.3.2	Validation procedure	44
2.3.3	Results and discussion	47
2.3.4	Conclusion	57
2.4	Comparison of various DTW versions for completing missing values in univariate time series	58
2.4.1	Introduction	58
2.4.2	Imputation based on DTW metrics	59
2.4.3	Data presentation	59
2.4.4	Results and discussion	60
2.4.5	Conclusion	64
2.5	Chapter conclusion	66

In this chapter, we present a detailed methodology to impute missing values in univariate time series based on combining the shape-feature extraction and Dynamic Time Warping (DTW) algorithms. Firstly, it is important to understand the meaning and context of the applied approach, so they are introduced in Section 2.1. Next in Section 2.2, we present the main theoretical background of DTW method and several of its variants. Then, in Section 2.3.1 we describe our approach for univariate time series imputation. Sections 2.3.2 and 2.3.3 are to validate the proposed method and to compare with state-of-the-art approaches. The next part 2.4, we perform a comparison of different DTW versions for the imputation of univariate time series.

2.1 Introduction

Time series with missing values occur in almost domains of applied sciences. These missing data may occur for a variety of reasons, for instance during maintenance, failure of measuring instruments, data transmission problem etc. This is particularly the case for marine samples ([1], [2]). Furthermore, most time series analysis algorithms and most statistical softwares are not designed to handle data with missing values. They often require complete data. However, the regularization of time series makes it possible to complete missing values [35]. For low frequency systems with monthly sampling, it is simple to apply a linear or polynomial regression or moving average to fill in the series. Problems arise when completing missing values of high frequency systems with quickly dynamics change.

For example, the MAREL-Carnot dataset, sampling frequency every 20 minutes, missing values are 72 points for one day, 504 points for a week, and 2,200 points for a month. In this case, the size of consecutive missing values (also called gap) is large. Example, the pH signal has 131,472 observations of which 72.78% are available values. It contains 3,392 isolated missing values and many consecutive missing data. The size of these gaps varies from one hour to few months; the largest gap is a 16,843 points corresponding to 234 days (approximately 8 months). Single holes and gaps having $T < \text{tide duration}$ -holes (807 missing points) could be easily replaced by local averages. For the other gaps, the phytoplankton bloom dynamics or composition changes too fast to use linear or spline imputation method.

In addition, collected data always contain noise due to high frequency, thus completion process becomes more complex. Other classical solution consists in ignoring missing data

or listwise deletion. But it is easy to imagine that this drastic solution may lead to serious problems, especially for time series data (the considered values depend on the past values). The first potential consequence of this method is information loss which could lose efficiency ([36]). The second consequence is about the systematic differences between observed and unobserved data that leads to biased and unreliable results ([4]).

Therefore, it is crucial to propose a new technique to estimate missing values. One prospective approach to solve missing data problems is the adoption of imputation techniques ([5]). These techniques should ensure that the obtained results are efficient (having minimal standard errors) and reliable (effective, curve-shape respect).

In the literature, regarding imputation methods, a large number of successful approaches have been proposed for completing missing data. For multivariate time series, efficient imputation algorithms estimate missing values based on the values of other variables (correlations between variables). However, handling missing values within univariate time series data differs from multivariate time series techniques. We must only rely on the available values of this unique variable to estimate the incomplete values of the time series. Moritz *et al.* [27] showed that imputing univariate time series data is a particularly challenging task.

Fewer studies are devoted to the imputation task for univariate time series. Allison [37] and Bishop [38] proposed to simply substitute the mean or the median of available values to each missing value. These simple algorithms provide the same result for all missing values leading to bias result and to undervalue standard error ([39], [40]). Other imputation techniques for univariate time series are linear interpolation, spline interpolation and the nearest neighbor interpolation. These techniques were studied for missing data imputation in air quality datasets ([5]). The results showed that univariate methods are dependent upon the size of the gap: the larger gap, the less effective technique. Walter *et al.* ([41]) carried out a performance comparison of three methods for univariate time series, namely, ARIMA (Autoregressive Integrated Moving Average), SARIMA (Seasonal ARIMA), and linear regression. The linear regression method is more efficient and effective than the other two methods, only when rearranging the data in periods. This study treated non-stationary seasonal time series data but it did not take into account series without seasonality. Chiewchanwattana *et al.* proposed the Varied-Window Similarity Measure (VWSM) algorithm ([42]). This method is better than the spline interpolation, the multiple imputation, and the optimal completion strategy fuzzy c-means algorithms. However, this research only focused on filling one isolated missing value, but did not consider sub-sequence missing. Moritz *et al.* [27] performed an overview about univariate time series

imputation comparing six imputation methods. Nevertheless, this study only considered the MCAR type.

Dynamic Time Warping (DTW) [7] is an effective and well-known method for measuring similarity between two linear/nonlinear time series. The success of DTW in data mining [8], information retrieval and pattern recognition [9, 10, 11] leads us to study its ability to complete missing values in time series. In addition, taking advantage of available values to estimate the missing values makes it possible to reconstruct data with more plausible values. Thus, the aim of this chapter is to propose an algorithm to fill *large gap(s)* in univariate time series based on Dynamic Time Warping ([7]) by exploiting the information of available values. We do not deal with all the missing data over the entire series, but we focus on each large gap where series-shape change could occur over the duration of this large gap.

Further, the distribution of missing values or entire signal could be very difficult to estimate, so it is necessary to make some assumptions. Our approach makes an assumption that the information on missing values exists within the univariate time series and takes into account the time series characteristics.

Here, the main focus of this chapter is to investigate and propose a new algorithm for completing large gap based on DTW method. Therefrom, we first introduce and discuss the main ideas of Dynamic Time Warping approach and then summarize several modifications of DTW.

2.2 Literature review of Dynamic Time Warping

2.2.1 Classical DTW algorithm

In time series analysis, finding out the similarity between two time series is a vital task for numerous applications of time series. However, how do we define the similarity of two sequences (i.e time series)? And how do we find similar sequences quickly in a large databases with different type of data format? Euclidean distance is the most popular measure that allows to determine similarity and to index between two time series. But this distance is a very brittle and it cannot index time series accurately with two different time phases. So we need a method that permits to shift elastically on the time axis, and to contain sequences that are similar, but out of time phase.

Dynamic Time Warping or elastic matching was initially proposed to recognize spoken

words [7], and then it has been widely used in many applied applications like pattern recognition [9, 10], shape retrieval [43, 44], gene expression [45], and so on. Unlike the Euclidean distance, DTW optimally aligns with "warps" the data points of two time series (see figure 2.1 and figure 2.2). It consists in calculating a geometric distance between two curves in order to find their similarity. The method accepts temporal and local deformations, i.e two curves may have different lengths. The algorithm involves finding the optimal match between pairs of points which minimizes an Euclidean distance with certain restrictions. Let us present the DTW algorithm in detail.

2.2.1.1 Time warping

Given two time series x and y of length N and M respectively, where: $x = \{x_1, x_2, \dots, x_N\}$ and $y = \{y_1, y_2, \dots, y_M\}$.

We want to align two time series based on minimized distance on a common time-axis.

Calculating DTW alignment between these two time series includes some steps. The first step is to create a cost matrix ($N \times M$), where each (i^{th}, j^{th}) item is the distance between x_i and y_j . This distance can be measured by *Manhattan* measure, *Euclidean* distance or *squared* distance Then, DTW algorithm builds a matching sequence (warping path) of points $P = (p_1, p_2, \dots, p_k)$ with $p_l = (i_l, j_l) \in [1 : N] \times [1 : M]$ for $l \in [1 : k]$, between the points of signals x and y according to some criteria (see Section Local path criteria and global path criteria).

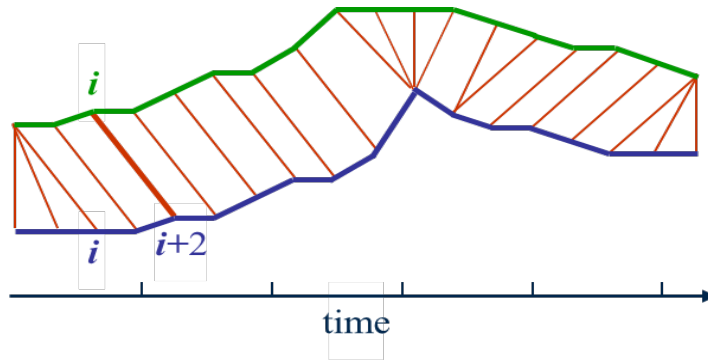


Figure 2.1: Dynamic Time Warping example [46]

The goal is to find a warping path which has the minimal overall distance.

Dynamic programming (DP) algorithm is used to find this warping path. DP is a robust method to deal with a big problem by dividing this problem into a collection of simple sub-problems. Then each sub-problem is individually solved. The final results are combined from

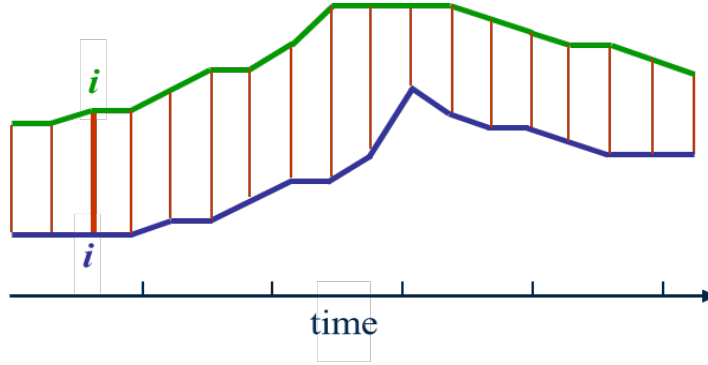


Figure 2.2: Euclidean example. Note that while the two sequences have an overall similar shape, they are not aligned in the time axis. Euclidean distance, which assumes the i^{th} point in one sequence is aligned with the i^{th} point in the other, will produce a pessimistic dissimilarity measure. The nonlinear Dynamic Time Warped alignment allows a more intuitive distance measure to be calculated [46]

all solutions to resolve the given problem. The next time, if the same sub-problem occurs, it will be simple to look up previously computed solution instead of recalculating its result.

DTW uses the dynamic programming equation (2.1) to determine $dist(i, j)$ - the cost matrix. The equation (2.1) can be considered as a symmetric formulation, because both points around the diagonal of the considered point have equal weights.

$$dist(i, j) = d(x_i, y_j) + \min\{dist(i-1, j-1), dist(i-1, j), dist(i, j-1)\} \quad (2.1)$$

The next step, the warping path between time series is found by using the cost matrix which is filled by accumulated distances (defined by eq.2.1). Figure 2.3 shows the DTW process to find the warping path between x and y time series. Back-tracking the cost matrix, the warping path can be retrieved by applying a greedy method. Searching the warping path begins from $dist(N, M)$ and backtracks to the bottom left, with the assessment of all the adjacent cells from left, down, diagonally. If one of these adjacent cells has the smallest value, it will be added to the starting point of the warping path until $dist(1, 1)$ is reached.

Many warping paths can be generated from the equation (2.1), so in order to find the optimal warping path from these achievable warping paths, some criteria (constraints) must be satisfied. These constraints make it possible to reduce the search space for warping paths and to increase the ability of the DTW algorithm. There are two types of constraints: the first one is local criteria and the other one is global constraints. Local constraints perform slopes of the warping path (local path) so this allows to calculate the accurate path. Global constraints make less the search space for warping paths, and enhance the efficiency of DTW algorithm. These global

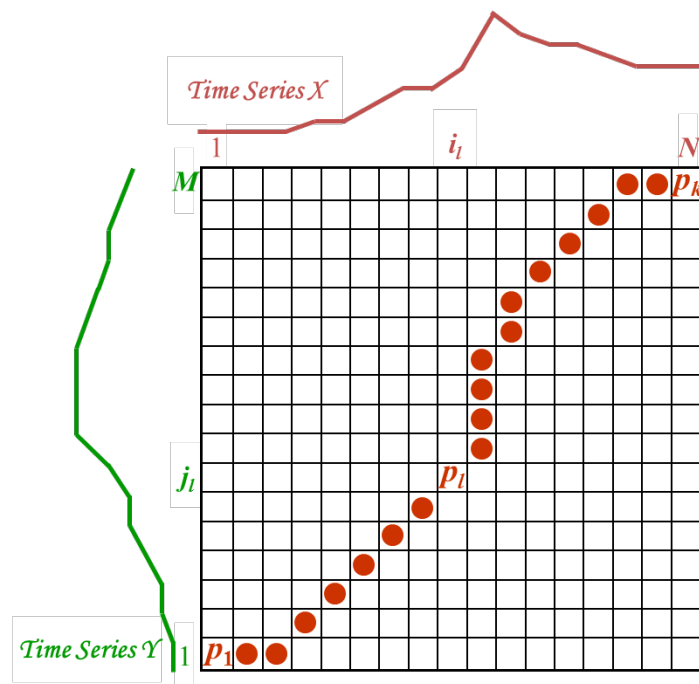


Figure 2.3: DTW cost matrix with an illustration of matching path (red circle) [46]

and local criteria are described in the following:

- **Local path criteria:**

1. Boundary condition: $p_1 = (1, 1)$ and $p_k = (N, M)$. The starting and ending points of the warping path must be the first and the last points of aligned sequences.
2. Monotonicity condition: $i_1 \leq i_2 \leq \dots \leq i_k$ and $j_1 \leq j_2 \leq \dots \leq j_k$. This condition preserves the time-ordering of points.
3. Step size condition (continuity): $i_l - i_{l-1} \leq 1$ and $j_l - j_{l-1} \leq 1$. This criteria limits the warping path from long jumps (shifts in time) while aligning sequences (all points are matched).

Although warping path satisfies local constraints but it demands computing time. A question arises, *how to speed up the calculation of DTW?* A solution is to use global path criteria.

- **Global path criteria:**

Warping path satisfies the global path constraints is a path should be close to the diagonal. This means that it restricts warping path how far it is from the diagonal (also called a warping window) in the cost matrix. This permits to improve the computing time of

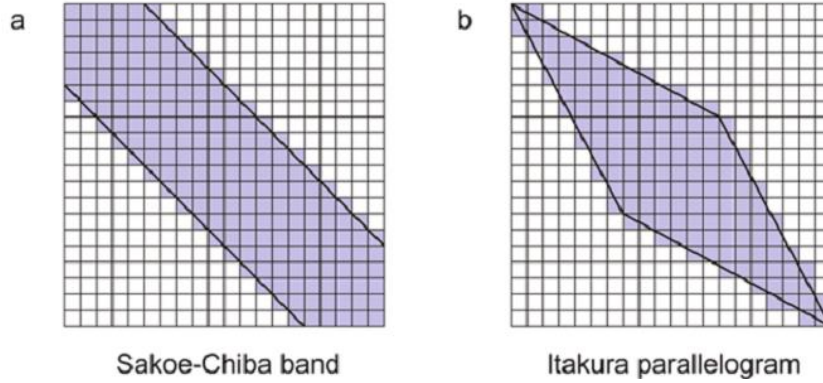


Figure 2.4: Examples of global constraints: (a) Sakoe-Chiba band; (b) Itakura parallelogram.

DTW algorithm from $O(N \times M)$ to $O(N \times r)$ where r is the size of warping window and to avoid a small segment of one series maps onto a relatively large segment of another series.

In the literature, many studies investigated to speed up the process of finding the warping path. Sakoe-Chiba band [7] and Itakura parallelogram [47] are two criteria widely used. Sakoe-Chiba is one of the simplest and most commonly used window, using equation (2.2) to decrease the calculation of cells in the cost matrix (figure 2.4a)

$$|i_l - j_l| \leq r \quad (2.2)$$

Itakura parallelogram [47] is one of the most popular global constraints but it is not as simple as Sakoe-Chiba window. Figure 2.4b presents the Itakura parallelogram. The warping path must be satisfied global constraints (i.e. it is in the lozenge).

DTW algorithm has been applied in numerous domains and has a wide range of applications. To make it more applicable, many improvements of classical DTW have been proposed, which produced diverse variants of DTW method. In the following sections, we will discuss several modifications of this algorithm.

2.2.2 DDTW - Derivative Dynamic Time Warping

DDTW [48] is the modification of classical DTW to improve the DTW limitations. DTW tries to explain variability in the y-axis by warping the x-axis (a single point on one time series maps onto a large subsection of another time series - called this undesirable behavior "singularities"). It fails to find obvious, natural alignments in two sequences simply because a feature

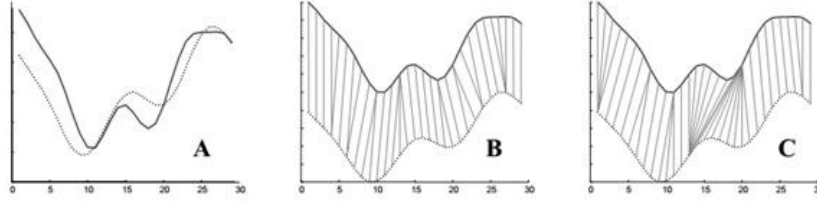


Figure 2.5: A) Two synthetic signals (with the same mean and variance). B) The natural "feature to feature" alignment. C) The alignment produced by dynamic time warping. Note that DTW failed to align the two central peaks because they are slightly separated in the Y-axis [48]

(i.e peak, valley, inflection point, plateau etc.) in one sequence is slightly higher or lower than its corresponding feature in the other sequence. Figure 2.5 illustrates this problem.

The modification is made on distance measure. In fact, DDTW estimates local derivatives of the data to find the correct warping. Keogh and Pazzani proposed to use square of distances of estimated derivatives instead of using Euclidean distance. With a given sequence $x = \{x_1, x_2, \dots, x_N\}$, its derivative can be calculated by following equation:

$$Dx = \frac{(x_i - x_{i-1}) + \frac{x_{i+1} - x_{i-1}}{2}}{2}, 1 < i < N \quad (2.3)$$

DDTW's time complexity is $O(M \times N)$, which is the same as DTW. It is simple to calculate and it does not need to remove offset translation.

2.2.3 AFBTW - Adaptive Feature Based Dynamic Time Warping

Although DDTW has taken into account local shape of time series (derivation) but it does not take care of global shape of the time series. Hence, both DTW and derivative DTW may fail to align a pair of sequences on their common trends or patterns. To avoid this, Xie *et al.* [49] proposed a new modification of DTW named Adaptive Feature Based Dynamic Time Warping. For each point in a sequence $x = \{x_1, x_2, \dots, x_N\}$, a global feature and a local feature are calculated as follows:

- $f_{local}(x_i)$, the local feature of the data point x_i , is defined as a vector of two components:

$$f_{local}(x_i) = (x_i - x_{i-1}, x_i - x_{i+1}) = ((f_{local}(x_i))_1, (f_{local}(x_i))_2) \quad (2.4)$$

- Global feature of a data point x_i :

$$f_{global}(x_i) = (x_i - \sum_{k=1}^{i-1} \frac{x_k}{i-1}, x_i - \sum_{k=i+1}^N \frac{x_k}{N-i}) = ((f_{global}(x_i))_1, (f_{global}(x_i))_2) \quad (2.5)$$

In this method, instead of using Euclidean distance between x_i and y_j , the authors proposed to use a distance calculating as follows:

$$dist(x_i, y_j) = w_1 dist_{local}(x_i, y_j) + w_2 dist_{global}(x_i, y_j) \quad (2.6)$$

where $dist(x_i, y_j)$ is the overall distance between x_i and y_j . w_1 and w_2 weights are used to adjust the percentage influence of local and global criteria, and $w_1 + w_2 = 1, 0 \leq w_1 \leq 1, 0 \leq w_2 \leq 1$. $dist_{local}(x_i, y_j)$ and $dist_{global}(x_i, y_j)$ are distances between x_i and y_j based on their local features and global features, and they are computed in the following:

$$dist_{local}(x_i, y_j) = |(f_{local}(x_i))_1 - (f_{local}(y_j))_1| + |(f_{local}(x_i))_2 - (f_{local}(y_j))_2| \quad (2.7)$$

$$dist_{global}(x_i, y_j) = |(f_{global}(x_i))_1 - (f_{global}(y_j))_1| + |(f_{global}(x_i))_2 - (f_{global}(y_j))_2| \quad (2.8)$$

2.2.4 Dissimilarity-based elastic matching

In the previous studies, the cost function provided by DTW, DDTW and AFBDTW is a relative measure, which cannot be easily interpreted by itself. It is a mean distance, which depends on the intensities of both signals. In order to make the response similar to the one of a human expert, Caillault *et al.* [50] proposed a bounded measure of dissimilarity, between 0 and 1, that adapts the DTW matching cost. The authors defined a dissimilarity s , replacing the Euclidean distance d , as a ratio of distances:

$$s(x_{i_l}, y_{j_l}) = \frac{d(x_{i_l}, y_{j_l})}{\max\{d(x_{i_l}, 0), d(y_{j_l}, 0)\}} \quad (2.9)$$

where $x = \{x_1, x_2, \dots, x_N\}$, $y = \{y_1, y_2, \dots, y_M\}$ and $P = \{(i_l, j_l), l = 1 \dots k, i_l = 1 \dots N, j_l = 1 \dots M\}$ is a matching path between the points of x and y signals.

In this work, an extended approach is also proposed allowing to calculate DTW distance on

multidimensional signals (see [50] for more detail).

2.2.5 Dynamic Time Warping-D algorithm (DTW-D)

Chen *et al.* [51] proposed an other version of DTW devoted to applications of time series semi-supervised learning. The authors exploited the difference/delta between DTW and Euclidean Distance (ED) for the time series classification task. They showed that DTW-D provides better discrimination than DTW through experiments. Given two time series x and y , DTW-D distance is defined as follows:

$$DTW - D(x, y) = DTW(x, y) / (ED(x, y) + \epsilon) \quad (2.10)$$

where ϵ is a very small positive number that is used to avoid divide-by-zero error.

2.2.6 Illustration

In order to better understand these DTW algorithms, we have conducted a number of experiments to compare DTW, DDTW and AFBDTW. To examine the performance of different DTW versions for detecting the correct warping between two sequences we reuse the same signals in Chapter 1. Here, we focus on 3 following cases (the remaining cases, see in the appendix B):

The first case: We build the Query, and the Reference is produced by shifting the Query. This means we know the correct warping.

The second case: We use the Query and create a line of 0 (we called the Reference4)

The third case: We take the Query and the Reference5 is yielded by making a copy of the Query and then adding small noise.

We can then use these pairs of signals as input of the three algorithms and compare warping paths.

Figure 2.6, 2.7 and 2.8 illustrate i) the matching paths producing by different versions of DTW, ii) signals after the deformation of three pairs: (Query vs Reference), (Query vs Reference4) and (Query with Reference5).

For the first case (Query vs Reference, figure 2.6), visually, matching path generated from DTW is the least effective of the three. The other DDTW and AFBDTW methods have a good warping path and a shape detection. However, for the second case (Query vs Reference4, figure 2.7), the warping path of DTW is less distorted as comparing with the one of DDTW

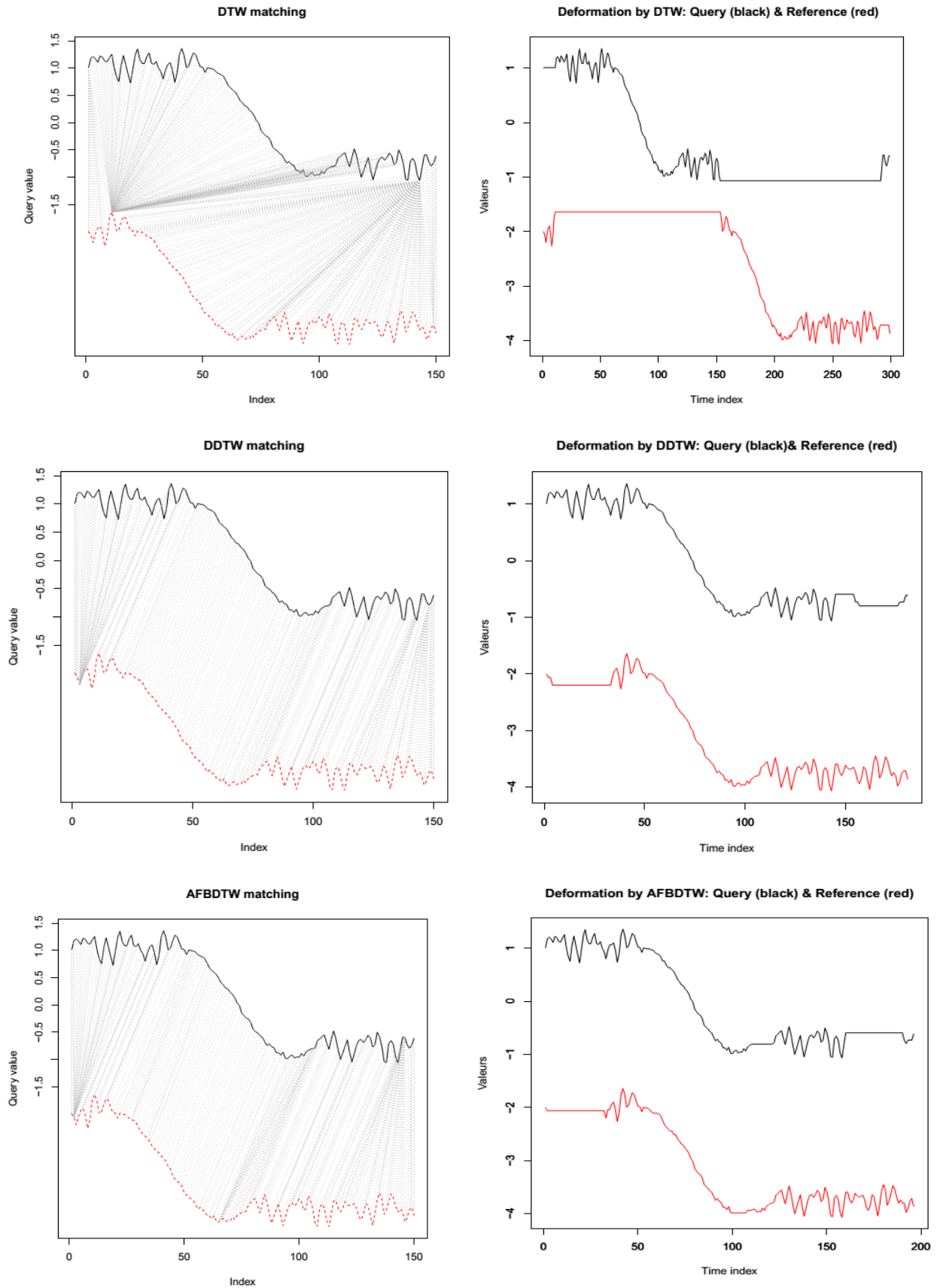


Figure 2.6: Query vs Reference

CHAPTER 2. DTW-BASED IMPUTATION APPROACH FOR UNIVARIATE TIME SERIES

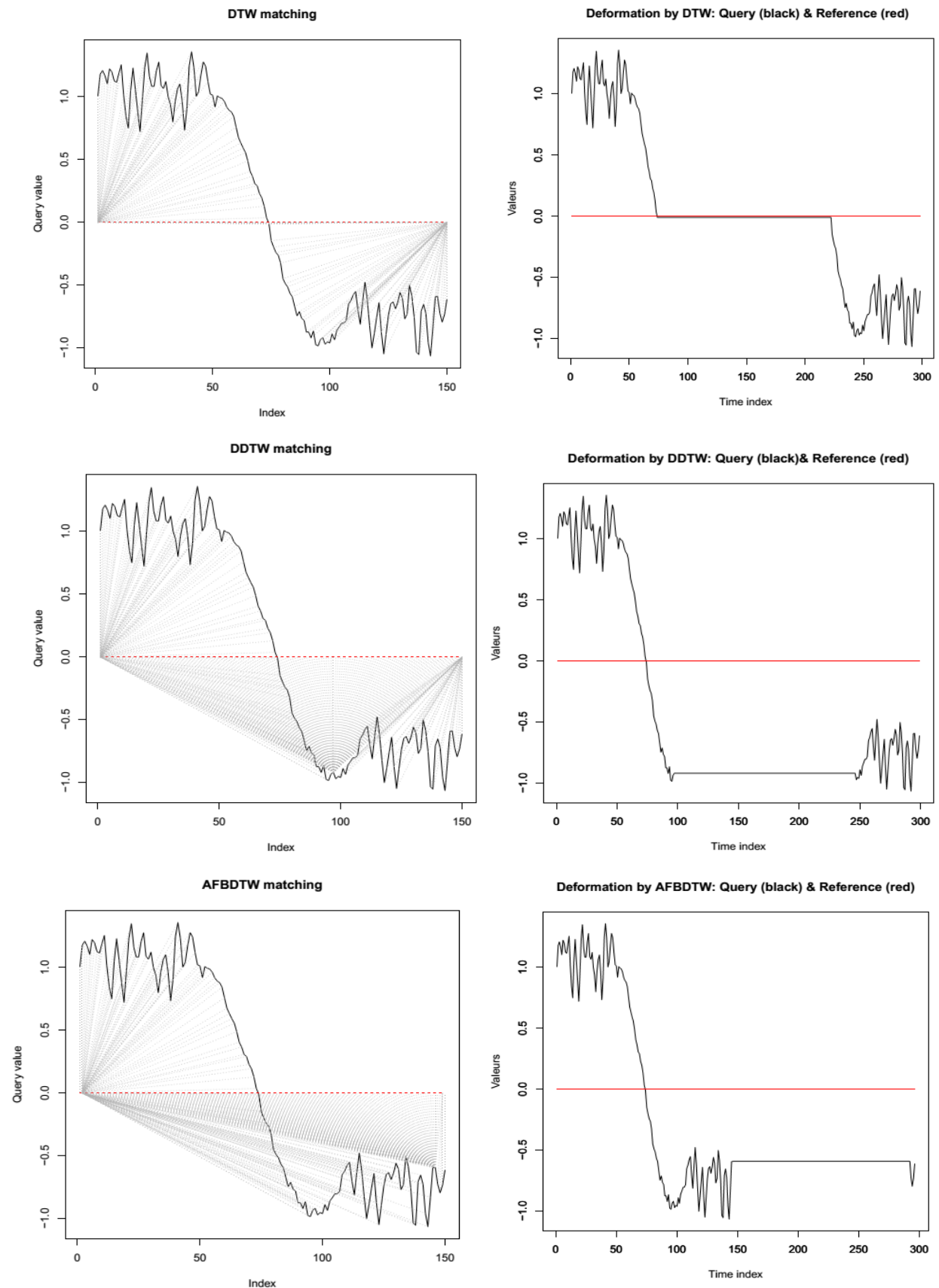


Figure 2.7: Query vs Reference4

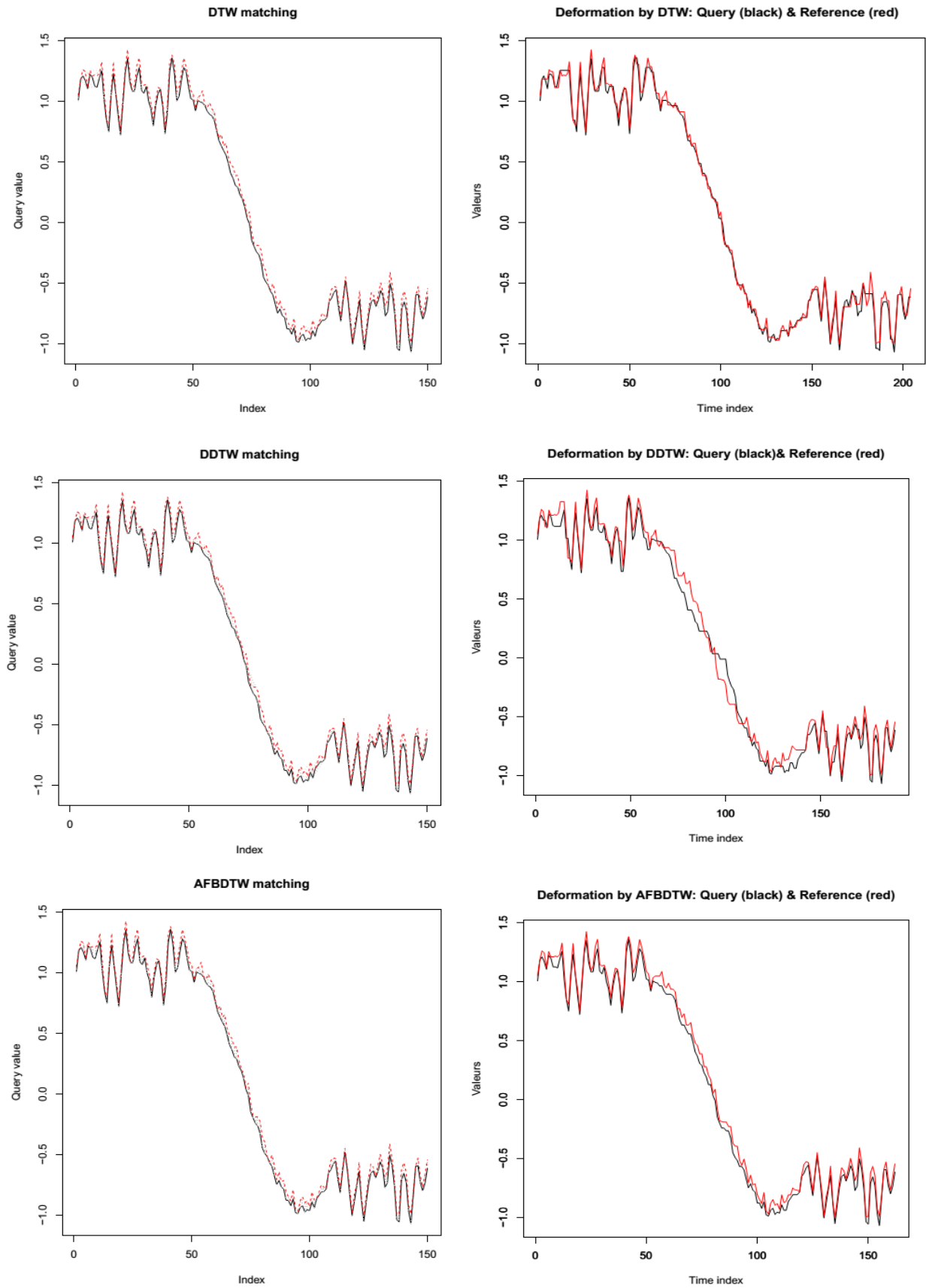


Figure 2.8: Query vs Reference5

and AFBDTW. For the last case (Query with Reference5, figure 2.8), because the difference between Query and Reference5 is very small. So we see the warping paths of all three methods are very good. But when looking at deformation signals, it strongly shows that DTW has more accurate matching than the two remaining cases.

In addition, we calculate the final matching cost of these methods between each pair of signals. These costs also show us the similarity between each pair. The objective of DTW methods is to find the warping path with minimal distance, thus when comparing the final matching cost of different pairs produced by various DTW variants: a pair has smaller distance means that this pair is more similar.

Table 2.1 presents costs of each pair calculated by different DTW methods.

- DTW: the smallest value is the 5th pair (Query and Reference5), the second one is the 4th pair (Query and Reference4), followed by the 2nd pair and the 1st pair, and finally is the 3rd pair.
- DDTW: the smallest distance is the 5th pair (Query and Reference5), the second one is the 1st pair (Query and Reference), followed by the 2nd and the 4th pair, and finally is the 3rd pair.
- AFBDTW: the smallest cost is the 5th pair (Query and Reference5), the second one is the 1st pair, then following by the 2nd pair, and lastly is the 3rd and 4th pairs.

Table 2.1: The matching cost of different methods

	DTW	DDTW	AFBDTW	ED	DTW-D
Query - Reference	2.09	0.04	200.28	41.90	0.05
Query - Reference2	0.56	0.05	200.61	18.05	0.03
Query - Reference3	2.27	0.06	201.25	37.21	0.06
Query - Reference4	0.42	0.05	201.25	10.68	0.04
Query - Reference5	0.03	0.02	200.11	0.72	0.05

From this table and from the figure 2.8, it obviously demonstrates that the 5th pair is the most similar. For the first pair, the Reference is created out of phase of the Query, and when looking at the figure 2.6, we see that DDTW gives the best warping path (this result is also shown in the table 2.1), following by AFBDTW and finally DTW with the most deformation. In contrast, for the 4th pair, DTW yields the best matching path with at least warping.

Table 2.2: Different indicators for evaluating the similarity between each pair of signals

Time series		1-Sim	1-R2	RMSE	NMAE	FSD	FB	1-FA2
Query	Reference	0.58	0.47	3.42	1.39	0.16	2.11	1
Deformation by DTW: Query	Reference	0.44	0.64	2.25	0.86	0.11	1.43	0.86
Deformation by DDTW: Query	Reference	0.56	0.02	3.05	1.26	0.08	1.93	1
Deformation by AFBDTW: Query	Reference	0.56	0.02	3.06	1.26	0.01	-1.94	1
Query	Reference2	0.36	0.19	1.47	0.58	0.39	1.78	0.78
Deformation by DTW: Query	Reference2	0.17	0.44	0.79	0.24	0.29	0.67	0.32
Deformation by DDTW: Query	Reference2	0.44	0.6	2.1	0.82	0.03	3.28	0.98
Deformation by AFBDTW: Query	Reference2	0.41	0.05	1.39	0.57	0.08	-1.71	0.96
Query	Reference3	0.53	NA	3.04	1.2	2	1.89	1
Deformation by DTW: Query	Reference3	0.47	NA	2.45	0.94	2	1.23	1
Deformation by DDTW: Query	Reference3	0.57	NA	3.5	1.41	2	2.63	1
Deformation by AFBDTW: Query	Reference3	1	NA	3.32	1.34	2	-2.36	1
Query	Reference4	0.25	NA	0.87	0.34	2	-2	1
Deformation by DTW: Query	Reference4	0.13	NA	0.62	0.17	2	-2	1
Deformation by DDTW: Query	Reference4	0.26	NA	0.9	0.36	2	-2	1
Deformation by AFBDTW: Query	Reference4	1	NA	0.75	0.29	2	2	1
Query	Reference5	0.02	0	0.06	0.02	0	0.46	0.01
Deformation by DTW: Query	Reference5	0.01	0	0.05	0.01	0	0.15	0.01
Deformation by DDTW: Query	Reference5	0.03	0.01	0.09	0.03	0.01	0.37	0.05
Deformation by AFBDTW: Query	Reference5	0.02	0	0.06	0.02	0	-0.45	0.01

In Chapter 1, we have introduced indicators to evaluate the similarity between two signals. To better assess the ability of finding the similarity of different DTW versions, we compute these indicators between Query and various References (table 2.2). Again, we see more clearly that the largest similarity and FA2, the smallest RMSE, NMAE and FB for all deformation signals are yielded by DTW. However, when considering FSD index, AFBDTW gives the smallest value (except for the second pair and the case of linear signals due to the same values of SD), which means that the AFBDTW's matching ability is better.

When we look at the R^2 index, we find that this indicator does not allow detecting the out of phase (the 1st pair, $R^2 \approx 1$) nor adding the noise (the 5th pair). The Sim indicator is insensitive to noise (Sim ≈ 1 for Query-Reference5) but it does not enable to discover the out of phase (Query-Reference). NMAE/RMSE cannot distinguish the shape of signals (their values $\in [0, 3]$) for all pairs. So depending on each application we use both these two indices or we use either NMAE (univariate time series) or RMSE. All FB values of the 5th pair are close to the acceptable threshold ($-0.3 < FB < 0.3$). It clearly indicates that it is a good indicator of shape. FA2 is strict criterion on the different possible amplitude between 2 signals and thus also

makes it possible to assess well the similarity of shape ($FA2 \approx 0.99$ for all cases of Reference5).

We can conclude that depending on the structure of each pair of signals, different versions of DTW will produce the matching path with different deformation level.

2.3 Dynamic Time Warping-based imputation for univariate time series

2.3.1 The proposed method - DTWBI

In this part, we present a new method for imputing missing values of univariate time series data based on the combination of shape-feature extraction and DTW algorithms.

Given an incomplete time series x , with T - gap at position t ($x_i = NA, i = t : t + T - 1$). Here, we consider a large gap when $T \geq 6\%N$ for small time series ($N < 10,000$) or when T is larger than the known-process change.

The general architecture of our proposal DTWBI (Dynamic Time Warping-Based Imputation) is shown in Figure 2.9. It involves 4 steps: 1- Building query, 2- Comparing sliding window, 3- Selecting window, 4-Filling gap.

The proposed approach consists in finding the most similar sub-sequence (Qs) to a query (Q) (Step 2-Comparing sliding window and step 3- Selecting window), with Q is the sub-sequence before a gap of T size at position t ($Q = x[t - T : t - 1]$) (Step 1-Building query), and completes this gap by Qfs - the following sub-sequence of the Qs (Step 4-Filling the gap).

In this work, we always create the query with the same size of the considered gap in order to look for the similar window having the same dynamics. Furthermore, the algorithm is expandable by choosing a window after the gap. Here we build a query before the gap if its position is in the second half of the signal otherwise after the gap. This ensures that there is always enough data to search similar window.

To find the Qs similar sub-sequence, we use the principles of Dynamic Time Warping - DTW ([7]), especially transformed from original data to Derivative Dynamic Time Warping - DDTW data ([48]). The DDTW data are used because we can obtain information about the shape of sequence ([48]). The dynamics and the shape of data before a gap are a key-point of our method. The elastic matching is used to find a similar window to the Q query of T size in the search database. Once the most similar window is identified, the following window will be copied to the location of missing values. Fig. 2.10 describes the different steps of our approach.

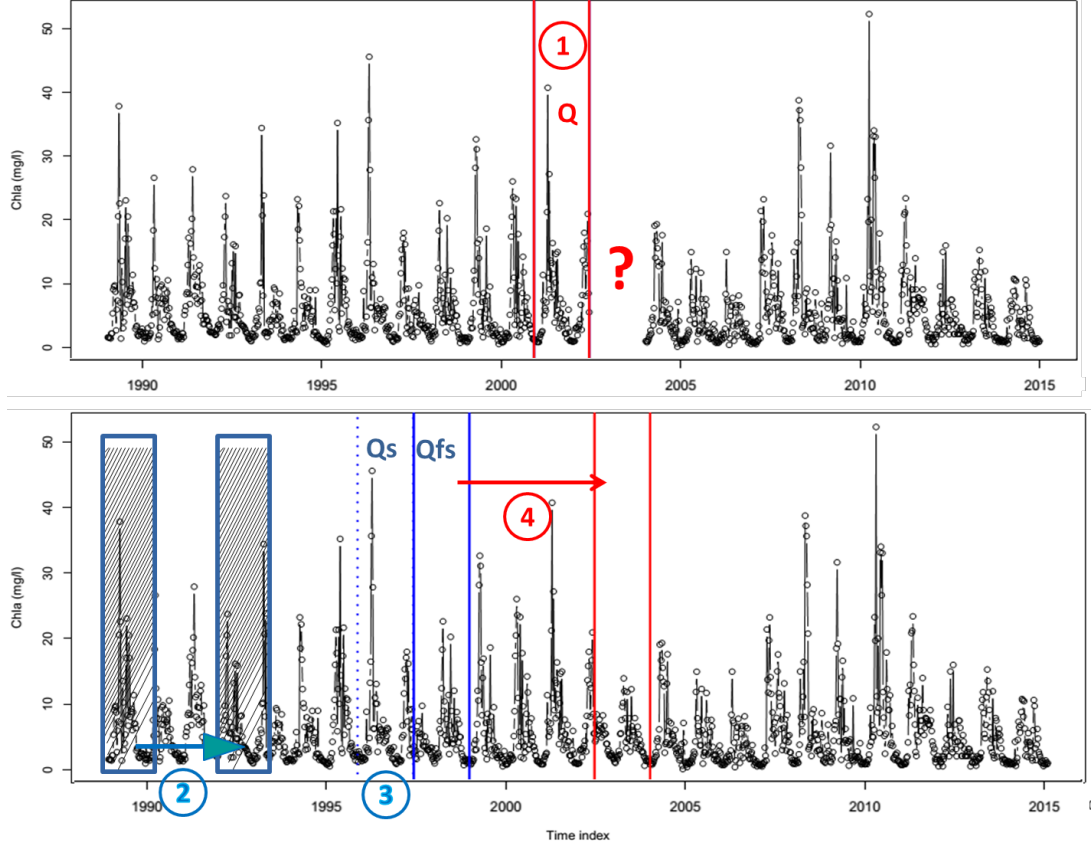


Figure 2.9: General architecture of DTWBI: 1- Building query, 2- Comparing sliding window, 3- Selecting window, 4- Filling gap

In the proposed method, the shape-feature extraction algorithm ([52]) is applied before using DTW algorithm (cf. Fig. 2.10) in order to reduce the computation time. In general, time complexity of DTW requires $O(N^2)$, so this is a very useful step to decrease computation time of the proposed method. A reference window is selected to calculate DTW cost only if the correlation between the shape-features (also called the global features) of this window and the ones of the query is very high. In addition, we apply the shape-feature extraction algorithm because it better presents the shape and dynamics of series through 9 elements, such as moments (the 1st moment, the 2nd moment, the 3rd moment), number of peaks, entropy, etc (see [52] for more detail). This is an important objective of the proposed method (i.e. we take into account the global shape of sequences before considering the local shape DTW). In Algorithm 1, we just mention the finding of similar windows before the gap. In case of finding similar windows after the gap, the method just needs to shift the corresponding index.

The detail of DTWBI (namely DTW-Based Imputation) algorithm is introduced in Algorithm 1. For each gap, DTWBI will be divided into 2 major stages.

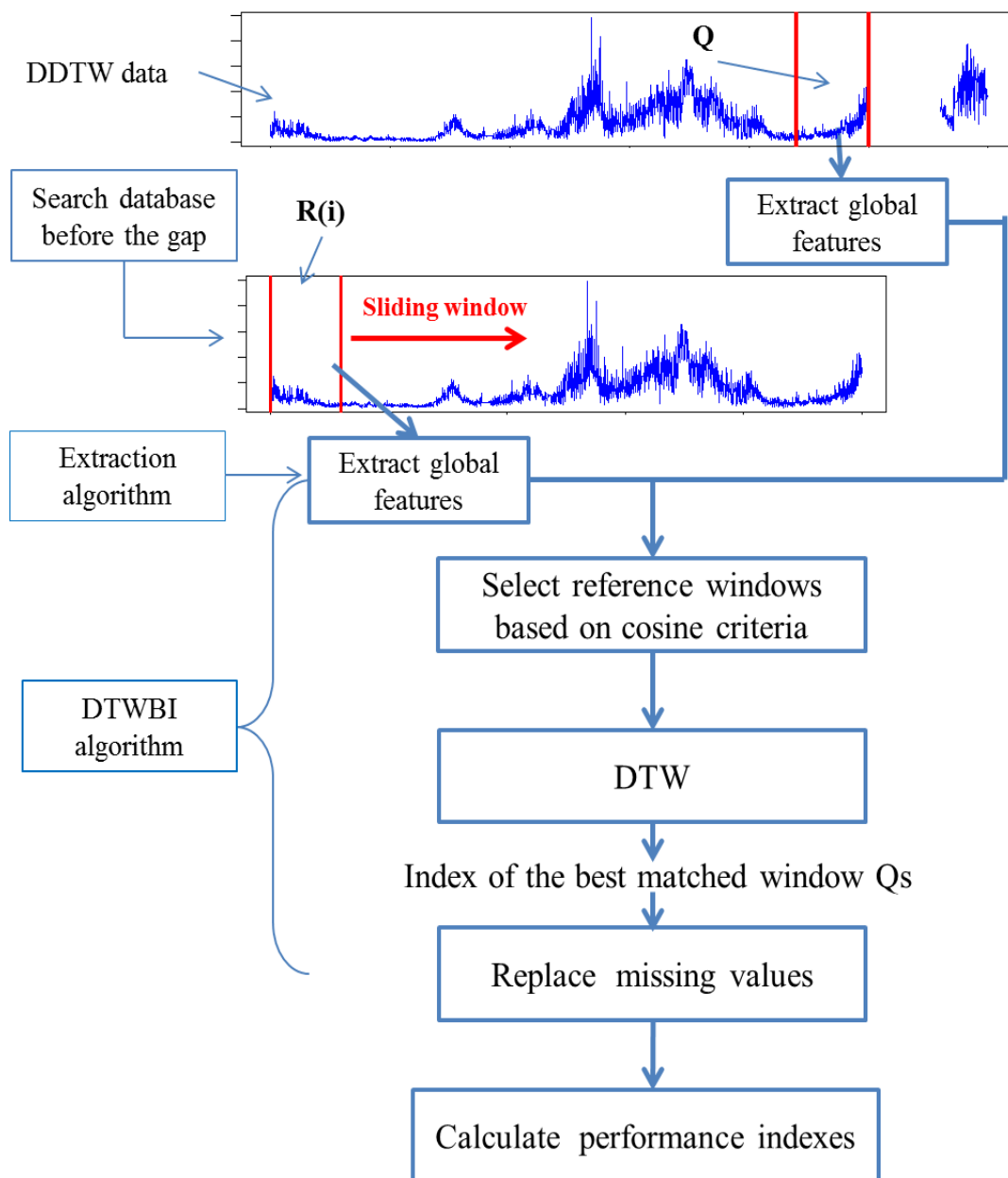


Figure 2.10: Detail diagram of DTWBI method for univariate time series imputation

The first stage is to find a global threshold to determine two sub-sequences being similar (**Step 4:** in Algorithm 1). This threshold is calculated as follows: after creating the query Q , for each $step_threshold$, if the global shape between a reference window R_i and the query Q is similar (this means that the cosine value between global features of the two windows is greater than θ_cos), we will calculate DTW-cost between R_i and Q . The DTW-threshold is estimated as the minimum distance obtained from all sequences R_i analyzed with Q .

The second stage is to retrieve the most similar window to the query. Similarly to the first stage, with each $step_sim_win$, we only compute DTW cost between a sliding reference R_i and the query Q as the correlation condition is satisfied. We then compare this DTW cost to the $threshold$ to determine if this R_i reference is similar to the query Q . R_i reference and Q query are considered similar if their DTW cost is less than the $threshold$. We thereafter select the most similar window Qs with the minimum DTW cost of all the similar windows (**Step 5:** in Algorithm 1). Lastly, the gap is completed by the Qfs vector after the Qs .

2.3.2 Validation procedure

This part is designed to validate our proposal and compare with state-of-the-art methods of data imputation (namely, na.interp, na.locf, na.approx, na.aggregate, na.spline). We assess these methods in terms of their efficacy of accuracy and shape between actual data with completion data using criteria for evaluation as defined in Chapter 1. In the following, we present the datasets, univariate time series imputation methods, and experimental results.

2.3.2.1 Data presentation

In this study, we analyze 8 datasets in order to evaluate the performance of the proposed technique. Four datasets come from TSA package ([53]). These datasets are chosen because they are usually used in the literature, including Airpassenger, Beersales, Google, and SP. Besides, we also choose other datasets from various domains in different places:

1. Airpassenger - Monthly total international airline passengers from 01/1960 to 12/1971.
2. Beersales - Monthly beer sales in millions of barrels, from 01/1975 to 12/1990.
3. Google - Daily returns of the google stock from 08/20/04 to 09/13/06.
4. SP - Quarterly S&P Composite Index, 1936Q1 - 1977Q4.

Algorithm 1 DTWBI algorithm

Input: $x = \{x_1, x_2, \dots, x_N\}$: incomplete time series

t : index of a gap (position of the first missing value of the gap)

T : size of the gap

θ_{cos} : cosine threshold (≤ 1)

$step_threshold$: increment for finding a threshold

$step_sim_win$: increment for finding a similar window

Output: y - completed (imputed) time series

- 1: **Step 1:** Transform x to DDTW data $Dx = DDTW(x)$
 - 2: **Step 2:** Construct a Q query - temporal window before the missing data $Q = Dx[t - T : t - 1]$
 - 3: **Step 3:** Build a search database before the gap: $SDB = Dx[1 : t - 2T]$ and deleting all lines containing missing parameter $SDB = SDB \setminus \{dx_j, dx_j = NA\}$
 - 4: **Step 4:** Find the threshold
 - 5: $i \leftarrow 1$; $DTW_costs \leftarrow NULL$
 - 6: **while** $i \leq \text{length}(SDB)$ **do**
 - 7: $k \leftarrow i + T - 1$
 - 8: Create a reference window: $R(i) = SDB[i : k]$
 - 9: Calculate global feature of Q and $R(i)$: gfQ, gfR
 - 10: Compute cosine coefficient: $cos = \text{cosine}(gfQ, gfR)$
 - 11: **if** $cos \geq \theta_{cos}$ **then**
 - 12: Calculate DTW cost: $cost = DTW_cost(Q, R(i))$
 - 13: Save the cost to DTW_costs
 - 14: **end if**
 - 15: $i \leftarrow i + step_threshold$
 - 16: **end while**
 - 17: $threshold = \min\{DTW_costs\}$
 - 18: **Step 5:** Find similar windows on the SDB
 - 19: $i \leftarrow 1$; $Lop \leftarrow NULL$
 - 20: **while** $i < \text{length}(SDB)$ **do**
 - 21: $k \leftarrow i + T - 1$
 - 22: Create a reference window: $R(i) = SDB[i : k]$
 - 23: Calculate global feature of Q and $R(i)$: gfQ, gfR
 - 24: Compute cosine coefficient: $cos = \text{cosine}(gfQ, gfR)$
 - 25: **if** $cos \geq \theta_{cos}$ **then**
 - 26: Calculate DTW cost: $cost = DTW_cost(Q, R(i))$
 - 27: **if** $cost < threshold$ **then**
 - 28: Save position of $R(i)$ to Lop
 - 29: **end if**
 - 30: **end if**
 - 31: $i \leftarrow i + step_sim_win$
 - 32: **end while**
 - 33: **Step 6:** Replace the missing values at the position t by vector after the Q s window having the minimum DTW cost in the Lop list.
 - 34: **return** y - with imputed series
-

5. CO2 concentrations - This dataset contains monthly mean CO2 concentrations at the Mauna Loa Observatory from 1974 to 1987 ([54]).
6. Mackey-Glass chaotic - The data is generated from the Mackey-Glass equation which is the nonlinear time delay differential ([55]).
7. Phu Lien temperature - This dataset is composed of monthly mean air temperature at the Phu Lien meteorological station in Vietnam from 1/1961 to 12/2014.
8. Water level - The MAREL Carnot data in France are acquired from 2005 up today. For our study, we focus on the water level, sampling frequency of 20 minutes from 01/1/2005 to 31/12/2009 ([3]).

As introduced in Chapter 1, characterizing data is an important step that allows to choose an appropriate algorithm as well as to easily interpret results. In order to obtain useful information from the dataset and makes the dataset easily exploitable, we analyzed these series. Table 2.3 summarizes characteristics of the datasets.

Table 2.3: Data characteristics

N0	dataset name	N0 of instants	Trend (Y/N)	Seasonal (Y/N)	Frequency
1	Air passenger	144	Y	Y	Monthly
2	Beersales	192	Y	Y	Monthly
3	Google	521	N	N	Daily
4	SP	168	Y	Y	Quarterly
5	CO2 concentrations	160	Y	Y	Monthly
6	Mackey-Glass chaotic	1201	N	N	
7	Phu Lien temperature	648	N	Y	Monthly
8	Water level	131472	N	Y	20 minutes

2.3.2.2 Univariate time series imputation algorithms

The performance of the proposed method is compared with 5 other existing methods for univariate time series including na.interp, na.locf, na.approx, na.aggregate, and na.spline. All these methods are implemented using R language (na stands for Not Available):

1. na.interp (forecast R-package): This approach uses linear interpolation for non-seasonal series and Seasonal Trend decomposition using Loess (STL decomposition) for seasonal series to replace missing values ([53]). A seasonal model is fitted to the data, and then

interpolation is made on the seasonally adjusted series, before re-seasonalizing. So, this method is especially devoted to strong and clear seasonality data.

2. `na.locf` (last observation carried forward) (zoo R-package): This method replaces any missing value by the most recent available value prior to it ([56]). This is one of the most simple algorithm which takes into account characteristics of time series. Because in fact, it has often a clear relation between a considered observation (at t_n) and its previous one (at t_{n-1}), so this method is quite strong. For all data with daily sampling, this method is suited: the value of the next day seems similar to its predecessor (for example daily temperature). But it has disadvantages when there are large differences between observed value at moment t_n and its previous point at t_{n-1} (especially in the case of time series having strong seasonality). In [57], the author pointed out that the mean and covariance structure are usually distorted when using this method. Molenberghs *et al.* showed that `locf` is generally biased even under MCAR ([58]).

In general, this method assumes that the outcome would not change after the last observed value. Therefore, there has been no time effect since the last observed data.

3. `na.approx` (zoo R-package): This method is integrated in the zoo R-package. It use a linear interpolation to estimate each missing value ([56]). The difference between this method and `na.interp` is that `na.interp` takes into account the seasonal component and `na.approx` does not take this. Therefore, with signals have no the seasonal factor, imputation results of the two methods are the same.
4. `na.aggregate` (zoo R-package): This algorithm applies a generic function to replace each NA with aggregated values. This allows to complete a NA by using the overall mean, monthly means, etc ([56]). In our experiment, we use the overall mean. With this computation, `na.aggregate` does not exploit the characteristics of time series. In particular, this method is not good when time series having a strong trend.
5. `na.spline` (zoo R-package): This algorithm uses a polynomial (cubic) interpolation to complete missing data ([56]).

2.3.3 Results and discussion

For assessing the results, we apply the experiment protocol as previously defined in Chapter

1. In the present study, 5 missing data levels are considered on 8 datasets. When the size of

a dataset (number of instants of the dataset) is less than or equal to 10,000 samples, we create gaps with different sizes: 6%, 7.5%, 10%, 12.5%, 15% of overall dataset size. In contrast, when the size of a dataset is greater than 10,000 sampling points, gaps are built at rates 0.6%, 0.75%, 1%, 1.25%, and 1.5% of the dataset size (here the largest gap of the water level time series is 1,972 missing values, corresponding to the missing rate 1.5%). For each missing rate, the algorithms are conducted 10 times by randomly selecting the missing positions on the data. We then run 50 iterations for each dataset.

Results are analyzed in two respects comprising quantitative performance and visual ability.

- **Comparison of quantitative performance**

For this part, we compare similarity (Sim), NAME, RMSE, FSD of the real data with the imputed data resulting from the six imputation methods. Table 2.4 and table 2.5 show imputation average results of DTWBI, na.interp, na.locf, na.approx, na.aggregate, na.spline methods applied on 8 datasets using these indicators.

Airpassenger, Beersales, Google, SP datasets

The Airpassenger dataset has both trend and seasonality components (tabel 2.3). The results from Table 2.4 indicate that when the gap size is greater than or equal to 10%, the proposed method has the highest similarity and the lowest NMAE and RMSE.

On the Beersales dataset, considering similarity and RMSE indicators: na.interp method provides the best result and the second one is our approach. By contrast to these two indicators, our method has better results on NMEA and FSD indicators at any missing rate. When comparing na.interp method to the na.approx one on the Airpassenger and Beersales datasets, we can see na.interp shows better performance than na.approx method on any indicators and at every level of missing data. It corresponds to the fact that these two datasets have a clear seasonality component. na.interp method takes into account the seasonality factor, so it can better handle seasonality than na.approx does, although both algorithms use the interpolation for completing missing data.

On Airpassenger and Beersales datasets, na.aggregate approach gives less efficient results than na.interp. But on Google series, na.aggregate method yields the best performance: the highest similarity and the smallest NMEA, RMSE indicators. Without any trend on this dataset, this method leads to the best result. For SP dataset, na.aggregate method still highlights a good performance on NMEA and RMSE, but this approach has lower

CHAPTER 2. DTW-BASED IMPUTATION APPROACH FOR UNIVARIATE TIME SERIES

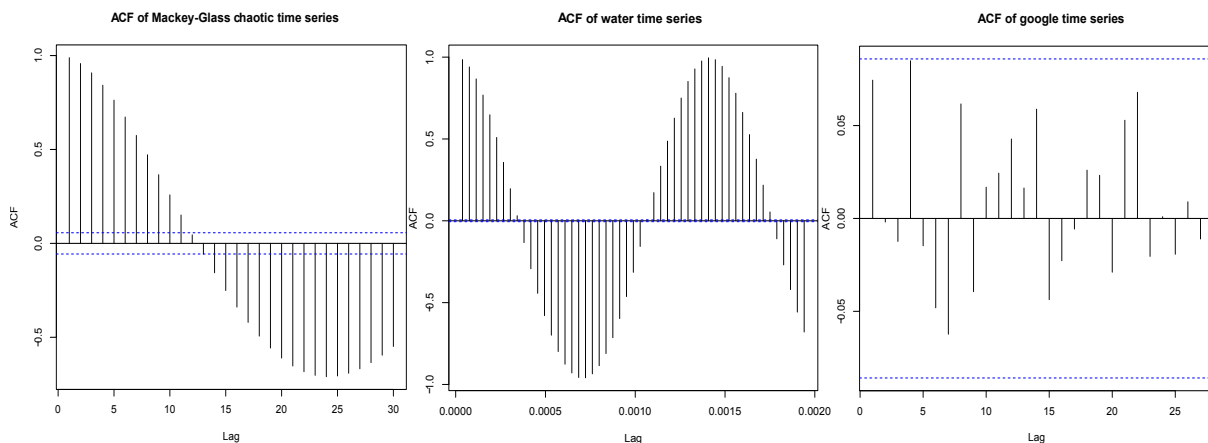


Figure 2.11: ACF of Mackey-Glass chaotic, water level and Google time series

similarity than it has on Google series. The `na.aggregate` method replaces missing values by overall mean. However, SP series has a clear trend; therefore, `na.aggregate` method seems not to be effective with series having a strong trend.

CO2 concentrations, Mackey-Glass chaotic, Phu Lien temperature, water level datasets

Table 2.5 illustrates the results of different methods on 4 datasets comprising CO2 concentrations, Mackey-Glass chaotic, Phu Lien temperature, water level datasets. These datasets have a seasonality component (except Mackey-Glass chaotic series but this dataset is regularly repeated), without any trend (excluding CO2 concentrations dataset) and high auto-correlation. Our method demonstrates the best ability for completing missing data on these series: the highest similarity, the lowest NMAE, RMSE and FSD at any missing level. Furthermore, on Airpassenger, Beersales, Google and SP datasets, the similarity of our approach is lower, but the difference value of this indicator between the proposed method and the best method is small. On the contrary, for these four datasets, our method outperforms the remaining techniques on any indicator and at any missing rate. The different values of these indicators between the proposed method and the other ones are quite large. The results confirm that the imputation values generated from the proposed method are close to the real values on datasets having high auto-correlation (see Fig. 2.11, the ACF maximum values of water and chaotic series are approximate 1), which means that there is a strong relationship between the available and the unknown values.

Following the proposed method, the second one is `na.aggregate` method applied on the Mackey-Glass chaotic series, Phu Lien temperature and water level series. As mentioned

2.3. Dynamic Time Warping-based imputation for univariate time series

Table 2.4: Average imputation performance indices of six methods on the Airpassenger, Beersales, Google and SP datasets. The best results are highlighted in bold.

Gap size	Method	Airpassenger					Beersales					Google					SP				
		1-Sim	NMAE	RMSE	FSD		1-Sim	NMAE	RMSE	FSD		1-Sim	NMAE	RMSE	FSD		1-Sim	NMAE	RMSE	FSD	
6%	DTWBI	0.22	0.034	21.1	0.24		0.12	0.035	0.7	0.14		0.17	0.14	0.034	0.44		0.26	0.026	35.5	0.7	
	na.interp	0.15	0.019	11.1	0.24		0.11	0.063	0.6	0.15		0.17	0.11	0.032	1.11		0.26	0.028	36.3	0.54	
	na.locf	0.24	0.044	26.3	2		0.19	0.129	1.2	2		0.19	0.13	0.036	2		0.25	0.022	29.2	2	
	na.prox	0.23	0.037	21.8	1.01		0.2	0.136	1.3	1.5		0.17	0.11	0.032	1.11		0.27	0.028	37	1.03	
	na.aggregate	0.2	0.033	20.1	2		0.17	0.11	1.1	2		0.14	0.08	0.024	2		0.22	0.021	26.5	2	
7.5%	na.spline	0.29	0.057	35.1	0.52		0.32	0.26	2.3	0.55		0.5	1.81	0.473	1.02		0.37	0.045	56.8	0.41	
	DTWBI	0.22	0.035	20.6	0.31		0.13	0.038	0.7	0.162		0.16	0.13	0.032	0.33		0.24	0.03	38.9	0.52	
	na.interp	0.14	0.023	13.6	0.3		0.11	0.067	0.6	0.163		0.17	0.12	0.034	1.18		0.22	0.024	33.1	0.67	
	na.locf	0.23	0.046	27.4	2		0.19	0.123	1.2	2		0.18	0.13	0.035	2		0.23	0.026	34.8	2	
	na.prox	0.26	0.053	31.3	1.49		0.2	0.132	1.3	1.51		0.17	0.12	0.034	1.18		0.22	0.025	34	1.1	
10%	na.aggregate	0.19	0.033	20.2	2		0.18	0.112	1.1	2		0.13	0.08	0.024	2		0.2	0.022	29.1	2	
	na.spline	0.4	0.112	65.4	0.45		0.4	0.404	3.5	0.43		0.56	3.65	0.963	1.38		0.31	0.042	54.5	0.55	
	DTWBI	0.11	0.02	12.7	0.36		0.16	0.054	1	0.13		0.16	0.13	0.032	0.23		0.19	0.029	40.1	0.57	
	na.interp	0.14	0.021	13.1	0.34		0.11	0.068	0.7	0.18		0.15	0.1	0.03	1.22		0.18	0.025	36.3	0.56	
	na.locf	0.21	0.042	26.1	2		0.18	0.13	1.3	2		0.17	0.13	0.035	2		0.19	0.026	36.9	2	
12.5%	na.prox	0.21	0.041	24.6	1.03		0.18	0.124	1.2	1.24		0.15	0.1	0.03	1.22		0.17	0.024	33.5	1.14	
	na.aggregate	0.19	0.035	22.1	2		0.16	0.111	1.1	2		0.13	0.08	0.024	2		0.18	0.023	31.7	2	
	na.spline	0.38	0.134	78.3	0.52		0.45	0.558	4.9	0.67		0.58	4.68	1.118	1.13		0.24	0.049	63.2	0.45	
	DTWBI	0.11	0.019	12.6	0.36		0.12	0.039	0.7	0.12		0.15	0.14	0.032	0.23		0.2	0.03	41.9	0.61	
	na.interp	0.14	0.023	14.8	0.39		0.11	0.068	0.6	0.15		0.15	0.12	0.032	1.27		0.19	0.028	38.8	0.52	
15%	na.locf	0.2	0.044	26.9	2		0.18	0.127	1.2	2		0.16	0.13	0.035	2		0.19	0.027	36.1	2	
	na.prox	0.21	0.043	26.7	0.95		0.2	0.147	1.4	1.28		0.15	0.12	0.032	1.27		0.185	0.027	35.6	1.06	
	na.aggregate	0.18	0.035	21.8	2		0.16	0.109	1.1	2		0.12	0.08	0.024	2		0.186	0.024	31	2	
	na.spline	0.36	0.129	76.8	0.67		0.39	0.458	4	0.77		0.61	2.14	0.532	1.4		0.39	0.113	132.4	0.69	
	DTWBI	0.1	0.02	12.8	0.36		0.16	0.054	1	0.1		0.15	0.13	0.031	0.29		0.19	0.029	40.7	0.59	
15%	na.interp	0.14	0.025	15.6	0.35		0.11	0.069	0.7	0.17		0.14	0.11	0.031	0.99		0.21	0.033	43.6	0.49	
	na.locf	0.21	0.047	28.2	2		0.18	0.126	1.2	2		0.16	0.13	0.034	2		0.19	0.028	36.3	2	
	na.prox	0.2	0.043	26.5	1.17		0.17	0.117	1.1	1.42		0.14	0.11	0.031	0.99		0.19	0.032	41	1	
	na.aggregate	0.17	0.035	22.1	2		0.16	0.11	1.1	2		0.11	0.08	0.023	2		0.18	0.025	32	2	
	na.spline	0.45	0.175	106.1	0.95		0.51	0.731	6.3	0.88		0.66	12.34	2.928	1.6		0.39	0.136	162.5	0.68	

above (Table 2.3), these datasets have no trend, that is why na.aggregate could demonstrate its ability. However, on the C02 series with clear trend, fully opposed to these 3 datasets, the performance of this method is the worst one.

Although na.interp method is well indicated for handling datasets with seasonality component: here for these 4 datasets this approach does not illustrate its capability. It gives the same results as na.approx method and lower results than our approach and the na.aggregate one (on the Mackey-Glass chaotic, Phu Lien temperature and water series). For any dataset, na.spline method indicates the lowest performance. However on the water series, this method has the least performance for completing missing values. This means that the spline method is not suitable for this task.

In all datasets, FSD value of na.aggregate and na.locf methods always equals 2, because they use the same value for all missing data (last value for na.locf method; overall mean for na.aggregate).

Also, to be more persuasive about imputation results, we have conducted a new comparison as follows: we randomly chose 10 windows having the same size of the gap, then compute the average values to fill in the gap. Next we compare the results with all the above methods using the same indicators as previously defined. Figure 2.12 illustrates this comparison. Looking at figure 2.12, once again DTWBI demonstrates its ability versus the random selection of windows for complete missing values: the largest similarity, the smallest RMSE and FSD.

- **Comparison of visual performance**

Tables 2.4, 2.5 indicate the quantitative comparison of 6 different methods for the task of completing missing values. In this part, figures 2.13, 2.14, 2.15, 2.17, and 2.18 show the comparison of visual imputation performance of different methods.

Fig. 2.13 presents the shape of imputation values of 5 existing methods (na.interp, na.locf, na.approx, na.aggregate and na.spline) with the true values at position 106, the gap size of 9 on the Airpassenger series. As we can notice on Table 2.4, considering low rates of missing data, the proposed approach is less effective than na.interp and na.aggregate methods for Airpassenger time series. However, when looking at Fig. 2.14, we find that the shape of the imputation values generated from DTWBI method is very similar to the shape of true values. Despite high similarity, low RMSE and NMAE, the shape of imputation values yielded from na.aggregate method (Fig. 2.13) is not as good as the

Table 2.5: Average imputation performance indices of six methods on CO2 concentrations, Mackey-Glass Chaotic, Phu Lien temperature and Water level datasets. The best results are highlighted in bold.

Gap size	Method	CO2 concentrations					Mackey-Glass Chaotic					Phu Lien temperature					Water level				
		1-Sim	NMAE	RMSE	FSD		1-Sim	NMAE	RMSE	FSD		1-Sim	NMAE	RMSE	FSD		1-Sim	NMAE	RMSE	FSD	
6%	DTWBI	0.07	0.001	0.3	0.04	0.05	0.005	0.01	0.03	0.12	0.06	1.7	0.08	0.05	0.009	0.1	0.05				
	na.interp	0.25	0.055	1.6	1.5	0.21	0.031	0.04	0.81	0.2	0.142	3.1	0.63	0.19	0.042	0.5	1.05				
	na.locf	0.27	0.059	1.7	2	0.23	0.036	0.05	2	0.23	0.173	3.8	2	0.2	0.043	0.4	2				
	na.prox	0.25	0.055	1.6	1.5	0.21	0.031	0.04	0.81	0.2	0.142	3.1	0.63	0.19	0.042	0.5	1.05				
	na.aggregate	0.55	0.185	4.7	2	0.18	0.025	0.03	2	0.17	0.114	2.4	2	0.17	0.035	0.4	2				
7.5%	na.spline	0.25	0.057	1.6	0.75	0.35	0.072	0.09	0.38	0.39	0.413	8.5	0.52	0.7	0.654	6.6	1.61				
	DTWBI	0.07	0.001	0.4	0.05	0.07	0.008	0.01	0.02	0.12	0.061	1.7	0.06	0.04	0.007	0.1	0.02				
	na.interp	0.26	0.057	1.6	1.38	0.2	0.031	0.04	1.04	0.21	0.147	3.2	0.98	0.18	0.038	0.4	0.97				
	na.locf	0.24	0.053	1.6	2	0.23	0.038	0.05	2	0.23	0.171	3.7	2	0.19	0.043	0.5	2				
	na.prox	0.26	0.057	1.6	1.38	0.2	0.031	0.04	1.04	0.21	0.147	3.2	0.98	0.18	0.038	0.4	0.97				
10%	na.aggregate	0.55	0.186	4.7	2	0.17	0.025	0.03	2	0.17	0.113	2.4	2	0.17	0.036	0.4	2				
	na.spline	0.26	0.058	1.6	0.79	0.31	0.062	0.08	0.39	0.42	0.701	14.5	0.8	0.8	1.228	12	1.71				
	DTWBI	0.07	0.001	0.4	0.04	0.07	0.008	0.01	0.01	0.12	0.063	1.8	0.05	0.03	0.005	0.1	0.03				
	na.interp	0.24	0.051	1.4	0.88	0.19	0.03	0.04	0.98	0.19	0.137	3	0.58	0.19	0.041	0.4	0.91				
	na.locf	0.24	0.054	1.6	2	0.21	0.036	0.05	2	0.23	0.176	3.8	2	0.19	0.043	0.5	2				
12.5%	na.prox	0.24	0.051	1.4	0.88	0.19	0.03	0.04	0.98	0.19	0.137	3	0.58	0.19	0.041	0.4	0.91				
	na.aggregate	0.56	0.197	4.9	2	0.17	0.025	0.03	2	0.17	0.114	2.4	2	0.17	0.036	0.4	2				
	na.spline	0.34	0.098	2.9	0.26	0.29	0.058	0.08	0.33	0.51	0.88	17.8	1.04	0.82	1.57	15.5	1.79				
	DTWBI	0.06	0.001	0.3	0.04	0.08	0.009	0.02	0.01	0.12	0.065	1.8	0.04	0.04	0.006	0.1	0.03				
	na.interp	0.22	0.049	1.5	1.39	0.2	0.033	0.04	1.13	0.21	0.163	3.5	1.44	0.19	0.044	0.5	1.21				
15%	na.locf	0.25	0.057	1.7	2	0.21	0.036	0.05	2	0.22	0.18	3.8	2	0.19	0.043	0.5	2				
	na.prox	0.22	0.049	1.5	1.39	0.2	0.033	0.04	1.13	0.21	0.163	3.5	1.44	0.19	0.044	0.5	1.21				
	na.aggregate	0.56	0.2	5	2	0.16	0.025	0.03	2	0.16	0.116	2.4	2	0.17	0.036	0.4	2				
	na.spline	0.29	0.073	2.2	0.38	0.39	0.093	0.12	0.63	0.45	0.653	13.7	0.99	0.75	0.96	9.8	1.74				
	DTWBI	0.06	0.001	0.3	0.04	0.08	0.01	0.02	0.01	0.12	0.066	1.8	0.05	0.04	0.007	0.1	0.04				
15%	na.interp	0.24	0.053	1.6	1.46	0.19	0.03	0.04	0.99	0.19	0.145	3.2	1	0.19	0.044	0.5	1.6				
	na.locf	0.23	0.052	1.6	2	0.21	0.037	0.05	2	0.21	0.175	3.8	2	0.19	0.043	0.5	2				
	na.prox	0.24	0.053	1.6	1.46	0.19	0.03	0.04	0.99	0.19	0.145	3.2	1	0.19	0.044	0.5	1.6				
	na.aggregate	0.57	0.202	5.1	2	0.16	0.025	0.03	2	0.16	0.117	2.5	2	0.17	0.036	0.4	2				
	na.spline	0.31	0.085	2.5	0.58	0.43	0.129	0.16	0.73	0.56	1.268	26.3	1.27	0.79	1.185	11.8	1.83				

CHAPTER 2. DTW-BASED IMPUTATION APPROACH FOR UNIVARIATE TIME SERIES

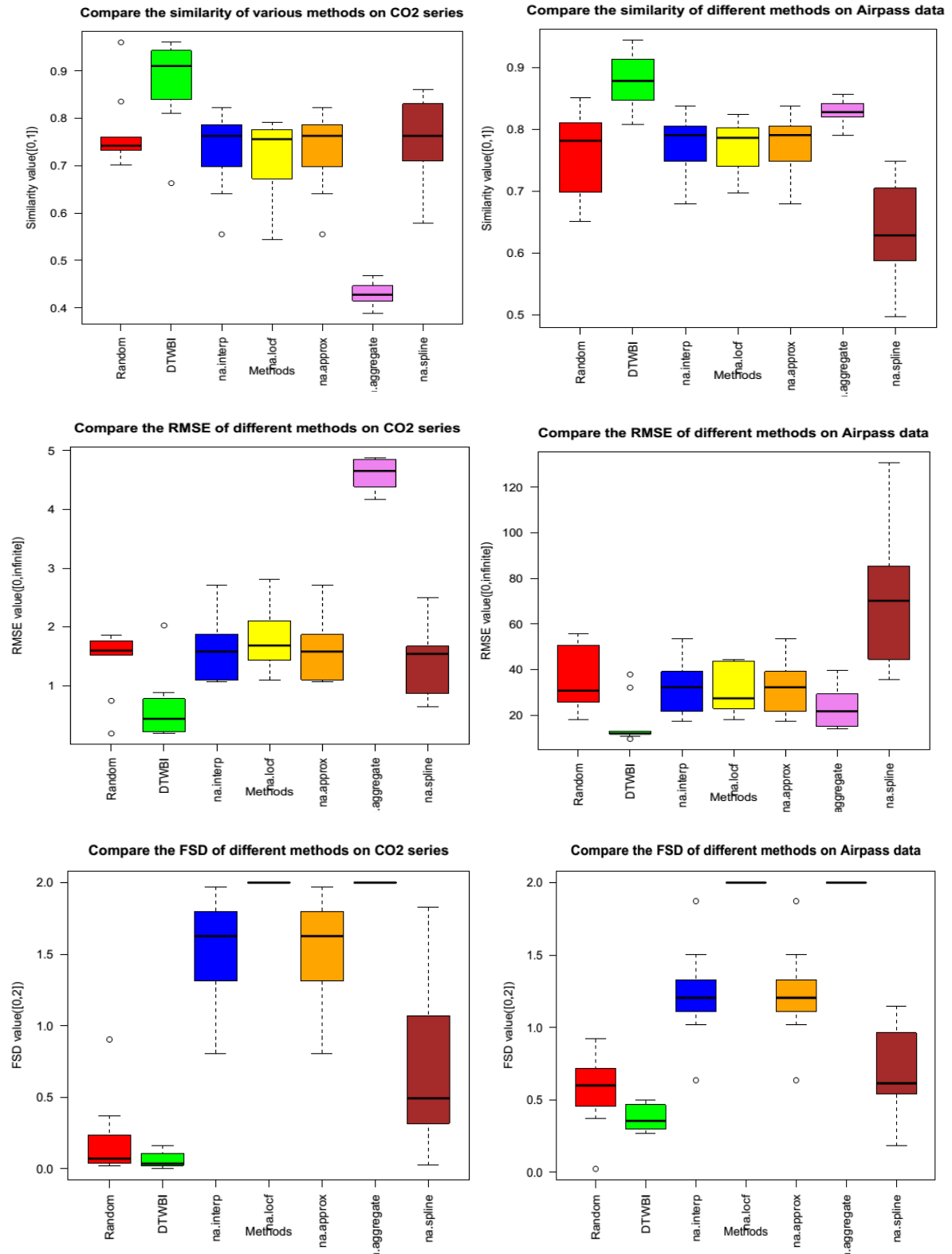


Figure 2.12: a) On the left, boxplot comparison of Similarity, RMSE and FSD on C02 dataset with a gap size of 6%, b) on the right boxplot comparison of Similarity, RMSE and FSD on Airpass dataset with a gap size of 15%

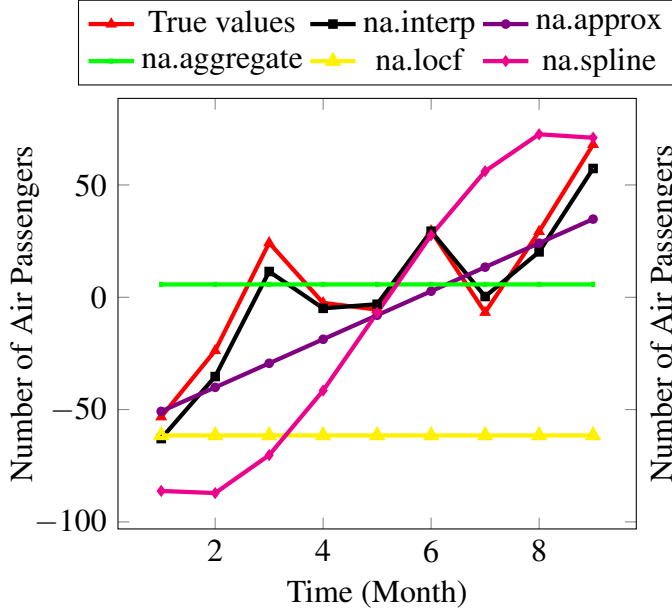


Figure 2.13: Visual comparison of imputed values of different imputation methods with true values on Airpassenger series at position 106 with the gap size of 9.

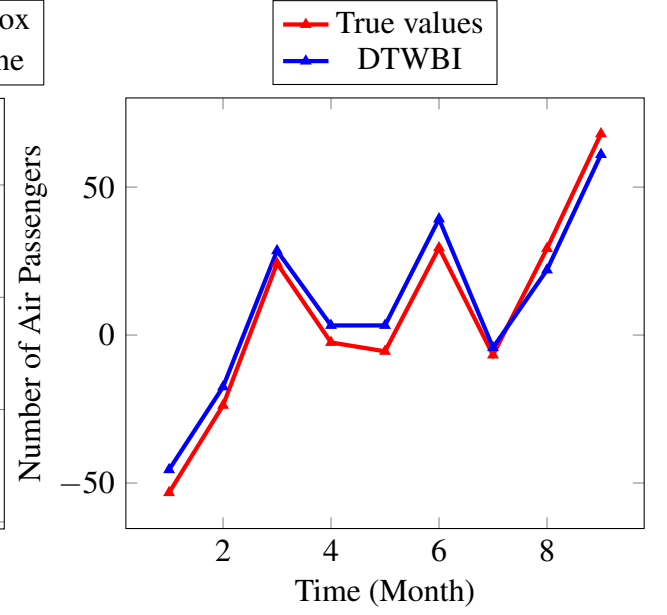


Figure 2.14: Visual comparison of imputed values of proposed method with true values on Airpassenger series at position 106 with the gap size of 9.

proposed method (Fig. 2.14). As analyzed above, the na.interp method better deals with seasonal factor, so their imputed values are asymptotic to the real values (Fig. 2.13).

Fig. 2.15 illustrates the visual comparison of DTWBI imputation values and real values on water level series at position 23,282, and at 0.6% rate of missing values (corresponding to 789 missing points). The proposed method proves again its capability for the task of completing missing values. We see that the shape of the imputation values generated from our method and the one of the true values are almost completely identical.

Fig. 2.16 shows the matching pairs between the query and the most similar reference window for the considered case. The values of matching pairs are very close, which indicates the reason why the DTWBI imputation values are very similar to the real values (fig. 2.15). In contrast to our approach, handling seasonal factor of na.interp method is ineffective on water level dataset. This method does not provide good result such as on Airpassenger series (Fig. 2.13); its performance is the same as na.approx method (Fig. 2.17). Fig. 2.18 especially points out the obvious inefficiency of na.spline method for the task of completing missing values, considering series with high auto-correlation and large gap size (789 missing values in this case).

In this work, we also calculate Cross-Correlation (CC) coefficients between the query with each

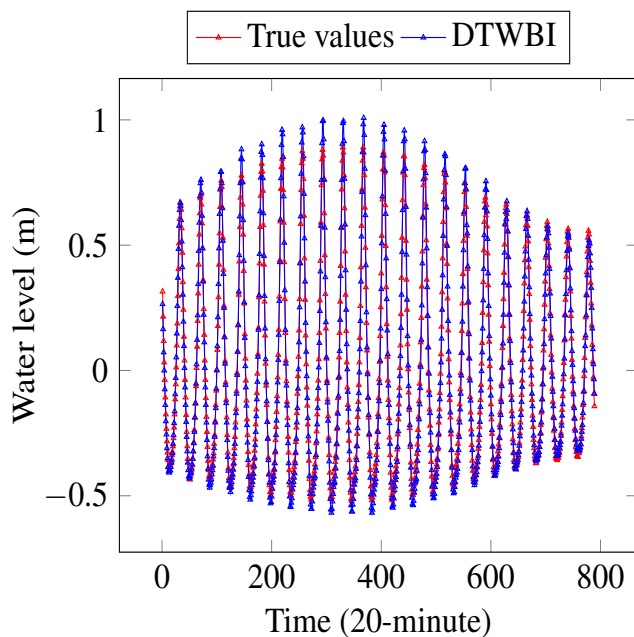


Figure 2.15: Visual comparison of imputed values of the proposed method with true values on water level series at position 23,282 with the gap size of 789.

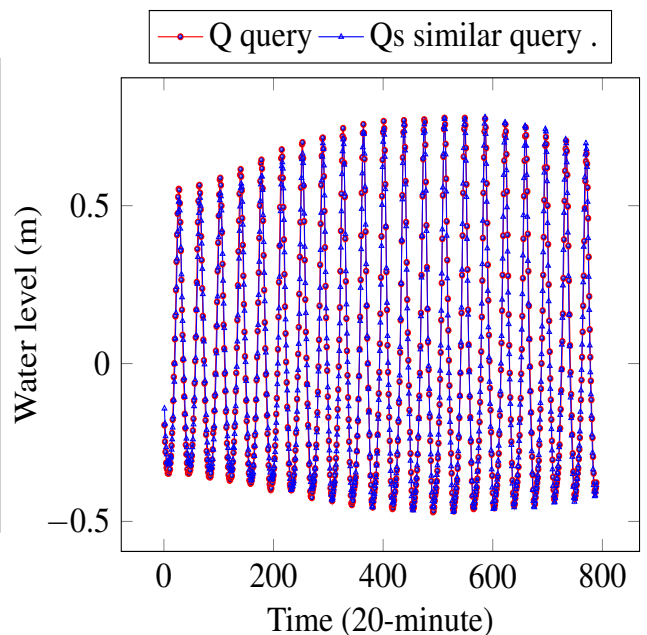


Figure 2.16: Visual comparison of the query with the similar window on water level series at position 23,282 with the gap size of 789.

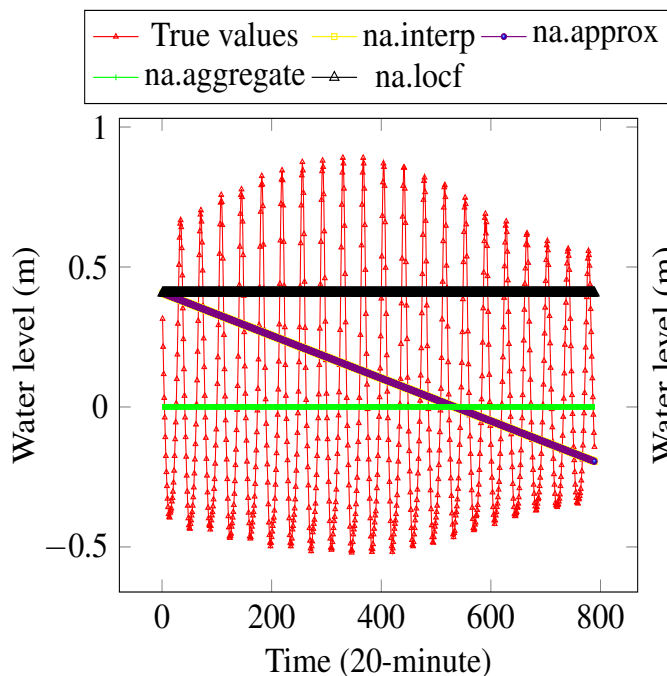


Figure 2.17: Visual comparison of imputed values of different methods with true values on water level series at position 23,282 with the gap size of 789.

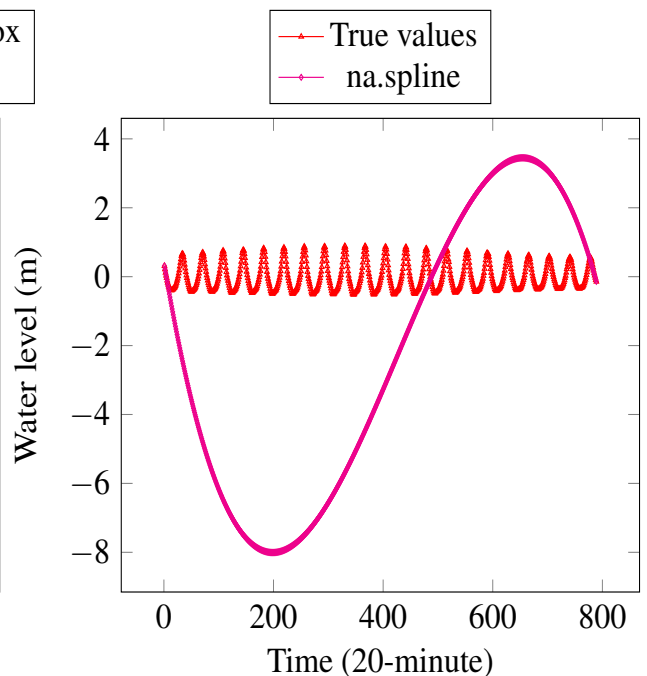


Figure 2.18: Visual comparison of imputed values of spline method with true values on water level series at position 23,282 with the gap size of 789.

reference window, and then we find the maximum coefficient. CC demonstrates that a pattern (here that is the query) exists or not in the database. High CC value means that there exists the recurrence of the pattern in the database. Therefore, we could easily find the pattern. Table 2.6 indicates the maximum of cross-correlation between the query and reference windows.

Table 2.6: The maximum of cross-correlation between the query and reference windows.

Gap size	dataset							
	#1	#2	#3	#4	#5	#6	#7	#8
6%	0.88	0.92	0.58	0.78	0.99	1	0.91	1
7.50%	0.91	0.91	0.55	0.74	0.99	0.99	0.91	1
10%	0.94	0.87	0.5	0.67	0.98	0.99	0.91	1
12.50%	0.95	0.89	0.44	0.65	0.98	0.99	0.9	1
15%	0.95	0.85	0.4	0.65	0.98	0.99	0.9	1

#1-Airpassenger, #2-Beersales, #3-Google, #4-SP, #5-Co2 concentrations
#6-Mackey-Glass chaotic, #7-Phu Lien temperature, #8-water level

This result is fully interpreted: for 4 datasets including CO2 concentrations, Mackey-Glass chaotic series, Phu Lien temperature and water level, their cross-correlation between the query and reference windows are very high for each missing level (Table 2.6). This corresponds to the results in Table 2.5: the proposed method yields the highest similarity and the lowest NMAE, RMSE, FSD. It also means that the imputation values generated from DTWBI method are very close to the true ones. For Google (#3) and SP (#4) datasets, we see that CC are not high, that is why our approach does not well prove its ability. With Airpassenger dataset (#1), when CC are greater than or equal to 0.94, the proposed method highlights better results than other methods. On Beersales dataset (#2), DTWBI gives improved results in the case of higher CC.

From these results, we can notice that the proposed method gives the best performance in the case of high CC coefficient (> 0.9). Indeed, CC is an indicator that gives information about the pattern recurrence in the data. Based on this indicator, we can predict if one pattern may occur in the past or in the following data from the position we are considering. From the above analyses, we can see that our algorithm outperforms other imputation methods when datasets have high auto-correlation and cross-correlation, no trend, strong seasonality, and complex distribution, especially in the case of large gap(s). High cross-correlation means that these datasets are recurrent, or in other words, these time series will repeat themselves over some periods. The drawback of this method is the computation time. The proposed algorithm may take a long time to find the imputation values when the size of the given data is large. The reason is the search for all possible sliding windows to find a reference window having the

maximum similarity to the query.

2.3.4 Conclusion

In this study, we complete missing data on univariate time series based on the combination of shape-feature extraction and DTW algorithms. The search of similar sequences by elastic matching makes it possible to complete a database with missing values while respecting as much as possible the dynamics and the shape of signals. Whereas applying the shape-feature extraction algorithm allows to reduce the computing time of the proposed method.

The proposed imputation approach, namely DTWBI, for univariate time series data with circular list permits to process a large dataset. DTWBI method has been tested on 8 datasets with various size, ranging from small to very large database (Airpassenger, Beersales, Google, SP, Co2 concentrations, Mackey-Glass chaotic, Phu Lien temperature, and water level). The accuracy of imputation values yielded by DTWBI is compared with 5 existing methods (na.interp, na.locf, na.approx, na.aggregate and na.spline) using 4 quantitative indicators (similarity, NMAE, RMSE and FSD) applied to 5 different simulation missing levels. We also compare the visual performance of these methods. The experiments show that our approach gives better results than the other existing methods, and is the best robust method in the case of time series having high cross-correlation and auto-correlation, large gap(s), complex distribution, and strong seasonality. However, the proposed framework is restricted to applications where the necessary assumption of recurring data in the time series is set up (high cross-correlation indicator), and it requires computation time for very large missing intervals.

In the past decades, several studies investigated to improve classical DTW for better comparing the similarity between two curves by integrating the notions of slope (DDTW [48]) and of curvature (AFBDTW [49]) or by changing the final DTW cost applied to classify [51] or by comparing multidimensional series [50]. In order to assess the ability of different DTW versions for filling in missing data, in the next section we perform a comparison of some DTW variants (including DWT, DDTW, AFBDTW, DTW-D) applied to univariate time series imputation.

2.4 Comparison of various DTW versions for completing missing values in univariate time series

2.4.1 Introduction

In the previous section, we have proposed DTWBI method using classical DTW for reconstructing database. And in the section 2.2 we have discussed several variants of DTW introduced to improve the finding the similar of two sequences. In order to identify which variant is more suitable for the imputation task, in this part, we carry out a comparison of the performance of different DTW metrics applied to univariate time series imputation.

Dynamic Time Warping (DTW) [7] approach is used when no information are available, the idea is to find a similar shape in a database to fill the missing values. Related works to DTW are cited below, rare works deal with large gaps in univariate time series.

Hsu *et al.* [59] used k-Nearest Neighbors (k-NN) and DTW algorithms for completing DNA data. They also performed comparing different versions of DTW algorithm for better prediction and computation performance. Nevertheless, the authors did not mention to complete long missing subsequences. In [60] a weighted k-NN version is combined with DTW to compare multiple points in time simultaneously. DTW-cost is used as distance metric instead of pointwise distance measurements. Kostadinova *et al.* [61] proposed an Integrative DTW-Based Imputation algorithm that is particularly suited for the estimation of missing values in gene expression time series data using multiple related information in datasets. This algorithm identifies an appropriate set of estimation matrices by using DTW-cost distance in order to measure similarities between gene expression matrices. Yang *et al.* [62] also developed a method to impute missing values in microarray time-series data based on the combination of k-NN and DTW. In these three last cited works, the authors applied DTW method for completing missing values in multivariate data. Imputation for consecutively missing values in univariate data is not considered.

On the other hand, there is no application for surveying imputation algorithms with large gap(s) size using directly DTW in the case of univariate time series. A gap is large when the process could have significant changes during this missing period. In addition, recall that for handling missing data within univariate time series, we must only rely on the available values of this unique variable to estimate the incomplete values.

Therefore, the objective of this part is to build a framework for filling missing values in

univariate time series and to perform a comparison of different similarity DTW metrics for the imputation task. This allows to suggest the most suitable metric for the imputation of marine univariate time series ensuring that results are reliable and high quality.

2.4.2 Imputation based on DTW metrics

We keep the same idea as DTWBI approach to perform completing missing data. That is, in the previous section we have used the original DTW, this section we apply 3 different versions of DTW for univariate time series imputation, namely, Derivative DTW (DDTW)[48], DTW-D [51], and AFBDTW (Adaptive Feature Based DTW) [49]).

The approach consists in finding the most similar sub-sequence (Q_s) to a query (Q), with Q is the sub-sequence before a gap of T size at position t ($Q = X[t - T : t - 1]$). Then, we complete this gap by the following sub-sequence of the Q_s when this window is determined. The mechanism is illustrated on the figure 2.9.

To obtain the Q_s similar sub-sequence, we used different versions of DTW (as above mentioned). The dynamics and the shape of data before (resp. after) a gap are key-point of this technique. The elastic matching is used to find similar window to the Q query of T size in the search database. Once the most similar window is identified Q_s , the following window Qfs will be copied to the location of missing values.

2.4.3 Data presentation

Five datasets are used for evaluating the performance of different DTW versions, including: Cua Ong temperature, Gas online, Chlorophyll- a , fluorescence, and water level. The last three datasets are collected by IFREMER (France) in the eastern English Channel [3]. We have chosen 4 new datasets and reused water level signal in order to focus on marine data which were provided by the project we participate (CPER MARCO of our university (Chlorophyll- a , fluorescence, water level) and Vietnam (Cua Ong temperature)). Another goal is also to test our algorithm for different applications (so that we use Gas online series).

- Cua Ong temperature in $^{\circ}\text{C}$ - daily mean air temperature at the Cua Ong meteorological station in Vietnam from 1/1/1973 to 31/12/1999.
- Gas online - weekly data on US finished motor gasoline products supplied (in thousands of barrels per day) from 8/2/1991 to 4/11/2016 [63].

2.4. Comparison of various DTW versions for completing missing values in univariate time series

- Chlorophyll-*a* (Chla) in $\mu\text{g/L}$ - weekly Chlorophyll-*a* time series from 01/1/1989 to 24/12/2014, Ifremer IGA-Gravelines monitoring [32].
- Water level in m - sampling frequency 20 minutes of water level from 01/1/2005 to 31/12/2009 [3].
- Fluorescence in FFU - sampling frequency 20 minutes of fluorescence from 1/1/2005 to 9/2/2009 [3].

In order to obtain useful information from the dataset and makes the dataset easily exploitable, we analyzed these series. Table 2.7 summarizes characteristics of the datasets.

Table 2.7: Data characteristics by dataset: Number of the dataset, its name, the number of time samples, presence (Y=Yes else N=No) of trend, presence of seasonal cycle and sampling frequency

N0	Dataset name	N0 of instants	Trend (Y/N)	Seasonal (Y/N)	Frequency
1	Cua Ong temperature	9859	N	Y	Daily
2	Gas online	1344	Y	Y	Weekly
3	<i>Chlorophyll-a</i>	1352	N	N	Weekly
4	Fluorescence	106000	N	Y	20 minutes
5	Water level	131472	N	Y	20 minutes

2.4.4 Results and discussion

For assessing the results of imputation algorithms, we use the experiment protocol as designed in Chapter 1. This consists of three steps. In the first step, we create artificial missing data by deleting data values from full time series. The second step consists in applying the imputation algorithms to complete missing data. Finally, the third step compares the performance of different DTW metrics on various indicators as previously defined. We consider 5 missing data levels on 5 datasets. Gaps are built at rates 0.6%, 0.75%, 1%, 1.25%, and 1.5% of the dataset size (here missing sequences of the water level time series correspond to around 10 days (789 NAs) to 1 month (1972 NAs)). For each gap, the algorithms are conducted 10 times by randomly selecting the missing positions on the data. We then run 50 iterations for each dataset. To assess accuracy and shape indices of these imputation methods, 6 indicators are divided into two group: the first group is accuracy indices (including Similarity, NMEA, RMSE) and the

CHAPTER 2. DTW-BASED IMPUTATION APPROACH FOR UNIVARIATE TIME SERIES

second one is shape indices (comprising FSD, FB and FA2). These measurements are defined in Chapter 1.

Tables 2.8, 2.9, 2.11, 2.10, and 2.12 show average results on 6 indicators (including similarity, NAME, RMSE, FSD, FA2, and FB) using different DTW versions for completing missing data applied on 5 time series.

From the results of these tables, we find that DTW metric provides the best results on the accuracy indices: the highest similarity and the lowest NMAE and RMSE at every missing level for all datasets. However, when considering on other indices such as FSD, FA2 and FB (we call shape indices), DTW no longer performs well as on the accuracy indicators.

Table 2.8: Average imputation performance indices of various similarity metrics on Cua Ong temperature series

Gap size	Metric	Accuracy indices			Shape indices		
		1-Sim	NMAE	RMSE	FSD	1-FA2	FB
0.6%	DTW	0.209	0.118	37.001	0.269	0.005	0.083
	DDTW	0.232	0.138	43.003	0.333	0.008	0.118
	DTW-D	0.273	0.160	48.372	0.307	0.005	0.152
	AFBDTW	0.228	0.126	39.099	0.252	0.000	0.103
0.75%	DTW	0.212	0.122	38.033	0.168	0.014	0.090
	DDTW	0.237	0.145	44.627	0.200	0.008	0.141
	DTW-D	0.270	0.184	53.756	0.267	0.064	0.175
	AFBDTW	0.224	0.142	44.297	0.188	0.030	0.131
1%	DTW	0.164	0.099	31.952	0.159	0	0.013
	DDTW	0.171	0.106	33.561	0.176	0.008	0.060
	DTW-D	0.188	0.123	39.209	0.228	0.010	0.078
	AFBDTW	0.173	0.104	33.537	0.125	0.005	0.043
1.25%	DTW	0.150	0.108	34.315	0.151	0.003	0.036
	DDTW	0.166	0.124	39.871	0.298	0.002	0.076
	DTW-D	0.160	0.119	37.711	0.228	0.008	0.074
	AFBDTW	0.155	0.113	36.699	0.181	0.003	0.072
1.5%	DTW	0.141	0.110	35.649	0.124	0.011	0.035
	DDTW	0.191	0.164	51.600	0.159	0.020	0.136
	DTW-D	0.147	0.115	36.399	0.088	0.005	0.060
	AFBDTW	0.142	0.111	36.656	0.102	0.009	0.048

With Cua Ong temperature (table 2.8) and Gas online (table 2.9) series, DTW still proves its ability on the FB index at all missing rate. For the remaining datasets (Fluorescence, water level, Chla datasets), DTW only highlights its performance at small missing rates.

2.4. Comparison of various DTW versions for completing missing values in univariate time series

Table 2.9: Average imputation performance indices of various similarity metrics on Gas online series

Gap size	Metric	Accuracy indices			Shape indices		
		1-Sim	NMAE	RMSE	FSD	1-FA2	FB
0.6%	DTW	0.293	0.094	392.806	0.385	0	0.031
	DDTW	0.303	0.100	413.314	0.355	0	0.033
	DTW-D	0.336	0.113	457.966	0.438	0	0.031
	AFBDTW	0.453	0.237	894.008	0.460	0	0.094
0.75%	DTW	0.287	0.106	452.470	0.328	0	0.031
	DDTW	0.330	0.137	560.240	0.484	0	0.051
	DTW-D	0.330	0.131	533.966	0.440	0	0.047
	AFBDTW	0.455	0.237	891.465	0.351	0	0.095
1%	DTW	0.276	0.115	476.098	0.203	0	0.039
	DDTW	0.328	0.146	575.640	0.311	0	0.053
	DTW-D	0.315	0.131	545.698	0.174	0	0.046
	AFBDTW	0.384	0.227	859.176	0.304	0	0.084
1.25%	DTW	0.288	0.102	433.679	0.266	0	0.028
	DDTW	0.299	0.116	473.552	0.325	0	0.036
	DTW-D	0.313	0.118	482.555	0.241	0	0.036
	AFBDTW	0.300	0.113	457.787	0.341	0	0.037
1.5%	DTW	0.234	0.131	549.911	0.201	0	0.047
	DDTW	0.277	0.168	655.410	0.238	0	0.066
	DTW-D	0.266	0.149	598.538	0.121	0	0.048
	AFBDTW	0.346	0.216	820.442	0.280	0	0.084

According to Keogh et Pazzani [48], DDTW method presents better performance than the original DTW by minimizing the number of duplicate points. However, the results in all the tables show that DDTW is not suitable for handling the imputation task, it does not prove its ability here.

AFBDTW was proposed in 2010 by Xie and Wiltgen [49]. This method takes into account both the local and global features of the series for correspondences points instead of the value itself or its derivative. That is the reason why AFBDTW proves the strength for the imputation task at large missing rates, specially in large datasets.

DTW-D method is proposed for semi-supervisor classification. Therefore, when we applied this method to complete missing values, DTW-D does not work well in all datasets at every missing level. Nevertheless, when looking at FSD indicator in the table 2.9, DTW-D gives the best results at large gaps ($\geq 1\%$). The reason may be that Gas online series has both trend and

Table 2.10: Average imputation performance indices of various similarity metrics on Fluorescence series

Gap size	Metric	Accuracy indices			Shape indices		
		1-Sim	NMAE	RMSE	FSD	1-FA2	FB
0.6%	DTW	0.160	0.028	1.569	0.531	0.462	0.423
	DDTW	0.189	0.032	1.767	1.120	0.662	0.871
	DTW-D	0.327	0.067	3.732	0.950	0.740	1.060
	AFBDTW	0.198	0.035	1.991	0.853	0.545	0.685
0.75%	DTW	0.187	0.032	1.800	0.616	0.512	0.505
	DDTW	0.190	0.034	1.883	1.364	0.731	0.974
	DTW-D	0.378	0.101	5.272	1.175	0.802	1.219
	AFBDTW	0.212	0.036	2.068	0.654	0.576	0.724
1%	DTW	0.150	0.027	1.579	0.838	0.550	0.711
	DDTW	0.172	0.035	1.963	1.411	0.854	1.236
	DTW-D	0.295	0.070	3.749	1.122	0.778	1.141
	AFBDTW	0.157	0.027	1.606	0.782	0.606	0.800
1.25%	DTW	0.157	0.027	1.655	0.913	0.630	0.794
	DDTW	0.175	0.034	1.925	1.415	0.825	1.132
	DTW-D	0.362	0.104	5.740	1.218	0.834	1.302
	AFBDTW	0.160	0.030	1.756	0.778	0.629	0.744
1.50%	DTW	0.119	0.028	1.689	1.033	0.659	0.790
	DDTW	0.123	0.031	1.820	1.270	0.813	0.957
	DTW-D	0.259	0.083	4.690	1.042	0.811	1.145
	AFBDTW	0.142	0.038	2.319	0.791	0.622	0.656

seasonality component.

Besides, the shape of imputation values generated from methods using various DTW metrics (DTW, DDTW, DTW-D, AFBDTW) are also analyzed. Fig. 2.19 presents the form of imputed values yielded by methods using different similarity metrics with the true values at position 444, the gap size of 14 (approximate 3 months of missing values) on the Chlorophyll-*a*. DTW metric proves again its capability to deal with missing subsequence. The shape of the imputation values generated from the method using DTW and the one of true values are very close.

After the comparison of quantitative and visual performance of different DTW versions, we carry out examining computational time of each metric. Table 2.13 shows that for large datasets or large gaps, AFBDTW requires the longest computational time and DTW has at least computing time.

2.4. Comparison of various DTW versions for completing missing values in univariate time series

Table 2.11: Average imputation performance indices of various similarity metrics on Chla series

Metric	Accuracy indices			Shape indices		
	1-Sim	NMAE	RMSE	FSD	1-FA2	FB
DTW	0.308	0.069	4.609	0.597	0.413	0.381
DDTW	0.339	0.091	5.707	0.692	0.463	0.476
DTW-D	0.356	0.090	5.915	0.831	0.450	0.543
AFBDTW	0.386	0.089	5.962	0.759	0.463	0.641
DTW	0.243	0.076	5.136	0.525	0.360	0.311
DDTW	0.254	0.076	5.171	0.582	0.400	0.355
DTW-D	0.303	0.094	6.481	0.897	0.480	0.492
AFBDTW	0.281	0.086	5.876	0.646	0.460	0.535
DTW	0.185	0.071	4.990	0.444	0.393	0.394
DDTW	0.205	0.088	6.207	0.501	0.443	0.468
DTW-D	0.236	0.093	6.557	0.642	0.486	0.637
AFBDTW	0.198	0.086	6.046	0.545	0.450	0.486
DTW	0.187	0.089	6.488	0.812	0.429	0.526
DDTW	0.203	0.103	7.076	0.687	0.500	0.475
DTW-D	0.216	0.105	7.352	0.775	0.518	0.409
AFBDTW	0.222	0.104	7.136	0.686	0.512	0.404
DTW	0.205	0.090	6.226	0.435	0.545	0.408
DDTW	0.216	0.097	6.772	0.407	0.515	0.460
DTW-D	0.218	0.097	6.865	0.655	0.550	0.463
AFBDTW	0.217	0.098	6.721	0.510	0.525	0.376

Also, we calculate Cross-Correlation (CC) coefficients between the query and each reference window and the maximum coefficient is extracted. CC demonstrates that a pattern (here that is the query) exists or not in the database. High CC value means that there exists one or more recurrence of the pattern in the database, that means: it is easy to find similar patterns. In Table 2.14, we see that only for water level series, CC values are very high (approximate 1), this explains why the similarity values are very high and the error index is very low.

2.4.5 Conclusion

This part compares a visual and quantitative performance of different DTW versions for univariate time series imputation. The obtained results show that when considering the accuracy of imputation values, DTW is the best robust and when regarding the shape of completed val-

CHAPTER 2. DTW-BASED IMPUTATION APPROACH FOR UNIVARIATE TIME SERIES

Table 2.12: Average imputation performance indices of various similarity metrics on water level series

Gap size	Metric	Accuracy indices			Shape indices		
		1-Sim	NMAE	RMSE	FSD	1-FA2	FB
0.6%	DTW	0.042	0.037	0.401	0.045	0	0.019
	DDTW	0.042	0.037	0.402	0.045	0	0.022
	DTW-D	0.139	0.141	1.434	0.103	0.059	0.005
	AFBDTW	0.079	0.074	0.765	0.051	0.002	0.019
0.75%	DTW	0.037	0.033	0.355	0.017	0	0.009
	DDTW	0.042	0.038	0.401	0.019	0	0.010
	DTW-D	0.154	0.162	1.624	0.075	0.082	0.010
	AFBDTW	0.076	0.073	0.750	0.039	0.008	0.022
1%	DTW	0.033	0.030	0.333	0.026	0	0.012
	DDTW	0.034	0.030	0.333	0.027	0	0.014
	DTW-D	0.107	0.108	1.141	0.047	0.034	0.013
	AFBDTW	0.082	0.080	0.828	0.025	0.009	0.017
1.25%	DTW	0.039	0.035	0.373	0.025	0	0.009
	DDTW	0.039	0.035	0.373	0.025	0	0.009
	DTW-D	0.086	0.086	0.965	0.034	0.019	0.019
	AFBDTW	0.047	0.044	0.471	0.018	0.001	0.009
1.5%	DTW	0.045	0.042	0.442	0.030	0	0.022
	DDTW	0.045	0.043	0.450	0.032	0	0.025
	DTW-D	0.073	0.073	0.841	0.021	0.012	0.008
	AFBDTW	0.061	0.060	0.635	0.020	0.009	0.015

Table 2.13: Computational time of methods using different DTW metrics at missing rate 0.6% on various series in second (s)

Method	Cua Ong temperature	Gas online	Chla	Fluorescence	Water level
DTW	12.459	1.670	1.08	774.718	2081.388
DDTW	13.112	1.700	1.07	786.543	2126.847
DTW-D	12.543	1.671	1.10	761.831	2088.375
AFBDTW	62.602	1.539	1.07	14219.51	49095.888

ues for the large gaps and datasets, AFBDTW is more suitable. This work highlights two mains contributions. Firstly, we perform completing large missing subsequences in univariate time series data. Secondly, we provide a quantitative and visual comparison of different DTW algorithms applied to various datasets.

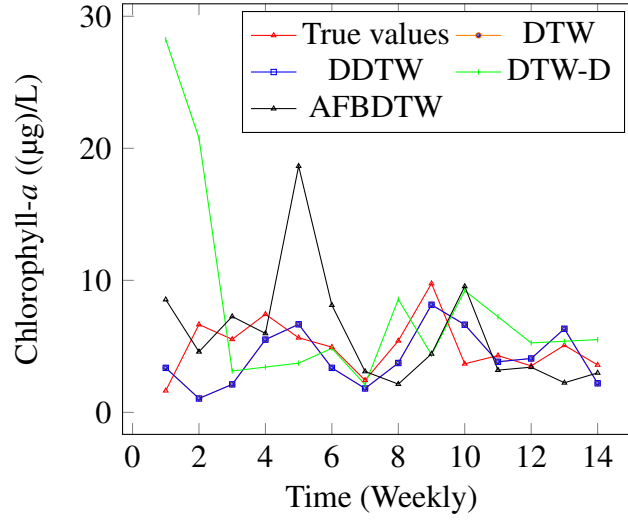


Figure 2.19: Visual comparison of imputed values using different DTW metrics with true values on *Chla* series at position 444 at missing rate 1% (correspond to 14 weeks missing).

Table 2.14: The maximum of cross-correlation between the query and reference windows.

Gap size	Cua Ong temperature	Gas online	Chla	Fluorescence	Water level
0.6%	0.751	0.921	0.93	0.657	0.997
0.75%	0.762	0.889	0.92	0.694	0.996
1%	0.780	0.819	0.86	0.710	0.996
1.25%	0.789	0.788	0.86	0.753	0.996
1.50%	0.825	0.778	0.87	0.731	0.996

2.5 Chapter conclusion

Missing data frequently occurs in many applied domains and poses serious problems such as loss of efficiency and unreliable results for various approaches. Thus, imputation (completing missing data) is very crucial task for many real applications. Over the years, numerous techniques have been developed by applying different approaches like model-based imputation, machine learning-based imputation or fuzzy logic-based imputation etc. However, few studies are dedicated for the univariate imputation, especially the completion of large gaps. We have therefore proposed in this chapter, a novel method, namely DTWBI, for completing large gaps in univariate time series data by combining shape-feature extraction and elastic matching (DTW) algorithms. Finding similar sequences by DTW metric allows to impute missing data considering the dynamics and shape of knowledge data, and using shape-feature extraction algorithm permits to reduce the computing time. Before describing our approach in detail in

Section 2.3.1, we present the basic of DTW and its variants in the first part of this chapter. In the last section, we perform a comparison of different versions of DTW in order to determine a more customized method for the imputation of marine univariate time series ensuring that results are reliable and high quality. From the results, we can conclude that when considering the accuracy of imputation values, DTW is the best robust and when regarding the shape of completed values for the large gaps and datasets, AFBDTW is more suitable.

List of Publications and valuations related to this chapter

1. Thi-Thu-Hong Phan, Emilie Poisson Caillault, Alain Lefebvre, André Bigand, "Dynamic Time Warping-based imputation for univariate time series data", Pattern Recognition Letters. Available online 16 August 2017. In Press, Accepted Manuscript. DOI: 10.1016/j.patrec.2017.08.019.
2. Emilie Poisson Caillault, Kelly Grassi, Thi Thu Hong Phan, Camille Dezechache, Jean Prygiel, Alain Lefebvre, "DTWBI & uHMM R-packages for multivariate time series pre-processing and interpretation", 26th Earth Science Meeting, 22-26 October 2018, Lille, France.
3. Thi-Thu-Hong Phan, Emilie Poisson Caillault, Alain Lefebvre, André Bigand, "Which DTW Method Applied to Marine Univariate Time Series Imputation", OCEANS 2017 MTS/IEEE, Aberdeen, Scotland, 06/2017. DOI: 10.1109/OCEANSE.2017.8084598.
4. Caillault-Poisson E., Lefebvre A., Hébert P.A., Phan, T.T.H., Ternynck P., Marson Q., Rizik A., Wacquet G., Artigas F., Bigand A, "Méthodologie(s) du traitement du signal à la classification/modélisation pour la compréhension de la dynamique des efflorescences phytoplanctoniques", Journée du CPER MARCO, 26 juin 2017, Boulogne sur Mer, France.
5. Caillault-Poisson E., Phan, T.T.H., Rizik A., Ternynck P., Bigand A, Lefebvre A, "New developments to fill the gap in high frequency data series and to integrate knowledge in Markov modeling of phytoplankton dynamics", EEC'2017: The Eastern English Channel Conference, Wimereux, 06/06/2017, France.
6. Thi-Thu-Hong Phan, Emilie Poisson Caillault, Alain Lefebvre, André Bigand. Which

DTW Method Applied to Marine Univariate Time Series Imputation, GRAISyHM: Séminaire des doctorants en traitement du signal et/ou de l'image, 26/04/2017, Lille, France.

7. Thi-Thu-Hong Phan, Emilie Poisson Caillault, Alain Lefebvre, André Bigand. Which DTW Method Applied to Marine Univariate Time Series Imputation, Journée Scientifique du Conseil Scientifique du GIS Campus de la Mer, 03/04/2017, Boulogne sur Mer, France.

8. R-Package

DWTBI R-package <https://cran.r-project.org/web/packages/DTWBI/index.html>

Imputation approaches for uncorrelated multivariate time series

Contents

3.1	Introduction	69
3.2	Dynamic Time Warping-based uncorrelated multivariate time series imputation	73
3.2.1	DTWUMI - Proposed approach	73
3.2.2	Validation procedure	75
3.2.3	Results and discussion	79
3.2.4	Conclusion	84
3.3	Proposed method based on an hybrid similarity measure	85
3.3.1	Methods based on fuzzy similarity measure	85
3.3.2	FSMUMI-Proposed approach	87
3.3.3	Validation procedure	93
3.3.4	Results and discussion	96
3.3.5	Conclusion	107
3.4	Chapter conclusion	107

3.1 Introduction

In the previous chapter we presented our proposal to fill missing data in univariate time series based on the combination of shape-feature extraction and DTW methods. The proposed ap-

proach exploits observed data on the univariate time series to estimate the missing values. In this chapter, we investigate to fill large incomplete data in low/un-correlated multivariate time series by taking advantage the property of uncorrelated multivariate data.

In the literature, many successful studies have been devoted to multivariate time series imputation such as [64, 65, 66, 67, 68, 69, 70, 71, 72, 73, 74, 75, 60]. Imputation techniques can be categorized in different perspectives: model-based, machine learning-based and clustering-based imputation techniques.

In view of the model-based imputation, two main methods were proposed. The first method was introduced by Schafer [64]. With the hypothesis that all variables follow a multivariate normal distribution, this approach is based on the multivariate normal (MVN) model to determine completion values. And, the second method, namely MICE, was developed by van Buuren *et al.* [65] and Raghunathan *et al.* [66]. This method uses chained equations to fill in incomplete data: for each variable with missing values, MICE computes the imputation data by exploiting the relations between all other variables.

According to the concept of machine learning-based imputation, many studies focus on completion of missing data in multivariate time series. Stekhoven and Bühlmann [76] implemented missForest based on the Random Forest (RF) method for multivariate imputation. P.Bonissone *et al.* [77] proposed a fuzzy version of RF that they named fuzzy random forest FRF. At the moment FRF is only devoted to classification and in our case FRF may be only interesting to separate correlated and un-correlated variables in multivariate time series if necessary. In [71], Shah *et al.* investigated a variant of MICE which fills in each variable using the estimation generated from RF. The results showed that the combination of MICE and RF was more efficient than original methods for multivariate imputation. K-Nearest Neighbors (k -NN)-based imputation is also a popular method for completing missing values such as [72, 78, 59, 62, 61, 60]. This approach identifies the k most similar patterns in the space of available features to impute missing data.

Besides these principal techniques, clustering-based imputation approaches are considered as power tools for completing missing values thanks to their ability to detect similar patterns. The objective of these techniques is to separate the data into several clusters when satisfying the following conditions: maximizing the intercluster similarity and minimizing intracluster dissimilarity. Li *et al.* [79] proposed the k -means clustering imputation technique that estimates missing values using the final cluster information. The fuzzy c -means (FcM) clustering is a common extension of k -means. The squared-norm is applied to measure the similarity between

cluster centers and data points. Different applications based on FcM are investigated for the imputation task as [80, 81, 82, 83, 84, 85, 86, 87]. Wang *et al.* [88] used FcM based on DTW to successfully forecast long-term time series.

In general, most of the imputation algorithms for multivariate time series take advantage of dependencies between attributes to predict missing values. The correlations make it possible to estimate missing data using the available values of the other variables. However, it is not efficient for multivariate series having low-or un-correlated features (case of MAREL Carnot dataset). For handling missing values or intervals in this case, we must only rely on the observed values of the unique variable containing missing data to predict the incomplete values. Besides, completion of missing values for this type of data has received little attention in the literature when comparing with the imputation of correlated multivariate time series.

One way to solve the problem of missing values in this case is to find the same behavior or shape. This is equivalent to retrieve similar values. In the literature, similarity measures are used for broad range of applications such as classification, anomaly detection [89], retrieval system [15], recommendation systems [17], imputation [90] and pattern recognition [20]. So, our idea to deal with large gaps in low/un-correlated multivariate time series, is to retrieve similar sub-sequences on unique signal having missing values by using a similarity measure.

Moreover, weighting of different similarity measures could provide better prediction accuracy in many applications such as [15, 17, 18, 19]. Particularly, imperfect time series can be modelled using fuzzy sets introduced by Zadeh [91, 92]. The fuzzy approach makes it possible to deal with imprecise and uncertain circumstances [15]. The successfully use of fuzzy-based similarity measure [20, 15, 17] and weighting of different similarity measures [17, 18, 19] leads us to study the ability of fuzzy-weighted similarity measure to complete missing values in un-correlated multivariate time series. To develop a new fuzzy-weighted similarity measure, in this study, we use a rule-based technique. This technique is power and widely employed in different studies like [15, 21, 22, 23, 24].

According to our knowledge, there is no application devoted to complete large gap(s) in uncorrelated multivariate time series using a fuzzy-weighted similarity measure and directly using DTW cost as a similarity criterion. Therefore, in this chapter, we propose two new approaches for filling large missing values in low/un-correlated multivariate time series by exploiting features of the uncorrelated data as follows:

1. DTWUMI method

- We extend our previous method (DTWBI) to impute large missing values in uncorrelated multivariate time series, namely DTWUMI.
- We just consider one query and this query is built by taking into account all the signals either before or after each gap (i.e. preserving the time index for all the variables). The last allows to assure an acceptable similarity for each signal within the time series in the same temporal window.
- We only find the most similar window to the query and only utilize DTW cost as the similarity criterion to retrieve similar windows.
- We directly use data from the window following or preceding of the most similar window on the signal containing the considered gap to fill in the missing values.

2. FSMUMI method

- Since time series data are multidimensional but they are uncorrelated (or low-correlated), so we take advantage of this feature to handle each signal one by one. This is explained in step of building queries: on each incomplete signal, for each gap, we build two queries, one query before the gap and one query after this gap.
- We take into account an uncertainty factor. So, we develop a new fuzzy-weighted similarity measure by weighting of different popular similarity distances based on fuzzy logic. To obtain this similarity measure we propose to use a new fuzzy-rule interpolation scheme that adapts to the fuzzy rule-based structure and adapts to the finding of missing patterns in time series.
- We retrieve the two most similar windows with two queries on the data before the gap and data after the gap (this means that we process two separated databases) on the signal containing the gap using the new similarity measure.
- The final imputation values are the average of 2 vectors following and preceding of the two most similar windows.

And then we will compare both methods with published algorithms

Moreover, estimating the distribution of missing values and whole signals is very difficult, so our approaches make an assumption of effective patterns (or recurrent data, here a pattern corresponds to the sub-sequence before (resp. after) a gap) on each signal.

The rest of this chapter is organized as follows. Section 3.2 details the DTWUMI approach based on the combination of DTW and shape-feature extraction methods, validation procedure (including data presentation, several state-of-the-art multivariate time series imputation algorithms), results and discussion, and conclusions for this part. Section 3.3 investigates the second proposal, FSMUMI, with the same subsections to the Section 3.2. Finally, conclusions are drawn and future work is presented in Section 3.4.

3.2 Dynamic Time Warping-based uncorrelated multivariate time series imputation

3.2.1 DTWUMI - Proposed approach

In this part, we present our method for imputing missing intervals of low/un-correlated multivariate time series data based on DTW metric, named DTWUMI.

Let us recall some notations of multivariate time series and the concept of large gap.

A multivariate time series is represented as a matrix $X_{N \times M}$ with M collected signals of size N . $x(t, i)$ is the value of the i -th signal at time t . $x_t = \{x(t, i), i = 1, \dots, M\}$ is the feature vector at the t -th observation of all variables.

X is referred as incomplete time series when it contains missing values (or values are Not Available-NA). We define the term gap of T -size at position t as a portion of X where at least one signal of X between t and $t + T - 1$ containing consecutive missing values ($\exists i | \forall t \in [t, t + T - 1], x(t, i) = NA$).

Here, we deal with large missing values in low/un-correlated multivariate time series. For isolated missing values ($T = 1$) or small T -gap, classical techniques can be applied such as the mean or the median of available values [37, 38]. A T -gap is large when the duration T is longer than known change process. For instance, in phytoplankton study, T is equal to one hour for characterizing *Langmuir* cells and one day for algal bloom processes [6]. For small time series ($N < 10,000$) without knowledge about an application and its change process (this depends on each application), we set a large gap when $T \geq 5\%N$.

Figure 3.1 illustrates the mechanism of DTWUMI method.

The major idea of our approach consists in finding the most similar sub-sequence (Qs) to a

query (Q), with Q is the sub-sequence before (resp. after) a gap,

$$Q = X[t - T : t - 1] = \begin{bmatrix} x^1[t - T] & x^1[t - T + 1] & \dots & x^1[t - 1] \\ \dots & \dots & \dots & \dots \\ x^M[t - T] & x^M[t - T + 1] & \dots & x^M[t - 1] \end{bmatrix}$$

We then complete this gap by the following (resp. preceding) sub-sequence of the Q_s of the signal containing the gap.

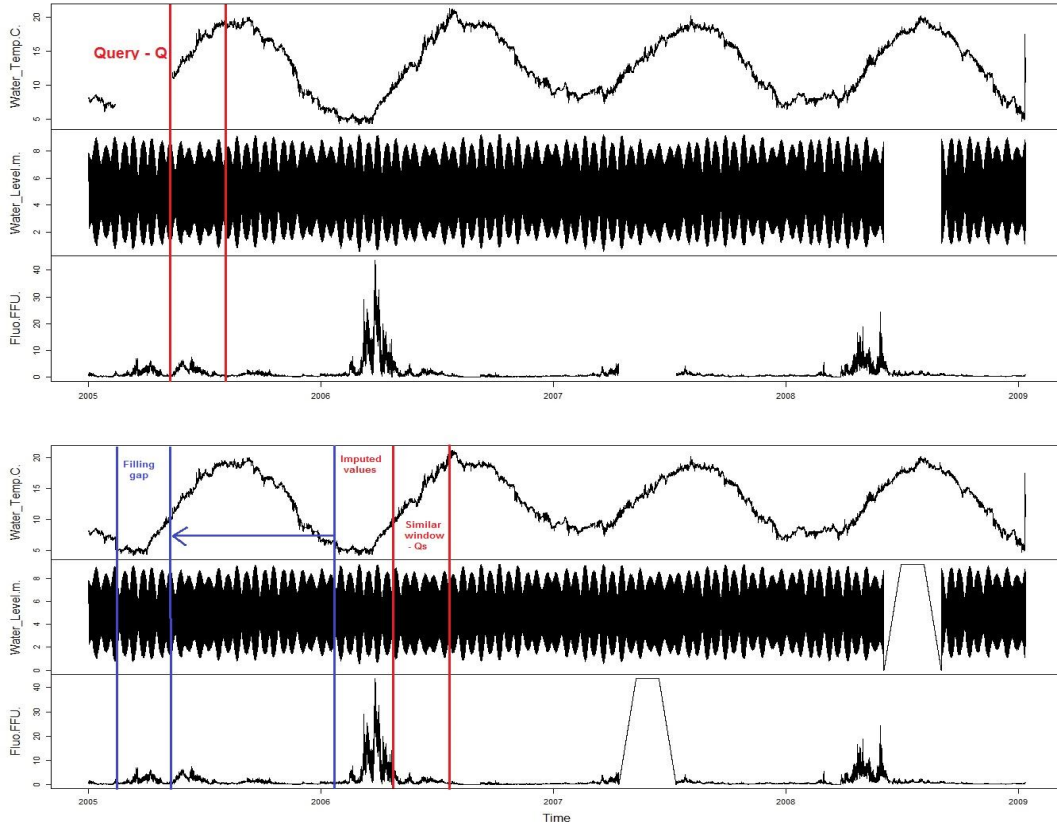


Figure 3.1: Illustration of the DTW-completion process: query building and similar sequence research, gap filling.

For multidimensional time series, the missing values may be on different variables. To deal with multivariate time series under DTW, the query and reference matrices must have no missing data. Hence, to increase the search space for similar values, in the proposed approach we make initial values for missing values. There are many ways to initialize these values, for example replacing missing values by 0, mean, or median, and so on. Here, on each signal we initially substitute missing values by the values generated from one trapezoidal curve multiply-

ing with the maximum of this signal. This makes it possible to manage the uncertainty of the imputation values. The trapezoid function f is defined as follows:

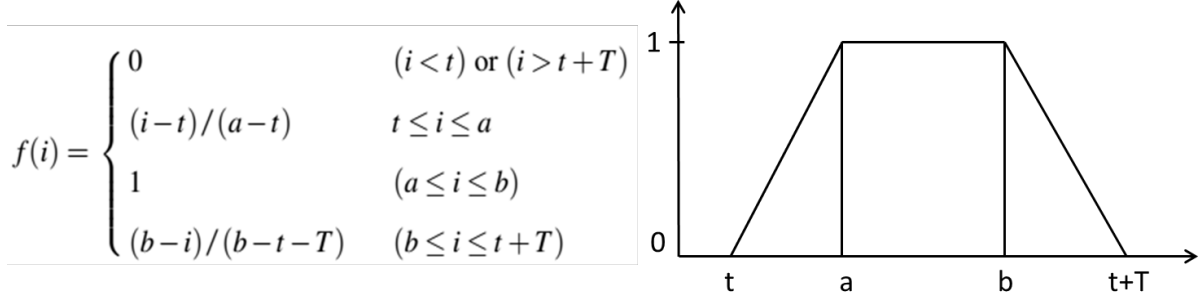


Figure 3.2: The trapezoid formula

To obtain the Q_s similar sub-sequence, we apply the principles of Dynamic Time Warping [7]. The dynamics and the shape of data before (resp. after) a gap are key point of this technique. Besides, conserving the same temporal window on all variables is another important factor of our algorithm. This means we create the query Q of size T on all variables (see figure 3.1) and look for the similar windows in the search database based on the elastic matching of multidimensional signals. Once the most similar window is identified, the previous window on the incomplete signal will be copied to the location of missing values.

In addition, the DTW algorithm requires long computational time. In order to decrease the computation time, before using DTW method to estimate imputation values, we deployed the shape-features extraction algorithm [52]. We only calculate DTW cost of the query and a reference window when the correlation between the shape-features of this window and the ones of the query is very high. The shape-features extraction algorithm is utilized because it better maintains the shape and dynamics of series through 9 global features (see [52] for more details).

3.2.2 Validation procedure

To validate our approach and compare with published methods (including MI, MICE, na.approx, missForest), we conduct experiments on 3 different datasets with the same protocol and gaps. The experiments process includes 3 steps as previously mentioned in Chapter 1. We assess these methods in terms of their efficacy of accuracy and shape between actual data and completion data using criteria for evaluation as defined in Chapter 1. In the following, we present the datasets and multivariate time series imputation methods.

3.2.2.1 Data presentation

Three multivariate time series are handled in this study. We choose one from KEEL repository, one simulated dataset (this permits to control the criterion of correlations and the amount of missing data) and one real dataset hourly collected by IFREMER (France) in the eastern English Channel.

NNGC1_F1_V1_003 (NNGC) dataset [93]: This time series contains transportation data (4 attributes and 1,745 instants) including highway traffic, traffic data of cars in tunnels, traffic at automatic payment systems on highways, traffic of individuals on subway systems, domestic aircraft flights, shipping imports, border crossings, pipeline flows and rail transportation. The data contains a time series of hourly frequency.

Simulated dataset: In the second experiment, a simulated dataset including 3 signals is produced in the following: For the first variable, we use 5 sine functions that have different frequencies and amplitudes $F = \{f_1, f_2, f_3, f_4, f_5\}$. Next, 3 various noise levels are added to data F , $S = \{F, F + noise1, F + noise2, F + noise3\}$. We then repeat S 4 times (this dataset has 32,000 sampled points). In this study, we treat with missing data in low/un-correlated multivariate time series. So to satisfy this condition, the two remaining signals are generated based on the first signal with the correlations between these signals are low ($\leq 0.1\%$). We apply the Corgen function of ecodist R-package [94] to create the second and the third variables.

MAREL-Carnot dataset [3]: The third experiment is conducted on MAREL-Carnot dataset. This dataset consists of nineteen series such as phosphate, salinity, turbidity, water temperature, fluorescence, water level,... that characterize seawater. These signals were collected from the 1st January 2005 to the 9th February 2009 at 20 minutes frequency. Here they were hourly sampled, so they have 35,334 time samples. But the data include many missing values, the size of missing data varies on each signal. For assessing the performance of the proposed method and comparing with other approaches, we chose a subgroup including fluorescence, water level, and water temperature (the water level and the fluorescence signals are complete data, while water temperature contains isolated missing values and gaps). We select these signals because their correlations are low.

After completing missing values, completion data will be compared with actual values in the full series to evaluate the ability of different imputation methods. Therefore, it is necessary to fill missing values in the water temperature. To ensure the fairness of all algorithms, filling in the water temperature series is performed by na.interp method ([53]).

3.2.2.2 Multivariate time series imputation algorithms

We compare our method with several commonly multivariate time series imputation approaches used state-of-the-art (including MI, MICE, na.approx, missForest). R language is applied to implement all these methods.

MI- Multiple Imputation

In the imputation methods introduced in Chapter 2 as na.approx, na.locf, . . . , each missing value is replaced by a value (in the literature, this is called a single imputation). Instead of completing a missing point by a single value, MI substitutes each missing value with a set of m plausible values [95]. MI procedure includes 3 steps (figure 3.3):

- Imputation: The missing data are completed m times to yield m complete data sets.
- Analysis: The m complete data sets are analyzed by using standard methods.
- Pooling: The m analyzed data sets are combined to a final result.

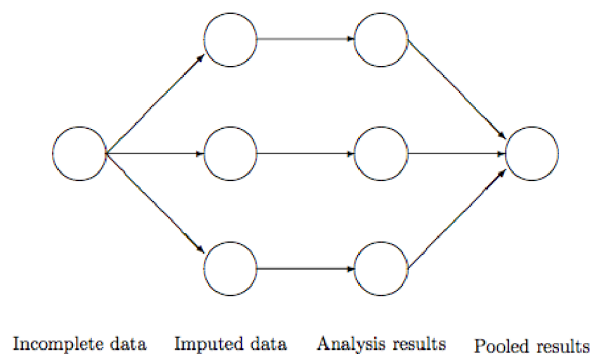


Figure 3.3: Schema of MI algorithm

Here, in this study we use mi R-package to complete incompleteness data [96]. This package constructs multiple imputation models and applies predictive mean matching method to estimate missing values. For each observation in a variable containing missing values, this method predicts imputed value by finding an observation (from available values) with the closest predictive mean to that variable. Bayesian models and weakly informative prior distributions are used to build more stable estimates of imputation models; multiple chains are run and convergence is assessed after a pre-specified number of iterations within each chain.

MICE - Multivariate Imputation via Chained Equations [97]: This method is based on the conditional (on all the other variables) distribution for each variable containing missing values to estimate imputed ones under the assumption that the missing data are missing at

At the end of a cycle, one imputed data set is generated. This process is iterated m time to produce m multiple data sets. And then these m sets are combined by applying rules of Rubin. m parameter should be specified by the user.

Linear interpolation - na.approx (zoo package) [56]: This algorithm uses a generic function with interpolated values to estimate missing data.

missForest [76]: This approach is based on random forest algorithm to fill in missing data, particularly in the case of mixed-type data. It involves 2 stages:

- The 1st stage: For each variable missForest builds a random forest model on the observed part.
- The 2nd stage: The model, is built in the first stage, is used to predict missing values in the variable.

The algorithm performs these two steps until a stopping criterion is met or the user specified maximum of iterations is reached. The difference between the previous and the new imputation data is computed after each iteration. The imputation process will stop as soon as the difference has become larger once. In other words, the last imputation was less accurate than the previous one. So, the final results are the imputation values of the before last iteration (excepting the case that the user provides a number of iterations). For further details see [76].

3.2.3 Results and discussion

For evaluating the results, we apply the experiment protocol as previously defined in the chapter 1. In the present study, 7 missing data levels are considered on 3 datasets. Gaps are built at rates 1%, 2%, 3%, 4%, 5%, 7.5% and 10% of the dataset size on every signal (here missing sequences on each variable of the MAREL Carnot series correspond to around 15 days (353 consecutive missing) to 5 months (3,533 NAs)). For each missing ratio, the algorithms are performed 5 times by randomly selecting the missing positions on the data. We then run 35 iterations for each data set.

Tables 3.1, 3.2 and 3.3 present the average performance evaluation of different imputation algorithms for NNGC, simulated and MAREL Carnot time series for the 6 indicators. The best results for each missing rate are highlighted in bold. These results confirm the good ability of DTWUMI for filling missing values in uncorrelated multivariate time series.

NNGC dataset: Table 3.1 shows a comparison of five imputation methods on NNGC dataset that has 7 missing ratios (1-10% missing values). We clearly find that missForest gives

the highest similarity, R^2 , FA2 and the lowest RMSE at every missing level. MICE is following the missForest method on these indicators. However, when considering on other indices such as FSD and FB, missForest only proves its performance at small missing rates ($\leq 3\%$). At larger missing levels (4%-7.5%), MICE provides the smallest FB indicator. And at 5%-10% missing rates MI gives best FSD. A lower value indicates better performance. The results can explain that NNGC dataset has high correlations between variables (approximate 0.79). MICE and missForest estimate missing data based on other observed variables. That is why these algorithms have better results and our algorithm does not prove its performance when completing datasets having high correlations. MI is also based on observed values for filling in missing data but under an assumption that all variables follow a multivariate normal distribution. So with this dataset, this method does not give good performance as MICE or missForest.

Simulated and MAREL Carnot datasets: From the results of tables 3.2 and 3.3, it is clear that missForest, MI, and MICE do not demonstrate their performance for completing missing data on these two datasets. For all missing rates, MissForest is ranked the second as considering similarity and RMSE indices (the simulation data) and the third or below for all indicators (MAREL Carnot series). Because these two datasets have very low correlations between variables, especially for the simulated series which is an almost uncorrelated dataset. That explains why, DTWUMI illustrates the best ability for imputation task: the highest similarity, R^2 , FA2 and the lowest RMSE, FSD for all missing ratios (table 3.5 - Simulated dataset). Regarding MAREL Carnot series, this dataset has low correlations (around 0.2), so that our approach, DTWUMI, does not show the capability to fill in missing values as it does in the simulated dataset (table 3.6 - MAREL Carnot dataset). However, this method definitely indicates its imputation performance when considering similarity, R^2 , FA2, RMSE indicators at every missing level. In particular, our method further proves the ability to fill in incomplete data with large missing rates (7.5% and 10% on MAREL Carnot dataset). These gaps correspond to 110.4 and 147.2 days sampled at hourly frequency.

With the NNGC series (table 3.1), the na.approx method always produces the worst result for every indicator. On the simulated and MAREL Carnot datasets, this method gives quite good results when comparing the quantitative performance: the lowest FB and/or FSD at some missing rates (simulated series), the second rank on similarity, R^2 , FA2 for all missing ratios (MAREL Carnot dataset). However, when looking at the shape of imputation values generated from of this method, it absolutely shows the worst shape (figure 3.5, 3.6).

In this study, we also carry out comparing the visualization performance of imputation val-

CHAPTER 3. IMPUTATION APPROACHES FOR UNCORRELATED MULTIVARIATE TIME SERIES

Table 3.1: Average imputation performance indices of various imputation methods on NNGC series (1745 collected points)

Gap size	Method	Accuracy indices			Shape indices		
		1-Sim	1- R^2	RMSE	FSD	FB	1-FA2
1%	na.approx	0.2	0.99	11786	0.41	0.19	0.52
	MI	0.1	0.32	5774	0.02	0.01	0.26
	MICE	0.03	0.06	2382	0.03	0.01	0.05
	missForest	0.02	0.02	1286	0.01	0.01	0.01
	DTWUMI	0.12	0.51	7591	0.03	0.12	0.3
2%	na.approx	0.18	0.96	11456	0.36	0.22	0.52
	MI	0.1	0.33	5644	0.04	0.05	0.31
	MICE	0.04	0.11	3025	0.02	0.01	0.05
	missForest	0.02	0.02	1210	0.01	0.01	0.01
	DTWUMI	0.12	0.51	7591	0.1	0.08	0.3
3%	na.approx	0.18	0.99	11329	0.66	0.29	0.55
	MI	0.1	0.29	5317	0.04	0.02	0.24
	MICE	0.03	0.11	3112	0.02	0.02	0.05
	missForest	0.02	0.02	1375	0.02	0.01	0.01
	DTWUMI	0.05	0.19	4219	0.05	0.08	0.08
4%	na.approx	0.18	0.99	11298	0.35	0.12	0.53
	MI	0.11	0.43	6647	0.05	0.06	0.3
	MICE	0.04	0.17	3730	0.02	0.01	0.08
	missForest	0.03	0.09	2405	0.06	0.03	0.05
	DTWUMI	0.1	0.48	6935	0.05	0.06	0.22
5%	na.approx	0.17	0.99	10848	0.73	0.26	0.54
	MI	0.11	0.43	6823	0.02	0.06	0.29
	MICE	0.04	0.14	3483	0.03	0.02	0.06
	missForest	0.03	0.09	2710	0.06	0.03	0.04
	DTWUMI	0.1	0.49	7116	0.05	0.04	0.22
7.5%	na.approx	0.19	0.99	11803	0.49	0.19	0.57
	MI	0.11	0.39	6408	0.01	0.05	0.28
	MICE	0.04	0.13	3375	0.02	0.01	0.05
	missForest	0.03	0.07	2197	0.05	0.02	0.03
	DTWUMI	0.04	0.14	3452	0.03	0.04	0.06
10%	na.approx	0.18	1	11419	0.62	0.25	0.56
	MI	0.1	0.35	5892	0.008	0.02	0.27
	MICE	0.04	0.13	3435	0.01	0.01	0.06
	missForest	0.02	0.05	1990	0.02	0	0.03
	DTWUMI	0.05	0.21	4402	0.02	0.04	0.08

3.2. Dynamic Time Warping-based uncorrelated multivariate time series imputation

Table 3.2: Average imputation performance indices of various imputation algorithms on simulated dataset (32,000 collected points)

Gap size	Method	Accuracy indices			Shape indices		
		1-Sim	1- R^2	RMSE	FSD	FB	1-FA2
1%	na.approx	0.126	0.994	1.99	0.52	1.86	0.81
	MI	0.14	0.999	2.22	0.12	1.89	0.79
	MICE	0.14	0.997	2.23	0.13	2.39	0.79
	missForest	0.11	0.996	1.69	0.89	5.49	0.85
	DTWUMI	0.085	0.51	1.22	0.01	5.86	0.58
2%	na.approx	0.11	0.998	1.99	0.48	2.41	0.8
	MI	0.13	0.997	2.31	0.06	7.12	0.8
	MICE	0.12	0.999	2.25	0.08	3.75	0.8
	missForest	0.1	0.998	1.7	0.94	2.48	0.86
	DTWUMI	0.064	0.45	1.17	0.01	0.79	0.55
3%	na.approx	0.11	0.998	1.88	0.69	2.08	0.81
	MI	0.13	1	2.27	0.03	2.63	0.8
	MICE	0.13	1	2.27	0.03	2.63	0.8
	missForest	0.1	1	1.71	0.91	2.49	0.85
	DTWUMI	0.064	0.45	1.16	0.01	1.72	0.54
4%	na.approx	0.11	0.999	2.14	0.42	2.08	0.79
	MI	0.12	1	2.3	0.03	5.66	0.8
	MICE	0.12	0.999	2.26	0.04	10.07	0.8
	missForest	0.09	1	1.73	0.94	3.81	0.86
	DTWUMI	0.065	0.46	1.19	0.01	4	0.56
5%	na.approx	0.12	1	2.12	0.66	2.09	0.79
	MI	0.12	1	2.27	0.04	3.67	0.79
	MICE	0.12	1	2.27	0.04	3.27	0.79
	missForest	0.1	1	1.75	0.94	1.92	0.85
	DTWUMI	0.07	0.46	1.19	0.01	2.55	0.58
7.5%	na.approx	0.11	1	1.86	0.84	2.09	0.82
	MI	0.12	0.999	2.24	0.03	7.95	0.79
	MICE	0.12	1	2.23	0.02	5.54	0.79
	missForest	0.1	1	1.69	0.9	2.7	0.86
	DTWUMI	0.078	0.58	1.37	0.01	5.57	0.6
10%	na.approx	0.11	1	2.01	0.46	2.02	0.79
	MI	0.12	1	2.24	0.02	2.18	0.79
	MICE	0.12	1	2.25	0.02	16.56	0.79
	missForest	0.09	1	1.7	0.91	1.35	0.86
	DTWUMI	0.064	0.47	1.18	0	4.49	0.56

CHAPTER 3. IMPUTATION APPROACHES FOR UNCORRELATED MULTIVARIATE TIME SERIES

Table 3.3: Average imputation performance indices of various imputation algorithms on Marel dataset (35,334 collected points)

Gap size	Method	Accuracy indices			Shape indices		
		1-Sim	1- R^2	RMSE	FSD	FB	1-FA2
1%	na.approx	0.068	0.15	1.62	0.07	0.03	0.21
	MI	0.19	0.44	4.48	0.42	0.24	0.48
	MICE	0.16	0.46	4.51	0.37	0.2	0.39
	missForest	0.15	0.26	3.2	0.35	0.18	0.32
	DTWUMI	0.056	0.04	1.02	0.11	0.05	0.15
2%	na.approx	0.07	0.13	1.73	0.06	0.12	0.18
	MI	0.17	0.41	3.81	0.23	0.12	0.43
	MICE	0.16	0.44	4.05	0.28	0.14	0.37
	missForest	0.13	0.24	2.76	0.24	0.14	0.26
	DTWUMI	0.06	0.04	1.07	0.1	0.03	0.16
3%	na.approx	0.08	0.17	1.8	0.09	0.07	0.19
	MI	0.21	0.49	4.53	0.41	0.33	0.47
	MICE	0.19	0.53	5.17	0.49	0.36	0.41
	missForest	0.18	0.37	4.09	0.39	0.37	0.36
	DTWUMI	0.056	0.06	1.07	0.09	0.02	0.12
4%	na.approx	0.057	0.09	1.68	0.06	0.07	0.22
	MI	0.15	0.41	4.51	0.31	0.2	0.47
	MICE	0.135	0.44	4.73	0.29	0.2	0.43
	missForest	0.12	0.22	3.46	0.31	0.18	0.34
	DTWUMI	0.048	0.05	1.27	0.06	0.05	0.19
5%	na.approx	0.064	0.11	1.81	0.06	0.06	0.21
	MI	0.15	0.41	4.36	0.21	0.21	0.44
	MICE	0.13	0.4	4.42	0.27	0.23	0.41
	missForest	0.12	0.23	3.52	0.28	0.23	0.28
	DTWUMI	0.054	0.08	1.59	0.12	0.09	0.13
7.5%	na.approx	0.07	0.3	3.2	0.19	0.16	0.24
	MI	0.14	0.54	4.76	0.26	0.17	0.48
	MICE	0.13	0.6	5.06	0.28	0.21	0.43
	missForest	0.1	0.41	3.35	0.28	0.14	0.33
	DTWUMI	0.061	0.25	2.11	0.12	0.08	0.18
10%	na.approx	0.083	0.23	3.09	0.15	0.16	0.27
	MI	0.13	0.43	4.35	0.16	0.14	0.46
	MICE	0.12	0.5	4.78	0.21	0.18	0.41
	missForest	0.1	0.29	3.47	0.25	0.15	0.3
	DTWUMI	0.065	0.2	2.58	0.12	0.13	0.2

ues generated from different methods. Figure 3.5 presents the shape of imputed values yielded by five different methods on the NNGC series. The missForest approach proves again the capability to deal with the successive missing values for a correlated dataset. The form of imputation values produced from missForest method is very close to the form of true values. However, with low-correlated dataset as MAREL Carnot data, missForest no longer demonstrates its ability (figure 3.6). In this case, our approach confirms its performance for the imputation task. The shape of DTWUMI’s imputed values is almost identical to the form of true values (figure 3.6).

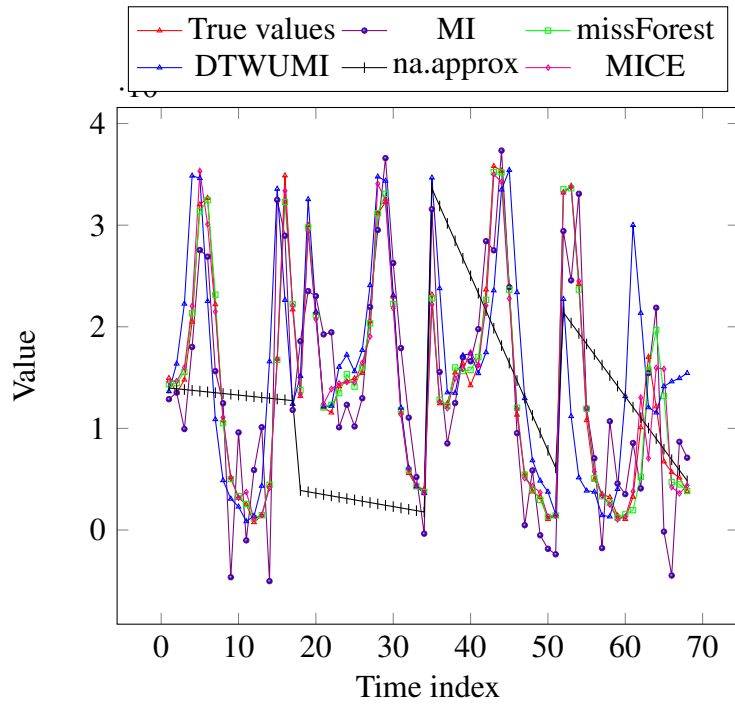


Figure 3.5: Visual comparison of imputed values of different imputation methods with true values on NNGC series with the gap size of 17 on each signal.

3.2.4 Conclusion

In this part, we propose an effective method for uncorrelated multivariate time series imputation, namely DTWUMI. We have performed several experiments on artificial and real datasets to demonstrate the capability of our approach and compared it with published algorithms (na.approx, MI, MICE, and missForest) on quantitative and shape indicators. The visual performance of these methods is also evaluated. The obtained results clearly show that our approach provides better performance than the other existing methods in case of time series having low or non-correlations between variables and large gap(s). However, the proposed algorithm is

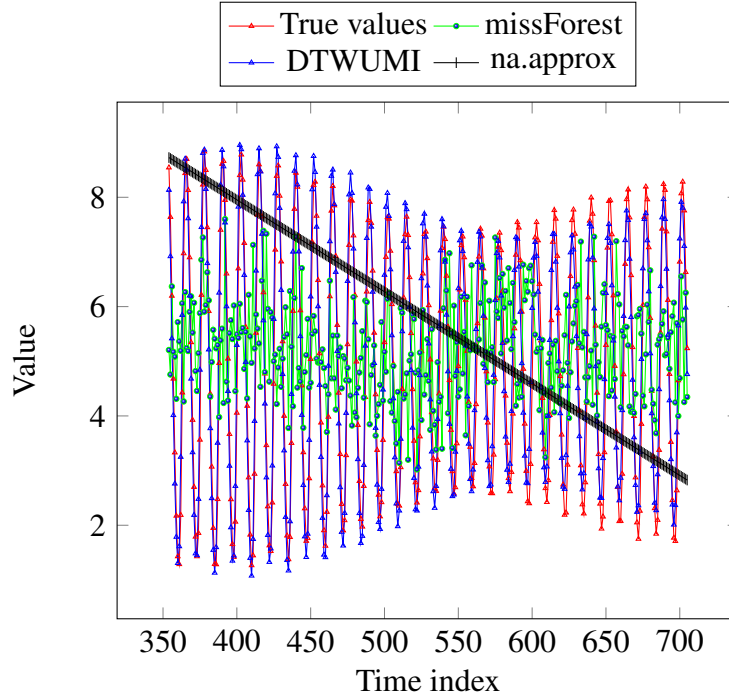


Figure 3.6: Visual comparison of imputed values of different imputation methods with true values on MAREL Carnot dataset with the gap size of 353 on the 2nd signal.

requires to applications with the necessary assumption of recurring data and sufficient large datasets size.

3.3 Proposed method based on an hybrid similarity measure

In the previous section, we have presented our first proposal to complete large gaps in uncorrelated multivariate time series using the DTW cost as a similarity criterion. In this section we continue to introduce our second proposal for the imputation task by exploiting the property of data (i.e uncorrelated between variables) and by taking into account an uncertainty factor. In this way we develop a new similarity measure which is used for finding similar patterns in each signal.

In this section, before focusing on our algorithms, we present a review on fuzzy similarity measure and its applications.

3.3.1 Methods based on fuzzy similarity measure

Indeed similarity-based approaches are a promising tool for time series analysis. However, many of these techniques rely on parameter tuning, and they may have shortcomings due to

dependencies between variables. The objective of this study is to fill large missing values in *uncorrelated multivariate time series*. Thus, we have to deal with a high level of uncertainty. There are many methods and theories to model uncertainties such as probabilistic models, belief function theory [98], Dempster-Shafer [99], fuzzy sets [91], etc. Mikalsen *et al.* [100] proposed to use GMM (Gaussian mixture models) and cluster kernel to deal with uncertainty. This method needs ensemble learning with numerous learning datasets that are not available in our case at the moment (marine data). So we have chosen to model this global uncertainty using fuzzy sets (FS) introduced by Zadeh [91]. These techniques consider that measurements have inherent imprecision rather than randomness.

Uncertainty is classically presented using three conceptually distinctive characteristics: fuzziness, randomness and incompleteness. This classification is interesting for many applications, like sensor management (image processing, speech processing, time series processing) and practical decision making. This paper focuses on (sensor) measurements treatment, but is also relevant for other applications.

Incompleteness often affects time series prediction (time series obtained from marine data such as salinity, temperature, ...). So it seems natural to use fuzzy similarity between sub-sequences of time series to deal with these three kinds of uncertainties (fuzziness, randomness and incompleteness). Fuzzy sets are now well-known and we only need to remind the basic definition of "FS". Considering the universe X , a fuzzy set $A \in X$ is characterized using a fuzzy membership function μ_A :

$$\mu_A : X \rightarrow [0, 1], \quad (3.1)$$

where $\mu_A(x)$ represents the membership of x to A and is associated to the uncertainty of x . In our case, we will consider similarity values between the sub-sequences as defined in the following. One solution to deal with uncertainty brought by multivariate time series is to use the concept of fuzzy time series [101]. In this framework, the variable observations are considered as fuzzy numbers instead of real numbers. In our case the same modelling is used considering distance measures between sub-sequences and then we compute the fuzzy similarities to find the similar successive values in time series.

Fuzzy similarity is a generalization of the classical concept of equivalence and defines the resemblance between two objects (here sub-sequences of time series). Similarity measures of fuzzy values have been compared in [102] and have been extended in [16]. In [102], Pappis and Karacapilidis presented three main kinds of similarity measures of fuzzy values, including:

- measures based on the operations of union and intersection,
- measures based on the maximum difference,
- measures based on the difference and the sum of membership grades.

In [103, 104], the authors used these definitions to propose a distance metric for a space of linguistic summaries based on fuzzy protoforms. Almeida *et al.* extended this work to put forward linguistic summaries of categorical time series [105]. The introduced similarity measure takes into account not only the linguistic meaning of the summaries, but also the numerical characteristic attached to them. In the same way, Gupta *et al.* [15] introduced this approach to create an hybrid similarity measure based on fuzzy logic. The approach is used to retrieve relevant documents. In the other research, Al-Shamri and Al-Ashwal presented fuzzy weightings of popular similarity measures for memory-based collaborative recommend systems [17].

Concerning the similarity between two sub-sequences of time series, we can use the DTW cost as a similarity measure. However, to deal with the high level of uncertainty of the processed signals, numerous similarity measures can be used to compute similarity like the cosine similarity, Euclidean distance, Pearson correlation coefficient, and so on. Moreover, a fuzzy-weighted combination of scores generated from different similarity measures could comparatively achieve better retrieval results than the use of a single similarity measure [15, 17].

Based on the same concepts, we propose to use a fuzzy rules interpolation scheme between grades of membership of similarities fuzzy values. This method makes it possible to build a new hybrid similarity measure for finding similar sub-sequence in time series.

3.3.2 FSMUMI-Proposed approach

The proposed imputation method is based on the retrieval and the similarity comparison of available sub-sequences (namely Fuzzy Similarity Measure-based Uncorrelated Multivariate Imputation, FSMUMI). In order to compare the sub-sequences, we create a new similarity measure applying a multiple fuzzy rules interpolation.

Figure 3.7 demonstrates the mechanism of FSMUMI approach. Without loss of generality, in this figure, we consider a multivariate time series including 3 variables whose correlations are low.

The proposed approach involves three major stages. The first stage is to build two queries Qa and Qb . The second stage is devoted to find the most similar windows to the queries.

3.3. Proposed method based on an hybrid similarity measure

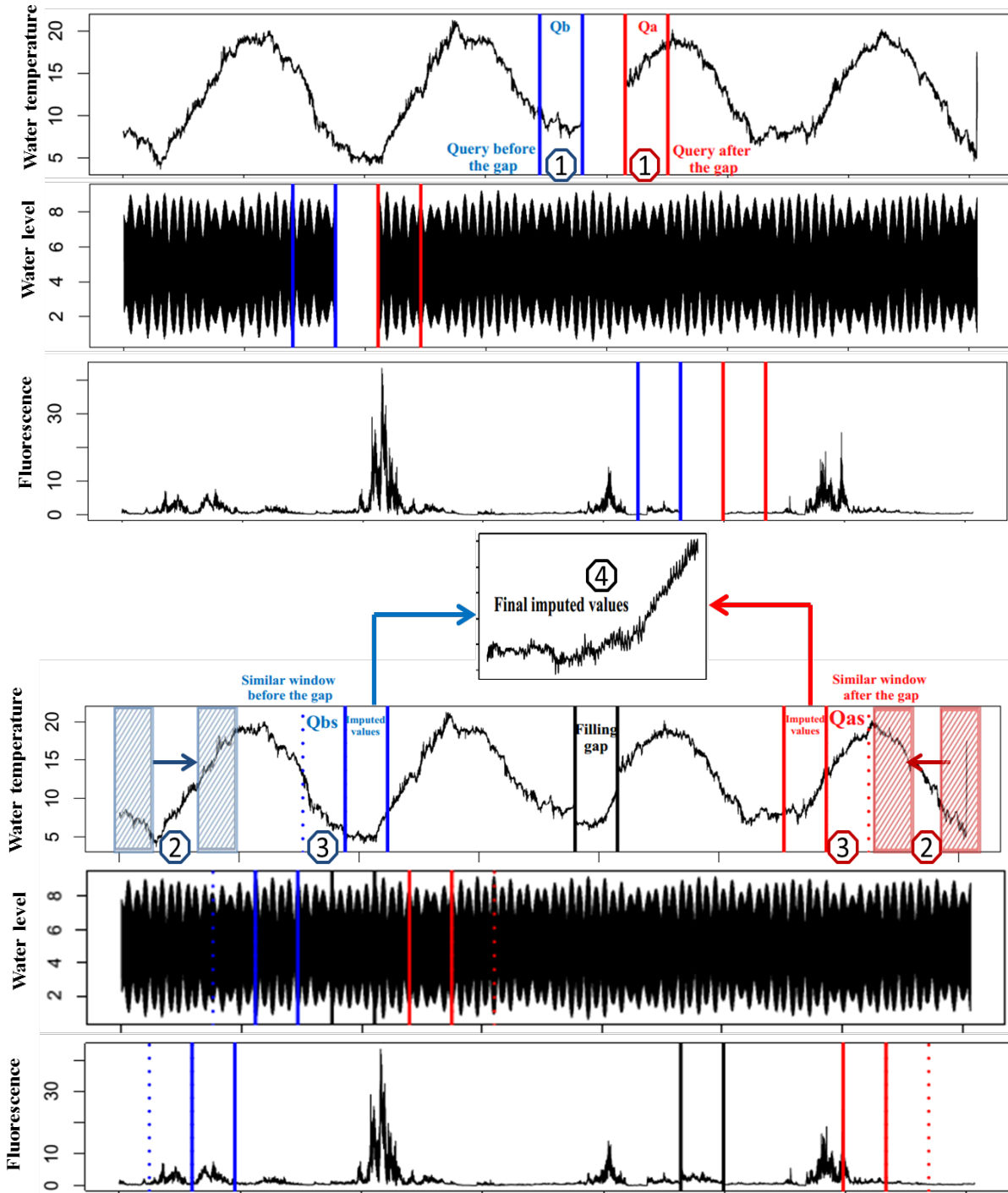


Figure 3.7: Scheme of the completion process: 1-Building queries, 2- Comparing sliding windows, 3- Selecting the most similar windows, 4- Completing gap.

This stage includes two minor steps, comparing sliding windows to queries by using the new similarity measure and selecting the similar windows Qas and Qbs . Finally, the imputation values are computed by averaging values of the window following Qbs and the one preceding Qas to complete the gap.

This method focus on filling large missing values in low/un-correlated multivariate time series. For this type of data, we cannot take advantage of the relations between features to estimate missing values. So we must base our approach on observed values on each signal to complete missing data on itself. This means that we can complete missing data on each variable, one by one. Further, an important point of our approach is that each incomplete signal is processed as two separated time series, one time series before the considered gap and one time series after this gap. This allows to increase the search space for similar values. Moreover, applying the proposed process (one by one), FSMUMI makes it possible to handle the problem of wholly missing variables (missing data at the same time index in the all variables).

In the next section, we present the way to compute the new similarity measure between sub-sequences. Then, we provide details of the proposed approach to impute the successive missing values of low/un-correlated multivariate time series.

3.3.2.1 Fuzzy weighted similarity measure between sub-sequences

To introduce a new similarity measure using multiple fuzzy rules interpolation to solve the missing problem, two questions arise here: which measures will be taken as fuzzy? How can they be "fuzzified"?

To answer the first question, we take into account 3 different distance measures between two sub-sequences Q ($Q = \{q_i, i = 1, \dots, T\}$) and R ($R = \{r_i, i = 1, \dots, T\}$) including: Cosine distance, Euclidean distance (these two measures are widely used in the literature) and Similarity distance (this one was presented in our previous study [90]). These three measures are defined as follows:

- Cosine distance is computed by eq 3.2. This coefficient presents the cosine of the angle between Q and R

$$Cosine(Q, R) = \frac{\sum_{i=1}^T q_i \cdot r_i}{\sum_{i=1}^T (q_i)^2 \cdot \sum_{i=1}^T (r_i)^2} \quad (3.2)$$

- Euclidean distance is calculated by eq 3.3

$$ED^*(Q,R) = \sqrt{\sum_{i=1}^T (q_i - r_i)^2} \quad (3.3)$$

To satisfy the input condition of fuzzy logic rules, we normalize this distance to $[0, 1]$ by this function $ED = 1 / (1 + ED^*(q, r))$.

- Similarity measure is defined by the function 3.4. This measure indicates the similarity percentage between Q and R

$$Sim(Q,R) = \frac{1}{T} \sum_{i=1}^T \frac{1}{1 + \frac{|q_i - r_i|}{\max(Q) - \min(Q)}} \quad (3.4)$$

To answer the second question, we use these 3 distance measures (or attributes) to generate 4 fuzzy similarities (see figure 3.9), then applied to a fuzzy rule interpolation scheme (see figure 3.8) using the 3 attributes which provides 3 coefficients to calculate a new interpolated similarity measure. The universe of discourse of each distance measure is normalized to the value 1.

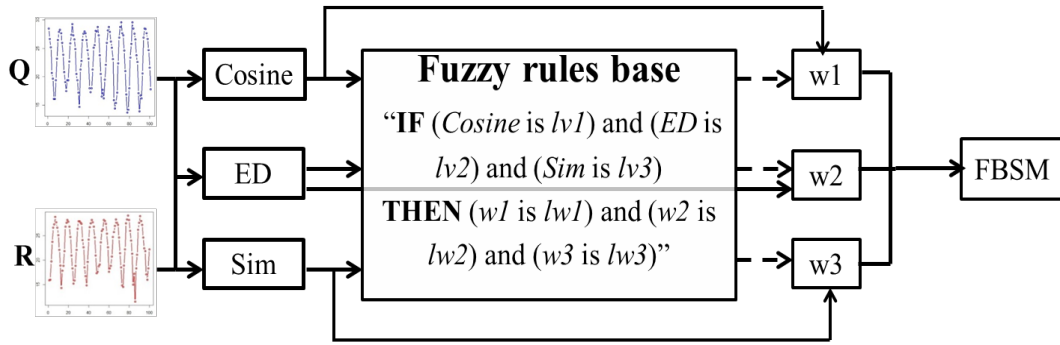


Figure 3.8: Computing scheme of the new similarity measure

And finally, the new (interpolated) similarity measure is given by eq 3.5:

$$FBSM = w1 * Cosine(Q,R) + w2 * ED(Q,R) + w3 * Sim(Q,R) \quad (3.5)$$

where $w1$, $w2$, $w3$ are the weights of the Cosine, ED and Sim measures respectively. Thus uncertainty modelled using FS is kept during the similarity computation and makes it possible

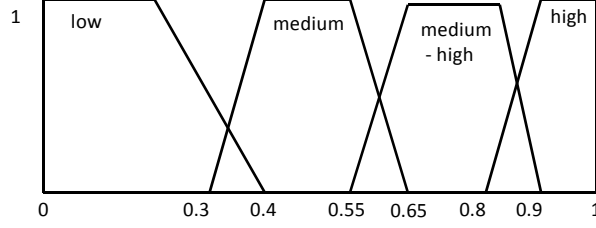


Figure 3.9: Membership function of fuzzy similarity values

to deal with a high level of uncertainty as shown in the sequel. The coefficients w_i are generated from the fuzzy system (figure 3.8). We use FuzzyR R-package [106] to develop this system. All input and output variables are expressed by 4 linguistic terms as low, medium, medium-high and high. A trapezoidal membership function is handled in this case to match input and output spaces to a degree of membership (figure 3.9). The multiple fuzzy rules interpolation is applied to create the fuzzy rules base. Thus, in our case 64 fuzzy rules are introduced. Each fuzzy rule is presented in the following form:

Rule R: **IF** (*Cosine* is lv_1) and (*ED* is lv_2) and (*Sim* is lv_3) **THEN** (w_1 is lw_1) and (w_2 is lw_2) and (w_3 is lw_3)

in which $lvi, lwi \in \{\text{low, medium, medium-high, high}\}$, and $i = 1, 2, 3$.

3.3.2.2 FSMUMI approach

This part presents the detail of FSMUMI method. The proposed model is described in Algorithm 2 and is mainly divided into three phases:

- The first phase - Building queries (cf. 1 in Fig 3.7)

For each incomplete signal and each T -gap, two referenced databases are extracted from the original time series and two query windows are built to retrieve similar windows. The data before the gap (noted Db) and the data after this gap (denoted Da) are considered as two separated time series. We noted Qb is the sub-sequence before the gap and Qa is the respective sub-sequence after the gap. These query windows have the same size T as the gap.

- The second phase - Finding the most similar windows (cf. 2 and 3 in Fig 3.7)

For the Db database, we build sliding reference windows (noted R) of size T . From these R windows, we retrieve the most similar window (Qbs) to the Qb query using the new

Algorithm 2 FSMUMI algorithm

Input: $X = \{x^1, x^2, \dots, x^M\}$: incomplete uncorrelated multivariate time series

N : size of time series

t : index of a gap (position of the first missing of the gap)

T : size of the gap

$step_threshold$: increment for finding a threshold

$step_sim_win$: increment for finding a similar window

Output: Y - completed (imputed) time series

```

1: for each incomplete signal  $x^j \in X$  do
2:   for each gap at  $t$  index in  $x^j$  do
3:     Divide  $x^j$  into two separated time series  $Da, Db$ :  $Da = x^j[t + T : N], Db = x^j[1 : t - 1]$ 
4:     Completing all lines containing missing parameter on  $Da, Db$  by a max trapezoid function
5:     Construct queries  $Qa, Qb$ -temporal windows after and before the gap  $Qa = Da[1 : T], Qb = Db[t - T + 1 : t - 1]$ 
6:     for  $Db$  data do
7:       Step a: Find the threshold in the  $Db$  database
8:        $i \leftarrow 1; FSM \leftarrow NULL$ 
9:       while  $i \leq length(Db)$  do
10:         $k \leftarrow i + T - 1$ 
11:        Create a reference window:  $R(i) = Db[i : k]$ 
12:        Calculate a fuzzy-based similarity measure between  $Qb$  and  $R(i)$ :  $fbsm$ 
13:        Save the  $fbsm$  to  $FMS$ 
14:         $i \leftarrow i + step\_threshold$ 
15:       end while
16:       return  $threshold = \max\{FBMS\}$ 
17:       Step b: Find similar windows in the  $Db$  database
18:        $i \leftarrow 1; Lopb \leftarrow NULL$ 
19:       while  $i \leq length(Db)$  do
20:         $k \leftarrow i + T - 1$ 
21:        Create a reference window:  $R(i) = Db[i : k]$ 
22:        Calculate a fuzzy-based similarity measure between  $Qb$  and  $R(i)$ :  $fbsm$ 
23:        if  $fbsm \geq threshold$  then
24:          Save position of  $R(i)$  to  $Lopb$ 
25:        end if
26:         $i \leftarrow i + step\_sim\_win$ 
27:       end while
28:       return position of  $Qbs$  - the most similar window to  $Qb$  having the maximum fuzzy similarity measure in the  $Lopb$  list.
29:     end for
30:   for  $Da$  data do
31:     Perform Step a and Step b for  $Da$  data
32:     return position of  $Qas$  - the most similar window to  $Qa$ 
33:   end for
34:   Replace the missing values at the position  $t$  by average vector of the window after  $Qbs$  and the one previous  $Qas$ 
35: end for
36: end for
37: return  $Y$  - imputed time series

```

similarity measure $fbsm$ as previously defined in subsection 3.3.2.1. Details are in the following:

We first find the threshold, which allows to consider two windows to be similar. For each increment $step_threshold$, we compute a $fbsm$ similarity measure between a sliding window R and the query Qb . The $threshold$ is the maximum value obtained from the all $fbsm$ calculated (**Step a:** in Algorithm 2).

We then find the most similar window to the Qb query. For each increment similar window $step_sim_win$, a $fbsm$ of a R sliding reference and the Qb query is estimated. We then compare this $fbsm$ to the $threshold$ to determine if this R reference is similar to the Qb query. We finally choose the most similar window Qbs with the maximum $fbsm$ of all the similar windows (**Step b:** in Algorithm 2).

The same process is performed to find the most similar window Qas in Da data.

In the proposed approach, the dynamics and the shape of data before and after a gap are a key-point. This means that we take into account both queries Qa (after the gap) and Qb (before the gap). This makes it possible to find out windows that have the most similar dynamics and shape to the queries.

- The third phase (cf. 4 in Fig 3.7)

When results from both referenced time series are available, we fill in the gap by averaging values of the window previous Qas and the one following Qbs . The average values are used in our approach because model averaging makes the final results more stable and unbiased [107].

3.3.3 Validation procedure

To analyze the relevance of the proposed approach, it is important to compare with state-of-the-art methods. This validation step will be conducted on the main application of this thesis. Our approach is compared with well-known methods (including Amelia II, FcM, MI, MICE, missForest, na.approx, and DTWUMI) and experiments are performed on three multivariate time series with the same protocol and the same gaps. The experiments process includes 3 steps as previously mentioned in Chapter 1. These methods are assessed in terms of their efficacy of accuracy and shape between true values and completion data using criteria for evaluation

as defined in Chapter 1. The datasets and multivariate time series imputation methods are described in detail below.

3.3.3.1 Datasets description

For assessment of the proposed approach and comparison of its performance to several published algorithms, we use 3 multivariate time series, one from UCI Machine Learning repository, one simulated dataset (this allows us to handle the correlations between variables and percentage of missing values) and finally a real time series hourly sampled by IFREMER (France) in the eastern English Channel. The two last datasets (**Simulated dataset** and **MAREL-Carnot dataset**) have been mentioned in the previous part (DTWUMI).

- **Synthetic dataset** [108]: The data are synthetic time series, including 10 features, 100,000 sampled points. All data points are in the range -0.5 to +0.5. The data appear highly periodic, but never exactly repeat. They have structure at different resolutions. Each of the 10 features is generated by independent invocations of the function:

$$y = \sum_{i=3}^7 \frac{1}{2^i} \sin(2\pi(2^{2+i} + \text{rand}(2^i))t); 0 \leq t \leq 1 \quad (3.6)$$

where $\text{rand}(x)$ produces a random integer between 0 and x .

These data are very large so we choose only a subset of 3 signals for performing experiments.

- **Simulated dataset**: see the section 3.2.2.1.
- **MAREL-Carnot dataset**: see the section 3.2.2.1.

3.3.3.2 Multivariate imputation approaches

In the present study, we perform a comparison of the proposed algorithm with 7 other approaches (comprising Amelia II, FCM, MI, MICE, missForest, na.approx, and DTWUMI) for the imputation of multivariate time series. We use R language to execute all these algorithms.

1. **Amelia II** (Amelia II R-package) [109]: This method supposes that all the variables in a dataset have Multivariate Normal Distribution (MVN) and missing data are Missing at Random. Figure 3.10 illustrates different steps of this approach.

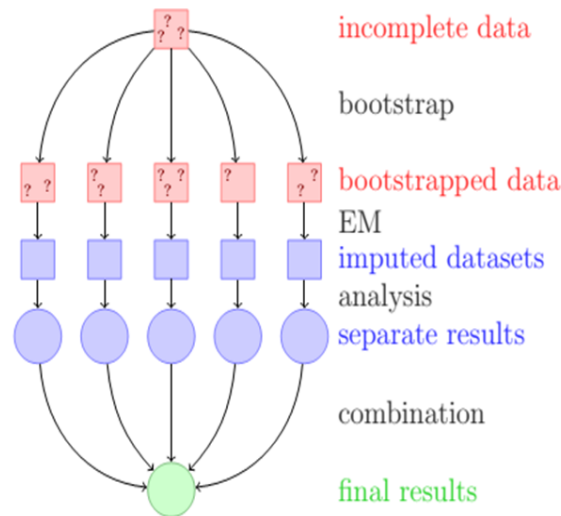


Figure 3.10: A schematic of Amelia II multiple imputation with the EMB algorithm.

The method uses the familiar expectation-maximization algorithm on multiple bootstrapped samples of the original incomplete data to draw values of the complete data parameters. The algorithm then draws imputed values from each set of bootstrapped parameters, replacing the missing values with these drawn values.

2. **FcM-Fuzzy c -means based imputation:** This approach involves 2 steps. The first step is to group the whole data into k clusters using fuzzy- c means technique. A cluster membership for each sample and a cluster center are generated for each feature. The second step is to fill in the incomplete data by using the membership degree and the center centroids [79]. We base on the principles of [79] and use the c -means function [110] to develop this approach.
3. **MI - Multiple Imputation** (MI R-package) [96]: This method has been presented in section 3.2.2.2.
4. **MICE - Multivariate Imputation via Chained Equations** (MICE R-package) [97]: This method has been presented in section 3.2.2.2.
5. **missForest** (missForest R-package) [76]: This method has been presented in section 3.2.2.2.
6. **Linear interpolation - na.approx** (zoo R-package) [56]: This method has been presented in section 3.2.2.2.

7. **DTWUMI** [111]: In the previous section, we have introduced details of this method.

3.3.4 Results and discussion

In comparison with our previous proposal and state-of-the art approaches, we implemented the same protocol and evaluation criteria: seven missing data levels on three large uncorrelated datasets. On each signal, we build simulated gaps in the complete signal with different rates ranging from 1%, 2%, 3%, 4%, 5%, 7.5% and 10% of the data (here the biggest gap of synthetic dataset is 10,000 missing values). For every missing ratio, the approaches are run 5 times by randomly choosing the positions of missing on the data. We then perform 35 iterations for each dataset.

This section provides experiment results obtained from the proposed approach and compares its ability with the seven published approaches. Results are discussed in three parts, i.e quantitative performance, visual performance and execution times.

3.3.4.1 Quantitative performance comparison

Tables 3.4, 3.5, 3.6 illustrate the average ability of various imputation methods for synthetic, simulated and MAREL-Carnot time series using 6 measurements as previously defined. For each missing level, the best results are highlighted in bold. These results demonstrate the improved performance of FSMUMI to complete missing data in low/uncorrelated multivariate time series.

Synthetic dataset: Table 3.4 presents a comparison of 8 imputation methods on synthetic dataset that contains 7 missing data levels (1-10%). The results clearly show that when a gap size is greater than 2%, the proposed method yields the highest similarity, R^2 , FA2 and the lowest RMSE, FB. With this dataset, na.approx gives the best performance at the smallest missing data level for all indices and is ranked second for other ratios of missing values (2-5%) for similarity and FA2, RMSE (2-4%), and R^2 (the 1st rank at 2% missing rate, the 2nd at 3%, 5%). The results can explain that the synthetic data are generated by a function (eq. 3.6). na.approx method which applies the interpolation function to estimate missing values. So it is easy to find a function to generate values that are approximate real values when missing data rates are small. But this work is more difficult when the missing sample size rises, that is why the ability of na.approx decreases as missing data levels increase, especially at 7.5% and 10% rates. Although this dataset never exactly repeats itself and our approach is proposed under

CHAPTER 3. IMPUTATION APPROACHES FOR UNCORRELATED MULTIVARIATE TIME SERIES

the assumption of recurrent data but the FSMUMI approach proves its performance for the imputation task even if the missing size increases.

Among the considered methods, the FcM-based approach is less accurate at lower missing rates but it provides better results at larger missing ratios as regards the accuracy indices.

Table 3.4: Average imputation performance indices of various imputation algorithms on synthetic dataset (100,000 collected points)

Gap size	Method	Accuracy indices			Shape indices		
		1-Sim	1- R^2	RMSE	FSD	FB	1-FA2
1%	FSMUMI	0.136	0.261	0.051	0.358	3.253	0.364
	Amelia	0.275	0.999	0.143	0.409	2.252	0.773
	FcM	0.231	0.722	0.096	1.889	2.208	0.996
	MI	0.275	0.999	0.142	0.421	2.091	0.773
	MICE	0.258	0.944	0.13	0.406	2.452	0.72
	missForest	0.248	0.915	0.122	0.389	3.976	0.744
	na.approx	0.052	0.066	0.019	0.054	0.29	0.074
	DTWUMI	0.257	0.713	0.88	0.725	0.405	0.69
2%	FSMUMI	0.1	0.295	0.046	0.155	0.395	0.337
	Amelia	0.259	0.998	0.147	0.275	2.005	0.803
	FcM	0.208	0.686	0.104	1.863	2.289	0.987
	MI	0.259	0.998	0.147	0.268	2.11	0.81
	MICE	0.244	0.968	0.14	0.255	7.616	0.759
	missForest	0.239	0.968	0.133	0.279	3.156	0.792
	na.approx	0.104	0.278	0.047	0.224	0.398	0.347
	DTWUMI	0.237	0.775	0.867	0.509	8.449	0.646
3%	FSMUMI	0.113	0.341	0.056	0.219	0.852	0.322
	Amelia	0.218	0.911	0.127	0.133	6.128	0.76
	FcM	0.214	0.601	0.1	1.832	1.759	0.989
	MI	0.253	0.993	0.141	0.236	2.295	0.775
	MICE	0.21	0.873	0.118	0.208	5.118	0.703
	missForest	0.188	0.796	0.102	0.215	1.846	0.627
	na.approx	0.148	0.43	0.072	0.372	2.382	0.577
	DTWUMI	0.231	0.799	0.874	0.332	27.952	0.69
4%	FSMUMI	0.06	0.146	0.037	0.099	0.738	0.299
	Amelia	0.208	1	0.14	0.213	2.171	0.807
	FcM	0.155	0.759	0.095	1.85	2.09	0.986
	MI	0.208	0.999	0.14	0.196	2.302	0.807

3.3. Proposed method based on an hybrid similarity measure

	MICE	0.209	0.987	0.138	0.22	3.748	0.801
	missForest	0.196	0.968	0.127	0.216	3.94	0.827
	na.approx	0.145	0.721	0.092	0.252	5.251	0.689
	DTWUMI	0.148	0.586	0.918	0.185	12.688	0.719
	FSMUMI	0.055	0.132	0.032	0.058	0.098	0.201
	Amelia	0.214	0.997	0.15	0.147	2.238	0.79
	FcM	0.179	0.715	0.108	1.818	2.194	0.993
5%	MI	0.231	0.996	0.167	0.206	3.094	0.808
	MICE	0.221	0.968	0.152	0.222	2.3	0.79
	missForest	0.212	0.944	0.143	0.315	4.547	0.819
	na.approx	0.16	0.8	0.118	0.352	18.217	0.622
	DTWUMI	0.186	0.885	0.88	0.213	0.723	0.694
	FSMUMI	0.049	0.071	0.027	0.069	0.505	0.184
	Amelia	0.197	0.998	0.147	0.045	1.305	0.792
	FcM	0.158	0.809	0.104	1.813	1.866	0.991
7.5%	MI	0.2	0.992	0.15	0.038	1.645	0.797
	MICE	0.205	0.988	0.15	0.057	10.744	0.799
	missForest	0.188	0.97	0.136	0.284	4.396	0.812
	na.approx	0.192	0.971	0.142	0.669	2.163	0.712
	DTWUMI	0.133	0.653	0.908	0.064	1.113	0.571
	FSMUMI	0.061	0.181	0.043	0.114	0.511	0.26
	Amelia	0.202	0.999	0.147	0.034	4.062	0.788
	FcM	0.164	0.872	0.104	1.837	2.201	0.992
10%	MI	0.21	0.997	0.155	0.12	2.954	0.785
	MICE	0.209	0.996	0.15	0.055	3.994	0.779
	missForest	0.194	0.97	0.135	0.308	3.024	0.811
	na.approx	0.183	0.997	0.129	0.372	1.455	0.719
	DTWUMI	0.155	0.782	0.893	0.026	1.182	0.626

Simulated dataset: Table 3.5 illustrates the evaluation results of various imputation algorithms on the simulated dataset. The best values for each missing level are highlighted in bold. Our proposed method outperforms other methods for the imputation task on accuracy indices: the highest similarity, R^2 and the lowest RMSE at every missing ratio. However, when considering other indices such as FA2, FSD and FB, FSMUMI no longer shows its performance. It gains only at a 4% rate for the FB index and at 10% ratio for FA2. In contrast to FSMUMI, DTWUMI provides the best results for FSD indicator at all missing levels and FA2 at the first 5 missing ratios (from 1% to 5%).

CHAPTER 3. IMPUTATION APPROACHES FOR UNCORRELATED MULTIVARIATE TIME SERIES

Different from the synthetic dataset, on the simulated dataset, the FcM-based method is always ranked the third at all missing rates for similarity and RMSE indicators. Following FcM is missForest algorithm for the both indices.

Although, in the second experiment, data are built by various functions but they are quite complex so that na.approx does not provide good results.

Table 3.5: Average imputation performance indices of various imputation algorithms on simulated dataset (32,000 collected points)

Gap size	Method	Accuracy indices			Shape indices		
		1-Sim	1- R^2	RMSE	FSD	FB	1-FA2
1%	FSMUMI	0.083	0.515	1.033	0.159	2.51	0.574
	Amelia	0.157	1	2.206	0.232	3.619	0.794
	FcM	0.118	0.998	1.483	1.98	2.015	0.998
	MI	0.16	0.999	2.241	0.2	0.915	0.799
	MICE	0.159	0.998	2.201	0.214	1.449	0.801
	missForest	0.127	0.998	1.608	0.836	12.034	0.861
	na.approx	0.146	0.992	1.901	0.393	18.997	0.777
	DTWUMI	0.09	0.552	1.156	0.007	6.022	0.562
2%	FSMUMI	0.068	0.487	1.166	0.194	1.971	0.611
	Amelia	0.12	0.998	2.312	0.107	2.191	0.794
	FcM	0.093	0.999	1.672	1.985	1.96	0.998
	MI	0.12	1	2.307	0.123	3.949	0.789
	MICE	0.119	0.999	2.282	0.114	8.881	0.789
	missForest	0.096	1	1.769	0.941	2.777	0.858
	na.approx	0.118	1	2.261	0.721	2.059	0.786
	DTWUMI	0.074	0.523	1.545	0.008	3.686	0.583
3%	FSMUMI	0.068	0.453	1.053	0.076	10.649	0.582
	Amelia	0.13	0.999	2.212	0.062	3.779	0.794
	FcM	0.098	0.999	1.526	1.984	2.22	0.997
	MI	0.13	0.999	2.197	0.078	9.374	0.795
	MICE	0.129	1	2.19	0.067	1.938	0.792
	missForest	0.102	0.999	1.626	0.855	2.407	0.851
	na.approx	0.116	0.997	1.938	0.518	1.974	0.818
	DTWUMI	0.073	0.526	1.189	0.01	8.725	0.567
4%	FSMUMI	0.064	0.412	1.067	0.061	1.374	0.568
	Amelia	0.122	1	2.305	0.032	2.446	0.764
	FcM	0.096	1	1.607	1.982	2.325	0.997

4%

3.3. Proposed method based on an hybrid similarity measure

	MI	0.125	1	2.261	0.043	2.391	0.792
	MICE	0.124	0.999	2.233	0.045	42.495	0.791
	missForest	0.101	1	1.726	0.876	2.901	0.854
	na.approx	0.109	1	1.99	0.475	1.94	0.811
	DTWUMI	0.066	0.465	1.172	0.004	2.079	0.547
5%	FSMUMI	0.063	0.404	1.062	0.062	4.508	0.577
	Amelia	0.122	1	2.273	0.028	4.109	0.798
	FcM	0.092	1	1.619	1.984	2.192	0.998
	MI	0.123	1	2.287	0.024	5.582	0.797
	MICE	0.121	1	2.267	0.044	2.326	0.792
	missForest	0.097	0.999	1.731	0.923	2.473	0.859
	na.approx	0.114	1	1.988	0.567	2.247	0.809
	DTWUMI	0.063	0.454	1.166	0.003	1.594	0.545
7.5%	FSMUMI	0.06	0.408	1.063	0.049	4.843	0.566
	Amelia	0.117	1	2.232	0.034	3.306	0.792
	FcM	0.09	1	1.605	1.981	3.562	0.998
	MI	0.119	0.999	2.259	0.025	1.946	0.793
	MICE	0.118	1	2.238	0.032	9.359	0.794
	missForest	0.094	0.999	1.695	0.907	1.259	0.858
	na.approx	0.108	1	1.958	0.461	3.089	0.816
	DTWUMI	0.065	0.477	1.19	0.004	3.851	0.566
10%	FSMUMI	0.061	0.4226	1.086	0.051	5.558	0.572
	Amelia	0.117	1	2.269	0.021	3.074	0.793
	FcM	0.089	1	1.607	1.981	2.683	0.997
	MI	0.118	0.9996	2.233	0.02	2.05	0.793
	MICE	0.118	0.9998	2.254	0.018	3.424	0.793
	missForest	0.094	0.9999	1.702	0.909	1.87	0.857
	na.approx	0.11	1	1.958	0.541	2.006	0.798
	DTWUMI	0.067	0.5371	1.293	0.012	3.093	0.577

MAREL Carnot dataset: Once again, as reported in table 3.6, our algorithm demonstrates its capability for the imputation task. FSMUMI method generates the best results as regarding accuracy indices for almost missing ratios (excluding at 2% missing level on all indices, and at 5% missing rate on R^2 score). But when considering shape indicators, FSMUMI only provides the highest FA2 values at several missing levels (3%, 5%-10%). In particular, our method illustrates the ability to fill in incomplete data with large missing rates (7.5% and 10%): the highest similarity, R^2 , FA2 and the lowest RMSE, FSD (excluding at 7.5%), and FB. These

gaps correspond to 110.4 and 147.2 days sampled at hourly frequency.

In contrast to the two datasets above, on the MAREL-Carnot data, na.approx indicates quite good results: the permanent second or third rank for the accuracy indices (the 1st order at 5% missing rate on R^2 score), the lowest FSD (from 3% to 5% missing rates) and FB at some other levels of missing data. But when looking at the shape of imputation values generated from this method, it absolutely gives the worst results (figure 3.13).

Other approaches (including FcM-based imputation, MI, MICE, Amelia, missForest) exploit the relations between attributes to estimate missing values. However, three considered datasets have low correlations between variables (roundly 0.2 for MAREL-Carnot data, ≤ 0.1 for simulated and synthetic datasets). So these methods do not demonstrate their performance for completing missing values in low/un-correlated multivariate time series. Otherwise, our algorithm shows its ability and stability when applying to the imputation task for this kind of data.

DTWUMI approach was proposed to fill large missing values in low/un-correlated multivariate time series. However, this method is not as powerful as the FSMUMI method. DTWUMI only produces the best results at 2% missing level on the MAREL-Carnot dataset, and is always at the second or the third rank at all the remaining missing rates on the MAREL-Carnot and the simulated datasets. That is because the DTWUMI method only finds the most similar window to a query either before a gap or after this gap, and it uses only one similarity measure, the DTW cost, to retrieve the most similar window. In addition, another reason may be that DTWUMI has directly used data from the window following or preceding the most similar window to completing the gap.

Table 3.6: Average imputation performance indices of various imputation algorithms on MAREL-Carnot dataset (35,334 collected points)

Gap size	Method	Accuracy indices			Shape indices		
		1-Sim	1- R^2	RMSE	FSD	FB	1-FA2
1%	FSMUMI	0.051	0.156	1.532	0.044	0.081	0.191
	Amelia	0.187	0.544	5.132	0.378	0.354	0.482
	FcM	0.156	0.342	4.037	0.4	0.347	0.338
	MI	0.192	0.561	5.282	0.396	0.365	0.497
	MICE	0.166	0.608	5.596	0.423	0.35	0.436
	missForest	0.165	0.472	4.422	0.385	0.355	0.381
	na.approx	0.061	0.171	1.748	0.067	0.06	0.161

3.3. Proposed method based on an hybrid similarity measure

	DTWUMI	0.084	0.181	2.466	0.214	0.149	0.198
	FSMUMI	0.045	0.037	1.446	0.053	0.083	0.182
	Amelia	0.146	0.369	4.743	0.211	0.222	0.429
	FcM	0.116	0.06	3.418	0.415	0.237	0.231
2%	MI	0.146	0.364	4.72	0.218	0.228	0.435
	MICE	0.129	0.369	4.711	0.197	0.21	0.413
	missForest	0.116	0.155	3.575	0.33	0.193	0.258
	na.approx	0.06	0.07	2.012	0.045	0.094	0.214
	DTWUMI	0.042	0.018	1.095	0.029	0.066	0.154
	FSMUMI	0.053	0.11	1.294	0.134	0.08	0.166
	Amelia	0.176	0.503	4.694	0.426	0.224	0.478
	FcM	0.139	0.251	3.35	0.441	0.237	0.314
3%	MI	0.17	0.531	4.474	0.354	0.221	0.476
	MICE	0.157	0.552	4.905	0.34	0.184	0.429
	missForest	0.139	0.345	3.556	0.422	0.184	0.346
	na.approx	0.068	0.224	1.79	0.062	0.056	0.169
	DTWUMI	0.096	0.216	2.587	0.329	0.136	0.223
	FSMUMI	0.059	0.058	1.466	0.094	0.101	0.183
	Amelia	0.171	0.44	4.389	0.287	0.2	0.456
	FcM	0.126	0.152	2.779	0.285	0.203	0.727
4%	MI	0.166	0.41	4.234	0.277	0.204	0.444
	MICE	0.15	0.379	4.15	0.268	0.19	0.411
	missForest	0.129	0.234	3.134	0.23	0.187	0.303
	na.approx	0.077	0.13	2.006	0.068	0.135	0.268
	DTWUMI	0.07	0.105	1.77	0.15	0.12	0.138
	FSMUMI	0.051	0.22	2.025	0.227	0.152	0.167
	Amelia	0.151	0.551	4.924	0.303	0.189	0.461
	FcM	0.113	0.337	3.606	0.301	0.199	0.254
5%	MI	0.143	0.567	4.612	0.249	0.123	0.448
	MICE	0.131	0.523	4.75	0.274	0.188	0.419
	missForest	0.104	0.371	3.443	0.229	0.147	0.274
	na.approx	0.065	0.213	2.071	0.175	0.038	0.233
	DTWUMI	0.067	0.275	2.363	0.22	0.157	0.242
	FSMUMI	0.043	0.056	1.52	0.075	0.039	0.189
	Amelia	0.14	0.42	4.546	0.191	0.197	0.437
	FcM	0.104	0.123	3.12	0.328	0.198	0.23
7.5%	MI	0.142	0.427	4.624	0.222	0.222	0.443
	MICE	0.126	0.38	4.375	0.206	0.208	0.437

CHAPTER 3. IMPUTATION APPROACHES FOR UNCORRELATED MULTIVARIATE TIME SERIES

	missForest	0.112	0.202	3.587	0.329	0.228	0.288
	na.approx	0.073	0.081	2.043	0.092	0.107	0.243
	DTWUMI	0.06	0.102	1.999	0.071	0.074	0.215
	FSMUMI	0.053	0.098	1.642	0.083	0.055	0.191
	Amelia	0.14	0.3	4.294	0.24	0.142	0.442
	FcM	0.1	0.098	3.68	0.136	0.101	0.303
10%	MI	0.14	0.112	4.294	0.24	0.142	0.442
	MICE	0.12	0.42	4.066	0.152	0.077	0.383
	missForest	0.097	0.461	3.049	0.104	0.117	0.255
	na.approx	0.071	0.529	1.873	0.098	0.094	0.253
	DTWUMI	0.081	0.381	3.293	0.119	0.124	0.224

3.3.4.2 Visual performance comparison

In this study, we also compare the visualization performance of completion values yielded by various algorithms. Figure 3.11 and figure 3.12 illustrate the form of imputed values generated from different approaches on the synthetic series at two missing ratios 1% and 5%.

At a 1% missing rate, the shape of imputation values produced by na.approx method is closer to the one of true values than the form of completion values given by our approach. However, at a 5% level of missing data, this method no longer shows the performance (figure 3.12). In this case, the proposed method proves its relevance for the imputation task. The shape of FSMUMI's imputation data is almost similar to the form of true values (figure 3.12).

Looking at figure 3.13, FSMUMI one more time proves its capability for uncorrelated multivariate time series imputation: completion values yielded by FSMUMI are virtually identical to the real data on the MAREL-Carnot dataset. When comparing DTWUMI with FSMUMI, it is clear that FSMUMI gives improved results (figure 3.11, 3.12 and 3.13).

3.3.4.3 Computation time

Besides, we perform a comparison of the computational time of each method on the synthetic series (in second - s). Table 3.7 indicates that na.approx method requires the shortest running time and DTWUMI approach takes the longest computing time. The proposed method, FSMUMI, demands more execution time as missing rates increase. However, considering the quantitative and visual performance of FSMUMI for the imputation task (table 3.4, figure 3.12 and figure 3.13), the required time of the proposed approach is fully acceptable.

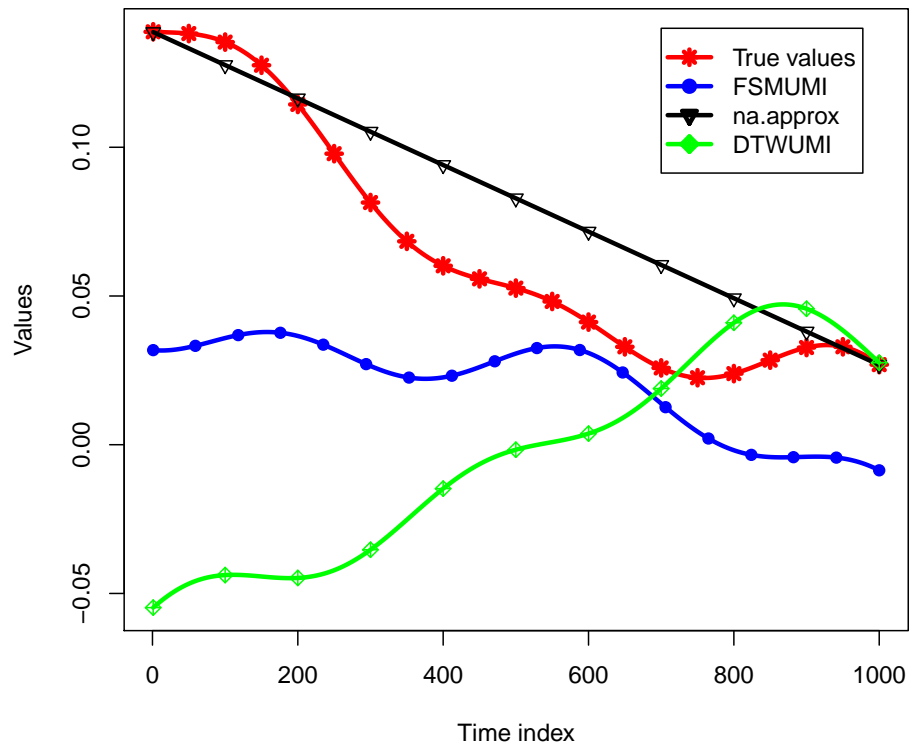


Figure 3.11: Visual comparison of completion data of different imputation approaches with real data on the 1st signal of synthetic series with the gap size of 1000

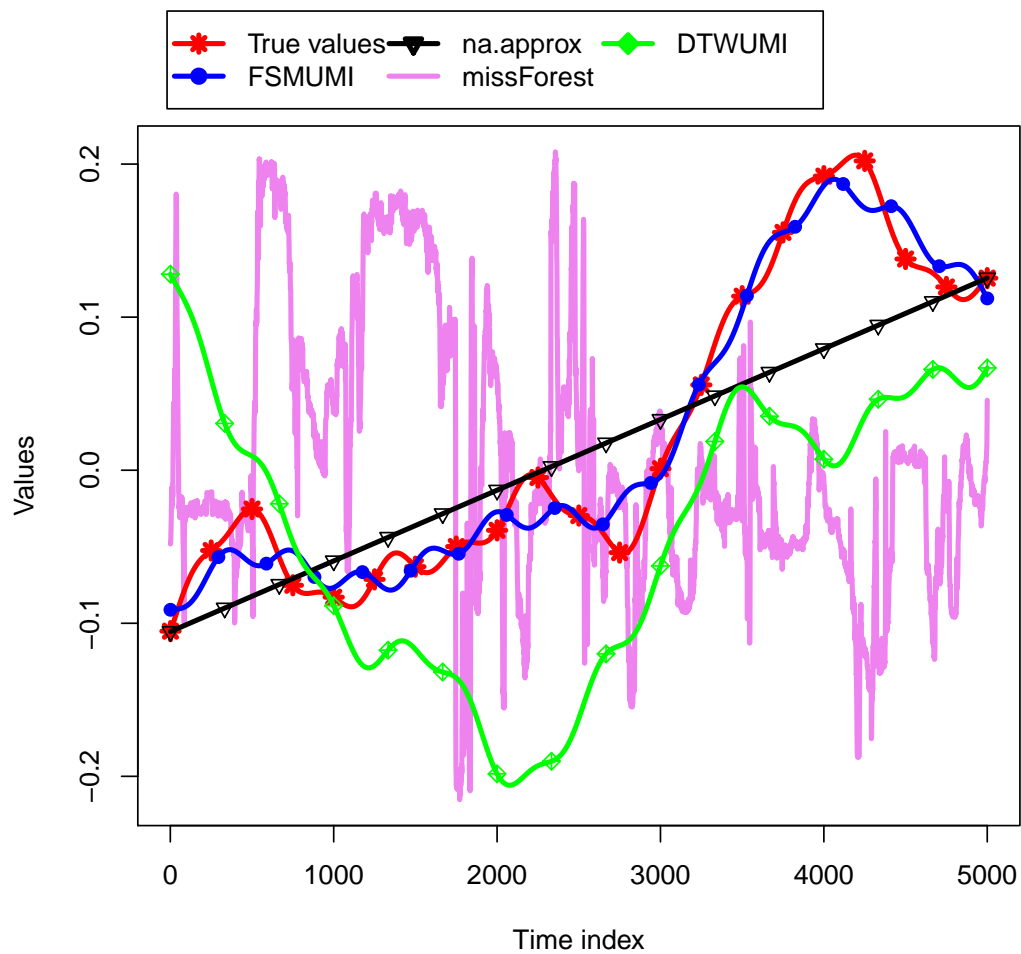


Figure 3.12: Visual comparison of completion data of different imputation approaches with real data on the 1st signal of synthetic series with the gap size of 5000

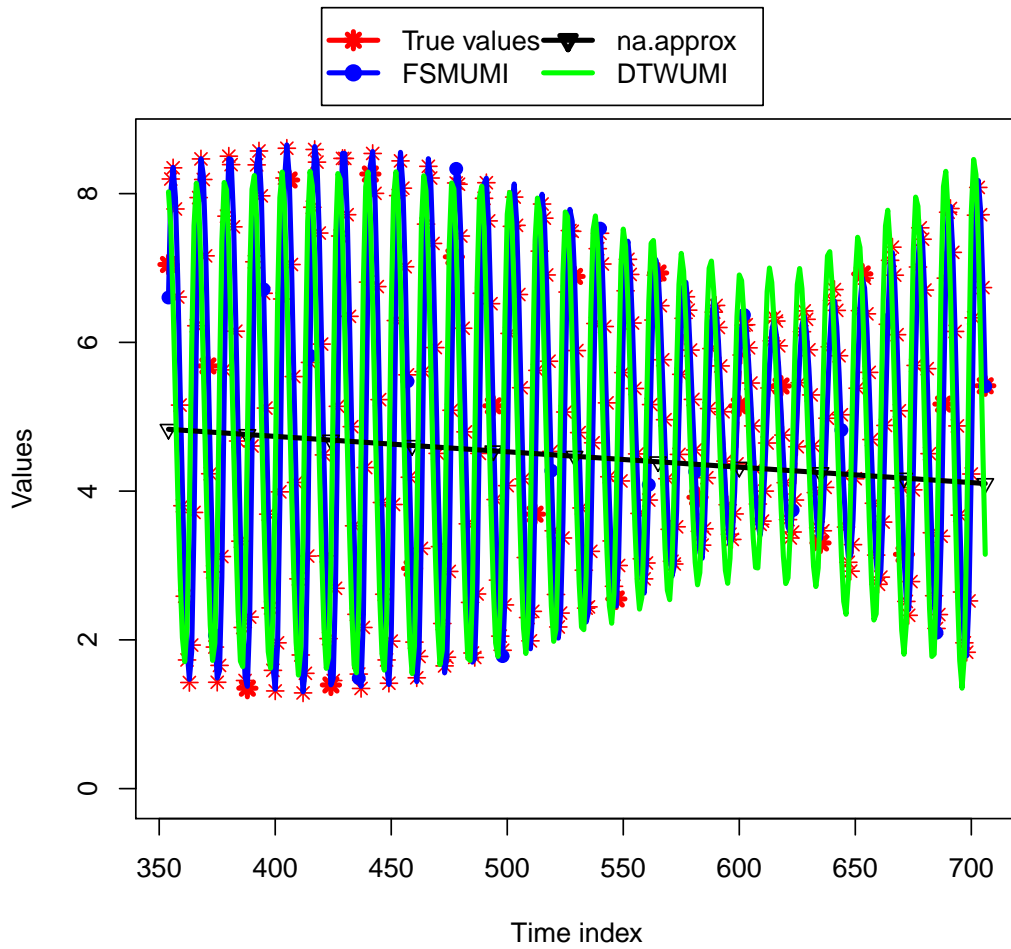


Figure 3.13: Visual comparison of completion data of different imputation approaches with real data on the 2nd signal of MAREL Carnot dataset with the gap size of 353

Table 3.7: Computational time of different methods on the synthetic series in second (s)

Method	Gap size (100,000 collected points)						
	1%	2%	3%	4%	5%	7.5%	10%
FSMUMI	353.9	427.5	701.9	1037.8	1423.6	2525.5	3556.8
Amelia	3.2	3.4	5.2	3.2	3.2	3.2	3.2
FcM	40.9	39.8	40.0	41.1	41.2	46.7	45.6
MI	844.1	714.0	739.1	723.3	724.5	719.7	726.5
MICE	7021.1	9187.7	21909.6	13041.9	14833.9	19417.7	23812.6
missForest	26833.8	24143.8	22969.9	32056.6	36485.8	42424.1	28521.1
na.approx	0.11	0.089	0.167	0.09	0.088	0.088	0.094
DTWUMI	5002.67	15714.8	37645.82	64669.71	86435.38	180887.78	273879

3.3.5 Conclusion

This work proposes a novel approach for uncorrelated multivariate time series imputation using a fuzzy- weighted similarity measure, namely FSMUMI. This method makes it possible to manage uncertainty with the comprehensibility of linguistic variables and parameter adaptation. FSMUMI has been tested on different datasets and compared with published algorithms (Amelia II, FcM, MI, MICE, missForest, na.approx, and DTWUMI) on accuracy and shape criteria. The visual ability of these approaches is also investigated. The experimental results definitely highlight that the proposed approach yielded improved performance in accuracy over previous methods in the case of multivariate time series having large gaps and low or non-correlation between variables. However, the proposed algorithm is necessary to make an assumption of recurrent data and sufficiently large dataset.

3.4 Chapter conclusion

The occurrence of missing data happens in most scientific domains and most kinds of data. This poses serious problems in data analysis and data mining such as bias results or loss of algorithms power. Therefore, imputation data are valuable/significant techniques to deal with incompleteness data. Imputation data process is to complete missing data in an incomplete dataset. Techniques of imputation are applied to retrieve efficient estimation of missing values based on available data. In this chapter, we propose two new approaches, namely DTWUMI and FSMUMI, for imputing large consecutive missing data in uncorrelated multivariate time series. Handling incompleteness for this type of data has received little attraction compared to the imputation task for correlated data. In these two approaches, we take advantage of the property of low/un-correlated multivariate data in two different aspects:

DTWUMI is an extension of our previous proposal (DTWBI). This approach is based on combining DTW and shape-feature extraction algorithms. To conserve time indices of all the variables in the dataset, only one query Q is built by taking into account all the signals either before or after each gap. DTWUMI thereafter finds the most similar window to the query using DTW cost as the similarity criterion. This approach applies shape-feature extraction method to decrease the computation time before using DTW algorithm to retrieve similar windows. Since data are low/uncorrelated, so imputation data are the vector following or preceding of the most similar window on the signal containing considered gap. In the DTWUMI, we take care of the same time index of all the variables by creating a query window (i.e Q is a matrix of all the signals) either before or after the gap, and find the most similar window (a matrix) to the query. But imputation values are only a vector in the signal having the considered gap.

In the second proposal, FSMUMI, we introduce an uncertain factor that allows to manage a high level of uncertainty, specifically:

- Develop a new similarity measure based on weighting some usually distances by applying fuzzy rules interpolation scheme.
- And then we use the new measure to find the most similar windows. There are some differences between these two methods:
 - Step of building query: FSMUMI builds two vector queries (instead of one query matrix as introduced in the DTWUMI): Qb - a vector previous the considered gap and Qa - a vector next to the gap. Accordingly, we create two search databases (i) Db - a database before the gap and (ii) Da - a database after the gap on the signal having the gap. And we find similar windows on these two databases.
 - Step of filling missing data: The final imputation data are the average of two vectors preceding and following of the most two similar windows.

The two proposed methods are mainly compared with state-of-the-art imputation approaches and comparisons are made in terms of accuracy and shape indices between real data and completion data. Also, the visual performance of these approaches is also investigated. DTWUMI is compared with missForest, MI, MICE and na.approx methods on NNGC, simulated and MAREL Carnot datasets. Whereas FSMUMI was compared with 6 well-known methods (MI, MICE, missForest, na.approx, Amelia, FCM) and with DTWUMI on simulated dataset, synthetic dataset and MAREL Carnot dataset.

The experimental results clearly show that our approaches yielded improved performance in accuracy than previous methods in the case of multivariate time series having large gaps and low or non-correlation between variables. However, the proposed algorithms are necessary to make an assumption of recurrent data and sufficient large dataset.

The present works open a broad range of applications, we plan to (i) combine FSMUMI/DTWUMI method with other algorithms such as Random Forest or Deep learning in order to efficiently fill incomplete data in any type of multivariate time series; (ii) investigate this approach applied to short-term/long-term forecasts in multivariate time series. We could also investigate type-2 fuzzy sets (T2FSs) [112] that are an extension of the ordinary fuzzy set (also called type-1 fuzzy sets, T1FS). Type-2 fuzzy set can handle more uncertainty because their membership functions are fuzzy. It is completely described by two functions (primary and secondary fuzzy grades). Further, collected data usually contain noise (real data plus noise). So that T2FS ([113]) should be considered to solve missing data problems in both types of time series: univariate and multivariate time series using a new similarity measure [114] for example. In case of bi-variate time series with small dataset, complex fuzzy sets ([113]) can be studied instead of ordinary FSs that have given good results using an adaptive scheme.

List of Publications and valuations related to this chapter

1. Thi-Thu-Hong Phan, André Bigand, Emilie Poisson Caillault, "A New Fuzzy Logic-based Similarity Measure applied to Large Gap Imputation for Uncorrelated Multivariate Time Series", *Applied Computational Intelligence and Soft Computing*. Available online August 2018. DOI: 10.1155/2018/9095683
2. Emilie Poisson Caillault, Camille Dezechache, Thi Thu Hong Phan, Kelly Grassi, Jean Prygiel, and Alain Lefebvre, "Data completion, characterization of environmental states and dynamics using multiparameter time series: DTWBI, DTWUMI and uHMM R-packages", 2nd General Assembly of JERICO-NEXT, Galway, Ireland, 24-27 September, 2018.
3. Thi-Thu-Hong Phan, Emilie Poisson Caillault, Alain Lefebvre, André Bigand, "Multivariate times series imputation by unsupervised and supervised approach", *journée IA LISIC*, 18/06/2018, Calais, France.
4. Thi-Thu-Hong Phan, Emilie Poisson Caillault, Alain Lefebvre, André Bigand, "DTW-

Approach For Uncorrelated Multivariate Time Series Imputation", IEEE International Workshop on Machine Learning for Signal Processing. MLSP 2017. September 25-28, 2017 Roppongi, Tokyo, Japan. DOI: 10.1109/MLSP.2017.8168165

5. Thi-Thu-Hong Phan, Emilie Poisson Caillault, Alain Lefebvre, André Bigand. DTW-Approach For Uncorrelated Multivariate Time Series Imputation, 5th édition de la Journée Doctorale du Campus de la Mer, 19 October, 2017 Boulogne sur Mer, France.
6. DTWUMI R-package <https://cran.r-project.org/web/packages/DTWUMI/index.html>

Applications: Toward classification and forecasting

Contents

4.1	Classification of phytoplankton species	112
4.1.1	Introduction	112
4.1.2	Feature-extraction algorithm	115
4.1.3	Methodology	116
4.1.4	Experiment and discussion	121
4.1.5	Conclusion	125
4.2	Event detection in a multidimensional time series	125
4.2.1	Data presentation	126
4.2.2	Preprocessing data	129
4.2.3	Event detection	132
4.2.4	Conclusion	134
4.3	Comparative Study on Univariate Forecasting Methods for Meteorological Time Series	136
4.3.1	Introduction	136
4.3.2	Time series forecasting methods	138
4.3.3	Experiment protocol	140
4.3.4	Results and discussion	141
4.3.5	Conclusion	145
4.4	Chapter conclusion	146

The two previous chapters explained how to complete large consecutive missing values in univariate time series and in uncorrelated multivariate time series. This chapter illustrates some concrete applications in relation to the marine focus and projects (CPER MARCO project in France and other projects in Vietnam). We begin the chapter by introducing our proposal (section 4.1), shape-feature extraction algorithm, which allows to effectively extract global features from a signal. Accordingly, to analyze pertinent of proposed algorithm we apply it to classify phytoplankton species. This proposed algorithm is already combined with DTWBI (Chapter 2) and DTWUMI (Chapter 3) in order to reduce computation time. In next sections, we present two other applications where DTWBI is applied. In the first application, DTWBI is employed to complete MAREL Carnot dataset, then we perform a detection of rare/extreme events (section 4.2). In the second application (section 4.3), based on the idea of imputation, we use DTWBI to forecast meteorological univariate time series.

4.1 Classification of phytoplankton species

Phytoplankton plays an important role in marine ecosystem. It is defined as a biological factor to assess marine quality. The identification of phytoplankton species has a high potential for monitoring environmental, climate changes and for evaluating water quality. However, phytoplankton species identification is not an easy task owing to their variability and ambiguity due to thousands of micro and pico-plankton species. Therefore, the aim of this part is to build a framework for identifying phytoplankton species and to perform a comparison on different features types and classifiers. We propose a new type of features extracted from raw signals of phytoplankton species in section 4.1.2. Then, in section 4.1.4 we analyze the performance of various classifiers on the proposed features type as well as two other features types for finding the most robust one.

4.1.1 Introduction

Phytoplankton is an important factor in environmental, economic and ecological policies. Being main producer of oxygen, phytoplankton is also an important food item in both aquaculture as well as mariculture. A question is raising: “how do changes in the global environment affect abundance, diversity, and production of plankton and nekton?” [115]. Many researchers show that environment changes strongly affect to phytoplankton and that it responds promptly

to chemical perturbation [116, 117, 118, 119, 120, 121]. The identification/classification of microscopic phytoplankton is therefore crucial for a wide variety of environmental monitoring applications in different domains such as: ecology (biodiversity), climate and economy. It is thus necessary to have a capable technique/tool which can provide detailed description of phytoplankton species population from water samples.

Up to now, studies in identification/classification of phytoplankton species are usually carried out by visual comparing the collected profiles with references ones, or by the microscope method [122, 123]. Using this microscope analysis method takes 3 to 4 hours for each sample (low frequency). It is laborious and extremely time-consuming. Hence, developing an automatic computer-aided machine system to identify/classify phytoplankton species is a required task.

Flow cytometry (FCM) analysis is a well-known and proven tool in aquatic ecology to quickly detect and quantify phytoplankton and bacteria (microorganism) from water samples [124, 125]. “The various light scatter, diffraction, and fluorescence parameters measured by analytic FCM can provide characteristic “signatures” for each microbial cell, which allow taxa to be discriminated with the use of pattern-recognition techniques” [126]. Thus, the task of identifying phytoplankton species becomes the classification of multidimensional signals [50].

Regarding pattern-recognition techniques, a number of successful approaches have been proposed for automated identification/classification of plankton species.

Concerning zooplankton identification/classification, several techniques including object classification technique for analyzing plankton images were developed by Hu and Davis [127] and Davis et al.[128]. In these two works, the images were collected from a plankton video recorder. A Support Vector Machine (SVM) is used for classifying a big image set (20,000 plankton images); the accuracy of classification on seven classes was achieved with the score of 71%. The performance of six classifiers: Multi-Layer Perceptron (MLP), K-Nearest Neighbors (5-NN), SVM (using linear and Radial Basis Function (RBF) kernels), Random Forest (RF), and C4.5 Decision Trees (DTs) were studied for classifying zooplankton images obtained from the ZooScan system [129]. In this study, RF demonstrates the best performance and was followed by SVM using the linear kernel. Irigoien *et al.* [130] carried out a research on classifying in zooplankton images with 17 categories and RF gives the highest result. The ZooScan digital imaging system for automatic analysis of zooplankton images is built by Grosjean et al. [115]. They tested individual classification algorithms as well as combinations of two or more different algorithms such as: double bagging associated with linear discriminant analysis, k -NN

with discriminant vector forest and specifically mix of linear discriminant analysis with learning vector quantization, and random forest. Accuracy of the last combination achieves around 75% in the task of categorizing 29 zooplankton species. In the work of classifying binary zooplankton images, Luo et al. [131] investigated the performance of some classifiers, namely: SVM, RF, C4.5 DTs, and the cascade correlation neural network. SVM proves the highest classification performance with 90% and 75% on the six and seven classes, respectively.

Concerning phytoplankton species identification/ classification, many classification algorithms were used for this task such as Artificial Neural Networks (ANNs) using FCM data [132, 133, 134, 135, 136, 137] (72 phytoplankton species have been successfully identified by ANN [134]). In another work, several methods namely: DTs, Naive Bayes (NB), ridge Linear Regression (LR), k -NN, SVM, bagged and boosted ensembles were applied to categorize phytoplankton images with 12 classes and an unknown class [138]. A system using SVM classifier for automated taxonomic classification of phytoplankton sampled with imaging-in-flow-cytometry is developed by Sosik and Olson [139]. In the work of Blaschko *et al.* [140], the accuracy of two modelling approaches for predicting boreal lake phytoplankton assemblages and their ability to detect human impact were studied. They used random forest to predict biological group membership and species. Verikas et al. [141] have recently investigated to detect, recognize, and estimate abundance objects representing the *P.minimum* species in phytoplankton images. The classification performance of SVM and RF methods was compared on 158 phytoplankton images.

It is found that the number of studies using plankton signals (FCM data) is less than the ones using plankton images. Most of studies based on signals used available features generated from a FCM system. However, only a few earlier studies used FCM signals (both available features and raw signals) to compare the performance of classification methods [50]. In addition, RF has proved its performance in many applications of plankton species identification/classification [115, 129, 130, 140]. With the best of our knowledge, there is no application that combines the FCM signals and RF to determine phytoplankton species.

Therefore, our main contributions in this part are: (1) to propose a new type of features extracted from the raw signals of phytoplankton species; (2) to perform a comparative analysis of identifying phytoplankton species using a variety of advance machine learning models such as K -NN (1-NN), SVM, RF and several modification versions of RF. This permits to determine the best type of features for representing phytoplankton species and classifier for classifying phytoplankton species with high accuracy.

4.1.2 Feature-extraction algorithm

The idea of our proposal is to propose some features that can better represent dynamics and shape of signals. Among of the possible features, signal moments and entropy give improved results. Denoted $x = \{x_i | i = 1, 2, \dots, N\}$ are the values of each signal (curve). With each raw signal, 9 elements are calculated as follows:

- Percentile: The per^{th} percentile of x 's values is the value that cuts off the first per percent of x 's values when these values are sorted in ascending order ($per = 30$ is used in this study).
- Max: It is the maximum of x 's values:

$$\max(x) = \max\{x_1, x_2, \dots, x_N\} \quad (4.1)$$

- First moment: It is the mean of x 's values:

$$\bar{x} = \text{mean}(x) = \frac{\sum_{i=1}^N x_i}{N} \quad (4.2)$$

- Standard derivation: It is the standard derivation of x 's values, based on the 2^{nd} moment central:

$$STD(x) = \sqrt{\frac{1}{N} \sum_{i=1}^N (x_i - \bar{x})^2} = \sqrt{\mu_2} \quad (4.3)$$

- Median: The median of x 's values is the value separating the higher half and the lower half. It is the middle number when the data is sorted from lowest value to highest value.
- Third moment: It is the 3^{rd} moment of x 's values:

$$\gamma_1 = \frac{\mu_3}{\mu_2^{3/2}} \quad (4.4)$$

where μ_2 and μ_3 are the second and third central moments. $\gamma_1 = 1$ is the normalized 3^{rd} moment central (Skewness coefficient). We can know the data distribution thanks to this coefficient.

- Nop: It is the number of peaks of x 's values calculated from the second derivative.
- Length: It is the length of the curve.

- Entropy: It is based on the Shannon entropy formula:

$$entropy(x) = - \sum_{i=1}^N p_i \log(p_i) \quad (4.5)$$

with p_i is the probability of x_i

Consequently, for each signal, a features vector of dimension 9 is extracted.

4.1.3 Methodology

4.1.3.1 Data presentation

In this study, we reuse the data of the previous study [50] (Data presentation and Signal acquisition). The data is acquired from 7 culture samples, whose particles belong to 7 distinct phytoplankton species: *Chaetoceros socialis*, *Emiliana Huxleyi*, *Lauderia annulata*, *Leptocylindrus minimus*, *Phaeocystis globosa*, *Skeletonema costatum* and *Thalassiosira rotula*. Each species is equally represented by 100 shape-profiles and each culture sample was labeled by biologists using a microscope [123]. So, the data set has 700 (100×7) phytoplankton cells.

Signal acquisition

Multi-signals were gathered in the LOG laboratory¹ from different phytoplankton species living in Eastern Channel, with a CytoSense flow cytometer (CytoBuoy²), and labeled by biologists [123] once having them isolated from the natural environment. Flow cytometry is a technique used to characterize individual particles (cells or bacteria) derived by a liquid flow at high speed in front of a laser light. Different signals either optical or physical are provided: forward scatter (reflecting the particle length), sideward scatter (being more dependent on the particle internal structure) and several wavelengths of fluorescence that depend upon the type of its photosynthetic pigments measures.

More precisely, in the used signal library, each detected particle is described by 8 mono-dimensional raw signals issued from the flow cytometer in identical experimental conditions (same sampling rates, same detection threshold, etc.):

- one signal on forward scatter (FWS), corresponding to the cell length;
- two signals on sideward scatter (SWS), corresponding to the internal structure, in high and low sensitivity levels (SWS HS, SWS LS);

¹Laboratoire d’Oceanologie et de Géosciences, UMR 8187: <http://log.univ-littoral.fr>

²Cytobuoy system: <http://www.cytobuoy.com>

- two signals on red fluorescence (FLR), $\lambda_{em} > 620\text{nm}$ in high and low sensitivity (FLR HS, FLR LS), which characterize chlorophyll pigments;
- one signal on orange fluorescence (FLO), $565\text{nm} < \lambda_{em} < 592\text{nm}$, in low sensitivity (FLO LS);
- two signals on yellow fluorescence (FLY), $545\text{nm} < \lambda_{em} < 570\text{nm}$, in high and low sensitivity (FLY HS, FLY LS).

These signals are composed of voltage measures (μV), and their sampling period was here chosen to correspond to $0.5\mu\text{m}$ displacement of the water flow. Consequently, the longer the cell is, the higher the number of sampled measures is, and the time axis can be interpreted as a spatial length axis. Phytoplankton species identification is a hard task so all these signals are used to make the particles characterization. Each particle of our experiment is consequently characterized by the 8 signals described above. Figure 4.1 present some signal samples of *Chaetoceros socialis*, *Lauderia annulata* and *Skeletonema costatum* species.

4.1.3.2 Phytoplankton descriptor

After acquiring phytoplankton raw signals from the FCM system, phytoplankton descriptor must be computed to represent the phytoplankton species, that will be presented to a classifier. The phytoplankton descriptor describes properties of a phytoplankton cell (for example length, number of peaks . . . of each raw signal or the ratio of dissimilarity of each pairs of phytoplankton cells). In this work, these properties are typically called “features”. We investigate three types of features : derived features, proposed features (as above mentioned) and dissimilarity features [50].

1. Derived features

For each signal, 4 elements are extracted by a Cytobuoy machine including: length, height, integral, and number of peaks. So each phytoplankton cell is represented by a vector of 32 features.

2. Proposed features

As mentioned above in our proposal, 9 characteristics will be extracted from each signal. However, when applying to the phytoplankton classification, we have modified some features to adapt the data in the following:

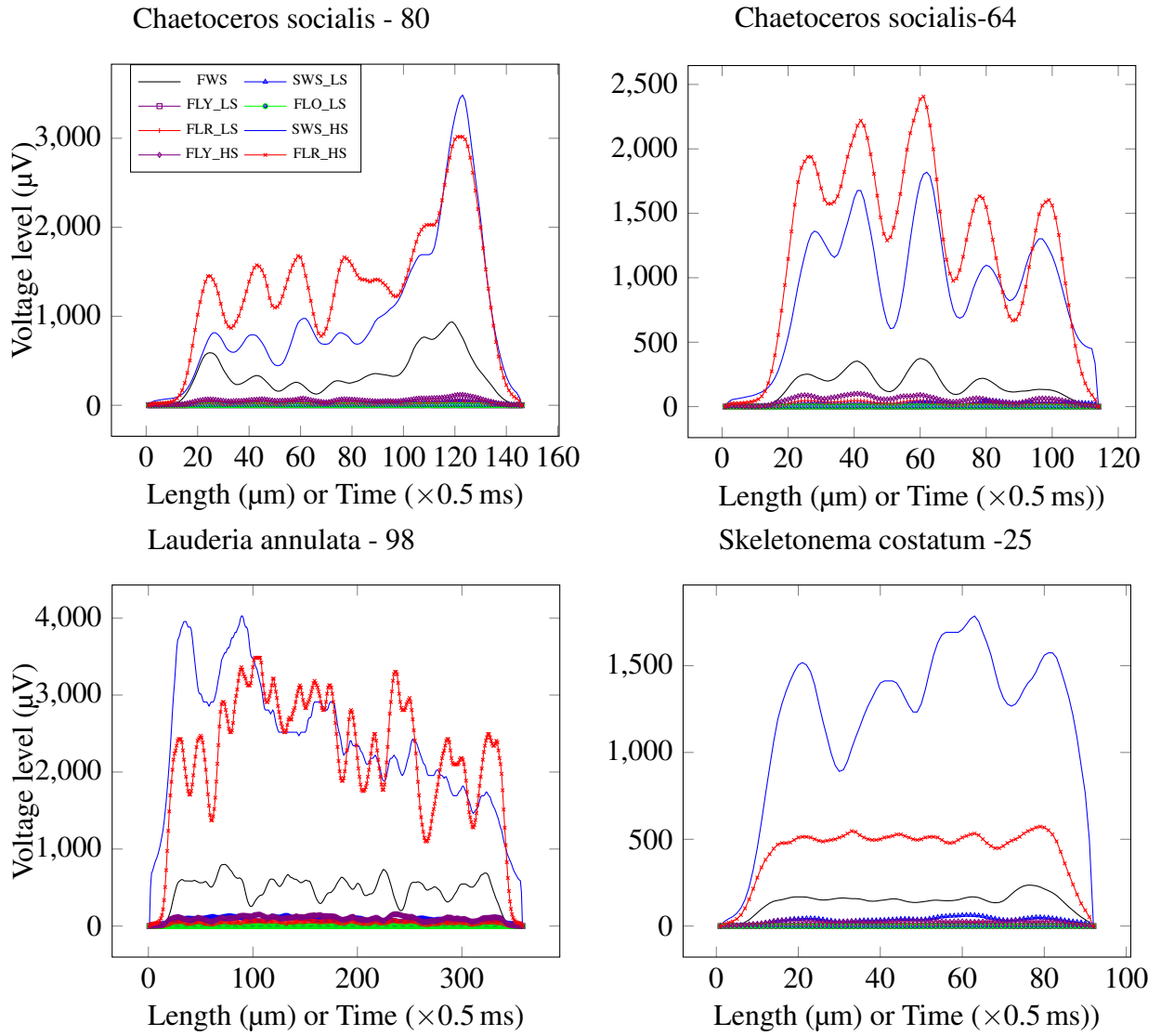


Figure 4.1: 8D-signals describing three species

- Third moment: we use the 3rd moment instead of utilizing the Skewness coefficient because some signals have all 0 values.
- Entropy: With this application p_i is computed as follows: $p_i = \frac{x_i}{\sum_{i=1}^N x_i}$ because we could exploit all the values of each signal.

For each signal 9 features are extracted. Consequently, the proposed features vector is 72 dimensions.

3. Dissimilarity features

As described in Chapter 2, Dynamic Time Warping [7] is an algorithm devoted to align two sequences (may vary in time) by warping the time axis until finding an optimal matching between the two sequences according to suitable metrics. However, it is not easy to interpret the matching cost. Thus, Caillaut *et al.* [50] proposed a dissimilarity distance that adapts the DTW matching cost and can deal with multidimensional signals. They replaced the distance d (L_1 -distance or L_2 -distance) by a dissimilarity s ($s \in [0, 1]$ -normalized dissimilarity degree):

$$s(x_{i_l}, y_{j_l}) = \frac{d(x_{i_l}, y_{j_l})}{\max\{d(x_{i_l}, 0), d(y_{j_l}, 0)\}} \quad (4.6)$$

where $x = \{x_1, x_2, \dots, x_N\}$ and $y = \{y_1, y_2, \dots, y_M\}$ are two signals of different size. The algorithm makes a matching $P = \{(i_l, j_l), l = 1 \dots k, i_l = 1 \dots N, j_l = 1 \dots M\}$ between the points of x and y signals, according to some time conditions.

Therefore, each phytoplankton cell is presented by a vector of 700 dissimilarity features, in which a feature is the DTW dissimilarity between considered cell and one cell in the dataset.

4.1.3.3 Classification

After feature extraction, a classifier is learned for identification of different phytoplankton species. In the following, we review several prominent classification models:

1. k -Nearest Neighbors

k -nearest neighbors [142] has been widely used in classification problems because it is simple, effective and nonparametric [143]. For each sample of a test set, we found k cases in the train set that is minimum distance between the feature vectors of the sample

and those of the train set. A decision of the label of a new sample is based on majority vote of the k label found.

2. Support Vector Machine

The basic idea of support vector machine [144] is to find an optimal hyper-plane for linearly separable patterns in a high dimensional space where features are mapped onto. The work is to detect the one that maximizes the margin around the separating hyper-plane from training set. A decision on the label of a new sample is based on its distance with the trained support vectors.

3. Random Forest

Breiman [145] proposed random forest, a classification technique obtained by constructing an ensemble of decision trees, in which each decision tree uses a different bootstrap sample of the response variables and at each node, a small subset of randomly selected variables from original ones for the binary splitting. For predicting new data, a RF aggregates the outputs of all trees.

4. Regularized Random Forest (RRF), Guided RRF (GRRF), Guided RF (GRF)

RRF, GRRF, GRF are different modified versions of the original RF. But these methods are just similar to initial RF method in the step of predicting new data, and they are different in step of finding features to build each decision tree of forest. Indeed, RRF was proposed for improving feature selection on the decision tree by limiting the choice of new feature at each tree node and evaluating features (using Gini index) on a part of the training data [146]. This process of feature selection is greedy because variables are selected based on a subsample of data variables at each node.

GRRF [147] is an enhanced RRF. This approach uses the feature importance scores generated from an initial random forest to guide the feature selection process in RRF for avoiding of selecting not strongly relevant features. While GRRF selects a subset of relevant and non-redundant features, GRF selects a subset of “relevant” features. So GRF often selects a lot more features than GRRF (sometimes most of the features), but it may lead to better classification accuracy than GRRF. Nevertheless, each tree of GRF is built independently and GRF can be implemented in a distributed computing framework [148].

4.1.4 Experiment and discussion

We have conducted a set of experiments on various types of features and classification models to evaluate their performance on phytoplankton species data (as mentioned above).

Experimental set up

To conduct all experiments, we use a computer with 64 bits Window 7, core i7, CPU 3.0 GHz and 8 GB main memory. For computing the proposed features we use the following R-packages: base, stats, moment [149], and entropy [150]. We utilize the latest R-packages of RF [145], RRF (RRF, GRRF, and GRF)[151], e1071 package (SVM) [152], class package (k -NN) [153] for classifying. Other R-packages like FactoMineR [154], lda [155], have been used to find the most important features.

Concerning SVM, after testing different kernels on different types of features, we choose polynomial kernel of SVM (degree =3) for the derived features and the dissimilarity features, RBF kernel of SVM for the proposed features (tune.svm function [152] is used to find out the optimal coefficients ($\gamma = 0.01$ and $C = 32$, for example)). With k -NN, one of the most important parameters is to choice of suitable value of K . In our experiment, we test with different values of k ($k = 1$ to 10) and this model gives the best results when $k = 1$.

For RF, the basic two parameters are specified to train the model are: *n tree* - number of trees to be constructed in the forest and *m try* - number of input variables randomly sampled as candidates at each node. In this study, *n tree* = 500 is fixed for all RF versions. *m try* of RF, γ of GRRF and γ of GRF are default values: the square root of the number of features [145], 0.1 [147] and 1 [151], respectively.

Each classifier is evaluated using a 4-fold cross validation to determine the recognition error rate and this cross validation is repeated 10 times. The data set of 700 (100×7) phytoplankton cells is divided into 4 subsets of 175 (25×7) cells. Each subset respects an equal target distribution. The learning phase uses three subsets and predicts the remains as test set. For classifying phytoplankton species, in the first step, we extract proposed features (derived features are available) and calculate dissimilarity of each pairs phytoplankton cells from the raw signals. In the next step, after finishing of the learning process, the classification models are used to predict test set. The average accuracy of classification methods are given in tables 4.1, 4.2, and 4.3. The results of contingency table between different models and between different features types of one in the 10 iterations are presented in tables 4.4, 4.5.

The reliability of classification models is evaluated based on classification accuracy of the test sets. The classification results of six methods using different features types are illustrated

4.1. Classification of phytoplankton species

Table 4.1: Accuracy of test recognition of different classification models on the derived features (%)

Classifier	SVM	<i>k</i> -NN	RF	RRF	GRRF	GRF
Fold1	95.89	88.63	96.91	95.37	95.66	95.94
Fold2	94.06	86.8	96.17	95.26	96.06	95.43
Fold3	95.03	87.6	96.63	95.54	96.06	94.97
Fold4	94.63	88.57	96.86	96.23	96.46	95.37
Average	94.9	87.9	96.64	95.6	96.06	95.43

Table 4.2: Accuracy of test recognition of different classification models on the proposed features (%)

Classifier	SVM	<i>k</i> -NN	RF	RRF	GRRF	GRF
Fold1	96.74	82.11	97.65	95.89	95.77	96.86
Fold2	97.54	83.12	98.57	96.29	94.83	97.37
Fold3	97.66	82.97	98.63	96.97	96.86	97.26
Fold4	97.32	82.74	98.12	96.68	96.69	97.54
Average	97.31	82.74	98.24	96.46	96.03	97.26

Table 4.3: Accuracy of test recognition of different classification models on the dissimilarity features (%)

Classifier	SVM	<i>k</i> -NN	RF	RRF	GRRF	GRF
Fold1	94.29	97.31	97.66	94.74	94.74	96.4
Fold2	94.91	97.72	97.43	95.66	94.34	96.57
Fold3	94.86	97.54	97.2	94.29	93.83	95.77
Fold4	94.97	97.2	97.49	95.54	94.57	96.57
Average	94.76	97.44	97.44	95.06	94.37	96.33

Table 4.4: Contingency table of RF model on the dissimilarity features and the proposed features (T: true label, F: false label)

Random Forest		Proposed features							
		Fold 1		Fold 2		Fold 3		Fold 4	
		T	F	T	F	T	F	T	F
Derived features	T	164	7	165	2	166	1	168	3
	F	1	3	8	0	0	9	3	1

Table 4.5: Contingency table of RF and k -NN models on the dissimilarity features

Dissimilarity features		<i>k</i> -NN							
		Fold 1		Fold 2		Fold 3		Fold 4	
		T	F	T	F	T	F	T	F
Random Forest	T	171	3	168	2	170	0	167	2
	F	0	1	2	3	3	2	2	4

in tables 4.1, 4.2, 4.3. These tables show that RF has the highest classification accuracy on all types of features when comparing to other classification methods. RRF, GRRF and GRF are improved versions of RF but they are recommended for high-dimensional data. In this study, all features types are not high-dimensional (number of dimensions are 32, 72, and 700 respectively), the RRF, GRRF as well as GRF therefore do not give the best results but they also provide good results on all features types.

Tables 4.1 and table 4.2 present the results of different classification models on the derived features and the proposed features. Regarding these two kinds of features, RF has proven the best capability for classifying on all folds, with classification accuracy average 96.64% (table 4.1) and 98.24% (table 4.2). The k -NN model and SVM model show a lower classification rate compared to all versions of RF with 87.90% and 94.90%, respectively (table 4.1).

Table 4.2 shows that when combining SVM with the proposed features gives better results (97.31%) than combining SVM with derived features (94.9%, Table 4.1) and dissimilarity features (94.76%, Table 4.3). In contrast to the SVM, k -NN has the lowest performance (82.74%, table 4.2), which implies that combining k -NN with the proposed features as well as with the derived features is not favorable for identifying phytoplankton species. This method drops its performance (table 4.2) because it is very sensitive to the 3rd moment (values of 3rd moment range from 0 to 69,000,000 while values of other features are too small). Besides, for more robust verification of the proposal features and classifiers, 5-fold cross validation is performed, in which 3 folds for learning, 1 fold for validation and 1 fold for testing. RF method always proves the best performance 98.57%, following by GRF 97.86%. SVM and GRRF have the same accuracy 97.14%. The performance of GRF is 95.71% and the last is k -NN with 79.29%.

Table 4.3 illustrates the classification results of different methods on the dissimilarity features. In contrast to the results in table 4.1 and table 4.2, k -NN method demonstrates superior capability for the task of identifying phytoplankton species. We find that when using the dis-

similarity features (based on DTW), the accuracy of the k -NN classifier is better than when combining k -NN with the derived features (L-1, 87.9% - table 4.1) or with the proposed features (L-2, 82.7% -table 4.2). This result is entirely interpretable because through experimental tests we demonstrate that the combination of 1-NN with DTW distance “has proven exceptionally difficult to beat” [13]. Concerning RRF, GRRF and GRF, with this type of features, the performance of these methods are less than their performance when they combine with the derived features and with the proposed features. However, RF has always stable in the best classification capacity, the same result as k -NN 97.44%.

In addition, in this study we also compare the results of target assignment of the same classifier on different features types (table 4.4) as well as different classifiers on the same features type (table 4.5). Table 4.5 is a contingency table of RF classifier on the derived features and the proposed features. In the 1st fold, RF classifies correctly 165 samples on the proposed features and 171 samples on the derived features. However, only 164 samples are the same classified on the both of features types. Table V is a contingency table of k -NN and RF methods based on the dissimilarity features. In the 4th fold, both RF and k -NN methods correctly classify 169 samples but only 167 samples are classified in common.

Besides the comparison of performance of different classifiers and results of target assignment, we carry out identifying which attribute affects the response variable (true label) on the derived features and the proposed features. A supervised technique: Linear Discriminant Analysis (LDA) [155] is used for analyzing. This technique permits to detect a linear combination of predictor variables (features) that best characterizes or separates two or more classes (targets). In fact, with the derived features, the hflo_ls feature (the height of signal on orange fluorescence FLO in low sensitivity, which corresponds to the maximum feature of the proposed features) is strong relative to the target variable (28.29% of contribution for all LD components). With the proposed features: the entropy_flo_ls variable (the entropy of signal on orange fluorescence FLO in low sensitivity) is the most important feature which affects the classification variable (46.15%). This result shows that, on the 8 signals, the signal on orange fluorescence FLO in low sensitivity is the most influential to the response variable. On the other hand, the classification results of all RF versions using the proposed features (table 4.2) are higher than their results using the derived features (table 4.1). From these analyses, we find that the proposed features are very significant for the task of classifying phytoplankton species.

Based on the results of classification of seven phytoplankton species (tables 4.1, 4.2, and 4.3), RF has proven its ability and stability for identifying phytoplankton species as combining

with different features types (the best performance when RF combining with the proposed features of 98.24%). In contrast, SVM and k -NN indicate less classification capability on the derived features and the proposed features although different kernels have been used and the parameters have been optimized to achieve the best result.

RF has high accuracy classifier and stability because for the classification situation, Breiman [145] pointed out that accuracy of classification can be improved by aggregating the results of many simple classifiers that have little bias by averaging or voting. From the above results and analysis, we suggest combining the proposed features with RF for identifying of phytoplankton species.

4.1.5 Conclusion

In this work, we compare a quantitative performance of six classification methods for identifying phytoplankton species. The obtained results prove that RF with the proposed features is the best robust for phytoplankton species identification. The study highlights two main contributions. Firstly, we propose new features extracted from raw FCM signals. Secondly, we provide a quantitative comparison of different classification algorithms applied to different features types. Besides, we also compare target assignment of the same classifier on different features types as well as different classifiers on the same features type. In addition, we carry out analyzing on the derived features and the proposed features to identify which attribute affect the target variable. The present work will permit combining classifiers (e.g. RF method with k -NN method) or features types (e.g. the derived features with the proposed features) to improve classification results.

4.2 Event detection in a multidimensional time series

As mentioned in the previous section, algal (including phytoplankton) bloom is a very important phenomenon that can help to develop appropriate strategies to avoid economic losses and environmental or ecosystem effect. This work is carried out within the framework of a collaboration between IFREMER and LISIC, especially for the CPER MARCO project. In this section, we emphasize the importance of completing missing data before classification and/or modelisation step to avoid incorrect interpretations of signal dynamics. We base on the previous work of Kevin Rousseeuw (PhD thesis) on a HMM/SC model. This model did not take

into account gaps. So here we complete the signals to improve the dynamic parameters of the HMMs. This study highlights to detect specific events in multivariate time series.

4.2.1 Data presentation

Before the step of detecting and modeling environmental states, it is necessary to characterize the acquired data. This step is essential in order to extract the useful information and make it easily exploitable. This is particularly interesting to carry out an exploratory data analysis to choose or propose adaptive algorithms of data processing.

Here, we explore the data acquired by the MAREL-Carnot station. These data are collected from 2005 to present. For our study, we only focus on the period 2005-2009, including 2009 (table 4.6). This represents a database of 131,472 data acquisition instants for physico-chemical and biological (frequency 20 minutes) signals. For nutrient data including nitrate, phosphate, silicate, in this study, we re-sample with daily frequency. Figures 4.2 and 4.3 illustrate these data.

Table 4.6: Number and percentage of missing values for each signal of the MAREL-Carnot station in the period 2005-2009.

Signal	Number of missing values	Percentage of missing values	Largest gap	Median gap	Number of gaps
Air temperature	18833	14.32%	1515	1	4738
Corrected dissolved-oxygen	21868	16.63%	3044	1	4942
Salinity	16440	12.50%	853	1	4783
Oxygen saturation	23764	18.08%	3044	1	5005
P.A.R	17501	13.31%	853	1	4915
Non-corrected -dissolved oxygen	21814	16.59%	3044	1	4932
pH	35789	27.22%	16843	1	4183
Turbidity	17177	13.07%	853	1	5236
Fluorescence	16182	12.31%	853	1	4816
Sea- level	1	7.610^{-6}	1	1	1
Water temperature	16428	12.5%	853	1	4780
Nitrate	506	27.7%	51	2	98
Phosphate	526	28.8%	56	2	97
Silicate	500	27.4%	70	2	74

Firstly, we notice that the signals appear as noise and some signals have visible cycles like the temperatures and P.A.R. (Photo-synthetically Active Radiation) parameters (figure 4.2 and

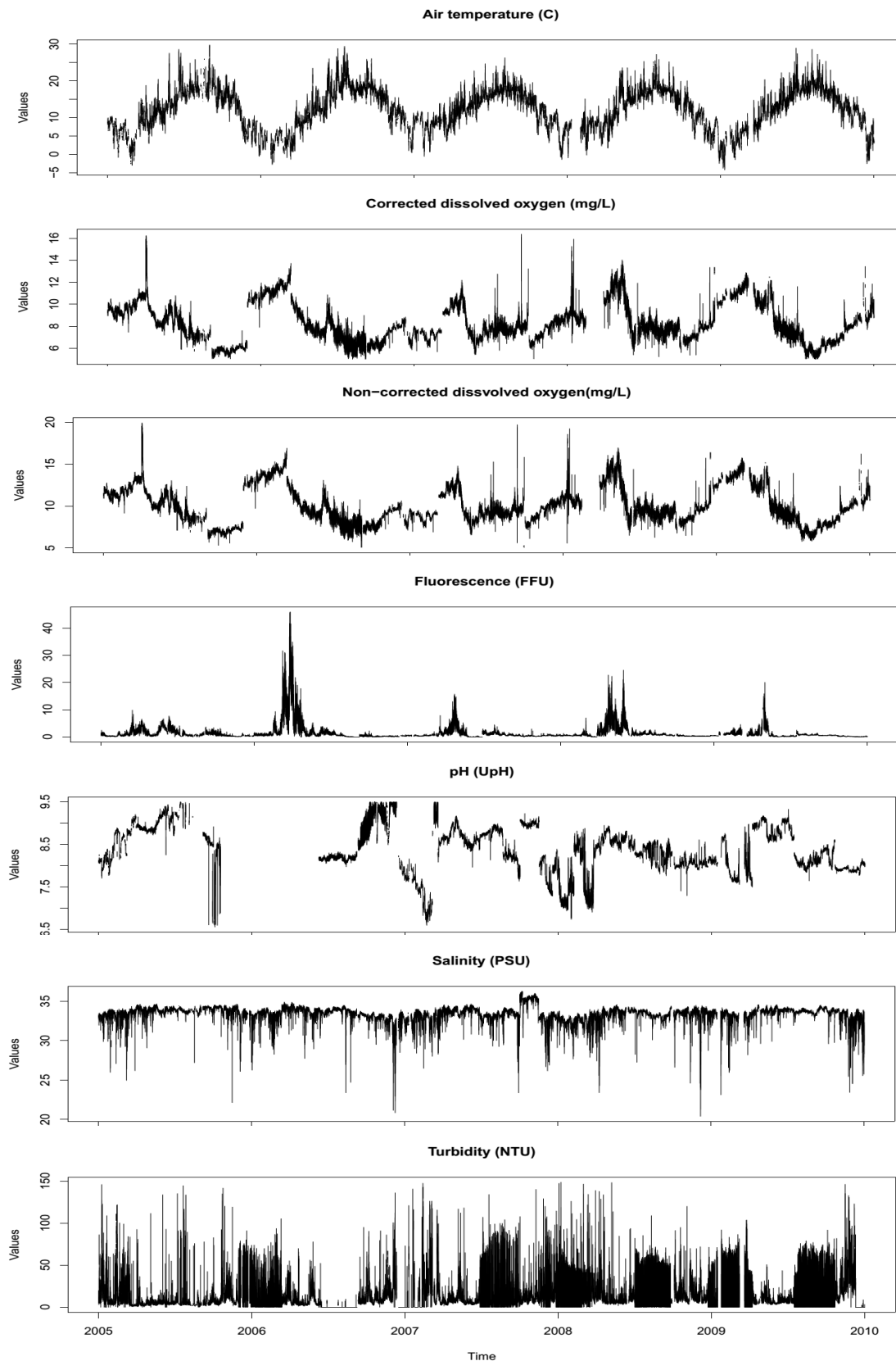


Figure 4.2: Signals collected from the MAREL-Carnot station during the period 2005-2009

4.2. Event detection in a multidimensional time series

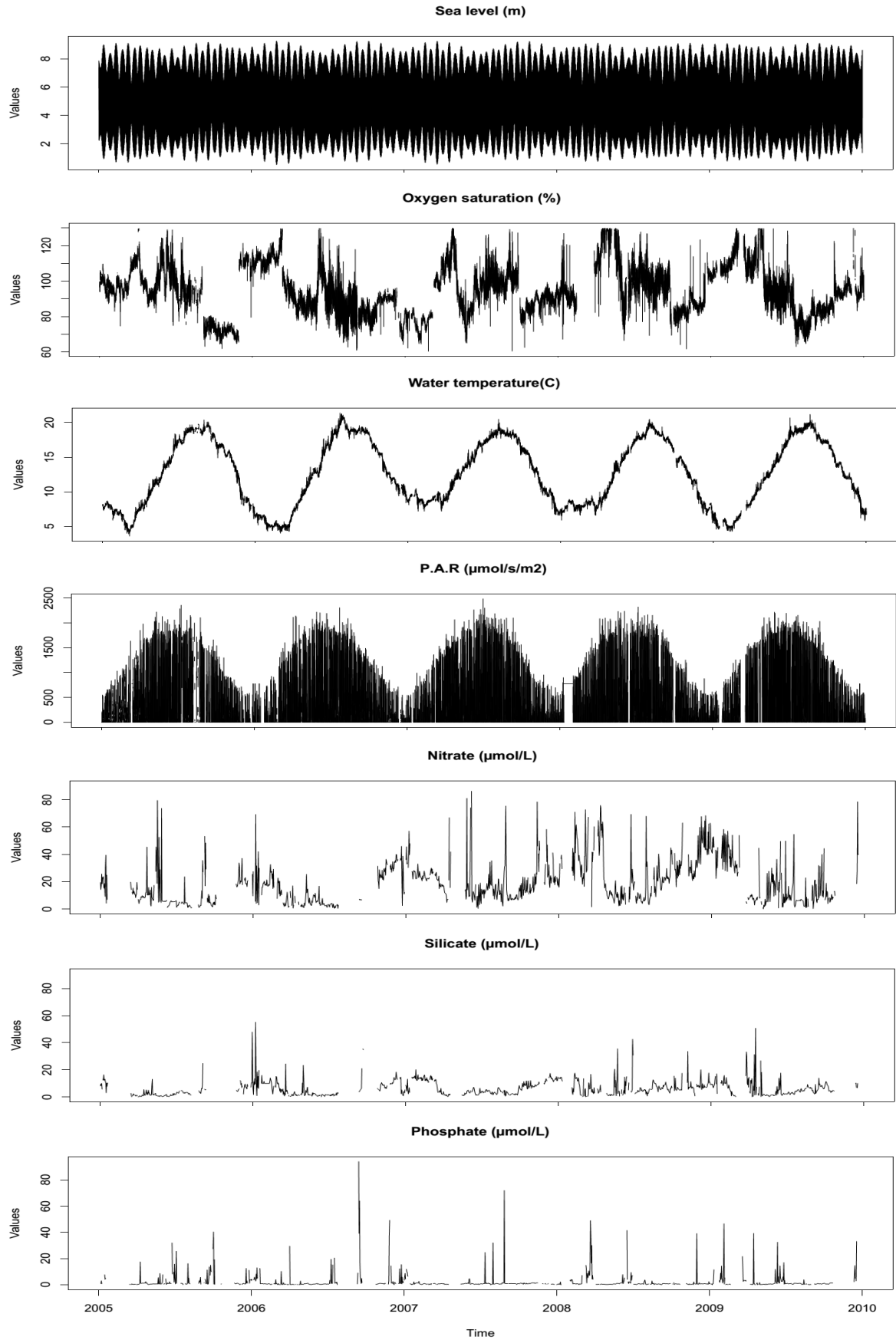


Figure 4.3: Signals collected from the MAREL-Carnot station during the period 2005-2009

4.3). Secondly, the data have episodic or continuous missing values over varying periods, for example in 2005-2006, no pH data were available for approximately 8 months (figure 4.2). The nutrient series have many holes (2005-2009) from one day to more than 2 months (70 days for silicate). After verifying that the data are in the expert range and re-sampling nutrient data, the percentage of missing values for these five years ranges from less than 1 % to more than 28% .

4.2.2 Preprocessing data

Before performing a detection of rare/extreme events on the MAREL Carnot dataset, we need to pre-process the data including data correction (this is based on sensor ranges and expert ranges), time alignment, completion of missing data and normalization of data. Figure 4.4 shows these steps. In this study, we choose 9 signals including: water temperature, salinity, dissolved oxygen, nitrate, phosphate, silicate, turbidity, water level and P.A.R.

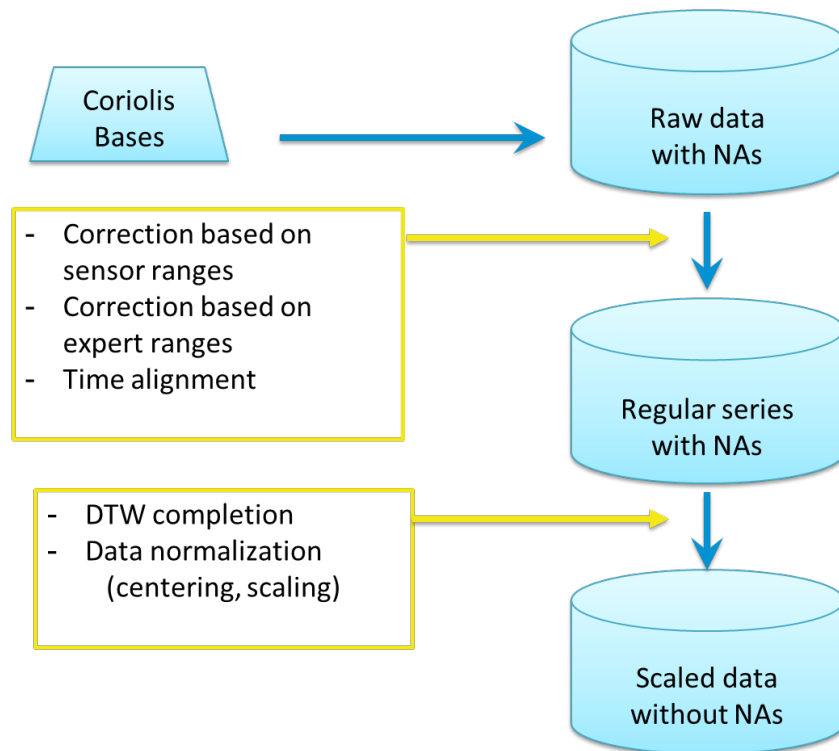


Figure 4.4: Schema of preprocessing data stage

• Correction of data

For all the selected signals, the values are corrected in the measurement range of the sensor and/or defined by the expert.

- **Time alignment**

The acquisition frequency of MAREL-Carnot data is 20 minutes. However, the measurements of various sensors are not done simultaneously, so there is a time shift that can range from a few seconds to a few minutes. The characteristics of the seawater do not radically change every minute, so in order to synchronize the measurements, after deleting the information on the seconds, a time alignment with interval of 20 minutes is performed. For each hour (noted hh), we obtain the alignment as follows:

- [hh:00, hh:20 [= hh:10
- [hh:20 , hh:40 [= hh:30
- [hh:40 , hh:59] = hh:50

So the moment 01:21 will be labeled as the moment 01:30. Our database therefore consists of = 131,472 times starting on 01/01/2005 at 00:10 and ending on 31/12/2009 at 23:50 with a sampling time of 20 minutes. For nutrients with a lower frequency (12 hours), we re-sample with daily frequency.

- **Completion of missing data**

As mentioned above, MAREL Carnot data contain a lot of missing values. There are many isolated missing points and gaps. We apply DTWBI to complete gaps when their size are larger or equal to 9 missing values (corresponding to 3 hours). For isolated missing values and gaps which are smaller than 9 missing points, we use two algorithms as following :

1. Imputing isolated missing - 1NA: replacing a missing value by the average of the previous value and the following one of the missing value at time index t .
2. Imputing small T-gaps (for Marel case $T \leq 9$ - corresponding to less than 3 hours): This method is an extension of the previous one (we named Weighted Moving Average method). The difference is in the update step of the considered window. This algorithm involves 3 steps as follows:
 - Calculate weighted moving average (direction left to right) w_l
 - Calculate weighted moving average (direction right to left) w_r
 - Compute the average of w_l and w_r to fill in missing values

Algorithm 3 Isolated-completion algorithm

Input: $x = \{x_1, x_2, \dots, x_N\}$: incomplete time series

Output: y - completed (imputed) time series

```

1: N=length(x)
2: for i=2 to N-1 do
3:   if ( $x(i) = NA$ ) then
4:      $x(i) = (x(i-1) + x(i+1))/2$ 
5:   end if
6: end for
7: if  $x_1 = NA$  then
8:    $x_1 = x_2$ 
9: end if
10: if  $x_N = NA$  then
11:    $x_N = x_{N-1}$ 
12: end if
13: Return  $y = x$  - with imputed series

```

Algorithm 4 Weighted moving average algorithm

Input: $x = \{x_1, x_2, \dots, x_N\}$: incomplete time series

t - the first position of a T-gap

T : size of the gap

Output: y - completed (imputed) time series

```

1: for each T-gap in the  $x$  do
2:   for  $i = t$  to  $t + T - 1$  do
3:     Calculate left weighted moving average  $w_l(i) = \sum_{j=1}^T \frac{j*x(i-T+j-1)}{T*(T+1)}$ 
4:     Calculate right weighted moving average  $w_r(i) = \sum_{j=1}^T \frac{j*x(i+2*T-j)}{T*(T+1)}$ 
5:      $x(i) = \frac{w_l(i) + w_r(i)}{2}$ 
6:   end for
7: end for
8: Return  $y = x$  - with imputed series

```

Table 4.7: Comparison of indicators between MAREL incomplete and complete Turbidity with satellite Turbidity

	1- Sim	NMAE	RMSE	FSD	1-FA2	FB
#1	0.069	0.079	12.311	0.732	0.767	0.903
#2	0.072	0.082	12.605	0.734	0.794	0.933
1. Imputation Turbidity with Satellite Turbidity						
2. Incomplete Turbidity with Satellite Turbidity						

In this part, we apply three proposed algorithms to fill missing values in MAREL Carnot data. In case of isolated missing values, algorithm 3 (Isolated-completion algorithm) is used. For the remaining cases, depending on the gap size that we apply either algorithm 4 (Weighted moving average algorithm) or DTWBI (detailed in Chapter 2). Thus we have completed 14 signals in which there are 9 signals mentioned above.

To illustrate the performance of proposed imputation algorithms, we here compare two turbidity series: one complete series daily collected by Satellite (latitude= 50.7449 and longitude= 1.54080) and the incomplete series collected by MAREL Carnot (this series has been daily re-sampled).

The table 4.7 shows results of performance indicators comparing between satellite Turbidity and MAREL Carnot Turbidity before and after completing gaps. These results clearly indicate that (it would be better to complete) the completion data is better although after re-sampling, the number of missing values is very small ($44/1821 \approx 2.41\%$) and gaps are small.

Here we see a big difference between values of satellite turbidity and MAREL turbidity (figure 4.5) because the satellite collects data far away from the MAREL Carnot station (the farthest point is 1.25km).

- **Normalization of data**

In this step, we perform scaling and centering data.

4.2.3 Event detection

To discover specific states in this large database, a multi-level spectral clustering approach [156] is performed. Figure 4.6 illustrates different steps to do this task. It consists in performing

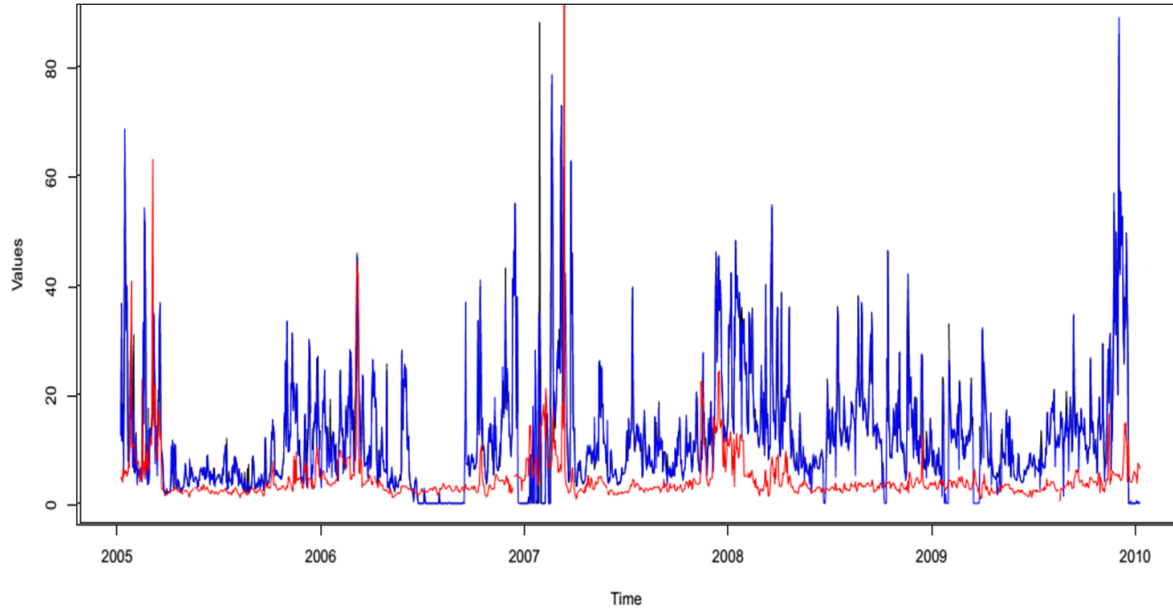


Figure 4.5: Comparison of incomplete(black) Turbidity, complete (blue) Turbidity and satellite Turbidity (red)

several spectral classifications in the spectral space. Here, a top-bottom strategy is deployed to generate states: for each detected state a spectral clustering (SC) algorithm is applied.

Figure 4.7c) presents the distribution of states labeled by the prediction of SC on learning database at the first level. In 2005-2008, the state s_2 , in green color, is related to the period beginning in April and ending in December with dominance in the period May-October. The state s_1 , in red, is dominant in the period from November to April (figure 4.7c). Here data are classified time non-dependent but the system is able to detect the seasonal dynamics when considering the temperature signal: the first state occurs in autumn and winter with low temperature, and the second state takes place in spring and summer with high temperature (figure 4.7b).

At the third level stopped by the expert interpretation, 8 new states has been discovered (figure 4.8). Figure 4.8a) illustrates these events and indicates that the 7th state has a punctual dynamics like intermittent¹ and extreme event². This is strongly correlated with high phosphate values (Figure 4.8b) highlighted by a PCA analysis.

The completion process allows now to better characterize the dynamics of these events

¹Intermittent: occurring at irregular intervals

²Extreme: out of statistic or small events like storm, dam opening, etc.

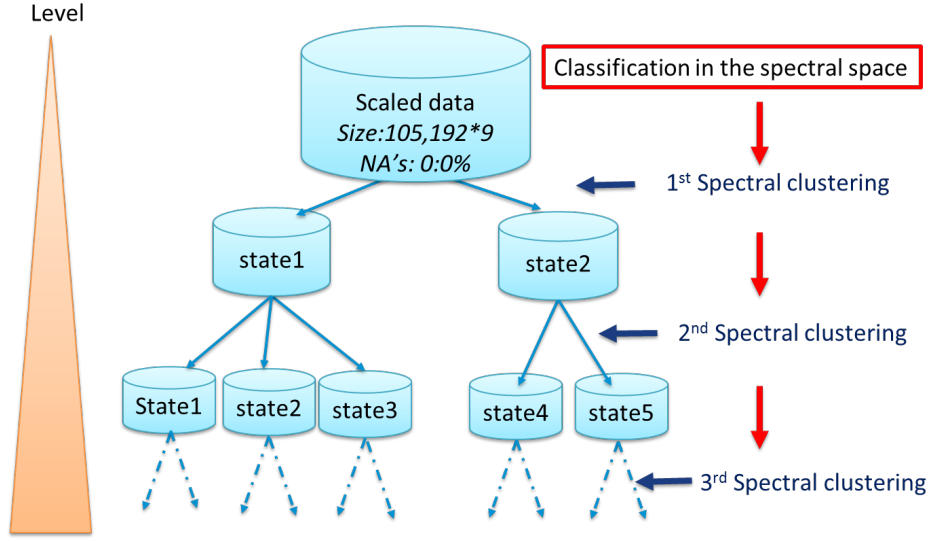


Figure 4.6: Extreme events detection

and to apply the unsupervised Hidden Markov Model (HMM) proposed in [1]. In particular, it enables to improved approximate the emission and transition matrices (A, B) of a HMM model. Another thesis is in progress (from October, 2017) and has promising results from this combination of imputation approach and clustering approach [156].

4.2.4 Conclusion

The goal of this application is to detect events in large MAREL-Carnot data without any priori biological knowledge. These data were collected from the high frequency multi-sensors of the MAREL-Carnot. Preprocessing is one of the essential steps before detecting rare/extreme events including correct out-of-range values, align the sensors on an identical time scale and complete the missing data using different proposed algorithms.

To detect specific events, multi-level spectral clustering approach has been applied. Experiment results show that this method allows to

- define states in multivariate time series,
- detect, identify and characterize these states,
- extract labels of rare or extreme events.

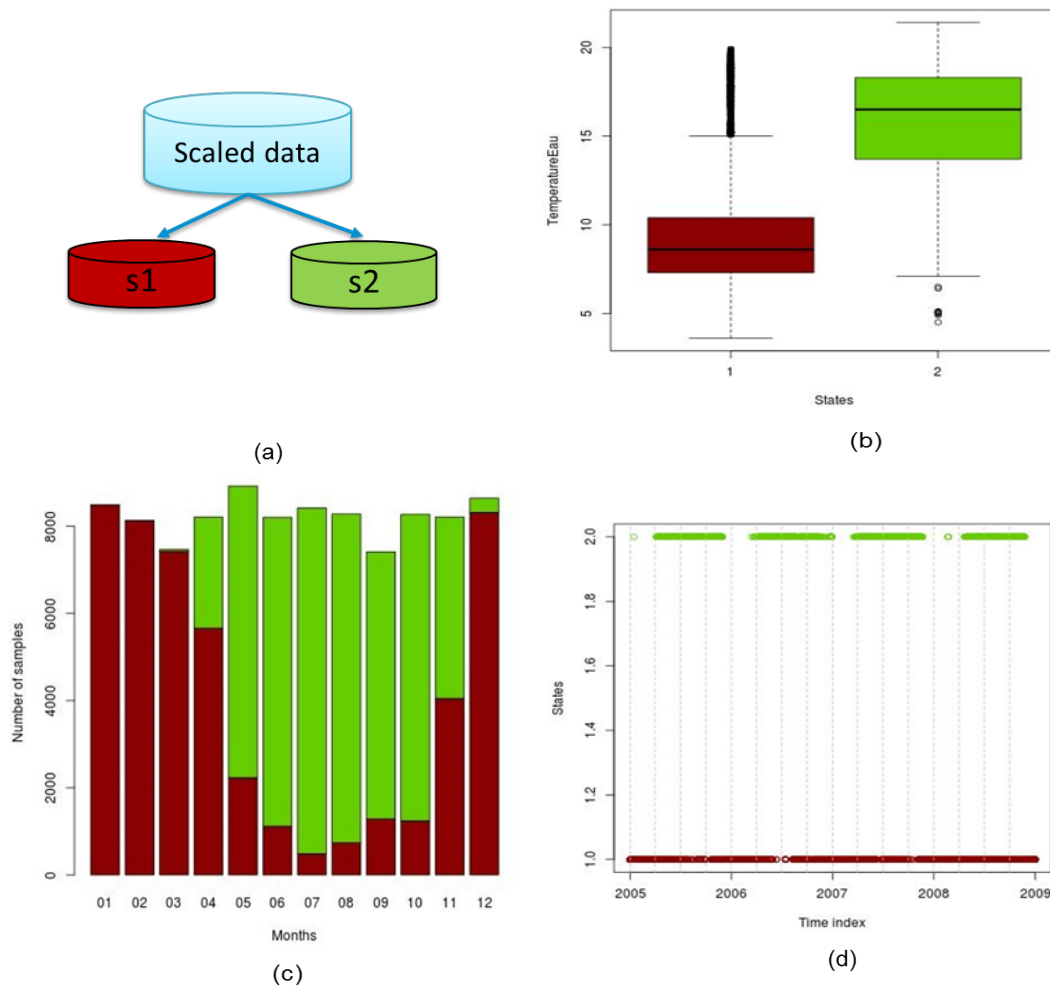


Figure 4.7: Results of the 1st spectral clustering (b) - boxplot of temperature dispersion (c) - states distribution per month with seasonal cycle in the period 2005-2008 and (d) - sequencing of the states in the period 2005-2008.

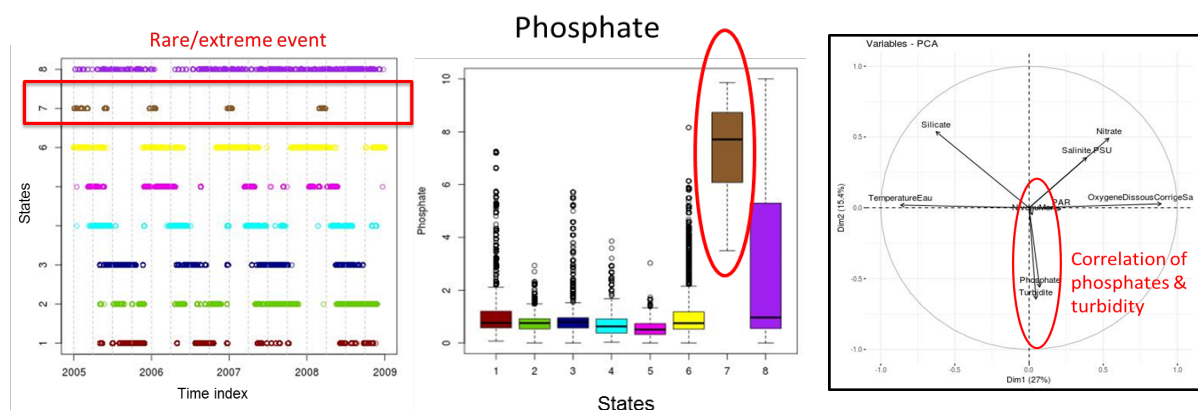


Figure 4.8

4.3 Comparative Study on Univariate Forecasting Methods for Meteorological Time Series

Time series forecasting has an important role in many real applications in meteorology and environment to understand phenomena as climate change and to adapt monitoring strategy. This part aims first to build a framework for forecasting meteorological univariate time series and then to carry out a performance comparison of different univariate models for forecasting task. Six algorithms are discussed: Single exponential smoothing (SES), Seasonal-naive (Snaive), Seasonal-ARIMA (SARIMA), Feed-Forward Neural Network (FFNN), Dynamic Time Warping-based Imputation (DTWBI), Bayesian Structural Time Series (BSTS). Four performance measures and various meteorological time series are used to determine a more customized method for forecasting.

4.3.1 Introduction

Time series forecasting is a matter of great importance in numerous domains [33, 157]. In particular, forecasting hydro-meteorological data plays a key role to better understand climate change, environmental change, and then to adapt monitoring strategy, to deploy preventive or corrective actions. This means to define how past events affect future events. But this task is a remaining challenge because hydro-meteorological data are impacted by diverse phenomena and factors from the environment.

Classic methods for forecasting hydro-meteorological time series were investigated to address the issue of linear models [157] such as linear regression, Exponential Smoothing (ES) or model fitting approaches based on moving average. Autoregressive Integrated Moving Average (ARIMA) is one of the most commonly model for this task [158, 159, 160, 161]. Mahmud *et al.* [162] investigated seasonal ARIMA model to monthly predict rainfall for 12 future months considering thirty rainfall stations in Bangladesh. Nury *et al.* [163] employed SARIMA to forecast future values of temperatures in the Sylhet Division of Bangladesh. The authors showed that the SARIMA is a powerful model for short-term forecasting of the two meteorological variables max. and min. temperature. In [164], Li *et al.* proposed Hadoop-based ARIMA algorithm to forecast weather.

These methods are well adapted to predict generic trends. However, they are not able (i) to determine nonlinear features in data and (ii) to predict quick change inside the process. In

the three past decades, numerous approaches have been proposed to improve accuracy and efficiency of time series forecasting, especially using nonlinear models. Cheng *et al.* [165] pointed out that nonlinear models outperform linear ones for time series forecasting in many applications, such as stock prices [33] and climatology [166].

Artificial Neural Networks (ANN) have become a useful approach to model nonlinear processes such as forecasting rainfall [167, 168], or predicting sea level [169]. In [170], Hung *et al.* investigated feed-forward neural network model and compared it with a simple persistent method for hourly rainfall forecasting (from 75 rain gauge stations) in Bangkok, Thailand. The results showed that FFNN model illustrated better ability to predict rainfall. Chattopadhyay and Chattopadhyay [171] performed a comparison of traditional statistical autoregressive models and autoregressive NN model for univariate prediction of rainfall time series. The results of these studies present the improved performance of NN model when comparing it with the traditional statistical approaches.

Dynamic Time Warping (DTW) [7] is an effective method for measuring similarity between two linear/nonlinear time series. This method is successfully applied in pattern recognition [9, 10], in imputation [90]. For the forecasting task, there are few studies using DTW to predict future values. In [172] Tsinaslanidis and Kugiumtzis used perceptually important points and DTW for stock market forecasting.

Compared to other methods, only few research has been devoted to predict time series using a Bayesian network-based method, although Aguilera *et al.* showed the capability of Bayesian networks in environmental modeling in [173].

Thus this work does not propose a novel forecasting method. However we emphasize on comparing the performances of different univariate approaches by building a framework for forecasting hydro-meteorological univariate time series. Five time series data are applied to the six models we choose for anticipating future values including SES, Snaive, SARIMA, FFNN, DTWBI, and BSTS. This allows to suggest the most suitable method, among the above-mentioned methods, for predicting hydro-meteorological univariate time series ensuring that results are reliable and of high quality.

In addition, for univariate forecasting methods, we must only rely on the available values of this unique variable to estimate future values, without other outside explanatory variables [174]. And, Smith and Agrawal [175] pointed out that "when attempting to forecast univariate time series data, it is generally accepted that parsimonious model techniques are followed.

In the next section, we focus on univariate forecasting methods. Then, Section 4.3.3 intro-

duces the experiments protocol. Results and discussion for forecasting meteorological univariate time series are provided in Section 4.3.4. Finally, conclusions are drawn and future work is presented.

4.3.2 Time series forecasting methods

In this part, several adapted methods for forecasting meteorological univariate time series are mentioned and then will be deployed.

- SES - Simple Exponential Smoothing: ES methods, including a number of ad hoc techniques, used for extrapolating different types of univariate time series. The new forecast at time $t + 1$ is the exponentially weighted average of all t past observations: y_1, y_2, \dots, y_t [157].

$$y_{t+1|t} = \sum_{n=0}^t \alpha(1 - \alpha)^n y_{t-n} \quad (4.7)$$

where $0 \leq \alpha \leq 1$

- Snaive - Seasonal-naive: sets all the forecast values to be the value of the last observation and takes into account the seasonal period as eq.4.8. Hence, this method considers that the most current observed value is the only important one and all the previous observations do not provide information to estimate future values.

$$y_{t+h} = y_{t+h-km} \quad (4.8)$$

where m is a seasonal period, $k = 1 + (h - 1) / m$, h is a number of periods for forecasting.

- SARIMA - Seasonal-ARIMA: the forecast values of a stationary time series can be estimated by an additive linear function composed of p past observations (autoregressive) and q random errors (moving average) as eq.4.9, denoted as $ARIMA(p, d, q)$ ([157]), and d is the differencing number used to make a series y to be stationary.

$$y_t = \sum_{n=1}^p \alpha_n \times y_{t-n} + \varepsilon_t + \sum_{n=1}^q \beta_n \times \varepsilon_{t-n} \quad (4.9)$$

Seasonal ARIMA model is developed from ARIMA by taking into account seasonal factors. SARIMA is labeled as $SARIMA(p, d, q)(P, D, Q)_s$, where upper-cases are counterpart of ARIMA model for the seasonal model and s is number of periods per season.

- **BSTS - Bayesian Structural Time Series:** This model applies Markov Chain Monte Carlo (MCMC) to sample the posterior distribution of a Bayesian structural time series model. The model involves 3 major steps:

Kalman filter: This step consists in decomposing a time series. Various state variables such as trend, seasonality, regression can be added in this step.

Spike-and-slab: This step selects the most important regression predictors.

Bayesian model averaging: This step combines the results and calculates prediction values.

- **DTWBI:** In a previous study [90], we proposed DTWBI approach for completing missing values. Here, we consider forecasting values as missing data, and then we apply DTWBI method to compute these future values. Forecasting process is based on past values. This is fully compatible with DTWBI approach that fills missing values according to the recorded data.

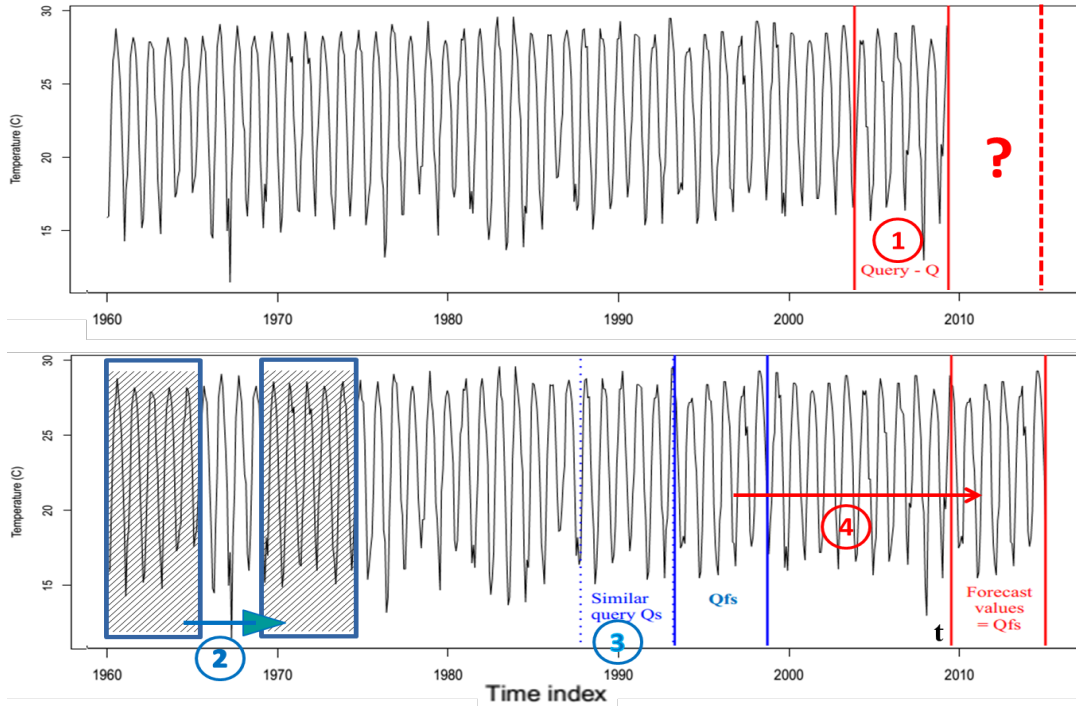


Figure 4.9: Illustration of the DTWBI for the forecasting task: 1-Query building, 2-Sliding window comparison, 3-Window selection, 4-Forecasting values

The approach consists in finding the most similar sub-sequence Q_s to a query Q (the sub-sequence before the predicted position) by sliding windows based on the combination of shape-feature extraction algorithm [52] and DTW method. This allows some distortions

both in the temporal and value axis. Once the most similar window is identified, the following sub-sequence Qfs of the Qs is considered as the forecast values. The dynamics and the shape of data before the forecast values are key-point of this technique (see [90]).

- **FFNN** - Feed-forward neural network: Artificial Neural Network is proposed from inspiring the interconnection neurons of the human. FFNN maps the set of inputs to the set of outputs (both data inputs and outputs are digital). FFNN allows to automatically extract global features before the last decision step (output layer) considering only one hidden layer. A FFNN with no hidden layers is also called linear perceptron: its inputs are directly mapped to the outputs unit via the weighted connections.

4.3.3 Experiment protocol

We have performed a set of experiments on five meteorological time series using six different univariate models to evaluate their forecasting performance.

4.3.3.1 Experiment set up

R language is used to conduct all experiments. We utilize the latest forecast R-packages [176] (for FFNN, Ses and Snaive), *astsa* [177] for SARIMA, *bsts* [178] (for BSTS). For DTWBI, we develop ourselves (upon request). For SARIMA, *auto.arima()* [176] is employed to optimize the parameters p, d, q, P, D, Q . For FFNN, we use the default parameters: input nodes are the number of seasonal lags applied to seasonally adjusted data, and number of nodes in the single hidden layer is half the number of input nodes. And for BSTS, we choose $niter = 50$ with specified seasonality component for each forecasting rate.

4.3.3.2 Data presentation

In this section, we describe the data used for the study. Five hydro-meteorological time series are used for evaluating the performance of forecasting methods (table 4.8). These five datasets were collected at three meteorological stations in Vietnam. They have different sampling frequency and time measurement duration (short or long period). In order to obtain useful information from the datasets and to make the datasets easily exploitable, we analyzed these series. Table 4.8 summarizes their characteristics. All the five datasets have a seasonality component (i.e. an annual cycle), without any linear trend.

Table 4.8: Characteristics of time series

N0	Dataset name	Period	# Samples	Frequency
1	Ba Tri humidity	2003-2007	7,304	6 hours
2	Ba Tri air temperature	2003-2007	7,304	6 hours
3	Cua Ong air temperature	1973-1999	9859	daily
4	Phu Lien humidity	1961-2015	692	monthly
5	Phu Lien air temperature	1961-2014	684	monthly

4.3.3.3 Experiment process

To assess the capacity of forecasting algorithms, we used a technique including three steps. In the first step, data segments are deleted from each time series with different size of consecutive data. In the second step, all forecasting algorithm are applied as mentioned above to estimate the forecast values. Finally, after forecasting data, four performance indicators are computed between the predicted segment and the deleted true values.

In this study, 5 forecasting data levels are considered on 5 datasets. For Phu Lien datasets with monthly sampling frequency, we predict 6, 12, 18, 24 and 30 future months. For the infra daily series, the forecasting size is ranged from 0.5% 0.75%, 1%, 1.25% and 1.5% of the dataset size. For each forecasting level, all the algorithms are conducted 5 times by back-warding the predicted position of each repetition with a size of forecasting. We then run 25 iterations for each dataset.

After the prediction of future values, we compared the performance of six different forecasting methods based on four evaluation metrics including Similarity, NMAE, RMSE and FB. These indicators have been defined in Chapter 1.

4.3.4 Results and discussion

Tables 4.9, 4.10 and 4.11 present average results of different forecasting algorithms on 5 univariate time series for the 4 indicators. The best results for each forecasting rate are bold highlighted.

These results show that FFNN method demonstrates better performance for forecasting future data on Phu Lien temperature, Ba Tri humidity and Ba Tri temperature series: the highest similarity, the lowest NMAE and RMSE at every forecasting levels. The highest similarity (close to 1 with $\text{Sim} \in [0, 1]$), lowest NMAE and RMSE highlight an improved capability for the forecasting task. The results illustrate that the forecast values generated from the FFNN

4.3. Comparative Study on Univariate Forecasting Methods for Meteorological Time Series

method are close to the real values. However, when considering the FB index, the indicator presents the bias of estimated values with real values, the FFNN only yields the best results at some levels.

On Phu Lien temperature data (table 4.10), following the FFNN approach is DTWBI as predicting values from 6 to 30 months on the first 3 indices (Similarity, RMSE and NMAE). For FB index, DTWBI outperformed other methods for larger sizes of forecasting values, from 18 to 30 months. The third one is BSTS on this dataset for all indicators.

In contrast to the three above datasets, BSTS method represents the best predictability on Sim, RMSE and NMAE measurements for all ratios on Phu Lien humidity (table 4.10). The second rank is SARIMA when considering the three indicators (excluding 2nd level for Sim index).

In addition, all five series have a seasonality component, so we choose SARIMA to make a prediction. Although ARIMA is a benchmark method for the forecasting task and for each time series we use R function `auto.arima()` [176] to optimize parameters but with these time series this model does not present its ability.

Looking at the Cua Ong temperature dataset (table 4.11), FFNN continues to demonstrate its predictability for meteorological univariate time series at the first two levels (0.5% and 0.75%). But at higher ratios from level 3 to level 5, DTWBI proves its predictability: the largest value for Similarity, and the smallest value considering error and bias indices.

Ses and Snaive methods were proposed for forecasting data with seasonality or no trend. When considering accuracy indices, they yield quite good results (table 4.9, 4.10 and 4.11).

In this study, we also compare the visualization performance of forecasting values generated from different methods.

Figure 4.10 presents the shape of forecast values yielded by different methods on the Phu Lien humidity series. From this figure, it is clear that SES and Snaive methods do not produce a similar shape as the shape of true values. When comparing the quantitative indicators, DTWBI is only second or third rank, but when considering the shape of forecasting values, DTWBI is better than other methods. The dynamics and the form of predicted values produced by the DTWBI method are very similar to the form of true values.

In this application, Cross-Correlation (CC) coefficients between the query and each sliding window (as defined in DTWBI method) are also calculated, and the maximum coefficient is computed. CC indicates the similarity of two series. For forecasting task, this coefficient demonstrates how past values affect future ones. High CC means that predicted values are

Table 4.9: Performance indices of various forecasting algorithms on Ba Tri datasets (**best results in bold**)

Method	Forecast size (%)	Ba Tri humidity				Ba Tri temperature			
		1-Sim	NMAE	RMSE	FB	1-Sim	NMAE	RMSE	FB
DTWBI	0.5	0.15	0.13	11.75	0.02	0.17	0.08	23.75	-0.01
FFNN		0.11	0.08	6.46	0	0.1	0.04	12.19	0.01
SARIMA		0.13	0.09	8.03	0.01	0.21	0.09	25.76	0.04
BSTS		0.19	0.16	13.14	-0.01	0.23	0.11	35.23	0
ses		0.17	0.14	11.75	0.02	0.19	0.08	25.21	0.01
snaive		0.22	0.18	14.55	-0.03	0.23	0.11	32.35	0.02
DTWBI	0.75	0.16	0.14	12.71	0.02	0.18	0.08	27.09	0.03
FFNN		0.1	0.08	6.62	0	0.14	0.06	17.59	0.02
SARIMA		0.13	0.11	8.81	0.01	0.19	0.08	24.37	0.03
BSTS		0.22	0.21	17.1	0.05	0.2	0.09	28.5	0.01
ses		0.17	0.14	11.9	0.01	0.18	0.08	25.29	0.01
snaive		0.2	0.19	15.56	0	0.22	0.11	34.51	0.01
DTWBI	1	0.16	0.14	13.1	0.03	0.16	0.08	25.46	0.03
FFNN		0.12	0.1	8.59	-0.01	0.11	0.05	15.95	0
SARIMA		0.13	0.11	9.55	0	0.17	0.08	24.27	0.02
BSTS		0.25	0.25	18.85	-0.13	0.28	0.17	52.62	-0.03
ses		0.17	0.15	12.81	0	0.16	0.07	23.46	0
snaive		0.25	0.25	19.56	-0.06	0.22	0.11	33.82	0.01
DTWBI	1.25	0.15	0.15	13.87	-0.01	0.16	0.08	24.75	0.03
FFNN		0.11	0.09	8.61	0	0.13	0.06	18.49	0
SARIMA		0.14	0.12	10.36	0	0.16	0.08	23.64	0.02
BSTS		0.24	0.25	20.42	-0.06	0.19	0.1	30.91	-0.02
ses		0.17	0.16	13.26	0	0.16	0.07	23.71	0.01
snaive		0.21	0.22	19.05	-0.04	0.19	0.1	31.73	-0.01
DTWBI	1.5	0.11	0.11	10.46	0.01	0.14	0.07	21.9	0.03
FFNN		0.09	0.08	7.91	-0.01	0.11	0.05	16.52	0.01
SARIMA		0.14	0.13	10.84	0	0.16	0.08	24.06	0.02
BSTS		0.23	0.24	19.56	-0.06	0.23	0.13	40.17	0.01
ses		0.17	0.17	13.77	0	0.16	0.08	24.8	0
snaive		0.18	0.19	16.81	0.05	0.18	0.09	30.07	-0.04

4.3. Comparative Study on Univariate Forecasting Methods for Meteorological Time Series

Table 4.10: Performance indices of various forecasting algorithms on Phu Lien datasets (**best results in bold**)

Method	Forecast size (month)	Phu Lien temperature				Phu Lien humidity			
		1-Sim	NMAE	RMSE	FB	1- Sim	NMAE	RMSE	FB
DTWBI	6	0.078	0.06	1.29	-0.03	0.24	0.12	5.5	0
FFNN		0.07	0.05	1.18	-0.02	0.25	0.11	4.97	0.02
SARIMA		0.12	0.09	1.78	-0.03	0.23	0.11	4.71	0.02
BSTS		0.07	0.06	1.18	0	0.2	0.08	3.51	0.01
ses		0.24	0.26	6.2	-0.01	0.22	0.11	4.84	0.02
snaive		0.24	0.26	6.2	-0.01	0.31	0.17	6.99	0.06
DTWBI	12	0.075	0.07	1.63	-0.02	0.2	0.12	5.86	-0.02
FFNN		0.06	0.05	1.24	0	0.17	0.1	4.5	0.01
SARIMA		0.08	0.07	1.63	-0.01	0.18	0.1	4.71	0.01
BSTS		0.08	0.07	1.48	0	0.14	0.08	3.64	0
ses		0.29	0.35	7.23	-0.26	0.17	0.1	4.73	0.01
snaive		0.29	0.35	7.23	-0.26	0.2	0.11	5.48	0.02
DTWBI	18	0.07	0.06	1.49	0	0.17	0.11	5.48	-0.02
FFNN		0.06	0.06	1.3	0	0.17	0.1	4.67	-0.03
SARIMA		0.08	0.08	1.82	-0.01	0.16	0.1	4.67	0
BSTS		0.07	0.07	1.54	0.02	0.12	0.07	3.41	-0.01
ses		0.24	0.31	7.18	0.01	0.16	0.1	4.81	-0.01
snaive		0.24	0.31	7.18	0.01	0.2	0.14	6.15	0.03
DTWBI	24	0.065	0.06	1.45	0	0.17	0.12	5.8	-0.03
FFNN		0.058	0.05	1.24	-0.01	0.15	0.11	5.08	0.01
SARIMA		0.09	0.08	1.8	-0.01	0.15	0.1	4.95	0.01
BSTS		0.08	0.08	1.67	0.01	0.13	0.09	3.85	-0.01
ses		0.26	0.31	6.55	-0.22	0.16	0.11	5.03	0.01
snaive		0.26	0.31	6.55	-0.22	0.16	0.11	5.15	0.02
DTWBI	30	0.07	0.07	1.6	0	0.16	0.11	5.34	-0.01
FFNN		0.059	0.05	1.27	-0.01	0.16	0.12	5.69	0.01
SARIMA		0.09	0.08	1.8	-0.01	0.15	0.11	5.08	0.01
BSTS		0.08	0.07	1.66	0.01	0.14	0.1	4.62	0.02
ses		0.23	0.29	6.49	0.04	0.15	0.11	5.28	0.01
snaive		0.23	0.29	6.49	0.04	0.15	0.11	5.56	0.03

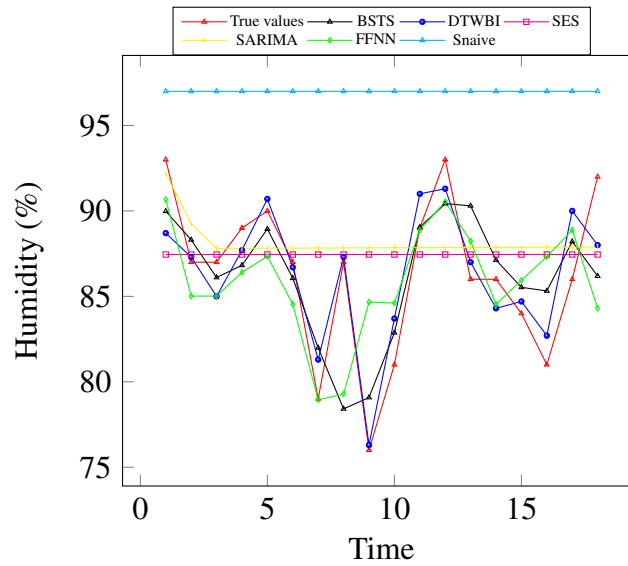


Figure 4.10: True values and forecast values generated from different univariate methods on Phu Lien humidity series (forecast size of 18 months)

close to past values. In table 4.12, we see that CC coefficients are very high only for Phu Lien temperature series, (approximate 1). These CC values make it possible to explain why the predicted values (generated from DTWBI, FFNN, SARIMA and BSTS) and the actual values are nearly identical: similarity values are very high, error and bias indices are very low.

From the above results and analysis, we suggest to use DTWBI approach for forecasting meteorological univariate time series when considering the shape of predicted values and to apply FFNN when regarding the quantitative accuracy.

4.3.5 Conclusion

This work proposes a framework for meteorological univariate time series forecasting. Quantitative performance of different methods are compared on 5 various datasets using 4 quantitative indicators (similarity, NMAE, RMSE and FB). The visual performance of these methods is also evaluated. The obtained results clearly demonstrate that FFNN yielded improved performance when considering accuracy of forecast values and DTWBI is more appropriate when regarding the shape and dynamics of predicted values for forecasting meteorological univariate time series. These results are original for hydro-meteorological univariate time series. The present work will allow to compare different type of univariate time series and to forecast multivariate time series in the future.

Table 4.11: Performance indices of various forecasting algorithms on Cua Ong temperature (best results in bold)

Method	Forecast size (%)	1-Sim	NMAE	RMSE	FB	Forecast size (%)	1-Sim	NMAE	RMSE	FB
DTWBI	0.5	0.21	0.09	30.29	-0.02	0.125	0.15	0.11	34.34	-0.06
FFNN		0.17	0.07	24.5	0.05		0.17	0.14	45.77	0.07
SARIMA		0.3	0.14	42.12	-0.03		0.22	0.15	44.71	-0.04
BSTS		0.48	0.65	202	0.65		0.70	3.47	1087	1.34
ses		0.21	0.1	31.8	0.04		0.2	0.16	48.97	0.04
snaive		0.21	0.1	31.8	0.04		0.2	0.16	48.97	0.04
DTWBI	0.75	0.18	0.11	34.59	0	0.15	0.14	0.11	35.1	-0.05
FFNN		0.16	0.09	28.85	0.08		0.15	0.13	41.57	0.09
SARIMA		0.24	0.14	43.61	0		0.2	0.16	49.46	-0.02
BSTS		0.66	1.48	418.77	-1121		0.32	0.53	199.05	0.20
ses		0.16	0.1	30.85	0		0.2	0.18	55.3	0.06
snaive		0.16	0.1	30.85	0		0.2	0.18	55.3	0.06
DTWBI	0.1	0.17	0.11	35.21	-0.04					
FFNN		0.18	0.13	40.66	0.1					
SARIMA		0.22	0.14	43.21	0.01					
BSTS		0.39	0.50	143.85	-0.89					
ses		0.19	0.14	42.95	0.11					
snaive		0.19	0.14	42.95	0.11					

Table 4.12: The maximum of cross-correlation between the query and sliding windows.

Size	#1	#2	Size (%)	#3	#4	#5
6	0.997	0.872	0.5	0.93	0.91	0.78
12	0.988	0.89	0.75	0.91	0.9	0.76
18	0.979	0.84	1	0.87	0.88	0.75
24	0.977	0.8	1.25	0.86	0.87	0.76
30	0.974	0.75	1.5	0.86	0.85	0.78

#1-Phu Lien temperature, #2-Phu Lien humidity, #3-Ba Tri temperature, #4-Ba Tri humidity, #5-Cua Ong temperature

4.4 Chapter conclusion

In this chapter we have presented three different applications:

The first application is devoted to identify phytoplankton species. In this work, we propose an algorithm that allows to extract the global characteristics of signal. Then it is applied to extract features of phytoplankton signals obtained from the FCM. Through experiments, it clearly shows that the combination of the proposed features with RF provides better results for the phytoplankton classification.

In the second application, we have applied the DTWBI algorithm to fill in large gaps, and two other algorithms to complete small gaps in the MAREL-Carnot dataset. We then have employed a multi-level spectral clustering approach to detect events in the data without any biological prior knowledge. The results show that this protocol allows to (i) determine states in multivariate time series; (ii) detect, identify and characterize states, for example, detecting inaccurate data in the salinity range; and (iii) extract labels of rare/extreme events.

The third application focuses on comparing of different univariate forecasting methods for meteorological time series. In this work, we also apply DTWBI to predict future values. Experiments show that DTWBI gives improved results when considering the shape of forecast values.

List of Publications and valuations related to this chapter

1. Thi-Thu-Hong Phan, Emilie Poisson Caillault, André Bigand, "Comparative Study on Univariate Forecasting Methods for Meteorological Time Series", 26th European Signal Processing Conference. Eusipco 2018. September 3-7, 2018, Rome, Italy.
2. Thi-Thu-Hong Phan, Emilie Poisson Caillault, André Bigand, "Comparative Study on Supervised Learning Methods for Identifying Phytoplankton Species", 2016 IEEE Sixth International Conference on Communications and Electronics (IEEE ICCE 2016). Full Accepted paper. July 27 - 29, 2016. Ha Long, Vietnam. DOI: 10.1109/CCE.2016.7562650
3. Lefebvre A., Grassi K., Phan T.T.H., Devreker D., Bigand A., Poisson-Caillault E., 2018, "Automated tools for analyzing outputs of automated sensors: High frequency Data", Third JERICO-NEXT Workshop on Phytoplankton Automated Observation. March 19-21, 2018 - M.I.O., Marseille, France.
4. Grassi K., Phan T.T.H., Poisson-Caillault E., Bigand A., Devreker D., Lefebvre A., "Results from measurements in the eastern English Channel : MAREL Carnot station", Third JERICO-NEXT Workshop on Phytoplankton Automated Observation. March 19-21, 2018 - M.I.O., Marseille, France.

Conclusions and future work

Conclusions

Missing data are the first weakness of most statistical models and data analysis methods. Despite their suitability of performances, missing data make them unable to operate. Completing missing data is a necessary precondition for a majority of approaches. Therefore, in this work we present our research on the missing data problem. The main contribution is the investigation and development of different techniques to impute large consecutive missing values in time series data. We focus on two types of data: univariate and uncorrelated multivariate time series. In the special case of those two types of time series, the imputation task is a remaining challenge because we cannot take advantage of inter-variable correlations to estimate missing values. Hence, we must exploit observed data in the incomplete time series itself to compute missing data.

The first main objective of this study is the proposition of an effective method to fill large missing values in univariate time series. In this context, we take into account time series characteristics to develop an appropriate and efficient strategy. We have opted for the elastic matching approach combined with a shape-feature extraction algorithm to propose DTWBI method. Experiments carried out on well-known and real-world datasets show that the completion of missing data by finding the most similar sequences using the elastic matching is a robust solution. Looking for similar sequences by elastic matching enables to complete missing values in database while conserving as much as possible the dynamics and the shape of signals. Using the shape-feature extraction algorithm greatly decreases the computing time. In addition, we study different variants of the DTW approach (including DDTW, AFBDTW and DTW-D) and in particular we focus on the comparison of these variants for the univariate imputation task.

The objective of this comparison is to suggest the most adaptable version to fill incompleteness in univariate time series according to the desired goal. Experimental results point out that when considering the accuracy of imputation values, DTW is more convenient and when regarding the shape of imputation values for the large gaps and big datasets, AFBDTW is more suitable.

The second major goal of this study is to deal with missing values in low/un-correlated multivariate time series. In the literature, most proposed approaches address the missing problem in correlated multivariate data by taking advantage of the relations between variables. Fewer studies pay attention to solve the incompleteness issue in low/un-correlated multivariate time series. Thus, we have investigated two algorithms to complete large missing values in low/uncorrelated multivariate data by exploiting the propriety of this type of data.

The first algorithm is an extension of DTWBI, namely DTWUMI (DTW-Uncorrelated Multivariate Imputation). As in DTWBI, we based our approach on the combination of DTW method and shape-feature extraction algorithm. DTWUMI's originality consists in a conjoint multivariate matching. So, we take care of the time index of all the variables. This is shown in the query creation (a matrix of all the variables before or after a gap) and finding similar windows steps. However, only a vector following (or preceding) of the most similar window in the signal containing the considered gap is used to complete the gap.

The second algorithm, namely FSMUMI, takes into account a factor of uncertainty. In this way, we develop a novel similarity measure based on fuzzy grades of basic similarity measures and fuzzy logic rules. In other words, the characteristic of low/un-correlation data is also exploited. Each signal is individually processed. Then, for each gap in this individual signal, we consider the data before this gap and after the gap as two separated univariate time series. The novel fuzzy-weighted similarity measure is applied to find similar windows in each univariate time series. Once imputation values from two separated time series are available, the gap is completed by averaging the both vectors of imputation values.

Experimental results on simulated and real datasets show that both proposed algorithms provide improved performance for the imputation task, not only in accuracy indices but also in the shape of imputation values. Moreover, they are capable of solving the problem of wholly missing variables (missing rows problem).

In this study, in addition to the investigation of various imputation techniques, we have also proposed an algorithm to extract global characteristics of signal (called the shape-feature extraction algorithm). This method is then applied to compute features of phytoplankton signals. Through experiments, it clearly indicates that the combination of the proposed features with

Random Forest provides better results for the phytoplankton classification. The shape-feature extraction algorithm is also combined with DTW approach in the two previous proposed algorithms (DTWBI and DTWUMI), with the aim of reducing the calculation time.

Besides, in this thesis DTWBI is applied in two specific applications. Experimental results are very promising:

In the first application, DTWBI is employed to complete large gaps in the MAREL Carnot dataset, then a multi-level spectral clustering approach is performed to detect rare/extreme events in the data without any prior biological knowledge. The results show that this protocol is able to detect/identify and characterize states and to extract labels of rare/extreme events.

In the second application, DTWBI is devoted to forecast meteorological univariate time series (section 4.3). We are based this work on the idea of imputation to predict future values in meteorological univariate time series. Experiments are conducted on five different univariate meteorological time series collected in Vietnam. The obtained results illustrate that DTWBI gives improved performance when considering the shape of forecast values.

Perspectives for future work

Based on the results presented in this thesis, we will now detail several perspectives for future research directions to improve the overall system.

Improvement of the performance of imputation algorithms

- In this thesis we propose DTWBI algorithm, which enables to impute large consecutive missing values in univariate time series, based on the combination of the shape-feature extraction and elastic matching approaches. This method is evaluated and compared with state-of-the-art approaches which do not allow to complete large periods of lacking data (detailed in Chapter 2). The obtained results are encouraging but in the DTWBI algorithm we only consider one query either before or after the considered gap. Therefore, an investigation of this algorithm should be expanded by taking into account two queries, one query before and one query after the gap. Moreover, data before and data after the gap will be considered as two referenced time series. This would, on the one hand, enrich the learning base and, consequently, improve the prediction ability of the method. On the other hand, this permits to envisage dynamics (important key) of data before and after

the gap to estimate imputation values.

- In the third proposal of this report, we develop a new fuzzy weighted-based similarity measure to fill large consecutive incompleteness in low/un-correlated multivariate time series (Chapter 3). Although this approach meets requirements and illustrates appealing results but there is still place for further development. The hybrid similarity measure is built based on fuzzy grades of basic similarity measures and on fuzzy-based rules (built from ordinary fuzzy set). Type-2 fuzzy set (T2FS) can handle more uncertainty because their membership functions are fuzzy themselves. So that T2FS should be investigated to solve missing data problems in both types of time series: univariate and multivariate time series using a new similarity measure for example.
- In the DTWUMI proposal, we initially use the trapezoid function to estimate initial values for missing data. With the promising results of the FSMUMI algorithm, we intend to use this algorithm instead of the trapezoid function in the DTWUMI algorithm to complete missing data.
- In the present work, we propose two algorithms to complete large missing values in low/un-correlated multivariate time series (Chapter 3). Experiment results show that the proposed algorithms provide improved performance for the imputation task. But in these studies, we only focus on dealing with large gaps in multivariate time series having low/un-correlation. Another solution would be studied to complete missing values in any type of multivariate time series by combining the proposed methods with other powerful approaches, for example Deep learning or random forest (RF).

Applications

- A further investigation on how to forecast multivariate time series can be conducted. As presented in Chapter 4, we have applied DTWBI for forecasting meteorological univariate time series. Results obtained are also promising and reliable. However, in the literature few studies have focused on multivariate time series forecasting. It would be interesting to investigate multivariate forecasting time series with a performance improvement.
- In this study, the detection of extreme/rare events in MAREL Carnot dataset using an unsupervised method (multi-level spectral clustering) has been discussed in Chapter 4.

Moreover, for imputation applications, we have applied similarity measures for retrieving similar subsequences (Chapter 2 and 3). For anomaly detection application, the similarity measure is also an important key to determine "how closely matched are two given observations" ([179]). Motivated from this, future research and further developments of anomaly detection in univariate/multivariate by using similarity measures could be considered.

- In Chapter 4, the shape-feature extraction algorithm is proposed and then applied to classify phytoplankton species. In section 4.1, a better ability for the classification task when combining RF and the proposed features is pointed out. Nevertheless, an improvement of this identification framework could be implemented as follows: firstly, we could combine different types of features, then apply feature-selection methods to select meaningful features which will be used to identify phytoplankton species. This would to extend our work in other learning contexts.

Appendices

List of publications and valuations related to the thesis

1. International journals with peer review

- Thi-Thu-Hong Phan, Emilie Poisson Caillault, Alain Lefebvre, André Bigand, "Dynamic Time Warping-based imputation for univariate time series data", Pattern Recognition Letters. Available online 16 August 2017. In Press.
DOI: 10.1016/j.patrec.2017.08.019
- Thi-Thu-Hong Phan, André Bigand, Emilie Poisson Caillault, "A New Fuzzy Logic-based Similarity Measure applied to Large Gap Imputation for Uncorrelated Multivariate Time Series", Applied Computational Intelligence and Soft Computing. Available online August 2018.
DOI: 10.1155/2018/9095683

2. International conferences with peer review

- Thi-Thu-Hong Phan, Emilie Poisson Caillault, André Bigand, "Comparative Study on Univariate Forecasting Methods for Meteorological Time Series", 26th European Signal Processing Conference. Eusipco 2018. September 3-7, 2018, Rome, Italy.
- Thi-Thu-Hong Phan, Emilie Poisson Caillault, Alain Lefebvre, André Bigand, "DTW-Approach For Uncorrelated Multivariate Time Series Imputation", IEEE International Workshop on Machine Learning for Signal Processing. MLSP 2017. September 25-28, 2017 Roppongi, Tokyo, Japan. DOI: 10.1109/MLSP.2017.8168165

-
- Thi-Thu-Hong Phan, Emilie Poisson Caillault, Alain Lefebvre, André Bigand, "Which DTW Method Applied to Marine Univariate Time Series Imputation", OCEANS 2017 MTS/IEEE, Aberdeen, Scotland, 06/2017. DOI: 10.1109/OCEANSE.2017.8084598
 - Thi-Thu-Hong Phan, Emilie Poisson Caillault, André Bigand, "Comparative Study on Supervised Learning Methods for Identifying Phytoplankton Species", 2016 IEEE Sixth International Conference on Communications and Electronics (IEEE ICCE 2016). Full Accepted paper. July 27 - 29, 2016. Ha Long, Vietnam. DOI: 10.1109/CCE.2016.7562650

3. Communication/National conferences

- Emilie Poisson Caillault, Kelly Grassi, Thi Thu Hong Phan, Camille Dezechache, Jean Prygiel, Alain Lefebvre, "DTWBI & uHMM R-packages for multivariate time series preprocessing and interpretation", 26th Earth Science Meeting, 22-26 October 2018, Lille, France.
- Emilie Poisson Caillault, Camille Dezechache, Thi Thu Hong Phan, Kelly Grassi, Jean Prygiel, and Alain Lefebvre, "Data completion, characterization of environmental states and dynamics using multiparameter time series: DTWBI, DTWUMI and uHMM R-packages", 2nd General Assembly of JERICO-NEXT, Galway, Ireland, 24-27 September, 2018.
- Lefebvre A., Grassi K., Phan T.T.H., Devreker D., Bigand A., Poisson-Caillault E., 2018, "Automated tools for analyzing outputs of automated sensors: High frequency Data", Third JERICO-NEXT Workshop on Phytoplankton Automated Observation. March 19-21, 2018 - M.I.O., Marseille, France.
- Grassi K., Phan T.T.H., Poisson-Caillault E., Bigand A., Devreker D., Lefebvre A., "Results from measurements in the eastern English Channel : MAREL Carnot station", Third JERICO-NEXT Workshop on Phytoplankton Automated Observation. March 19-21, 2018 - M.I.O., Marseille, France.
- Caillault-Poisson E., Lefebvre A., Hébert P.A., Phan, T.T.H., Ternynck P., Marson Q., Rizik A., Wacquet G., Artigas F., Bigand A, "Méthodologie(s) du traitement du signal à la classification/modélisation pour la compréhension de la dynamique des efflorescences phytoplanctoniques", Journée du CPER MARCO, 26 juin 2017, Boulogne sur Mer, France.

APPENDIX A. LIST OF PUBLICATIONS AND VALUATIONS RELATED TO THE THESIS

- Caillault-Poisson E., Phan, T.T.H., Rizik A., Ternynck P., Bigand A, Lefebvre A, "New developments to fill the gap in high frequency data series and to integrate knowledge in Markov modeling of phytoplankton dynamics", EEC'2017: The Eastern English Channel Conference, Wimereux, 06/06/2017, France.

4. Package

- DWTBI R-package <https://cran.r-project.org/web/packages/DTWBI/index.html>
- DTWUMI R-package <https://cran.r-project.org/web/packages/DTWUMI/index.html>

5. Doctoriales

- Thi-Thu-Hong Phan, Emilie Poisson Caillault, Alain Lefebvre, André Bigand. DTW-Approach For Uncorrelated Multivariate Time Series Imputation, 5th édition de la Journée Doctorale du Campus de la Mer, 19 October, 2017 Boulogne sur Mer, France.
- Thi-Thu-Hong Phan, Emilie Poisson Caillault, Alain Lefebvre, André Bigand. Comparative Study on Supervised Learning Methods for Identifying Phytoplankton Species, 4th édition de la Journée Doctorale du Campus de la Mer, 20 October, 2016 Boulogne sur Mer, France.

6. Seminars

- Thi-Thu-Hong Phan, Emilie Poisson Caillault, Alain Lefebvre, André Bigand, "Multivariate times series imputation by unsupervised and supervised approach", journée Intelligence Artificielle LISIC, 18/06/2018, Calais, France.
- Thi-Thu-Hong Phan, Emilie Poisson Caillault, Alain Lefebvre, André Bigand. Which DTW Method Applied to Marine Univariate Time Series Imputation, GRAISyHM: Séminaire des doctorants en traitement du signal et/ou de l'image, 26/04/2017, Lille, France.
- Thi-Thu-Hong Phan, Emilie Poisson Caillault, Alain Lefebvre, André Bigand. Which DTW Method Applied to Marine Univariate Time Series Imputation, Journée Scientifique du Conseil Scientifique du GIS Campus de la Mer, 03/04/2017, Boulogne sur Mer, France.
- Thi-Thu-Hong Phan. Elasting matching for classification and modelisation of incomplete time series, 28/11/2015, IFREMER, Boulogne sur Mer, France.

-
- E. Poisson Caillault, Grassi K., Phan T.T.H., A. Lefebvre et al., Aide à l'interprétation des données : du prétraitement à la classification de signaux temporels et d'images. Séminaire SFR Mer, 22 mai 2017, Boulogne-sur-MER.

Appendix B

Illustration of different DTW versions matching

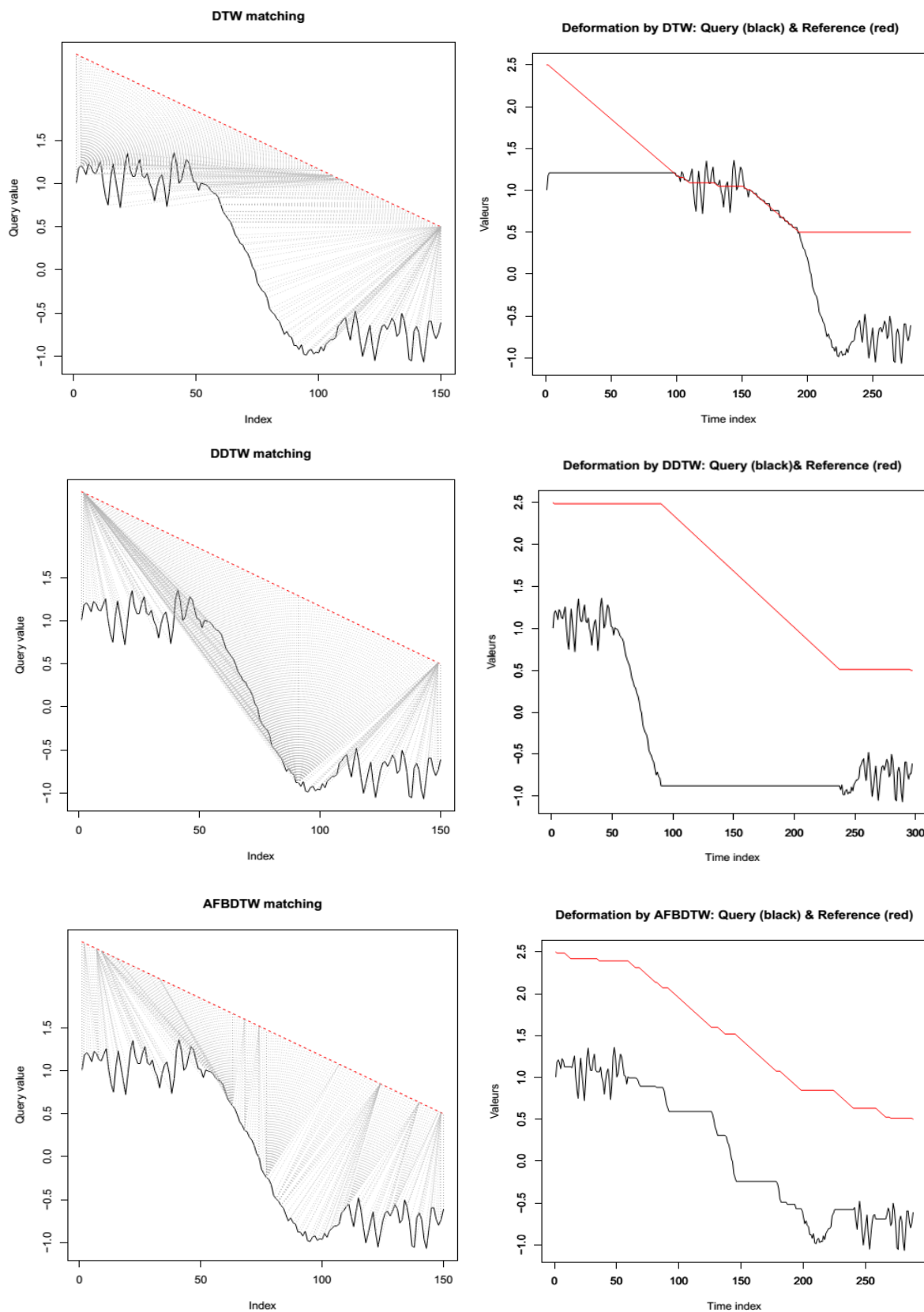


Figure B.1: Query-Reference2

APPENDIX B. ILLUSTRATION OF DIFFERENT DTW VERSIONS MATCHING

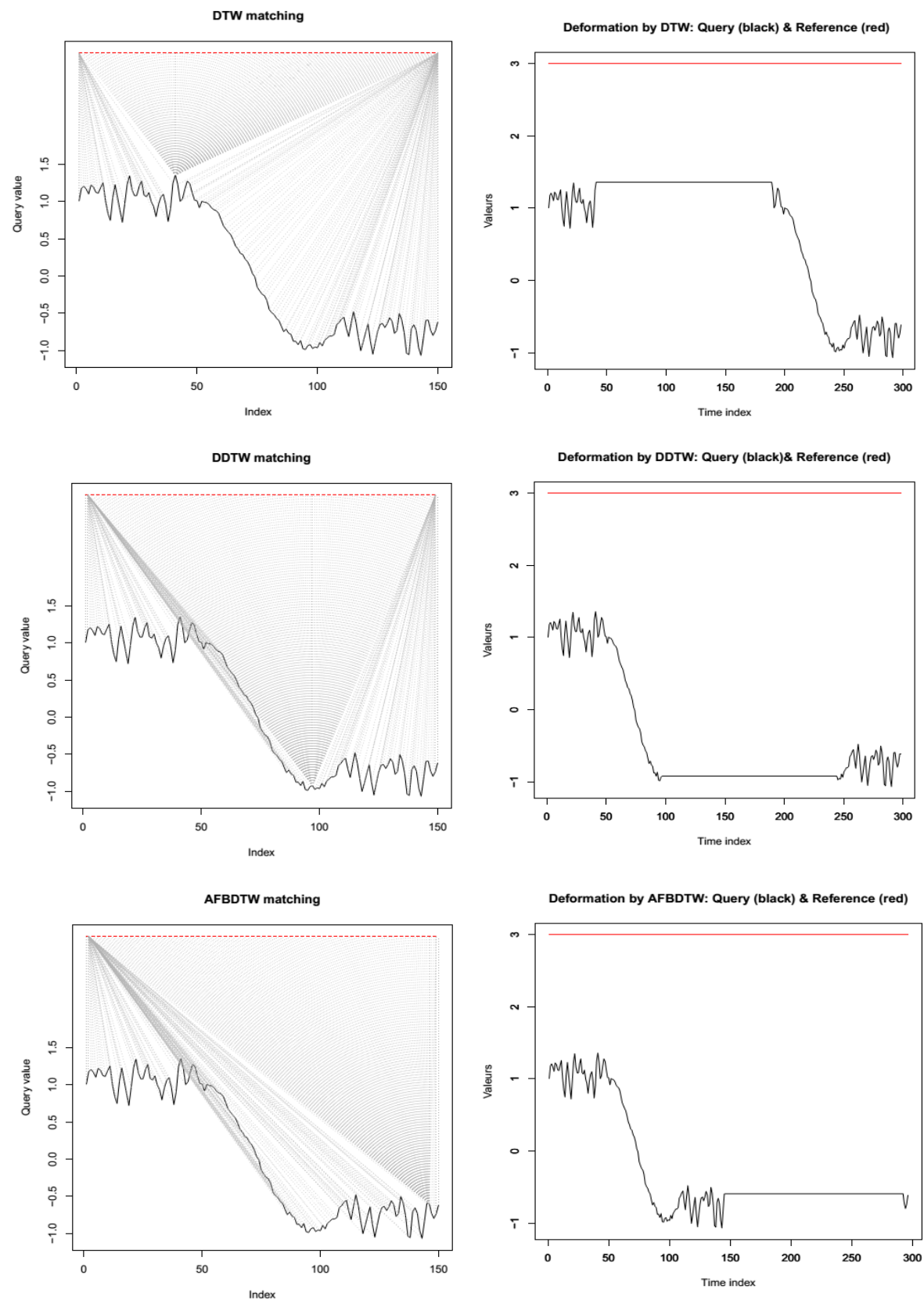


Figure B.2: Query-Reference3

List of fuzzy rules

If (Cosine is Low) and (ED is Low) and (Sim is Low) then (w1 is Low) (w2 is Low) (w3 is Low)

If (Cosine is Low) and (ED is Low) and (Sim is medium) then (w1 is Low) (w2 is Low) (w3 is medium)

If (Cosine is Low) and (ED is Low) and (Sim is medium-high) then (w1 is Low) (w2 is Low) (w3 is medium-high)

If (Cosine is Low) and (ED is Low) and (Sim is high) then (w1 is Low) (w2 is Low) (w3 is high)

If (Cosine is Low) and (ED is medium) and (Sim is Low) then (w1 is Low) (w2 is medium) (w3 is Low)

If (Cosine is Low) and (ED is medium) and (Sim is medium) then (w1 is Low) (w2 is medium) (w3 is medium)

If (Cosine is Low) and (ED is medium) and (Sim is medium-high) then (w1 is Low) (w2 is medium) (w3 is medium-high)

If (Cosine is Low) and (ED is medium) and (Sim is high) then (w1 is Low) (w2 is medium) (w3 is high)

If (Cosine is Low) and (ED is medium-high) and (Sim is Low) then (w1 is Low) (w2 is medium-high) (w3 is Low)

If (Cosine is Low) and (ED is medium-high) and (Sim is medium) then (w1 is Low) (w2 is medium-high) (w3 is medium)

If (Cosine is Low) and (ED is medium-high) and (Sim is medium-high) then (w1 is Low) (w2 is medium-high) (w3 is medium-high)

If (Cosine is Low) and (ED is medium-high) and (Sim is high) then (w1 is Low) (w2 is medium-high) (w3 is high)

If (Cosine is Low) and (ED is high) and (Sim is Low) then (w1 is Low) (w2 is high) (w3 is Low)

If (Cosine is Low) and (ED is high) and (Sim is medium) then (w1 is Low) (w2 is high) (w3 is medium)

If (Cosine is Low) and (ED is high) and (Sim is medium-high) then (w1 is Low) (w2 is high) (w3 is medium-high)

If (Cosine is Low) and (ED is high) and (Sim is high) then (w1 is Low) (w2 is high) (w3 is high)

If (Cosine is medium) and (ED is Low) and (Sim is Low) then (w1 is medium) (w2 is Low) (w3 is Low)

If (Cosine is medium) and (ED is Low) and (Sim is medium) then (w1 is medium) (w2 is Low) (w3 is medium)

If (Cosine is medium) and (ED is Low) and (Sim is medium-high) then (w1 is medium) (w2 is Low) (w3 is medium-high)

If (Cosine is medium) and (ED is Low) and (Sim is high) then (w1 is medium) (w2 is Low) (w3 is high)

If (Cosine is medium) and (ED is medium) and (Sim is Low) then (w1 is medium) (w2 is medium) (w3 is Low)

If (Cosine is medium) and (ED is medium) and (Sim is medium) then (w1 is medium) (w2 is medium) (w3 is medium)

If (Cosine is medium) and (ED is medium) and (Sim is medium-high) then (w1 is medium) (w2 is medium) (w3 is medium-high)

If (Cosine is medium) and (ED is medium) and (Sim is high) then (w1 is medium) (w2 is medium) (w3 is high)

If (Cosine is medium) and (ED is medium-high) and (Sim is Low) then (w1 is medium) (w2 is medium-high) (w3 is Low)

If (Cosine is medium) and (ED is medium-high) and (Sim is medium) then (w1 is medium) (w2 is medium-high) (w3 is medium)

If (Cosine is medium) and (ED is medium-high) and (Sim is medium-high) then (w1 is medium) (w2 is medium-high) (w3 is medium-high)

If (Cosine is medium) and (ED is medium-high) and (Sim is high) then (w1 is medium) (w2 is medium-high) (w3 is high)

If (Cosine is medium) and (ED is high) and (Sim is Low) then (w1 is medium) (w2 is high) (w3 is Low)

If (Cosine is medium) and (ED is high) and (Sim is medium) then (w1 is medium) (w2 is high) (w3 is medium)

If (Cosine is medium) and (ED is high) and (Sim is medium-high) then (w1 is medium) (w2 is high) (w3 is medium-high)

If (Cosine is medium) and (ED is high) and (Sim is high) then (w1 is medium) (w2 is high) (w3 is high)

If (Cosine is medium-high) and (ED is Low) and (Sim is Low) then (w1 is medium-high) (w2 is Low) (w3 is Low)

If (Cosine is medium-high) and (ED is Low) and (Sim is medium) then (w1 is medium-high) (w2 is Low) (w3 is medium)

If (Cosine is medium-high) and (ED is Low) and (Sim is medium-high) then (w1 is medium-high) (w2 is Low) (w3 is medium-high)

If (Cosine is medium-high) and (ED is Low) and (Sim is high) then (w1 is medium-high) (w2 is Low) (w3 is high)

If (Cosine is medium-high) and (ED is medium) and (Sim is Low) then (w1 is medium-high) (w2 is medium) (w3 is Low)

If (Cosine is medium-high) and (ED is medium) and (Sim is medium) then (w1 is medium-high) (w2 is medium) (w3 is medium)

If (Cosine is medium-high) and (ED is medium) and (Sim is medium-high) then (w1 is medium-high) (w2 is medium) (w3 is medium-high)

If (Cosine is medium-high) and (ED is medium) and (Sim is high) then (w1 is medium-high) (w2 is medium) (w3 is high)

If (Cosine is medium-high) and (ED is medium-high) and (Sim is Low) then (w1 is medium-high) (w2 is medium-high) (w3 is Low)

If (Cosine is medium-high) and (ED is medium-high) and (Sim is medium) then (w1 is medium-high) (w2 is medium-high) (w3 is medium)

If (Cosine is medium-high) and (ED is medium-high) and (Sim is medium-high) then (w1 is medium-high) (w2 is medium-high) (w3 is medium-high)

If (Cosine is medium-high) and (ED is medium-high) and (Sim is high) then (w1 is medium-high) (w2 is medium-high) (w3 is high)

If (Cosine is high) and (ED is Low) and (Sim is Low) then (w1 is high) (w2 is Low) (w3 is Low)

If (Cosine is high) and (ED is Low) and (Sim is medium) then (w1 is high) (w2 is Low) (w3 is medium)

If (Cosine is high) and (ED is Low) and (Sim is medium-high) then (w1 is high) (w2 is Low) (w3 is medium-high)

If (Cosine is high) and (ED is Low) and (Sim is high) then (w1 is high) (w2 is Low) (w3 is high)

If (Cosine is high) and (ED is medium) and (Sim is Low) then (w1 is high) (w2 is medium) (w3 is Low)

If (Cosine is high) and (ED is medium) and (Sim is medium) then (w1 is high) (w2 is medium) (w3 is medium)

APPENDIX C. LIST OF FUZZY RULES

If (Cosine is high) and (ED is medium) and (Sim is medium-high) then (w1 is high) (w2 is medium) (w3 is medium-high)

If (Cosine is high) and (ED is medium) and (Sim is high) then (w1 is high) (w2 is medium) (w3 is high)

If (Cosine is high) and (ED is medium-high) and (Sim is Low) then (w1 is high) (w2 is medium-high) (w3 is Low)

If (Cosine is high) and (ED is medium-high) and (Sim is medium) then (w1 is high) (w2 is medium-high) (w3 is medium)

If (Cosine is high) and (ED is medium-high) and (Sim is medium-high) then (w1 is high) (w2 is medium-high) (w3 is medium-high)

If (Cosine is high) and (ED is medium-high) and (Sim is high) then (w1 is high) (w2 is medium-high) (w3 is high)

If (Cosine is high) and (ED is high) and (Sim is Low) then (w1 is high) (w2 is high) (w3 is Low)

If (Cosine is high) and (ED is high) and (Sim is medium) then (w1 is high) (w2 is high) (w3 is medium)

If (Cosine is high) and (ED is high) and (Sim is medium-high) then (w1 is high) (w2 is high) (w3 is medium-high)

If (Cosine is high) and (ED is high) and (Sim is high) then (w1 is high) (w2 is high) (w3 is high)

Dynamic Time Warping-based imputation for univariate time series data

Thi-Thu-Hong Phan, Emilie Poisson Caillault, Alain Lefebvre, André Bigand, "Dynamic Time Warping-based imputation for univariate time series data", Pattern Recognition Letters. Available online 16 August 2017. In Press, Accepted Manuscript



Contents lists available at ScienceDirect

Pattern Recognition Letters

journal homepage: www.elsevier.com/locate/patrec

Dynamic time warping-based imputation for univariate time series data

Thi-Thu-Hong Phan^{a,b,*}, Émilie Poisson Caillault^{a,c,*}, Alain Lefebvre^c, André Bigand^a

^a University Littoral Côte d'Opale, EA 4491-LISIC, F-62228 Calais, France

^b Vietnam National University of Agriculture, Department of Computer Science, Hanoi, Vietnam

^c IFREMER, IER BL, F-62321 Boulogne-sur-mer, France

ARTICLE INFO

Article history:
Available online xxx

Keywords:
Imputation
Missing data
Univariate time series
DTW
Similarity

ABSTRACT

Time series with missing values occur in almost any domain of applied sciences. Ignoring missing values can lead to a loss of efficiency and unreliable results, especially for large missing sub-sequence(s). This paper proposes an approach to fill in large gap(s) within time series data under the assumption of effective information. To obtain the imputation of missing values, we find the most similar sub-sequence to the sub-sequence before (resp. after) the missing values, then complete the gap by the next (resp. previous) sub-sequence of the most similar one. Dynamic Time Warping algorithm is applied to compare sub-sequences, and combined with the shape-feature extraction algorithm for reducing insignificant solutions. Eight well-known and real-world data sets are used for evaluating the performance of the proposed approach in comparison with five other methods on different indicators. The obtained results proved that the performance of our approach is the most robust one in case of time series data having high auto-correlation and cross-correlation, strong seasonality, large gap(s), and complex distribution.

© 2017 Elsevier B.V. All rights reserved.

1. Introduction

Recent advances in monitoring systems, communication and information technology, storage capacity and remote sensing systems make it possible to consider huge time series databases. These databases have been collected over many years with intraday samplings. However, they are usually incomplete due to sensor failures, communication/transmission problems or bad weather conditions for manual measures or maintenance. This is particularly the case for marine samples [3,26]. Incomplete missing data are problematic [8] because most data analysis algorithms and most statistical softwares are not designed to handle this kind of data.

Let consider some terminologies and a real marine data set to illustrate the problem. A time series $x = \{x_t | t = 1, 2, \dots, N\}$ is a set of N observations successive indexed in time, occurring in uniform intervals. A single hole at index t is an isolated missing value where observations at time $t - 1$ and $t + 1$ are available, we note $x_t = NA$ (NA stands for not available). A hole of size T , also called gap, is an interval $[t : t + T - 1]$ of consecutive missing values and is denoted $x[t : t + T - 1] = NA$. We define a large gap when T is larger than the known-process change, so it depends

on each application. At the MAREL Carnot station, a marine water monitoring platform in the eastern English Channel, France [15], 19 large time series are collected every 20 min as fluorescence, turbidity, oxygen saturation and so on. These data contain single and large holes. For example, oxygen saturation series has 131,472 observations and only 81.9% available. This series comprises 4004 isolated missing values and many consecutive missing data. The size of these gaps are various from one hour to few months; the largest gap is a 3044 points corresponding to 42 days. Single holes and gaps having $T < \text{tide duration-holes}$ (807 missing points) could be easily replaced by local averages. For the other gaps, the phytoplankton bloom dynamics or composition changes too fast to use linear or spline imputation method.

Other classical solution consists in ignoring missing data or listwise deletion. But it is easy to imagine that this drastic solution may lead to serious problems, especially for time series data (the considered values would depend on the past values). The first potential consequence of this method is information loss which could lose efficiency [20]. The second consequence is about systematic differences between observed and unobserved data that leads to biased and unreliable results [9].

Therefore, it is crucial to propose a new technique to estimate missing values. One prospective approach to solve missing data problems is the adoption of imputation techniques [12]. These techniques should ensure that the obtained results are

* Corresponding authors.

E-mail addresses: pthong@vnu.edu.vn, hongptvn@gmail.com (T.-T.-H. Phan), emilie.poisson@univ-littoral.fr (É. Poisson Caillault).

<http://dx.doi.org/10.1016/j.patrec.2017.08.019>

0167-8655/© 2017 Elsevier B.V. All rights reserved.

Please cite this article as: T.-T.-H. Phan et al., Dynamic time warping-based imputation for univariate time series data, Pattern Recognition Letters (2017), <http://dx.doi.org/10.1016/j.patrec.2017.08.019>

efficient (having minimal standard errors) and reliable (effective, curve-shape respect).

According to our knowledge, there is no application for filling time series data with large missing gap(s) size for univariate time series. We therefore investigate and propose an algorithm to complete large gap(s) of univariate time series based on Dynamic Time Wrapping [28]. We do not deal with all the missing data over the entire series, but we focus on each large gap where series-shape change could occur over the duration of this large gap. Further, the distribution of missing values or entire signal could be very difficult to estimate, so it is necessary to make some assumptions. Our approach makes the assumption that the information about missing values exists within the univariate time series and takes into account the time series characteristics.

This paper is organized as follows. First, we discuss the related work in Section 2. The analysis of time series data is discussed in Section 3. The proposed approach is introduced in Section 4. Experimental results and discussion on 8 data sets are illustrated in Section 5. Conclusion is set out in Section 6.

2. Related work

In the literature, missing data mechanisms can be divided into three categories. Each category is based on one possible cause: "Missing data are completely random" (Missing Completely At Random, MCAR, in the literature), "Missing data are random" (Missing At Random, MAR) and "Missing data are not random" (Not Missing At Random, NMAR) [17]. It is important to understand the causes that produce missing data to develop an imputation task. This can help to select an appropriate imputation algorithm [19]. But in practice, understanding the causes remains a challenging task when missing data cannot be known at all, or when these data have a complex distribution [8]. Similarly, assigning sub-sequences of missing values to a category can be blurry [19]. Commonly, most current research works focus on the three types of missing data previously defined to find out corresponding imputation methods. Regarding imputation methods, a large number of successful approaches have been proposed for completing missing data.

Concerning the imputation task for multivariate time series, many studies have been investigated using machine learning techniques as [16,25,30] and model techniques such as [6,7,11,14,23,24,27,29,31,33,35]. The efficiency of these algorithms is based on correlations between signals or their features, and missing values are estimated from the observed values. However, handling missing values within univariate time series data differs from multivariate time series techniques. We must only rely on the available values of this unique variable to estimate the incomplete values of the time series. Moritz et al. [19] showed that imputing univariate time series data is a particularly challenging task.

Fewer studies are devoted to the imputation task for univariate time series. Allison [1] and Bishop [2] proposed to simply substitute the mean or the median of available values to each missing value. These simple algorithms provide the same result for all missing values leading to bias result and to undervalue standard error [5,32]. Other imputation techniques for univariate time series are linear interpolation, spline interpolation and the nearest neighbor interpolation. These techniques were studied for missing data imputation in air quality data sets [12]. The results showed that univariate methods are dependent on the size of the gap in time: the larger gap, the less effective technique. Walter et al. [36] carried out a performance comparison of three methods for univariate time series, namely, ARIMA (Autoregressive Integrated Moving Average), SARIMA (Seasonal ARIMA), and linear regression. The linear regression method was more efficient and effective than the other two methods, only when rearranging the data in periods. This study treated non-stationary seasonal time series data but it

did not take into account series without seasonality. Chiewchan-wattana et al. proposed the Varied-Window Similarity Measure (VWSM) algorithm [4]. This method is better than the spline interpolation, the multiple imputation, and the optimal completion strategy fuzzy c-means algorithms. However, this research only focused on filling one isolated missing value, but did not consider sub-sequence missing. Moritz et al. [19] performed an overview about univariate time series imputation comparing six imputation methods. Nevertheless, this study only considered the MCAR type.

3. Time series characterization

Filling large gaps within time series requires firstly to characterize the data. This step permits to extract useful information from the data set and makes the data set easily exploitable. The four specific components of time series are trend, seasonal, cyclical and random change:

1. *Trend component*: That is the change of variable(s) in terms of monitoring for a long time. If there exists a trend within the time series data (i.e. on the average data), the measurements tend to increase (or decrease) over time.
2. *Seasonal component*: This component takes into account intra-interval fluctuations. That means there is a regular and repeated pattern of peaks and valleys within the time series related to a calendar period such as seasons, quarters, months, weekdays, and so on.
3. *Cyclical component*: This component equals the seasonal one, the difference is that its cycle duration is more than one year.
4. *Random change component*: This component considers random fluctuations around the trend; this could affect the cyclical and seasonal variations of the observed sequence, but it cannot be predicted by previous data (in the past of time series).

There are different techniques to decompose time series into components. "Decompose a time series into seasonal, trend and irregular components using moving averages" (R-starts package, [22]) is the most common technique. In this study, we use this technique to analyze time series data. *Auto-correlation function* (ACF) provides an additional important indication of the properties of time series (i.e. how past and future data points are related). Therefore, it can be used to identify the possible structure of time series data, and to create reliable forecasts and imputations [19]. High auto-correlation values mean that the future is strongly correlated to the past. Fig. 1 indicates the auto-correlation of Mackey-Glass chaotic, water level and Google data sets in our experiment.

4. The proposed method - DTWBI

In this part, we present a new method for imputing missing values of univariate time series data.

A time series x is referred as incomplete time series when it contains missing values (or values are Not Available-NA). Recall that the portion of a time series between two points x_t and x_{t+T-1} with $x_i = NA$ ($i = t : t + T - 1$) is called a gap of T -size at position t . In this paper, we consider a large gap when $T \geq 6\%N$ for small time series ($N < 10,000$) or when T is larger than the known-process change.

The proposed approach finds the most similar sub-sequence (Q_s) to a query (Q), with Q (cf. Fig. 2) is the sub-sequence before a gap of T size at position t ($Q = x[t - T : t - 1]$), and completes this gap by the following sub-sequence of the Q_s .

To find the Q_s similar sub-sequence, we use the principles of Dynamic Time Warping - DTW [28], especially transformed from original data to Derivative Dynamic Time Warping - DDTW data [13]. The DDTW data are used because we can obtain information about the shape of sequence [13]. The dynamics and the shape

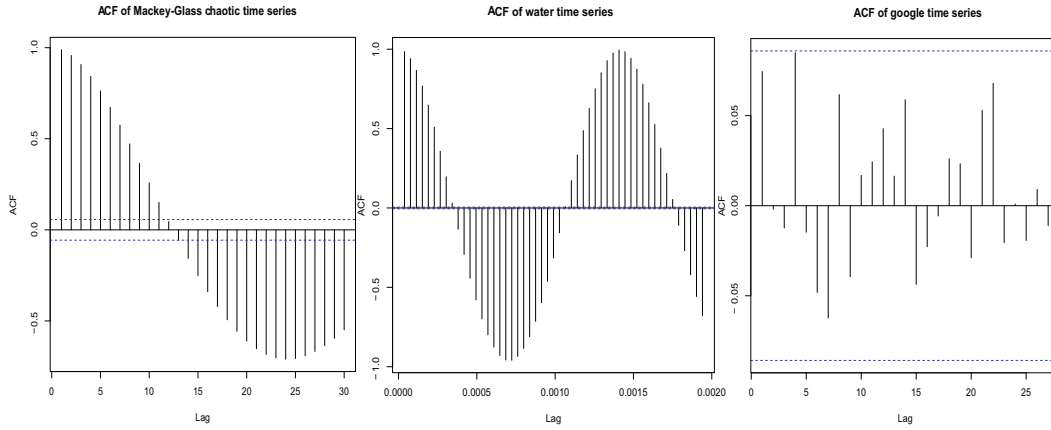


Fig. 1. ACF of Mackey-Glass chaotic, water level and Google time series.

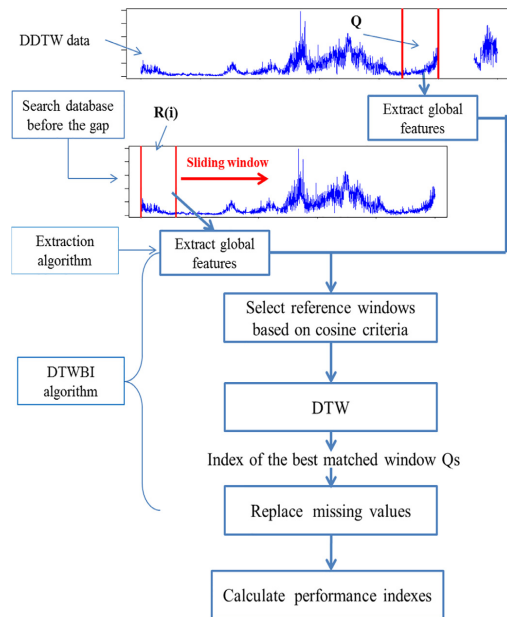


Fig. 2. Diagram of DTWBI method for univariate time series imputation.

of data before a gap are a key-point of our method. The elastic matching is used to find a similar window to the Q query of T size in the search database. Once the most similar window is identified, the following window will be copied to the location of missing values. Fig. 2 describes the different steps of our approach.

The detail of DTWBI (namely DTW-Based Imputation) algorithm is introduced in Algorithm 1. In the proposed method, the shape-feature extraction algorithm [21] is applied before using DTW algorithm in order to reduce the computation time. As we know DTW's time complexity is $O(N^2)$, so this is a very useful step to decrease computation time of DTW method. A reference

window is selected to calculate DTW cost only if the correlation between the shape-features (also called the global features) of this window and the ones of the query is very high. In addition, we apply the shape-feature extraction algorithm because it better presents the shape and dynamics of series through 9 elements, such as moments (the 1st moment, the 2nd moment, the 3rd moment), number of peaks, entropy, etc (see [21] for more detail). This is an important objective of the proposed method. In Algorithm 1, we just mention the finding of similar windows before the gap. In case of finding similar windows after the gap, the method just needs to shift the corresponding index.

5. Experimental results and discussion

5.1. Data presentation

In this study, we analyzed 8 data sets in order to evaluate the performance of the proposed technique. 4 data sets come from TSA package [10]. These data sets are chosen because they are usually used in the literature, including Airpassenger, Beersales, Google, and SP. Besides, we also choose other data sets from various domains in different places:

1. Airpassenger - Monthly total international airline passengers from 01/1960 to 12/1971.
2. Beersales - Monthly beer sales in millions of barrels, from 01/1975 to 12/1990.
3. Google - Daily returns of the google stock from 08/20/04 to 09/13/06.
4. SP - Quarterly S&P Composite Index, 1936Q1–1977Q4.
5. CO₂ concentrations - This data set contains monthly mean CO₂ concentrations at the Mauna Loa Observatory from 1974 to 1987 [34].
6. Mackey-Glass chaotic - The data is generated from the Mackey-Glass equation which is the nonlinear time delay differential [18].
7. Phu Lien temperature - This data set is composed of monthly mean air temperature at the Phu Lien meteorological station in Vietnam from 1/1961 to 12/2014.
8. Water level - The MAREL Carnot data in France acquired from 2005 up today. For our study, we focus on the water level, sampling frequency of 20 min from 01/1/2015 to 31/12/2009 [15].

Table 1 summarizes characteristics of the data sets.

Please cite this article as: T.-T.-H. Phan et al., Dynamic time warping-based imputation for univariate time series data, Pattern Recognition Letters (2017), <http://dx.doi.org/10.1016/j.patrec.2017.08.019>

APPENDIX D. DYNAMIC TIME WARPING-BASED IMPUTATION FOR UNIVARIATE TIME SERIES DATA

ARTICLE IN PRESS

JID: PATREC

[m5G;August 30, 2017;13:44]

4

T.-T.-H. Phan et al. / Pattern Recognition Letters 000 (2017) 1–9

Table 1
Data characteristics.

N0	Data set name	N0 of instants	Trend (Y/N)	Seasonal (Y/N)	Frequency
1	Air passenger	144	Y	Y	Monthly
2	Beersales	192	Y	Y	Monthly
3	Google	521	N	N	Daily
4	SP	168	Y	Y	Quarterly
5	CO ₂ concentrations	160	Y	Y	Monthly
6	Mackey-Glass chaotic	1201	N	N	
7	Phu Lien temperature	648	N	Y	Monthly
8	Water level	131,472	N	Y	20 min

5.2. Univariate time series imputation algorithms

The performance of the proposed method compared with 5 other existing methods for univariate time series (namely, na.interp, na.locf, na.approx, na.aggregate, na.spline) is evaluated in this paper. All these methods are implemented using R language (na stands for Not Available):

1. na.interp (forecast R-package): linear interpolation for non-seasonal series and Seasonal Trend decomposition using Loess (STL decomposition) for seasonal series to replace missing values [10]. A seasonal model is fitted to the data, and then interpolation is made on the seasonally adjusted series, before re-seasonalizing. So, this method is especially devoted to strong and clear seasonality data.
2. na.locf (last observation carried forward) (zoo R-package): any missing value is replaced by the most recent non-NA value prior to it [37]. Conceptually, this method assumes that the outcome would not change after the last observed value. Therefore, there has been no time effect since the last observed data.
3. na.approx (zoo R-package): generic function for replacing each NA with interpolated values [37].
4. na.aggregate (zoo R-package): generic function for replacing each NA with aggregated values. This allows imputing using the overall mean, by monthly means, etc [37]. In our experiment, we use the overall mean.
5. na.spline (zoo R-package): polynomial (cubic) interpolation to fill in missing data [37].

5.3. Imputation performance indicators

After the completion of missing values, we assess the performance of our method, and then compare it with existing imputation methods based on four different metrics described as follows:

1. Similarity: $Sim(y, x)$ indicates the similarity between actual data (X) and imputation data (Y). It is calculated by:

$$Sim(y, x) = \frac{1}{T} \sum_{i=1}^T \frac{1}{1 + \frac{|y_i - x_i|}{\max(x) - \min(x)}} \quad (1)$$

Where T is the number of missing values. A higher similarity (similarity value $\in [0, 1]$) highlights a better ability method for the task of completing missing values.

2. NMAE: The Normalized Mean Absolute Error between the imputed value y and the respective true value time series x is computed as:

$$NMAE(y, x) = \frac{1}{T} \sum_{i=1}^T \frac{|y_i - x_i|}{V_{\max} - V_{\min}} \quad (2)$$

Where V_{\max} , V_{\min} are the maximum and the minimum values of input time series (time series has missing data) by ignoring the missing values. A lower NMAE means better performance method for the imputation task.

3. RMSE: The Root Mean Square Error is defined as the average squared difference between the imputed value y and the respective true value time series x . This indicator is very useful for measuring overall precision or accuracy. In general, the most effective method would have the lowest RMSE.

$$RMSE(y, x) = \sqrt{\frac{1}{T} \sum_{i=1}^T (y_i - x_i)^2} \quad (3)$$

4. FSD: Fraction of Standard Deviation of the imputed value y and the respective true value time series x is defined as follows:

$$FSD(y, x) = 2 * \frac{|SD(y) - SD(x)|}{SD(y) + SD(x)} \quad (4)$$

This fraction indicates whether a method is acceptable or not (here SD stands for Standard Deviation). For the imputation task, FSD should be closer to 0, the imputation values are closer to the real values.

5.4. Experiment protocol

Indeed, we could not compare the ability of imputation algorithms on real missing data because the true values are not available. Therefore, we have to create simulated missing values on full data to compare the performance of imputation algorithms. For assessing the results, we use a technique based on three steps. In the first step, we create artificial missing data by deleting data values from known time series. The second step consists in applying the imputation algorithms to complete missing data. Finally, the third step compares the performance of the proposed method with published methods using the different imputation performance indicators as previously defined.

In the present study, 5 missing data levels are considered on 8 data sets. If the size of a data set (number of instants of the data set) is less than or equal to 10,000 samples, we create gaps with different sizes: 6%, 7.5%, 10%, 12.5%, 15% of overall data set size. In contrast, when the size of a data set is greater than 10,000 sampling points, gaps are built at rates 0.6%, 0.75%, 1%, 1.25%, and 1.5% of the data set size (here the largest gap of the water level time series is 1972 missing values, corresponding to the missing rate 1.5%). For each missing rate, the algorithms are conducted 10 times by randomly selecting the missing positions on the data. We then run 50 iterations for each data set.

5.5. Results and discussion

5.5.1. Comparison of quantitative performance

Table 2 shows imputation average results of DTWBI, na.interp, na.locf, na.approx, na.aggregate, na.spline methods applied on 8 data sets using 4 indicators: similarity, NAME, RMSE, FSD.

• Airpassenger, Beersales, Google, SP data sets

The Airpassenger data set has both trend and seasonality components. The result from Table 2 indicates that when the gap

Please cite this article as: T.-T.-H. Phan et al., Dynamic time warping-based imputation for univariate time series data, Pattern Recognition Letters (2017), <http://dx.doi.org/10.1016/j.patrec.2017.08.019>

Table 2

Average imputation performance indexes of six methods on eight data sets (best results in bold).

Gap size	Method	Airpassenger				Beersales				Google				SP			
		Sim	NMAE	RMSE	FSD	Sim	NMAE	RMSE	FSD	Sim	NMAE	RMSE	FSD	Sim	NMAE	RMSE	FSD
6%	DTWBI	0.777	0.034	21.1	0.24	0.88	0.035	0.7	0.14	0.83	0.14	0.034	0.43	0.74	0.026	35.5	0.7
	na.interp	0.85	0.019	11.1	0.24	0.89	0.063	0.6	0.15	0.83	0.11	0.032	1.11	0.74	0.028	36.3	0.54
	na.locf	0.76	0.044	26.3	2	0.81	0.129	1.2	2	0.81	0.126	0.036	2	0.75	0.022	29.2	2
	na.approx	0.77	0.037	21.8	1.01	0.8	0.136	1.3	1.5	0.83	0.11	0.032	1.11	0.73	0.028	37	1.03
	na.aggregate	0.8	0.033	20.1	2	0.83	0.11	1.1	2	0.86	0.082	0.024	2	0.78	0.021	26.5	2
7.5%	na.spline	0.71	0.057	35.1	0.52	0.68	0.26	2.3	0.55	0.5	1.813	0.473	1.02	0.63	0.045	56.8	0.41
	DTWBI	0.782	0.035	20.6	0.3	0.87	0.038	0.7	0.1629	0.84	0.131	0.032	0.33	0.76	0.03	38.9	0.52
	na.interp	0.86	0.023	13.6	0.3	0.885	0.067	0.6	0.163	0.83	0.119	0.034	1.18	0.78	0.024	33.1	0.67
	na.locf	0.77	0.046	27.4	2	0.81	0.123	1.2	2	0.82	0.126	0.035	2	0.77	0.026	34.8	2
	na.approx	0.74	0.053	31.3	1.49	0.8	0.132	1.3	1.51	0.83	0.119	0.034	1.18	0.78	0.025	34	1.1
10%	na.aggregate	0.81	0.033	20.2	2	0.82	0.112	1.1	2	0.87	0.081	0.024	2	0.8	0.022	29.1	2
	na.spline	0.6	0.112	65.4	0.45	0.6	0.404	3.5	0.43	0.44	3.652	0.963	1.38	0.69	0.042	54.5	0.55
	DTWBI	0.887	0.02	12.7	0.36	0.84	0.054	1	0.13	0.84	0.132	0.032	0.23	0.81	0.029	40.1	0.57
	na.interp	0.86	0.021	13.1	0.34	0.89	0.068	0.7	0.18	0.85	0.105	0.03	1.22	0.82	0.025	36.3	0.56
	na.locf	0.79	0.042	26.1	2	0.82	0.13	1.3	2	0.83	0.131	0.035	2	0.81	0.026	36.9	2
12.5%	na.approx	0.79	0.041	24.6	1.03	0.82	0.124	1.2	1.24	0.85	0.105	0.03	1.22	0.83	0.024	33.5	1.14
	na.aggregate	0.81	0.035	22.1	2	0.84	0.111	1.1	2	0.87	0.084	0.024	2	0.82	0.023	31.7	2
	na.spline	0.62	0.134	78.3	0.52	0.55	0.558	4.9	0.67	0.42	4.684	1.118	1.13	0.76	0.049	63.2	0.45
	DTWBI	0.893	0.02	12.6	0.36	0.87	0.039	0.7	0.12	0.85	0.138	0.032	0.23	0.8	0.03	41.9	0.61
	na.interp	0.86	0.023	14.8	0.39	0.89	0.068	0.6	0.15	0.85	0.115	0.032	1.27	0.81	0.028	38.8	0.52
15%	na.locf	0.8	0.044	26.9	2	0.82	0.127	1.2	2	0.84	0.129	0.035	2	0.81	0.027	36.1	2
	na.approx	0.79	0.043	26.7	0.95	0.8	0.147	1.4	1.28	0.85	0.115	0.032	1.27	0.825	0.027	35.6	1.06
	na.aggregate	0.82	0.035	21.8	2	0.84	0.109	1.1	2	0.88	0.083	0.024	2	0.824	0.024	31	2
	na.spline	0.64	0.129	76.8	0.67	0.61	0.458	4	0.77	0.39	2.143	0.532	1.4	0.61	0.113	132.4	0.69
	DTWBI	0.895	0.02	12.8	0.36	0.84	0.054	1	0.1	0.85	0.133	0.031	0.29	0.81	0.029	40.7	0.59
15%	na.interp	0.86	0.025	15.6	0.35	0.89	0.069	0.7	0.17	0.86	0.11	0.031	0.99	0.79	0.033	43.6	0.49
	na.locf	0.79	0.047	28.2	2	0.82	0.126	1.2	2	0.84	0.127	0.034	2	0.81	0.028	36.3	2
	na.approx	0.8	0.043	26.5	1.17	0.83	0.117	1.1	1.42	0.86	0.11	0.031	0.99	0.81	0.032	41	1
	na.aggregate	0.83	0.035	22.1	2	0.84	0.11	1.1	2	0.89	0.079	0.023	2	0.82	0.025	32	2
	na.spline	0.55	0.175	106.1	0.95	0.49	0.731	6.3	0.88	0.34	12.339	2.928	1.6	0.61	0.136	162.5	0.68
		CO ₂ concentrations				Mackey-Glass Chaotic				Phu Lien temperature				Water level			
6%	DTWBI	0.93	0.001	0.3	0.04	0.95	0.005	0.01	0.03	0.88	0.06	1.7	0.08	0.95	0.009	0.1	0.05
	na.interp	0.75	0.055	1.6	1.5	0.79	0.031	0.04	0.81	0.8	0.142	3.1	0.63	0.81	0.042	0.5	1.05
	na.locf	0.73	0.059	1.7	2	0.77	0.036	0.05	2	0.77	0.173	3.8	2	0.8	0.043	0.4	2
	na.approx	0.75	0.055	1.6	1.5	0.79	0.031	0.04	0.81	0.8	0.142	3.1	0.63	0.81	0.042	0.5	1.05
	na.aggregate	0.45	0.185	4.7	2	0.82	0.025	0.03	2	0.83	0.114	2.4	2	0.83	0.035	0.4	2
7.5%	na.spline	0.75	0.057	1.6	0.75	0.65	0.072	0.09	0.38	0.61	0.413	8.5	0.52	0.3	0.654	6.6	1.61
	DTWBI	0.93	0.001	0.4	0.05	0.93	0.008	0.01	0.02	0.8788	0.061	1.7	0.06	0.96	0.007	0.1	0.02
	na.interp	0.74	0.057	1.6	1.38	0.8	0.031	0.04	1.04	0.79	0.147	3.2	0.98	0.82	0.038	0.4	0.97
	na.locf	0.76	0.053	1.6	2	0.77	0.038	0.05	2	0.77	0.171	3.7	2	0.81	0.043	0.5	2
	na.approx	0.74	0.057	1.6	1.38	0.8	0.031	0.04	1.04	0.79	0.147	3.2	0.98	0.82	0.038	0.4	0.97
10%	na.aggregate	0.45	0.186	4.7	2	0.83	0.025	0.03	2	0.83	0.113	2.4	2	0.83	0.036	0.4	2
	na.spline	0.74	0.058	1.6	0.79	0.69	0.062	0.08	0.39	0.58	0.701	14.5	0.8	0.2	1.228	12	1.71
	DTWBI	0.93	0.001	0.4	0.04	0.93	0.008	0.01	0.01	0.8791	0.063	1.8	0.05	0.97	0.005	0.1	0.03
	na.interp	0.76	0.051	1.4	0.88	0.81	0.03	0.04	0.98	0.81	0.137	3	0.58	0.81	0.041	0.4	0.91
	na.locf	0.76	0.054	1.6	2	0.79	0.036	0.05	2	0.77	0.176	3.8	2	0.81	0.043	0.5	2
12.5%	na.approx	0.76	0.051	1.4	0.88	0.81	0.03	0.04	0.98	0.81	0.137	3	0.58	0.81	0.041	0.4	0.91
	na.aggregate	0.44	0.197	4.9	2	0.83	0.025	0.03	2	0.83	0.114	2.4	2	0.83	0.036	0.4	2
	na.spline	0.66	0.098	2.9	0.26	0.71	0.058	0.08	0.33	0.49	0.88	17.8	1.04	0.18	1.57	15.5	1.79
	DTWBI	0.94	0.001	0.3	0.04	0.92	0.009	0.02	0.01	0.881	0.065	1.8	0.04	0.96	0.006	0.1	0.03
	na.interp	0.78	0.049	1.5	1.39	0.8	0.033	0.04	1.13	0.79	0.163	3.5	1.44	0.81	0.044	0.5	1.21
15%	na.locf	0.75	0.057	1.7	2	0.79	0.036	0.05	2	0.78	0.18	3.8	2	0.81	0.043	0.5	2
	na.approx	0.78	0.049	1.5	1.39	0.8	0.033	0.04	1.13	0.79	0.163	3.5	1.44	0.81	0.044	0.5	1.21
	na.aggregate	0.44	0.2	5	2	0.84	0.025	0.03	2	0.84	0.116	2.4	2	0.83	0.036	0.4	2
	na.spline	0.71	0.073	2.2	0.38	0.61	0.093	0.12	0.63	0.55	0.653	13.7	0.99	0.25	0.96	9.8	1.74
	DTWBI	0.94	0.001	0.3	0.04	0.92	0.01	0.02	0.01	0.882	0.066	1.8	0.05	0.96	0.007	0.1	0.04
15%	na.interp	0.76	0.053	1.6	1.46	0.81	0.03	0.04	0.99	0.81	0.145	3.2	1	0.81	0.044	0.5	1.6
	na.locf	0.77	0.052	1.6	2	0.79	0.037	0.05	2	0.79	0.175	3.8	2	0.81	0.043	0.5	2
	na.approx	0.76	0.053	1.6	1.46	0.81	0.03	0.04	0.99	0.81	0.145	3.2	1	0.81	0.044	0.5	1.6
	na.aggregate	0.43	0.202	5.1	2	0.84	0.025	0.03	2	0.84	0.117	2.5	2	0.83	0.036	0.4	2
	na.spline	0.69	0.085	2.5	0.58	0.57	0.129	0.16	0.73	0.44	1.268	26.3	1.27	0.21	1.185	11.8	1.83

size is greater than or equal to 10%, the proposed method has the highest similarity and the lowest NMAE and RMSE.

On the Beersales data set, considering similarity and RMSE indicators: na.interp method provides the best result and the second one is our approach. By contrast to these two indicators,

our method has better results on NMAE and FSD indicators at any missing rate. When comparing na.interp method to the na.approx one on the Airpassenger and Beersales data sets, we can see na.interp shows better performance than na.approx method on any indicators and at every level of missing data. It corresponds to

APPENDIX D. DYNAMIC TIME WARPING-BASED IMPUTATION FOR UNIVARIATE TIME SERIES DATA

ARTICLE IN PRESS

JID: PATREC

[m5G;August 30, 2017;13:44]

6

T.-T.-H. Phan et al. / Pattern Recognition Letters 000 (2017) 1–9

Algorithm 1 DTWBI algorithm.

Input: $x = \{x_1, x_2, \dots, x_N\}$: incomplete time series
 t : index of a gap (position of the first missing of the gap)
 T : size of the gap
 θ_cos : cosine threshold (≤ 1)
 $step_threshold$: increment for finding a threshold
 $step_sim_win$: increment for finding a similar window
Output: y - completed (imputed) time series

- 1: **Step 1:** Transform x to DDTW data $Dx = DDTW(x)$
- 2: **Step 2:** Construct a Q query - temporal window before the missing data $Q = Dx[t - T : t - 1]$
- 3: **Step 3:** Build a search database before the gap: $SDB = Dx[1 : t - 2T]$ and deleting all lines containing missing parameter $SDB = SDB \setminus \{dx_j, dx_j = NA\}$
- 4: **Step 4:** Find the threshold
- 5: $i \leftarrow 1$; $DTW_costs \leftarrow NULL$
- 6: **while** $i \leq \text{length}(SDB)$ **do**
- 7: $k \leftarrow i + T - 1$
- 8: Create a reference window: $R(i) = SDB[i : k]$
- 9: Calculate global feature of Q and $R(i)$: gfQ, gfR
- 10: Compute cosine coefficient: $cos = \text{cosine}(gfQ, gfR)$
- 11: **if** $cos \geq \theta_cos$ **then**
- 12: Calculate DTW cost: $cost = DTW_cost(Q, R(i))$
- 13: Save the cost to DTW_costs
- 14: **end if**
- 15: $i \leftarrow i + step_threshold$
- 16: **end while**
- 17: $threshold = \min(DTW_costs)$
- 18: **Step 5:** Find similar windows on the SDB
- 19: $i \leftarrow 1$; $Lop \leftarrow NULL$
- 20: **while** $i \leq \text{length}(SDB)$ **do**
- 21: $k \leftarrow i + T - 1$
- 22: Create a reference window: $R(i) = SDB[i : k]$
- 23: Calculate global feature of Q and $R(i)$: gfQ, gfR
- 24: Compute cosine coefficient: $cos = \text{cosine}(gfQ, gfR)$
- 25: **if** $cos \geq \theta_cos$ **then**
- 26: Calculate DTW cost: $cost = DTW_cost(Q, R(i))$
- 27: **if** $cost < threshold$ **then**
- 28: Save position of $R(i)$ to Lop
- 29: **end if**
- 30: **end if**
- 31: $i \leftarrow i + step_sim_win$
- 32: **end while**
- 33: **Step 6:** Replace the missing values at the position t by vector after the Q s window having the minimum DTW cost in the Lop list.
- 34: **return** y - with imputed series

the fact that these two data sets have a clear seasonality component. Na.interp method takes into account the seasonality factor, so it can better handle seasonality than na.approx does, although both algorithms use the interpolation for completing missing data.

On Airpassenger and Beersales data sets, na.aggregate approach gives less efficient results than na.interp. But on Google series, na.aggregate method yields the best performance: the highest similarity and the smallest NMEA, RMSE indicators. Without any trend on this data set, this method leads to the best result. For SP data set, na.aggregate method still highlights a good performance on NMEA and RMSE, but this approach has lower similarity than it has on Google series. The na.aggregate method replaces missing values by overall mean. However, SP series has a clear trend; therefore, na.aggregate method seems not to be effective with series having a strong trend.

In all data sets, FSD value of na.aggregate and na.locf methods always equals 2, because they use the same value for all missing data (last value for na.locf method; overall mean for na.aggregate).

• CO₂ concentrations, Mackey-Glass chaotic, Phu Lien temperature, water level data sets

These data sets have a seasonality component (except Mackey-Glass chaotic series but this data set is regularly repeated), without any trend (excluding CO₂ concentrations data set) and high auto-correlation. Our method demonstrates the best ability for completing missing data on these series: the highest similarity, the lowest NMAE, RMSE and FSD at any missing level. Furthermore, on Airpassenger, Beersales, Google and SP data sets, the similarity of our approach is lower, but the difference value of this indicator between the proposed method and the best method is small. On the contrary, for these four data sets, our method outperforms the existing techniques on any indicator and at any missing rate. The different values of these indicators between the proposed method and the other ones are quite large. The results confirm that the imputation values generated from the proposed method are close to the real values on data sets having high auto-correlation (see Fig. 1, the ACF maximum values of water and chaotic series are approximate 1), which means that there is a strong relationship between the available and the unknown values.

Following the proposed method, the second one is na.aggregate one applied on the Mackey-Glass chaotic series, Phu Lien temperature and water level series. As mentioned above (Table 1), these data sets have no trend, that is why na.aggregate could demonstrate its ability. However, on the CO₂ series with clear trend, fully opposed to these 3 data sets, the performance of this method is the worst one.

Although na.interp method is well indicated for handling data sets with seasonality component: here with these 4 data sets this approach does not illustrate its capability. It gives the same results as na.approx method and lower results than our approach and the na.aggregate one (on the Mackey-Glass chaotic, Phu Lien temperature and water series). For any data set, na.spline method indicates the lowest performance. However on the water series, this method has the least performance for completing missing values. This means that the spline method is not suitable for this task.

5.5.2. Comparison of the visual performance

Table 2 indicates the quantitative comparison of 6 different methods for the task of completing missing values. In this part, Figs. 3–5, 7, and 8 show the comparison of visual imputation performance of different methods.

Fig. 3 presents the shape of imputation values of 5 existing methods (na.interp, na.locf, na.approx, na.aggregate and na.spline) with the true values at position 106, the gap size of 9 on the Airpassenger series. As we can notice on Table 2, considering low rates of missing data, the proposed approach is less effective than na.interp and na.aggregate methods for Airpassenger time series. However, when looking at Fig. 4, we find that the shape of the imputation values generated from DTWBI method is very similar to the shape of true values. Despite high similarity, low RMSE and NMAE, the shape of imputation values yielded from na.aggregate method (Fig. 3) is not as effective as the proposed method (Fig. 4). As analyzed above, the na.interp method better deals with seasonal factor, so their imputed values are asymptotic to the real values (Fig. 3).

Fig. 5 illustrates the visual comparison of DTWBI's imputation values and real values on water level series at position 23,282, and at 0.6% rate of missing values (corresponding to 789 missing points). The proposed method proves again its capability for the task of completing missing values. We see that the shape of the imputation values generated from our method and the one of

Please cite this article as: T.-T.-H. Phan et al., Dynamic time warping-based imputation for univariate time series data, Pattern Recognition Letters (2017), <http://dx.doi.org/10.1016/j.patrec.2017.08.019>

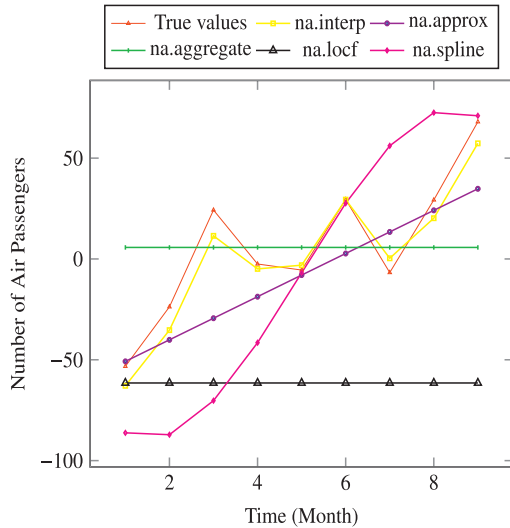


Fig. 3. Visual comparison of imputed values of different imputation methods with true values on Airpassenger series at position 106 with the gap size of 9.

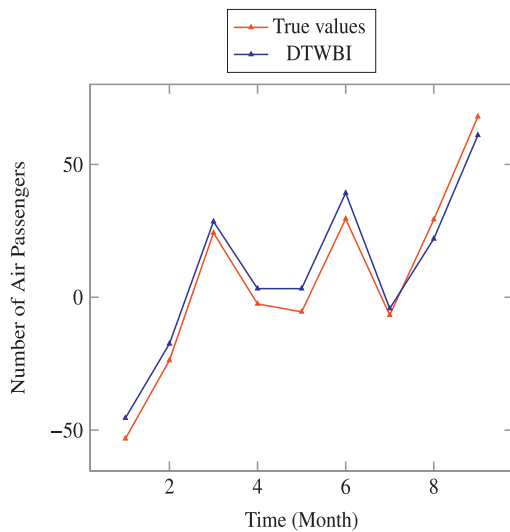


Fig. 4. Visual comparison of imputed values of proposed method with true values on Airpassenger series at position 106 with the gap size of 9.

the true values are almost completely identical. Fig. 6 shows the matching pairs between the query and the most similar reference window for the considered case. The values of matching pairs are very close, which indicates the reason why the imputation values generated from DTWBI are very similar to the real values. In contrast to our approach, handling seasonal factor of na.interp method is ineffective on water level data set. This method does not provide good result such as on Airpassenger series (Fig. 3); its perfor-

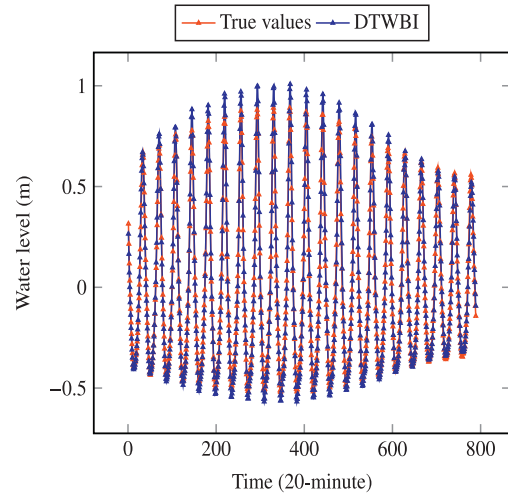


Fig. 5. Visual comparison of imputed values of the proposed method with true values on water level series at position 23,282 with the gap size of 789.

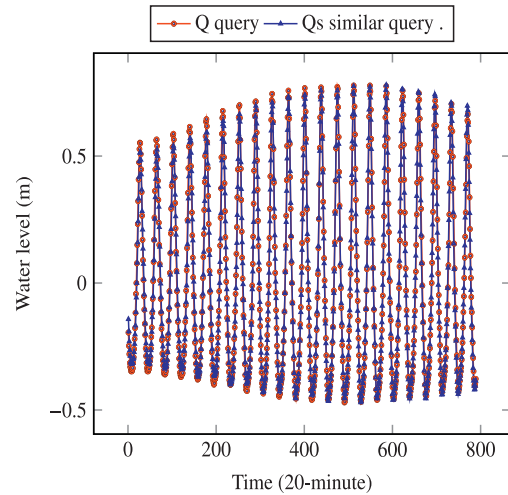


Fig. 6. Visual comparison of the query with the similar window on water level series at position 23,282 with the gap size of 789.

mance is the same as na.approx method (Fig. 7). Fig. 8 especially points out the obvious inefficiency of na.spline method for the task of completing missing values, considering series with high autocorrelation and large gap size (789 missing values in this case).

In this paper, we also calculate Cross-Correlation (CC) coefficients between the query with each reference window, and then we find the maximum coefficient. CC demonstrates that a pattern (here that is the query) exists or not in the database. High CC value means that there exists the recurrence of the pattern in the database. Therefore, we could easily find the pattern. Table 3 indicates the maximum of cross-correlation between the query and reference windows.

APPENDIX D. DYNAMIC TIME WARPING-BASED IMPUTATION FOR UNIVARIATE TIME SERIES DATA

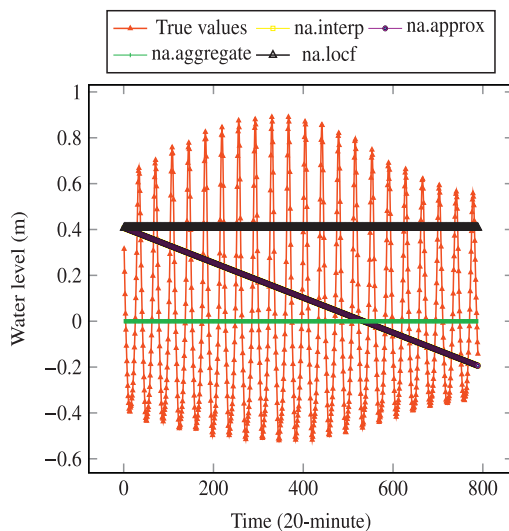


Fig. 7. Visual comparison of imputed values of different methods with true values on water level series at position 23,282 with the gap size of 789.

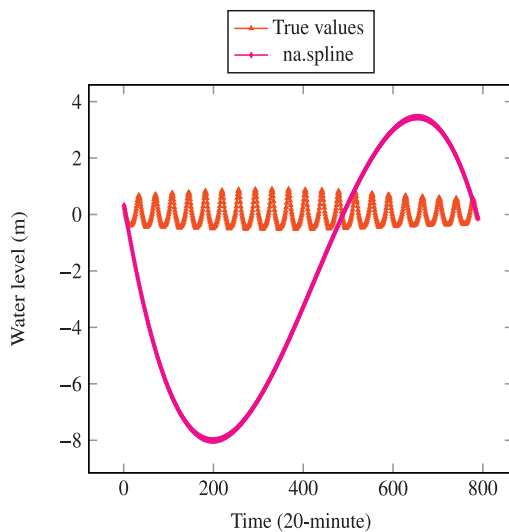


Fig. 8. Visual comparison of imputed values of spline method with true values on water level series at position 23,282 with the gap size of 789.

This result is fully interpreted: for 4 data sets including CO₂ concentrations, Mackey-Glass chaotic series, Phu Lien temperature and water level, their cross-correlation between the query and reference windows are very high for each missing level (Table 3). This corresponds to the results in Table 2: the proposed method yields the highest similarity and the lowest NMAE, RMSE, FSD. It also means that the imputation values generated from DTWBI method are very close to the true ones. For Google (#3) and SP (#4) data

Table 3

The maximum of cross-correlation between the query and reference windows.

Gap size	Data set							
	#1	#2	#3	#4	#5	#6	#7	#8
6%	0.88	0.92	0.58	0.78	0.99	1	0.91	1
7.50%	0.91	0.91	0.55	0.74	0.99	0.99	0.91	1
10%	0.94	0.87	0.5	0.67	0.98	0.99	0.91	1
12.50%	0.95	0.89	0.44	0.65	0.98	0.99	0.9	1
15%	0.95	0.85	0.4	0.65	0.98	0.99	0.9	1

#1-Airpassenger, #2-Beersales, #3-Google, #4-SP, #5-CO₂ concentrations, #6-Mackey-Glass chaotic, #7-Phu Lien temperature, #8-water level.

sets, we see that CC are not high, that is why our approach does not well prove its ability. With Airpassenger data set (#1), when CC are greater than or equal to 0.94, the proposed method highlights better results than other methods. On Beersales data set (#2), in case of higher CC, DTWBI gives better results in case of lower CC.

From these results, we can notice that the proposed method gives the best performance in case of high CC coefficient (> 0.9). Indeed, CC is an indicator that gives information about the pattern recurrence in the data. Based on this indicator, we can predict if one pattern may occur in the past or in the following data from the position we are considering. From the above analyses, we can see that our algorithm outperforms other imputation methods when data sets have high auto-correlation and cross-correlation, no trend, strong seasonality, and complex distribution, especially in case of large gap(s). High cross-correlation means that these data sets are recurrent, or in other words, these time series will repeat themselves over some periods. The drawback of this method is the computation time. The proposed algorithm may take a long time to find the imputation values when the size of the given data is large. The reason is the search for all possible sliding windows to find a reference window having the maximum similarity to the query.

6. Conclusion

In this paper, we have proposed a new imputation method for univariate time series data, namely DTWBI method. This methodology has been tested using 8 data sets: Airpassenger, Beersales, Google, SP, CO₂ concentrations, Mackey-Glass chaotic, Phu Lien temperature, and water level. The accuracy of imputation values produced by DTWBI is compared with 5 existing methods (na.interp, na.locf, na.approx, na.aggregate and na.spline) using 4 quantitative indicators (similarity, NMAE, RMSE and FSD). We also compare the visual performance of these methods. The experiments show that our approach gives better results than the other existing methods, and is the best robust method in case of time series having high cross-correlation and auto-correlation, large gap(s), complex distribution, and strong seasonality. However, the proposed framework is restricted to applications where the necessary assumption of recurring data in the time series is set up (high cross-correlation indicator), and it requires computation time for very large missing intervals. The present work will allow to extend the proposed approach to complete missing values of multivariate time series data in the future.

Acknowledgments

This work was kindly supported by the Ministry of Education and Training Vietnam International Education Development, the French government, the region Hauts-de-France in the framework of the project CPER 2014–2020 MARCO and the European Commission's H2020 program with the Joint European Research Infrastructure for Coastal Observations JERICO-Next.

References

- [1] P.D. Allison, *Missing Data, Quantitative Applications in the Social Sciences*, 136, Sage Publication, 2001.
- [2] C.M. Bishop, *Pattern Recognition and Machine Learning* (Information Science and Statistics), Springer-Verlag New York, Inc., Secaucus, NJ, USA, 2006.
- [3] H.-T. Ceong, H.-J. Kim, J.-S. Park, Discovery of and recovery from failure in a costal marine usn service, *J. Inf. Commun. Convergence Eng.* 1 (1) (2012).
- [4] S. Chiewchanwattana, C. Lursinsap, C.-H. Henry Chu, Imputing incomplete time-series data based on varied-window similarity measure of data sequences, *Pattern Recognit. Lett.* 28 (9) (2007) 1091–1103.
- [5] S.L. Crawford, S.L. Tennstedt, J.B. McKinlay, A comparison of analytic methods for non-random missingness of outcome data, *J. Clin. Epidemiol.* 48 (2) (1995) 209–219.
- [6] Y. Deng, C. Chang, M.S. Ido, Q. Long, Multiple imputation for general missing data patterns in the presence of high-dimensional data, *Sci. Rep.* 6 (2016) 21689.
- [7] A. Gelman, J. Hill, Y.-S. Su, M. Yajima, M. Pittau, B. Goodrich, Y. Si, J. Kropko, *Mi: missing data imputation and model checking*, 2015.
- [8] M. Gómez-Carracedo, J. Andrade, P. López-Mahía, S. Munieategui, D. Prada, A practical comparison of single and multiple imputation methods to handle complex missing data in air quality datasets, *Chemometr. Intell. Lab. Syst.* 134 (2014) 23–33.
- [9] G. Hawthorne, P. Elliott, Imputing cross-sectional missing data: comparison of common techniques, *Aust. N. Z. J. Psychiatry* 39 (7) (2005) 583–590.
- [10] R. Hyndman, Y. Khandakar, Automatic time series forecasting: the forecast package for r, used package in 2016, *J. Stat. Softw.* (2008) 1–22.
- [11] J.G. Joseph, A.A.E. El-Mohandes, M. Kiely, M.N. El-Khorazaty, M.G. Gantz, A.A. Johnson, K.S. Katz, S.M. Blake, M.W. Rossi, S. Subramanian, Reducing psychosocial and behavioral pregnancy risk factors: results of a randomized clinical trial among high-risk pregnant African American women, *Am. J. Public Health* 99 (6) (2009) 1053–1061.
- [12] H. Junninen, H. Niska, K. Tuppurainen, J. Ruuskanen, M. Kolehmainen, Methods for imputation of missing values in air quality data sets, *Atmos. Environ.* 38 (18) (2004) 2895–2907.
- [13] E.J. Keogh, M.J. Pazzani, Derivative dynamic time warping, in: *Sdm*, 1, SIAM, 2001, pp. 5–7.
- [14] K.J. Lee, J.B. Carlin, Multiple imputation for missing data: fully conditional specification versus multivariate normal imputation, *Am. J. Epidemiol.* 171 (5) (2010) 624–632.
- [15] A. Lefebvre, *MAREL Carnot data and metadata from Coriolis data centre*, SEANO, <http://doi.org/10.17882/39754>, 2015.
- [16] S.G. Liao, Y. Lin, D.D. Kang, D. Chandra, J. Bon, N. Kaminski, F.C. Sciruba, G.C. Tseng, Missing value imputation in high-dimensional phenomic data: imputable or not, and how? *BMC Bioinform.* 15 (2014) 346.
- [17] R.J.A. Little, D.B. Rubin, *Statistical Analysis with Missing Data*, John Wiley & Sons, 2014. Google-Books-ID: AyVeBAAQBAJ.
- [18] M.C. Mackey, L. Glass, *Oscillation and Chaos in Physiological Control Systems*, 197, Science (New York, N.Y.), 1977, pp. 287–289.
- [19] S. Moritz, A. Sardá, T. Bartz-Beielstein, M. Zaefferer, J. Stork, Comparison of different methods for univariate time series imputation in r, *arXiv preprint arXiv:1510.03924* (2015).
- [20] N.M. Noor, M.M. Al Bakri Abdullah, A.S. Yahaya, N.A. Ramli, Comparison of linear interpolation method and mean method to replace the missing values in environmental data set, *Mater. Sci. Forum* 803 (2014) 278–281.
- [21] T.T.H. Phan, E.P. Caillault, A. Bigand, Comparative study on supervised learning methods for identifying phytoplankton species, in: *2016 IEEE Sixth International Conference on Communications and Electronics (ICCE)*, IEEE, 2016, pp. 283–288.
- [22] R Core Team, *R: A Language and Environment for Statistical Computing*, R Foundation for Statistical Computing, Vienna, Austria, 2016.
- [23] T.E. Raghunathan, J.M. Lepkowski, J. Van Hoewyk, P. Solenberger, A multivariate technique for multiply imputing missing values using a sequence of regression models, *Surv. Methodol.* 27 (1) (2001) 85–96.
- [24] T.E. Raghunathan, D.S. Siscovick, A multiple-imputation analysis of a case-control study of the risk of primary cardiac arrest among pharmacologically treated hypertensives on JSTOR, *R. Stat. Soc. Ser. C (Appl. Stat.)* 45 (1996) 335–352.
- [25] S.A. Rahman, Y. Huang, J. Claassen, N. Heintzman, S. Kleinberg, Combining Fourier and lagged k-nearest neighbor imputation for biomedical time series data, *J. Biomed. Inform.* 58 (2015) 198–207.
- [26] K. Rousseeuw, E.P. Caillault, A. Lefebvre, D. Hamad, Monitoring system of phytoplankton blooms by using unsupervised classifier and time modeling, in: *2013 IEEE International Geoscience and Remote Sensing Symposium-IGARSS*, IEEE, 2013, pp. 3962–3965.
- [27] P. Royston, Multiple imputation of missing values: further update of ice, with an emphasis on interval censoring, *Stata J.* 7 (4) (2007) 445–464.
- [28] H. Sakoe, S. Chiba, Dynamic programming algorithm optimization for spoken word recognition, *IEEE Trans. Acoust., Speech, Signal Process.* 16 (1978) 43–49.
- [29] J. Schafer, *Analysis of Incomplete Multivariate Data*, Chapman and Hall, London, 1997.
- [30] A.D. Shah, J.W. Bartlett, J. Carpenter, O. Nicholas, H. Hemingway, Comparison of random forest and parametric imputation models for imputing missing data using MICE: a CALIBER study, *Am. J. Epidemiol.* 179 (6) (2014) 764–774.
- [31] M. Spratt, J. Carpenter, J.A.C. Sterne, J.B. Carlin, J. Heron, J. Henderson, K. Tilling, Strategies for multiple imputation in longitudinal studies, *Am. J. Epidemiol.* 172 (4) (2010) 478–487.
- [32] J.A.C. Sterne, I.R. White, J.B. Carlin, M. Spratt, P. Royston, M.G. Kenward, A.M. Wood, J.R. Carpenter, Multiple imputation for missing data in epidemiological and clinical research: potential and pitfalls, *BMJ (Clin. Resear. ed.)* 338 (2009) b2393.
- [33] E.A. Stuart, M. Azur, C. Frangakis, P. Leaf, Multiple imputation with large data sets: a case study of the children's mental health initiative, *Am. J. Epidemiol.* 169 (9) (2009) 1133–1139.
- [34] K.W. Thoning, P.P. Tans, W.D. Komhyr, Atmospheric carbon dioxide at mauna loa observatory. II - analysis of the NOAA GMCC data, 1974–1985 94 (1989) 8549–8565.
- [35] S. Van Buuren, H.C. Boshuizen, D.L. Knook, others, Multiple imputation of missing blood pressure covariates in survival analysis, *Stat. Med.* 18 (6) (1999) 681–694.
- [36] Y. Walter, O. J.M. Kihoro, K.H.O. Athiany, K.H. W. Imputation of incomplete non-stationary seasonal time series data, *Math. Theory Model.* 3 (12) (2013) 142–154.
- [37] A. Zeileis, G. Grothendieck, zoo: S3 infrastructure for regular and irregular time series, used package in 2016, 2005, doi:10.18637/jss.v014.i06.

Bibliography

- [1] K. Rousseeuw, É P. Caillault, A. Lefebvre, and D. Hamad. Monitoring system of phytoplankton blooms by using unsupervised classifier and time modeling. In *2013 IEEE International Geoscience and Remote Sensing Symposium - IGARSS*, pages 3962–3965, July 2013.
- [2] Hee-Taek Ceong, Hae-Jin Kim, and Jeong-Seon Park. Discovery of and recovery from failure in a costal marine usn service. *Journal of Information and Communication Convergence Engineering*, 1(1), Mar 2012.
- [3] Alain Lefebvre. MAREL Carnot data and metadata from Coriolis Data Centre. SEA-NOE. <http://doi.org/10.17882/39754>, 2015.
- [4] Graeme Hawthorne and Peter Elliott. Imputing cross-sectional missing data: Comparison of common techniques. *The Australian and New Zealand Journal of Psychiatry*, 39(7):583–590, July 2005.
- [5] Heikki Junninen, Harri Niska, Kari Tuppurainen, Juhani Ruuskanen, and Mikko Kolehmainen. Methods for imputation of missing values in air quality data sets. *Atmospheric Environment*, 38(18):2895–2907, June 2004.
- [6] Tommy D. Dickey. Emerging ocean observations for interdisciplinary data assimilation systems. *Journal of Marine Systems*, 40-41:5–48, April 2003.
- [7] Hiroaki Sakoe and Seibi Chiba. Dynamic Programming Algorithm Optimization for Spoken Word Recognition. *IEEE transactions on acoustics, speech, and signal processing*, 16:43–49, 1978.

- [8] Eamonn J. Keogh and Michael J. Pazzani. Scaling up dynamic time warping for datamining applications. In *Proceedings of the sixth ACM SIGKDD international conference on Knowledge discovery and data mining*, pages 285–289. ACM, 2000.
- [9] Donald J. Berndt and James Clifford. Using dynamic time warping to find patterns in time series. In *Proceedings of the 3rd International Conference on Knowledge Discovery and Data Mining, AAAIWS’94*, pages 359–370. AAAI Press, 1994.
- [10] Y. Jeong, M. K. Jeong, and O. A. Omitaomu. Weighted dynamic time warping for time series classification. *Pattern Recognition*, 44(9):2231–2240, September 2011.
- [11] Harold Mouchère, Jinpeng Li, Christian Viard-Gaudin, and Zhaoxin Chen. A dynamic Time Warping Algorithm for Recognition of Multi-Stroke On-Line Handwritten Characters. *Natural Science Edition, Journal of South China University of Technology*, 41(7):pp. 107–113, June 2013.
- [12] Toni M. Rath and R. Manmatha. Word image matching using dynamic time warping. In *CVPR (2)*, pages 521–527. IEEE Computer Society, 2003.
- [13] Xiaopeng Xi, Eamonn Keogh, Christian Shelton, Li Wei, and Chotirat Ann Ratanamahatana. Fast time series classification using numerosity reduction. pages 1033–1040. ACM Press, 2006.
- [14] François Petitjean, Alain Ketterlin, and Pierre Gançarski. A global averaging method for dynamic time warping, with applications to clustering. *Pattern Recognition*, 44(3):678–693, March 2011.
- [15] Y. Gupta, A. Saini, and A. Saxena. Fuzzy logic-based approach to develop hybrid similarity measure for efficient information retrieval. *Journal of Information Science*, 40(6):846–857, December 2014.
- [16] Shyi-Ming Chen, Ming-Shiow Yeh, and Pei-Yung Hsiao. A comparison of similarity measures of fuzzy values. *Fuzzy Sets and Systems*, 72(1):79–89, May 1995.
- [17] Mohammad Yahya H. Al-Shamri and Nagi H. Al-Ashwal. Fuzzy-Weighted Similarity Measures for Memory-Based Collaborative Recommender Systems. *Journal of Intelligent Learning Systems and Applications*, 06(01):1–10, 2014.

- [18] Parivash Pirasteh, Dosam Hwang, and Jai E. Jung. Weighted Similarity Schemes for High Scalability in User-Based Collaborative Filtering. *Mobile Netw Appl*, 20(4):497–507, August 2015.
- [19] Yong Wang, Jiangzhou Deng, Jerry Gao, and Pu Zhang. A hybrid user similarity model for collaborative filtering. *Information Sciences*, 418(Supplement C):102–118, December 2017.
- [20] Sina Shahmoradi and Saeed Bagheri Shouraki. Evaluation of a novel fuzzy sequential pattern recognition tool (fuzzy elastic matching machine) and its applications in speech and handwriting recognition. *Applied Soft Computing*, 62:315–327, January 2018.
- [21] Plamen P. Angelov and Dimitar Filev. Flexible models with evolving structure. *Int. J. Intell. Syst.*, 19(4):327–340, 2004.
- [22] P. Angelov and R. Buswell. Identification of evolving fuzzy rule-based models. *IEEE Transactions on Fuzzy Systems*, 10(5):667–677, October 2002.
- [23] Plamen P. Angelov and Ronald R. Yager. A new type of simplified fuzzy rule-based system. *Int. J. General Systems*, 41(2):163–185, 2012.
- [24] Chao-Chih Tsai and Ke-Chih Chen. An application of fuzzy rule-based system: to the economic equilibrium considering the shift in demand curve. In *Proceedings Joint 9th IFSA World Congress and 20th NAFIPS International Conference (Cat. No. 01TH8569)*, pages 2608–2611 vol.5, July 2001.
- [25] Roderick J. A. Little and Donald B. Rubin. *Statistical Analysis with Missing Data*. John Wiley & Sons, August 2014. Google-Books-ID: AyVeBAAAQBAJ.
- [26] Yiran Dong and Joanne Peng. Principled missing data methods for researchers. *Springer-Plus*, 2:222, 12 2013.
- [27] Steffen Moritz, Alexis Sardá, Thomas Bartz-Beielstein, Martin Zaefferer, and Jörg Stork. Comparison of different Methods for Univariate Time Series Imputation in R. *arXiv preprint arXiv:1510.03924*, 2015.
- [28] M.P. Gómez-Carracedo, J.M. Andrade, P. López-Mahía, S. Muniategui, and D. Prada. A practical comparison of single and multiple imputation methods to handle complex

- missing data in air quality datasets. *Chemometrics and Intelligent Laboratory Systems*, 134:23–33, May 2014.
- [29] Geert Molenberghs, Garrett Fitzmaurice, Michael G. Kenward, Geert Verbeke, and Anastasios Tsiatis. *Handbook of missing data methodology*. CRC Press, 2014.
- [30] Alain Lefebvre. MAREL Carnot data and metadata from Coriolis Data Centre. SEA-NOE. <http://doi.org/10.17882/39754>, 2015.
- [31] R Core Team. *R: A Language and Environment for Statistical Computing*. R Foundation for Statistical Computing, Vienna, Austria, 2016.
- [32] D. Woehrling, A. Lefebvre, and R. Le Fèvre-Lehoërff, G. and Delesmont. Seasonal and longer term trends in sea temperature along the french north sea coast, 1975 to 2002. *Journal of the Marine Biological Association U.K.*, 85 (1), pages 39–48, 2005.
- [33] Chris Chatfield. *The Analysis of Time Series: An Introduction, Sixth Edition*. CRC Press, March 2016.
- [34] Norman R. Draper and Harry Smith. *Applied Regression Analysis*. Wiley, April 1998.
- [35] P. Grosjean and F. Ibanez. *PASTECS. Manuel de l'utilisateur de la librairie de fonctions pour R et pour S+ Package for Analysis of Space-Time Ecological Series*, 2002.
- [36] Norazian Mohamed Noor, Mohd Mustafa Al Bakri Abdullah, Ahmad Shukri Yahaya, and Nor Azam Ramli. Comparison of Linear Interpolation Method and Mean Method to Replace the Missing Values in Environmental Data Set. *Materials Science Forum*, 803:278–281, August 2014.
- [37] Paul D. Allison. *Missing Data*, volume 136 of *Quantitative Applications in the Social Sciences*. Sage Publication, 2001.
- [38] Christopher M. Bishop. *Pattern Recognition and Machine Learning (Information Science and Statistics)*. Springer-Verlag New York, Inc., Secaucus, NJ, USA, 2006.
- [39] S. L. Crawford, S. L. Tennstedt, and J. B. McKinlay. A comparison of analytic methods for non-random missingness of outcome data. *Journal of Clinical Epidemiology*, 48(2):209–219, February 1995.

- [40] Jonathan A. C. Sterne, Ian R. White, John B. Carlin, Michael Spratt, Patrick Royston, Michael G. Kenward, Angela M. Wood, and James R. Carpenter. Multiple imputation for missing data in epidemiological and clinical research: Potential and pitfalls. *BMJ (Clinical research ed.)*, 338:b2393, 2009.
- [41] Yodah Walter.O, J. M. Kihoro, K. H. O. Athiany, and Kibunja H. W. Imputation of incomplete non- stationary seasonal time series data. *Mathematical Theory and Modeling*, 3(12):142–154, 2013.
- [42] Sirapat Chiewchanwattana, Chidchanok Lursinsap, and Chee-Hung Henry Chu. Imputing incomplete time-series data based on varied-window similarity measure of data sequences. *Pattern Recognition Letters*, 28(9):1091–1103, July 2007.
- [43] Ilaria Bartolini, Paolo Ciaccia, and Marco Patella. Warp: Accurate retrieval of shapes using phase of fourier descriptors and time warping distance. *IEEE transactions on pattern analysis and machine intelligence*, 27(1):142–147, 2005.
- [44] Andrés Marzal, Vicente Palazón, and Guillermo Peris. Contour-Based Shape Retrieval Using Dynamic Time Warping. In *Current Topics in Artificial Intelligence*, Lecture Notes in Computer Science, pages 190–199. Springer, Berlin, Heidelberg, November 2005.
- [45] J. Aach and G. M. Church. Aligning gene expression time series with time warping algorithms. *Bioinformatics (Oxford, England)*, 17(6):495–508, June 2001.
- [46] GenTXWarper - Dynamic Time Warping algorithm for gene expression time series. [Online]. Available: <http://www.psb.ugent.be/cbd/papers/gentxwarper/DTWalgorithm.htm>.
- [47] F. Itakura. Minimum prediction residual principle applied to speech recognition. *IEEE Transactions on Acoustics, Speech, and Signal Processing*, 23(1):67–72, February 1975.
- [48] Eamonn J. Keogh and Michael J. Pazzani. Derivative dynamic time warping. In *Proceedings of the 2001 SIAM International Conference on Data Mining*, pages 1–11. SIAM, 2001.
- [49] Xie Ying and Wiltgen Bryan. Adaptive Feature Based Dynamic Time Warping. *IJCSNS International Journal of Computer Science and Network Security*, 10:264–273, January 2010.

- [50] Émilie Caillault, Pierre-Alexandre Hébert, and Guillaume Wacquet. Dissimilarity-Based Classification of Multidimensional Signals by Conjoint Elastic Matching: Application to Phytoplanktonic Species Recognition. In *Engineering Applications of Neural Networks*, number 43 in Communications in Computer and Information Science, pages 153–164. Springer Berlin Heidelberg, 2009-08-27.
- [51] Yanping Chen, Bing Hu, Eamonn Keogh, and Gustavo EAPA Batista. DTW-D: Time series semi-supervised learning from a single example. In *Proceedings of the 19th ACM SIGKDD International Conference on Knowledge Discovery and Data Mining*, pages 383–391. ACM, 2013.
- [52] T. T. H. Phan, E. P. Caillault, and A. Bigand. Comparative study on supervised learning methods for identifying phytoplankton species. In *2016 IEEE Sixth International Conference on Communications and Electronics (ICCE)*, pages 283–288. IEEE, July 2016.
- [53] RJ Hyndman and Y Khandakar. Automatic time series forecasting: the forecast package for r, used package in 2016. *Journal of Statistical Software*, pages 1–22, September 2008.
- [54] Kirk W Thoning, Pieter P Tans, and Walter D Komhyr. Atmospheric carbon dioxide at Mauna Loa Observatory. II - Analysis of the NOAA GMCC data, 1974-1985. *Journal of Geophysical Research-Atmospheres*, 94:8549–8565, June 1989.
- [55] M. C. Mackey and L. Glass. Oscillation and chaos in physiological control systems. *Science (New York, N.Y.)*, 197(4300):287–289, July 1977.
- [56] Achim Zeileis and Gabor Grothendieck. zoo: S3 infrastructure for regular and irregular time series. *Journal of Statistical Software*, 14(6):1–27, 2005.
- [57] David L. Streiner. Missing data and the trouble with LOCF. *Evidence-Based Mental Health*, 11(1):3–5, February 2008.
- [58] Geert Molenberghs, Herbert Thijs, Ivy Jansen, Caroline Beunckens, Michael G. Kenward, Craig Mallinckrodt, and Raymond J. Carroll. Analyzing incomplete longitudinal clinical trial data. *Biostatistics (Oxford, England)*, 5(3):445–464, July 2004.
- [59] Hui-Huang Hsu, Andy C. Yang, and Ming-Da Lu. KNN-DTW Based Missing Value Imputation for Microarray Time Series Data. *Journal of Computers*, 6(3), March 2011.

- [60] Stefan Oehmcke, Oliver Zielinski, and Oliver Kramer. kNN ensembles with penalized DTW for multivariate time series imputation. In *Neural Networks (IJCNN), 2016 International Joint Conference On*, pages 2774–2781. IEEE, 2016.
- [61] Elena Kostadinova, Veselka Boeva, Liliana Boneva, and Elena Tsiporkova. An Integrative DTW-based imputation method for gene expression time series data. In *Intelligent Systems (IS), 2012 6th IEEE International Conference*, pages 258–263. IEEE, 2012.
- [62] Andy C. Yang, Hui-Huang Hsu, and Ming-Da Lu. Missing Value Imputation in Microarray Gene Expression Data. In *Conference on Information Technology and Applications in Outlying Islands*, 2009.
- [63] US Energy Information Administration. Product Supplied for Finished Gasoline. http://www.eia.gov/dnav/pet/PET_SUM_SNDW_A_EPMOF_VPP_MBBLPD_W.htm, 2016. gas_online_product_2016.
- [64] J.L. Schafer. *Analysis of Incomplete Multivariate Data*. Chapman and Hall, London, 1997.
- [65] Stef Van Buuren, Hendriek C. Boshuizen, Dick L. Knook, and others. Multiple imputation of missing blood pressure covariates in survival analysis. *Statistics in medicine*, 18(6):681–694, 1999.
- [66] Trivellore E. Raghunathan, James M. Lepkowski, John Van Hoewyk, and Peter Solenberger. A multivariate technique for multiply imputing missing values using a sequence of regression models. *Survey methodology*, 27(1):85–96, 2001.
- [67] J Engels and Paula Diehr. Imputation of missing longitudinal data: A comparison of methods. *Journal of Clinical Epidemiology*, 56(10):968–976, October 2003.
- [68] Patrick Royston. Multiple imputation of missing values: Further update of ice, with an emphasis on interval censoring. *Stata Journal*, 7(4):445–464, 2007.
- [69] Elizabeth A. Stuart, Melissa Azur, Constantine Frangakis, and Philip Leaf. Multiple Imputation With Large Data Sets: A Case Study of the Children’s Mental Health Initiative. *American Journal of Epidemiology*, 169(9):1133–1139, May 2009.

- [70] Katherine J. Lee and John B. Carlin. Multiple Imputation for Missing Data: Fully Conditional Specification Versus Multivariate Normal Imputation. *American Journal of Epidemiology*, 171(5):624–632, March 2010.
- [71] Anoop D. Shah, Jonathan W. Bartlett, James Carpenter, Owen Nicholas, and Harry Hemingway. Comparison of random forest and parametric imputation models for imputing missing data using MICE: A CALIBER study. *American Journal of Epidemiology*, 179(6):764–774, March 2014.
- [72] Serena G. Liao, Yan Lin, Dongwan D. Kang, Divay Chandra, Jessica Bon, Naftali Kaminski, Frank C. Sciurba, and George C. Tseng. Missing value imputation in high-dimensional phenomic data: Imputable or not, and how? *BMC Bioinformatics*, 15:346, 2014.
- [73] Shah Atiqur Rahman, Yuxiao Huang, Jan Claassen, Nathaniel Heintzman, and Samantha Kleinberg. Combining Fourier and lagged k -nearest neighbor imputation for biomedical time series data. *Journal of Biomedical Informatics*, 58:198–207, December 2015.
- [74] Andrew Gelman, Jennifer Hill, Yu-Sung Su, Masanao Yajima, Maria Pittau, Ben Goodrich, Yajuan Si, and Jon Kropko. Mi: Missing Data Imputation and Model Checking, April 2015.
- [75] Yi Deng, Changgee Chang, Moges Seyoum Ido, and Qi Long. Multiple Imputation for General Missing Data Patterns in the Presence of High-dimensional Data. *Scientific Reports*, 6:21689, February 2016.
- [76] Daniel J. Stekhoven and Peter Bühlmann. MissForest—non-parametric missing value imputation for mixed-type data. *Bioinformatics*, 28(1):112–118, 2012.
- [77] Piero Bonissone, José M. Cadenas, M. Carmen Garrido, and R. Andrés Díaz-Valladares. A fuzzy random forest. *International Journal of Approximate Reasoning*, 51(7):729–747, September 2010.
- [78] Shah Atiqur Rahman, Yuxiao Huang, Jan Claassen, Nathaniel Heintzman, and Samantha Kleinberg. Combining Fourier and lagged k -nearest neighbor imputation for biomedical time series data. *Journal of Biomedical Informatics*, 58:198–207, December 2015.

- [79] Dan Li, Jitender Deogun, William Spaulding, and Bill Shuart. Towards missing data imputation: A study of fuzzy k-means clustering method. In *Rough Sets and Current Trends in Computing*, pages 573–579. Springer, 2004.
- [80] Jinjun Tang, Guohui Zhang, Yinhai Wang, Hua Wang, and Fang Liu. A hybrid approach to integrate fuzzy C-means based imputation method with genetic algorithm for missing traffic volume data estimation. *Transportation Research Part C: Emerging Technologies*, 51:29–40, February 2015.
- [81] Ibrahim Berkan Aydılek and Ahmet Arslan. A hybrid method for imputation of missing values using optimized fuzzy c-means with support vector regression and a genetic algorithm. *Information Sciences*, 233:25–35, June 2013.
- [82] Takashi Furukawa, Shin-ichi Ohnishi, and Takahiro Yamanoi. On c-means Algorithm for Mixed Incomplete Data Using Partial Distance and Imputation. In *Proceedings of the International MultiConference of Engineers and Computer Scientists*, volume 1, 2014.
- [83] S. Azim and S. Aggarwal. Hybrid model for data imputation: Using fuzzy c means and multi layer perceptron. In *2014 IEEE International Advance Computing Conference (IACC)*, pages 1281–1285, February 2014.
- [84] Jinjun Tang, Yinhai Wang, Shen Zhang, Hua Wang, Fang Liu, and Shaowei Yu. On Missing Traffic Data Imputation Based on Fuzzy C -Means Method by Considering Spatial–Temporal Correlation. *Transportation Research Record: Journal of the Transportation Research Board*, 2528:86–95, September 2015.
- [85] P. Saravanan and P. Sailakshmi. Missing value imputation using fuzzy possibilistic c means optimized with support vector regression and genetic algorithm. *Journal of Theoretical and Applied Information Technology*, 72(1):34–39, 2015.
- [86] Hidetomo Ichihashi, Katsuhiko Honda, Akira Notsu, and Takafumi Yagi. Fuzzy c-Means classifier with deterministic initialization and missing value imputation. In *Foundations of Computational Intelligence, 2007. FOCI 2007. IEEE Symposium On*, pages 214–221. IEEE, 2007.
- [87] Takashi Furukawa, Shin-ichi Ohnishi, and Takahiro Yamanoi. Missing Categorical Data Imputation for FCM Clusterings of Mixed Incomplete Data. In *COGNITIVE 2014*, 2014. bibtex: furukawa_missing_2014.

- [88] Weina Wang, Witold Pedrycz, and Xiaodong Liu. Time series long-term forecasting model based on information granules and fuzzy clustering. *Engineering Applications of Artificial Intelligence*, 41:17–24, May 2015.
- [89] Jiawei Han, Jian Pei, and Micheline Kamber. *Data Mining: Concepts and Techniques*. Elsevier, 2011.
- [90] Thi-Thu-Hong Phan, Émilie Poisson Caillault, Alain Lefebvre, and André Bigand. Dynamic time warping-based imputation for univariate time series data. *Pattern Recognition Letters*, August 2017.
- [91] L.A. Zadeh. Fuzzy sets. *Inform. and Control*, 8:338–353, 1965.
- [92] L. A. Zadeh. The concept of a linguistic variable and its application to approximate reasoning. *Information Sciences*, 8(3):199–249, January 1975.
- [93] J. Alcalá, A. Fernández, J. Luengo, J. Derrac, S. García, L. Sánchez, and F. Herrera. Keel data-mining software tool: Data set repository, integration of algorithms and experimental analysis framework. *Journal of Multiple-Valued Logic and Soft Computing*, 17(2-3):255–287, 2010.
- [94] Sarah C. Goslee, Dean L. Urban, and others. The ecodist package for dissimilarity-based analysis of ecological data. *Journal of Statistical Software*, 22(7):1–19, 2007.
- [95] D. B. Rubin. *Multiple Imputation for Nonresponse in Surveys*. Wiley, 1987.
- [96] Yu-Sung Su, Andrew Gelman, Jennifer Hill, Masanao Yajima, and others. Multiple imputation with diagnostics (mi) in R: Opening windows into the black box. *Journal of Statistical Software*, 45(2):1–31, 2011.
- [97] Stef Buuren and Karin Groothuis-Oudshoorn. Mice: Multivariate imputation by chained equations in R. *Journal of statistical software*, 45(3), 2011.
- [98] Wafa Rekik, Sylvie Le Hégarat-Masclé, Roger Reynaud, Abdelaziz Kallel, and Ahmed Ben Hamida. Dynamic object construction using belief function theory. *Inf. Sci.*, 345:129–142, 2016.
- [99] Gang Niu and Bo-Suk Yang. *Mechanical Systems and Signal Processing*.

- [100] Karl Øyvind Mikalsen, Filippo Maria Bianchi, Cristina Soguero-Ruiz, and Robert Jenssen. Time series cluster kernel for learning similarities between multivariate time series with missing data. *Pattern Recognition*, 76:569–581, April 2018.
- [101] H.J.Sadael, F.G.Guimaraes, C.José da Silva, M.H.Lee, and T.Eslami. Short-term load forecasting method based on fuzzy time series, seasonality and long memory process. *Int. Journal of Approximate Reasoning*, 83:196–217, 2017.
- [102] Costas P. Pappis and Nikos I. Karacapilidis. A comparative assessment of measures of similarity of fuzzy values. *Fuzzy Sets and Systems*, 56(2):171–174, 1993.
- [103] Anna Wilbik and James M. Keller. A distance metric for a space of linguistic summaries. *Fuzzy Sets and Systems*, 208:79–94, December 2012.
- [104] Anna Wilbik and James M.Keller. A fuzzy measure similarity between sets of linguistic summaries. *IEEE Trans.on Fuzzy Systems vol.21 (1) (2012)*, 2012.
- [105] Rui Jorge Almeida, Marie-Jeanne Lesot, Bernadette Bouchon-Meunier, Uzay Kaymak, and Gilles Moyse. Linguistic summaries of categorical time series for septic shock patient data. In *IEEE International Conference On Fuzzy Systems (FUZZ’2013)*, pages 1–8. IEEE, 2013.
- [106] Jon Garibaldi, Chao Chen, and Tajul Razak. *FuzzyR: Fuzzy Logic Toolkit for R*, 2017. R package version 2.1.
- [107] Michael Schomaker and Christian Heumann. Model Selection and Model Averaging After Multiple Imputation. *Comput. Stat. Data Anal.*, 71:758–770, March 2014.
- [108] Eamonn J. Keogh and Michael J. Pazzani. An indexing scheme for fast similarity search in large time series databases. In *Scientific and Statistical Database Management, 1999. Eleventh International Conference On*, pages 56–67. IEEE, 1999.
- [109] James Honaker, Gary King, and Matthew Blackwell. Amelia II: A program for missing data. *Journal of Statistical Software*, 45(7):1–47, 2011.
- [110] David Meyer, Evgenia Dimitriadou, Kurt Hornik, Andreas Weingessel, and Friedrich Leisch. *e1071: Misc Functions of the Department of Statistics, Probability Theory Group (Formerly: E1071), TU Wien*, 2015. R package version 1.6-7.

- [111] T. T. H. Phan, É P. Caillault, A. Bigand, and A. Lefebvre. DTW-Approach for uncorrelated multivariate time series imputation. In *2017 IEEE 27th International Workshop on Machine Learning for Signal Processing (MLSP)*, pages 1–6, Tokyo, Japan, September 2017.
- [112] Jerry M Mendel and R.B.John. Type-2 fuzzy made simple. *IEEE Transactions on Fuzzy Systems*, 10(2):117–127, 2002.
- [113] Omolbanin Yazdanbakhsh and Scott Dick. A systematic review of complex fuzzy sets and logic. *Fuzzy Sets and Systems*, 338:1–22, May 2018.
- [114] Kifayat Ullah, Tahir Mahmood, and Naeem Jan. Similarity measures for t-spherical fuzzy sets with applications in pattern recognition. *Symmetry*, 10(6), 2018.
- [115] Philippe Grosjean, Marc Picheral, Caroline Warembourg, and Gabriel Gorsky. Enumeration, measurement, and identification of net zooplankton samples using the ZOOSCAN digital imaging system. *ICES Journal of Marine Science: Journal du Conseil*, 61(4):518–525, January 2004.
- [116] Mustafa Kansiz, Philip Heraud, Bayden Wood, Frank Burden, John Beardall, and Don McNaughton. Fourier transform infrared microspectroscopy and chemometrics as a tool for the discrimination of cyanobacterial strains. *Phytochemistry*, 52(3):407–417, 1999.
- [117] Felix Schläpfer and Bernhard Schmid. Ecosystem effects of biodiversity: a classification of hypotheses and exploration of empirical results. *Ecological Applications*, 9(3):893–912, 1999.
- [118] Mario Giordano, Mustafa Kansiz, Philip Heraud, John Beardall, Bayden Wood, and Don McNaughton. Fourier Transform Infrared Spectroscopy as a Novel Tool to Investigate Changes in Intracellular Macromolecular Pools in the Marine Microalga *Chaetoceros Muellerii* (bacillariophyceae). *Journal of Phycology*, 37(2):271–279, April 2001.
- [119] Gerald Niemi, Denice Wardrop, Robert Brooks, Susan Anderson, Valerie Brady, Hans Paerl, Chet Rakocinski, Marius Brouwer, Barbara Levinson, and Michael McDonald. Rationale for a New Generation of Indicators for Coastal Waters. *Environmental Health Perspectives*, 112(9):979–986, May 2004.

- [120] Christopher D. G. Harley, A. Randall Hughes, Kristin M. Hultgren, Benjamin G. Miner, Cascade J. B. Sorte, Carol S. Thornber, Laura F. Rodriguez, Lars Tomanek, and Susan L. Williams. The impacts of climate change in coastal marine systems. *Ecology Letters*, 9(2):228–241, February 2006.
- [121] Alberto Domenighini and Mario Giordano. Fourier Transform Infrared Spectroscopy of Microalgae as a Novel Tool for Biodiversity Studies, Species Identification, and the Assessment of Water Quality¹. *Journal of Phycology*, 45(2):522–531, April 2009.
- [122] J. W. G. Lund, C. Kipling, and E. D. Le Cren. The inverted microscope method of estimating algal numbers and the statistical basis of estimations by counting. *Hydrobiologia*, 11(2):143–170, April 1958.
- [123] Natacha Guiselin, Lucie Courcot, Luis Felipe Artigas, Aude Le Jéloux, and Jean-Michel Brylinski. An optimised protocol to prepare *Phaeocystis globosa* morphotypes for scanning electron microscopy observation. *Journal of Microbiological Methods*, 77(1):119–123, April 2009.
- [124] P. H. Burkill, R. F. C. Mantoura, and M. Cresser. The Rapid Analysis of Single Marine Cells by Flow Cytometry [and Discussion]. *Philosophical Transactions: Physical Sciences and Engineering*, 333(1628):99–112, 1990.
- [125] J. W. Hofstraat, W. J. M. van Zeijl, M. E. J. de Vreeze, J. C. H. Peeters, L. Peperzak, F. Colijn, and T. W. M. Rademaker. Phytoplankton monitoring by flow cytometry. *Journal of Plankton Research*, 16(9):1197–1224, 1994-01-01.
- [126] Malcolm F. Wilkins, Sam A. Hardy, Lynne Boddy, and Colin W. Morris. Comparison of five clustering algorithms to classify phytoplankton from flow cytometry data. *Cytometry*, 44(3):210–217, 2001.
- [127] Qiao Hu and Cabell Davis. Automatic plankton image recognition with co-occurrence matrices and support vector machine. *Marine Ecology Progress Series*, 295:21–31, 2005.
- [128] Cabell S. Davis, HU QIAO, Scott M. Gallager, TANG XIAOOU, and Carin J. Ashjian. Real-time observation of taxa-specific plankton distributions: an optical sampling method. *Marine ecology. Progress series*, 284:77–96, 2004.

- [129] G. Gorsky, M. D. Ohman, M. Picheral, S. Gasparini, L. Stemann, J.-B. Romagnan, A. Cawood, S. Pesant, C. Garcia-Comas, and F. Prejger. Digital zooplankton image analysis using the ZooScan integrated system. *Journal of Plankton Research*, 32(3):285–303, March 2010.
- [130] X. Irigoien, J. A. Fernandes, P. Grosjean, K. Denis, A. Albaina, and M. Santos. Spring zooplankton distribution in the Bay of Biscay from 1998 to 2006 in relation with anchovy recruitment. *Journal of Plankton Research*, 31(1):1–17, September 2008.
- [131] T. Luo, K. Kramer, D.B. Goldgof, L.O. Hall, S. Samson, A. Remsen, and T. Hopkins. Recognizing Plankton Images From the Shadow Image Particle Profiling Evaluation Recorder. *IEEE Transactions on Systems, Man and Cybernetics, Part B (Cybernetics)*, 34(4):1753–1762, August 2004.
- [132] H. W. Balfoort, J. Snoek, J. R. M. Smiths, L. W. Breedveld, J. W. Hofstraat, and J. Ringelberg. Automatic identification of algae: neural network analysis of flow cytometric data. *Journal of Plankton Research*, 14(4):575–589, 1992.
- [133] Lynne Boddy, C. W. Morris, M. F. Wilkins, G. A. Tarran, and P. H. Burkill. Neural network analysis of flow cytometric data for 40 marine phytoplankton species. *Cytometry*, 15(4):283–293, 1994.
- [134] Lynne Boddy, C. W. Morris, M. F. Wilkins, Luan AlHaddad, G. A. Tarran, R. R. Jonker, and P. H. Burkill. Identification of 72 phytoplankton species by radial basis function neural network analysis of flow cytometric data. *Marine Ecology Progress Series*, 195:47–59, March 2000.
- [135] Donald S. Frankel, Robert J. Olson, Sheila L. Frankel, and Sallie W. Chisholm. Use of a neural net computer system for analysis of flow cytometric data of phytoplankton populations. *Cytometry*, 10(5):540–550, 1989.
- [136] Donald S. Frankel, Sheila L. Frankel, Brian J. Binder, and Robert F. Vogt. Application of neural networks to flow cytometry data analysis and real-time cell classification. *Cytometry*, 23(4):290–302, 1996.
- [137] M. F. Wilkins, Lynne Boddy, C. W. Morris, and R. R. Jonker. Identification of phytoplankton from flow cytometry data by using radial basis function neural networks. *Applied and environmental microbiology*, 65(10):4404–4410, 1999.

- [138] Matthew B. Blaschko, Gary Holness, Marwan A. Mattar, Dimitri Lisin, Paul E. Utgoff, Allen R. Hanson, Howard Schultz, and Edward M. Riseman. Automatic in situ identification of plankton. In *Application of Computer Vision, 2005. WACV/MOTIONS'05 Volume 1. Seventh IEEE Workshops on*, volume 1, pages 79–86. IEEE, 2005.
- [139] Heidi M. Sosik and Robert J. Olson. Automated taxonomic classification of phytoplankton sampled with imaging-in-flow cytometry. *Limnol. Oceanogr. Methods*, 5(204):e216, 2007.
- [140] Simon Hallstan, Richard K. Johnson, Eva Willén, and Ulf Grandin. Comparison of classification-then-modelling and species-by-species modelling for predicting lake phytoplankton assemblages. *Ecological Modelling*, 231:11–19, April 2012.
- [141] Antanas Verikas, Adas Gelzinis, Marija Bacauskiene, Irina Olenina, and Evaldas Vaiciukynas. An Integrated Approach to Analysis of Phytoplankton Images. *IEEE Journal of Oceanic Engineering*, 40(2):315–326, April 2015.
- [142] Naomi S. Altman. An introduction to kernel and nearest-neighbor nonparametric regression. *The American Statistician*, 46(3):175–185, 1992.
- [143] David W. Aha, Dennis Kibler, and Marc K. Albert. Instance-based learning algorithms. *Machine Learning*, 6(1):37–66, January 1991.
- [144] Vladimir N. Vapnik. *The Nature of Statistical Learning Theory*. Springer New York, New York, NY, 1995.
- [145] Leo Breiman. Random forests. *Machine learning*, 45(1):5–32, 2001.
- [146] Houtao Deng and George Runger. Feature selection via regularized trees. In *Neural Networks (IJCNN), The 2012 International Joint Conference on*, pages 1–8. IEEE, 2012.
- [147] Houtao Deng and George Runger. Gene selection with guided regularized random forest. *Pattern Recognition*, 46(12):3483–3489, December 2013.
- [148] Houtao Deng and George Runger. Gene selection with guided regularized random forest. *Pattern Recognition*, 46(12):3483–3489, 2013.
- [149] Lukasz Komsta and Frederick Novomestky. *moments: Moments, cumulants, skewness, kurtosis and related tests*, 2015. R package version 0.14.

- [150] Jean Hausser and Korbinian Strimmer. *entropy: Estimation of Entropy, Mutual Information and Related Quantities*, 2014. R package version 1.2.1.
- [151] Houtao Deng. Guided random forest in the rrf package. *arXiv:1306.0237*, 2013.
- [152] David Meyer, Evgenia Dimitriadou, Kurt Hornik, Andreas Weingessel, and Friedrich Leisch. *e1071: Misc Functions of the Department of Statistics, Probability Theory Group (Formerly: E1071), TU Wien*, 2015. R package version 1.6-7.
- [153] W. N. Venables and B. D. Ripley. *Modern Applied Statistics with S*. Springer, New York, fourth edition, 2002. ISBN 0-387-95457-0.
- [154] Sébastien Lê, Julie Josse, and François Husson. FactoMineR: A package for multivariate analysis. *Journal of Statistical Software*, 25(1):1–18, 2008.
- [155] Jonathan Chang. *lda: Collapsed Gibbs Sampling Methods for Topic Models*, 2015. R package version 1.4.2.
- [156] Grassi K., Phan T.T.H., Poisson-Caillault E., Bigand A., Devreker D., and Lefebvre A. Results from measurements in the eastern English Channel : MAREL Carnot station. In *Third JERICO-NEXT Workshop on Phytoplankton*, Marseille, France, March 2018.
- [157] J. G. De Gooijer and R. J. Hyndman. 25 years of time series forecasting. *International Journal of Forecasting*, 22(3):443–473, January 2006.
- [158] Uruya Weesakul and Sudajai Lowanichchai. Rainfall forecast for agricultural water allocation planning in Thailand. *Science & Technology Asia*, 10(3):18–27, 2005.
- [159] Inderjeet Kaushik and Sabita Madhvi Singh. Seasonal ARIMA model for forecasting of monthly rainfall and temperature. *Journal of Environmental Research and Development*, 3(2), 2008.
- [160] P. E. Naill M. Momani and P. E. Naill M. Momani. Time Series Analysis Model for Rainfall Data in Jordan: Case Study for Using Time Series Analysis. *American Journal of Environmental Sciences*, 5(5):599–604, October 2009.
- [161] Byung Sik Kim, Syed Zakir Hossein, and Gyewoon Choi. Evaluation of temporal-spatial precipitation variability and prediction using seasonal ARIMA model in Mongolia. *KSCE Journal of Civil Engineering*, 15(5):917–925, May 2011.

- [162] Ishtiaq Mahmud, Sheikh Hefzul Bari, and M. Tauhid Ur Rahman. Monthly rainfall forecast of Bangladesh using autoregressive integrated moving average method. *Environmental Engineering Research*, 22(2):162–168, November 2016.
- [163] A. H. Nury, M. Koch, and M. J. B. Alam. Time Series Analysis and Forecasting of Temperatures in the Sylhet Division of Bangladesh. In *4th International Conference on Environmental Aspects of Bangladesh (ICEAB), August*, pages 24–26, 2013.
- [164] Leixiao Li, Zhiqiang Ma, Limin Liu, and Yuhong Fan. Hadoop-based ARIMA Algorithm and its Application in Weather Forecast. *International Journal of Database Theory and Application*, 6(5):119–132, October 2013.
- [165] C. Cheng, A. Sa-Ngasoongsong, O. Beyca, T. Le, H. Yang, Z. (James) Kong, and Satish T. S. Bukkapatnam. Time series forecasting for nonlinear and non-stationary processes: A review and comparative study. *IIE Transactions*, 47(10):1053–1071, October 2015.
- [166] M. Mudelsee. *Climate Time Series Analysis*. Springer, 2013.
- [167] T. Mandal and V. Jothiprakash. Short-term rainfall prediction using ANN and MT techniques. *ISH Journal of Hydraulic Engineering*, 18(1):20–26, March 2012.
- [168] A. El-Shafie, A. Nouredin, M. Taha, A. Hussain, and M. Mukhlisin. Dynamic versus static neural network model for rainfall forecasting at Klang River Basin, Malaysia. *Hydrology and Earth System Sciences*, 16(4):1151–1169, April 2012.
- [169] M. Imani, R.-J. You, and C.-Y. Kuo. Caspian Sea level prediction using satellite altimetry by artificial neural networks. *International Journal of Environmental Science and Technology*, 11(4):1035–1042, May 2014.
- [170] Nguyen Q. Hung, Mukand S. Babel, S. Weesakul, and N. K. Tripathi. An artificial neural network model for rainfall forecasting in Bangkok, Thailand. *Hydrology and Earth System Sciences*, 13(8):1413–1425, 2009.
- [171] Surajit Chattopadhyay and Goutami Chattopadhyay. Univariate modelling of summer-monsoon rainfall time series: Comparison between ARIMA and ARNN. *Comptes Rendus Geoscience*, 342(2):100–107, February 2010.

- [172] Prodromos E. Tsinaslanidis and Dimitris Kugiumtzis. A prediction scheme using perceptually important points and dynamic time warping. *Expert Systems with Applications*, 41(15):6848–6860, November 2014.
- [173] P.A. Aguilera, A. Fernández, R. Fernández, R. Rumí, and A. Salmerón. Bayesian networks in environmental modelling. *Environmental Modelling & Software*, 26(12):1376–1388, December 2011.
- [174] Celia Frank, Ashish Garg, Les Sztandera, and Amar Raheja. Forecasting women’s apparel sales using mathematical modeling. *International Journal of Clothing Science and Technology*, 15(2):107–125, April 2003.
- [175] Mick Smith and Rajeev Agrawal. A Comparison of Time Series Model Forecasting Methods on Patent Groups. In *MAICS*, pages 167–173, 2015.
- [176] Rob J Hyndman and Yeasmin Khandakar. Automatic time series forecasting: the forecast package for R. *Journal of Statistical Software*, 26(3):1–22, 2008.
- [177] David Stoffer. *astsa: Applied Statistical Time Series Analysis*, 2017. R package version 1.8.
- [178] Steven L. Scott. *bsts: Bayesian Structural Time Series*, 2017. R package version 0.7.1.
- [179] Haibin Cheng, Pang-Ning Tan, Christopher Potter, and Steven Klooster. Detection and Characterization of Anomalies in Multivariate Time Series. In *Proceedings of the 2009 SIAM International Conference on Data Mining*, pages 413–424. Philadelphia, PA, April 2009.

List of Tables

1.1	Values of different indicators between the Query and various references	24
2.1	The matching cost of different methods	39
2.2	Different indicators for evaluating the similarity between each pair of signals .	40
2.3	Data characteristics	46
2.4	Average imputation performance indices of six methods on the Airpassenger, Beersales, Google and SP datasets. The best results are highlighted in bold. . .	50
2.5	Average imputation performance indices of six methods on CO2 concentrations, Mackey-Glass Chaotic, Phu Lien temperature and Water level datasets. The best results are highlighted in bold.	52
2.6	The maximum of cross-correlation between the query and reference windows. .	56
2.7	Data characteristics by dataset: Number of the dataset, its name, the number of time samples, presence (Y=Yes else N=No) of trend, presence of seasonal cycle and sampling frequency	60
2.8	Average imputation performance indices of various similarity metrics on Cua Ong temperature series	61
2.9	Average imputation performance indices of various similarity metrics on Gas online series	62
2.10	Average imputation performance indices of various similarity metrics on Fluorescence series	63
2.11	Average imputation performance indices of various similarity metrics on Chla series	64
2.12	Average imputation performance indices of various similarity metrics on water level series	65

2.13	Computational time of methods using different DTW metrics at missing rate 0.6% on various series in second (s)	65
2.14	The maximum of cross-correlation between the query and reference windows. .	66
3.1	Average imputation performance indices of various imputation methods on NNGC series (1745 collected points)	81
3.2	Average imputation performance indices of various imputation algorithms on simulated dataset (32,000 collected points)	82
3.3	Average imputation performance indices of various imputation algorithms on Marel dataset (35,334 collected points)	83
3.4	Average imputation performance indices of various imputation algorithms on synthetic dataset (100,000 collected points)	97
3.5	Average imputation performance indices of various imputation algorithms on simulated dataset (32,000 collected points)	99
3.6	Average imputation performance indices of various imputation algorithms on MAREL-Carnot dataset (35,334 collected points)	101
3.7	Computational time of different methods on the synthetic series in second (s) .	107
4.1	Accuracy of test recognition of different classification models on the derived features (%)	122
4.2	Accuracy of test recognition of different classification models on the proposed features (%)	122
4.3	Accuracy of test recognition of different classification models on the dissimi- larity features (%)	122
4.4	Contingency table of RF model on the dissimilarity features and the proposed features (T: true label, F: false label)	122
4.5	Contingency table of RF and k -NN models on the dissimilarity features	123
4.6	Number and percentage of missing values for each signal of the MAREL- Carnot station in the period 2005-2009.	126
4.7	Comparison of indicators between MAREL incomplete and complete Turbidity with satellite Turbidity	132
4.8	Characteristics of time series	141
4.9	Performance indices of various forecasting algorithms on Ba Tri datasets (best results in bold)	143

4.10	Performance indices of various forecasting algorithms on Phu Lien datasets (best results in bold)	144
4.11	Performance indices of various forecasting algorithms on Cua Ong temperature (best results in bold)	146
4.12	The maximum of cross-correlation between the query and sliding windows. . .	146

List of Figures

1.1	Illustration of isolated and T-gap missing values	14
1.2	Decomposition of weekly data (average) of <i>Chla</i> from the Ifremer IGA-Gravelines monitoring station over the period 1989 to 2014 using R-starts package.	17
1.3	ACF of <i>Chla</i> time series	18
1.4	Simulated signals	23
2.1	Dynamic Time Warping example [46]	29
2.2	Euclidean example. Note that while the two sequences have an overall similar shape, they are not aligned in the time axis. Euclidean distance, which assumes the i^{th} point in one sequence is aligned with the i^{th} point in the other, will produce a pessimistic dissimilarity measure. The nonlinear Dynamic Time Warped alignment allows a more intuitive distance measure to be calculated [46]	30
2.3	DTW cost matrix with an illustration of matching path (red circle) [46]	31
2.4	Examples of global constraints: (a) Sakoe-Chiba band; (b) Itakura parallelogram.	32
2.5	A) Two synthetic signals (with the same mean and variance). B) The natural "feature to feature" alignment. C) The alignment produced by dynamic time warping. Note that DTW failed to align the two central peaks because they are slightly separated in the Y-axis [48]	33
2.6	Query vs Reference	36
2.7	Query vs Reference4	37
2.8	Query vs Reference5	38
2.9	General architecture of DTWBI: 1- Building query, 2- Comparing sliding window, 3- Selecting window, 4-Filling gap	42
2.10	Detail diagram of DTWBI method for univariate time series imputation	43

2.11	ACF of Mackey-Glass chaotic, water level and Google time series	49
2.12	a) On the left, boxplot comparison of Similarity, RMSE and FSD on C02 dataset with a gap size of 6%, b) on the right boxplot comparison of Similarity, RMSE and FSD on Airpass dataset with a gap size of 15%	53
2.13	Visual comparison of imputed values of different imputation methods with true values on Airpassenger series at position 106 with the gap size of 9.	54
2.14	Visual comparison of imputed values of proposed method with true values on Airpassenger series at position 106 with the gap size of 9.	54
2.15	Visual comparison of imputed values of the proposed method with true values on water level series at position 23,282 with the gap size of 789.	55
2.16	Visual comparison of the query with the similar window on water level series at position 23,282 with the gap size of 789.	55
2.17	Visual comparison of imputed values of different methods with true values on water level series at position 23,282 with the gap size of 789.	55
2.18	Visual comparison of imputed values of spline method with true values on water level series at position 23,282 with the gap size of 789.	55
2.19	Visual comparison of imputed values using different DTW metrics with true values on <i>Chla</i> series at position 444 at missing rate 1% (correspond to 14 weeks missing).	66
3.1	Illustration of the DTW-completion process: query building and similar sequence research, gap filling.	74
3.2	The trapezoid formula	75
3.3	Schema of MI algorithm	77
3.4	Main steps used in multiple imputation.	78
3.5	Visual comparison of imputed values of different imputation methods with true values on NNGC series with the gap size of 17 on each signal.	84
3.6	Visual comparison of imputed values of different imputation methods with true values on MAREL Carnot dataset with the gap size of 353 on the 2 nd signal. . .	85
3.7	Scheme of the completion process: 1-Building queries, 2- Comparing sliding windows, 3- Selecting the most similar windows, 4- Completing gap.	88
3.8	Computing scheme of the new similarity measure	90
3.9	Membership function of fuzzy similarity values	91

3.10	A schematic of Amelia to multiple imputation with the EMB algorithm.	95
3.11	Visual comparison of completion data of different imputation approaches with real data on the 1 st signal of synthetic series with the gap size of 1000	104
3.12	Visual comparison of completion data of different imputation approaches with real data on the 1 st signal of synthetic series with the gap size of 5000	105
3.13	Visual comparison of completion data of different imputation approaches with real data on the 2 nd signal of MAREL Carnot dataset with the gap size of 353	106
4.1	8D-signals describing three species	118
4.2	Signals collected from the MAREL-Carnot station during the period 2005-2009	127
4.3	Signals collected from the MAREL-Carnot station during the period 2005-2009	128
4.4	Schema of preprocessing data stage	129
4.5	Comparison of incomplete(black) Turbidity, complete (blue) Turbidity and satel- lite Turbidity (red)	133
4.6	Extreme events detection	134
4.7	Results of the 1 st spectral clustering (b) - boxplot of temperature dispersion (c) - states distribution per month with seasonal cycle in the period 2005-2008 and (d) - sequencing of the states in the period 2005-2008.	135
4.8	135
4.9	Illustration of the DTWBI for the forecasting task: 1-Query building, 2-Sliding window comparison, 3-Window selection, 4-Forecasting values	139
4.10	True values and forecast values generated from different univariate methods on Phu Lien humidity series (forecast size of 18 months)	145
B.1	Query-Reference2	162
B.2	Query-Reference3	163

Abstract

Missing data are a prevalent problem in many domains of pattern recognition and signal processing. Most of the existing techniques in the literature suffer from one major drawback, which is their inability to process incomplete datasets. Missing data produce a loss of information and thus yield inaccurate data interpretation, biased results or unreliable analysis, especially for large missing sub-sequence(s). So, this thesis focuses on dealing with large consecutive missing values in univariate and low/un-correlated multivariate time series.

We begin by investigating an imputation method to overcome these issues in univariate time series. This approach is based on the combination of shape-feature extraction algorithm and Dynamic Time Warping method. A new R-package, namely DTWBI, is then developed.

In the following work, the DTWBI approach is extended to complete large successive missing data in low/un-correlated multivariate time series (called DTWUMI) and a DTWUMI R-package is also established. The key of these two proposed methods is that using the elastic matching to retrieving similar values in the series before and/or after the missing values. This optimizes as much as possible the dynamics and shape of knowledge data, and while applying the shape-feature extraction algorithm allows to reduce the computing time.

Successively, we introduce a new method for filling large successive missing values in low/un-correlated multivariate time series, namely FSMUMI, which enables to manage a high level of uncertainty. In this way, we propose to use a novel fuzzy based on fuzzy grades of basic similarity measures and fuzzy logic rules. Finally, we employ the DTWBI to (i) complete the MAREL Carnot dataset and then we perform a detection of rare/extreme events in this database (ii) forecast various meteorological univariate time series collected in Vietnam.

Keywords: Imputation, missing data, univariate time series, uncorrelated multivariate time series, Dynamic Time Warping, similarity measure, fuzzy inference system.

RÉSUMÉ

Les données manquantes constituent un challenge commun en reconnaissance de forme et traitement de signal. Une grande partie des techniques actuelles de ces domaines ne gère pas l'absence de données et devient inutilisable face à des jeux incomplets. L'absence de données conduit aussi à une perte d'information, des difficultés à interpréter correctement le reste des données présentes et des résultats biaisés notamment avec de larges sous-séquences absentes. Ainsi, ce travail de thèse se focalise sur la complétion de large séquences manquantes dans les séries monovariées puis multivariées peu ou faiblement corrélées.

Un premier axe de travail a été une recherche d'une requête similaire à la fenêtre englobant (avant/après) le trou. Cette approche est basée sur une comparaison de signaux à partir d'un algorithme d'extraction de caractéristiques géométriques (formes) et d'une mesure d'appariement élastique (DTW - Dynamic Time Warping). Un package R CRAN a été développé, DTWBI pour la complétion de série monovariée et DTWUMI pour des séries multidimensionnelles dont les signaux sont non ou faiblement corrélés. Ces deux approches ont été comparées aux approches classiques et récentes de la littérature et ont montré leur faculté de respecter la forme et la dynamique du signal. Concernant les signaux peu ou pas corrélés, un package DTWUMI a aussi été développé.

Le second axe a été de construire une similarité floue capable de prendre en compte les incertitudes de formes et d'amplitude du signal. Le système FSMUMI proposé est basé sur une combinaison floue de similarités classiques et un ensemble de règles floues.

Ces approches ont été appliquées à des données marines et météorologiques dans plusieurs contextes : classification supervisée de cytogrammes phytoplanctoniques, segmentation non supervisée en états environnementaux d'un jeu de 19 capteurs issus d'une station marine MAREL CARNOT en France et la prédiction météorologique de données collectées au Vietnam.

Mots-clés: Imputation, données manquantes, séries temporelles univariées, séries temporelles multivariées non corrélées, Dynamic Time Warping, mesure de similarité, système d'inférence floue.